T-CELL IMMUNITY AGAINST INFLUENZA AND SARS-COV-2 IN THE FERRET MODEL

TOWARDS UNIVERSAL VACCINES

Koen van de Ven

T-cell immunity against influenza and SARS-CoV-2 in the ferret model
Towards universal vaccines

Koen Cornelis Gerardus Petrus van de Ven

Colofon

Scan to view the digital version of this thesis

ISBN: 978-94-6458-496-7

Provided by thesis specialist Ridderprint, ridderprint.nl
Printing: Ridderprint
Layout and design: Mila Slappendel, persoonlijkproefschrift.nl

T-cell immunity against influenza and SARS-CoV-2 in the ferret model

Towards universal vaccines

T-cel immuniteit tegen influenza en SARS-CoV-2 in het fretten model

Op weg naar universele vaccins

(met een samenvatting in het Nederlands)

Proefschrift

ter verkrijging van de graad van doctor aan de Universiteit Utrecht op gezag van de rector magnificus, prof.dr. H.R.B.M. Kummeling, ingevolge het besluit van het college voor promoties in het openbaar te verdedigen op

dinsdag 20 september 2022 des middags te 12.15 uur

door

Koen Cornelis Gerardus Petrus van de Ven

Geboren op 18 december 1990
te Oirschot

Promotor
Prof. dr. D. van Baarle

Co-promotor
Dr. J.M. de Jonge

Beoordelingscommissie:
Prof. dr. L. Koenderman (voorzitter)
Prof. dr. F.J.M. van Kuppeveld
Prof. dr. J.A.M. Borghans
Prof. dr. A.L.W. Huckriede
Dr. S. Herfst

Printing of this thesis was financially supported by The National Institute for Public Health and the Environment (RIVM).

Table of contents

General introduction

1

Influenza viruses – a brief introduction

In 412 BC, Hippocratus described the 'Cough of Perinthus' in the "Book of Epidemics" [1]. He noted that during the winter season, patients in the town of Perinthus were suffering from coughing, a sore throat and aches, among several other symptoms. With this written account, Hippocratus might have been the first to record what we now know as 'the flu', although the Cough of Perinthis likely involved multiple infectious diseases [2]. The flu – or influenza – is caused by the influenza virus. Its name originates from the Latin '*influentia*' (to flow into), referring to the belief that some disease outbreaks were influenced by the stars [3]. It was only in 1743 when an unknown epidemic was sweeping across Europe, that the term 'influenza' became common in the English language.

We have come a long way from the initial description of influenza. In 1933, Smith, Andrewes and Laidlaw isolated and for the first time identified a human influenza virus [4]. They infected ferrets with filtered throat washes from influenza patients, thereby establishing that the infectious particle should be a virus, as bacteria would have been filtered out. Perhaps unknowingly, their work created the basis for the ferret model that we are using today for influenza research. Through the work of later scientists we now know that influenza viruses are negative-sense single stranded RNA viruses of the *Orthomyxoviridae* family [5]. Based on their genetics, influenza viruses can be further divided into influenza A, B, C and D viruses. Only types A and B regularly infect humans, whereas influenza C virus has been shown to infect humans but is relatively rare. Influenza D virus can infect pigs and cattle, but no human cases have been identified up till now [6].

Despite decades of research and the development of vaccines, viral influenza remains a problem. It is estimated that 5-15% of the world population gets infected yearly with circulating influenza viruses [1, 2]. According to the World Health Organization (WHO), this leads to approximately 290.000-650.000 deaths every year, especially in the very young and elderly [7]. In addition to the seasonal influenza epidemic, new influenza viruses can be introduced from animal reservoirs into the human population. These newly introduced viruses might escape pre-existing immunity, leading to influenza virus pandemics with corresponding high morbidity and mortality. Vaccination could be an effective countermeasure against seasonal and pandemic influenza. Unfortunately, while influenza virus vaccines are available, the immunity they induce is too narrow to cope with the continuously evolving influenza viruses.

Influenza A virus – a continuously evolving threat

Of the influenza viruses, the most-studied is influenza A virus (IAV) due to its history of pandemic outbreaks. IAV can be divided into multiple subtypes based on the composition of haemagglutinin (HA) and neuraminidase (NA); two immunodominant proteins on the surface of the IAV virion ([8] and Figure 1). Up to date, 18 HA (H1-H18) and 11 NA (N1-N11) classes have been identified based on antigenic dissimilarities, which means that approximately 200 HA-NA combinations are possible [8, 9]. There are however several restrictions in place due to which not every combination is prevalent in nature [9]. Furthermore, not all IAV subtypes can infect humans. Only H1N1 and H3N2 are currently circulating among humans [10]. The H2N2 subtype has also circulated in the past, but disappeared from the human population in 1968 [10]. Besides these three human IAVs, there are sporadic zoonotic infections with IAV strains from animal reservoirs. Infections with swine IAV variants of the H1N1, H1N2 and H3N2 subtypes have been reported [11]. Additionally, in places with high bird-human contacts such as live bird markets, primarily H5- and H7-based IAV strains have been found to occasionally infect humans [12]. Zoonotic IAV infections rarely transmit from human-to-human as the virus is not sufficiently adapted to its human host. Still, influenza viruses mutate over time and it has been shown that as little as five mutations are required to enhance the transmission of an avian H5N1 virus [13, 14].

IAV possesses two features that equip the virus with the ability to produce variant viruses that may be more fit to a given environment: a segmented RNA genome and an error prone RNA polymerase (Figure 1). Due to a lack of proofreading and repair activity in the RNA polymerase, mutations are introduced into the IAV genome with every replication cycle ([15-18], more information about the IAV replication cycle can be found in Box 1). Over time, these mutations accumulate, which causes the influenza virus genome to drift further away from its original genome. Hence, this process is termed *antigenic drift* (Figure 2). Mutations mainly accrue in HA and NA genes, as evidenced by their low protein conservation between IAV isolates [19, 20]. This is in part due to immunological pressure, as the virus is forced to alter its HA and NA epitopes in order to escape the antibody response of the host [19, 21]. The gradual mutation of HA and NA is also the reason why people can get infected repeatedly with the same subtype of influenza virus (e.g. H1N1 or H3N2) and why influenza virus vaccines need to be updated yearly. Importantly, a mismatch between the vaccine and circulating influenza virus strains can severely diminish the vaccine effectiveness. This has occurred during multiple seasons, which resulted in vaccine effectiveness dropping to less than 20% [22-24].

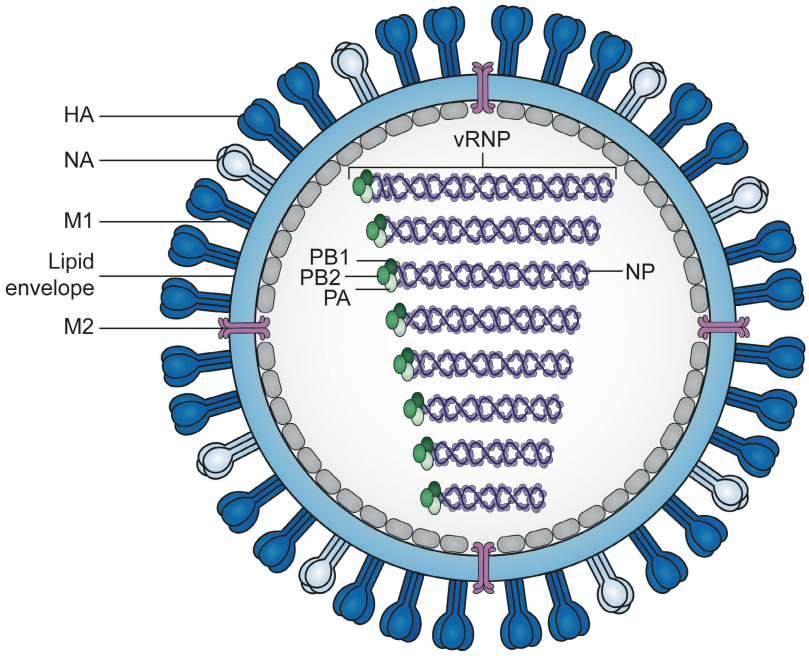

Figure 1: Overview of influenza A virus (IAV) particle with. The lipid envelope of IAV is coated with haemagglutinin (HA) and neuraminidase (NA) molecules and the transmembrane ion channel matrix protein 2 (M2). The inside of the lipid envelope is covered with matrix protein 1 (M1) molecules and contains 8 segmented RNA molecules that are wrapped around nucleoprotein (NP). These molecules are capped with the polymerase protein consisting of the subunits polymerase basic protein 1 (PB1), 2 (PB2) and polymerase acidic protein (PA). The viral RNA together with the polymerase complex forms the viral ribonucleoprotein complex (vRNP).

In addition to the antigenic drift that leads to gradual changes in seasonal influenza viruses, there is another process by which influenza viruses can escape the immune response. New IAV strains can emerge by a process termed *antigenic shift*, in which two or more IAV strains infect the same host and exchange genetic material (Figure 2; reviewed in [10]). The relatively easy exchange of genetic material is made possible by the segmented genome of IAV and the wide spread of IAV in animal reservoirs. Antigenic shift events can create new IAV strains that possesses HA and/or NA molecules that are no longer recognized by the existing antibody response. This can have severe consequences. If multiple IAV strains combine into a new strain that – by coincidence – possesses the ability to infect and transmit between humans, a possible pandemic strain might have been generated. For example, the strain responsible for the 2009 H1N1 pandemic can be traced back to a reassorting event in swine. Multiple IAV lineages reassorted into a strain that was able to infect humans and was not recognized sufficiently by the then existing immune response in the population [25,

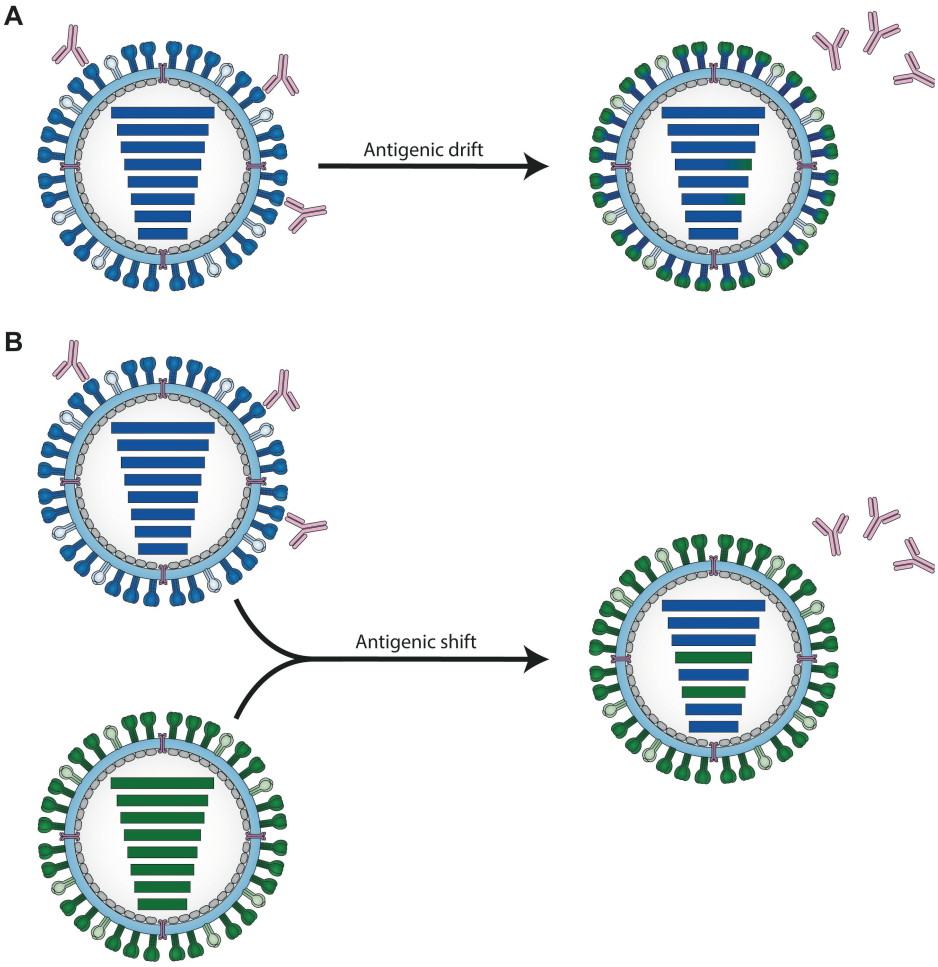

Figure 2: The continuous evolution of IAV. A) Antigenic drift and **B)** antigenic shift are processes by which influenza virus mutate and escape host immunity.

26]. Combined with the high mobility of our current society, this resulted in a fast and global spread of this pandemic H1N1 (pH1N1) virus. Other past IAV pandemics that resulted from antigenic shift are the 1957 H2N2 and 1968 H3N2 pandemics [27-29]. Thankfully, animal-derived IAV relatively rarely transmit to humans as their genes are not fully adapted to the human host, which also prevents sustained human-to-human transmission of these viruses.

The continuous changes in circulating IAV strains driven by antigenic drift and shift, poses a tangible threat to public health. This is clearly illustrated by the observation that all past influenza pandemics in which the causative agent has been isolated

can be attributed to IAV [30]. With the high mutation rate of IAV, the risk of new strains appearing due to antigenic shift and the close animal-to-human contact, it is not the question if, but when a new influenza pandemic will occur. Therefore, the development and introduction of improved influenza virus vaccines is crucial for dampening the impact of seasonal influenza epidemics and future pandemics.

Box 1: IAV replication cycle

The IAV genome is divided over eight RNA-segments that code for ten essential and several non-essential proteins (reviewed in [5]). The virion consists of a lipid envelope that is covered with HA and NA molecules (Figure 1). Interspersed between HA and NA is the small matrix protein 2 (M2). The inside of the lipid membrane is coated with matrix protein 1 (M1) molecules and harbors the segmented-RNA genome that is tightly wrapped around nucleoprotein (NP). Each RNA-segment is capped with a polymerase unit consisting of three subunits: polymerase acidic protein (PA), polymerase basic protein 1 (PB1) and 2 (PB2). Together, the viral RNA wrapped around NP and the polymerase unit form the viral ribonucleoprotein complex (vRNP). Other proteins that are encoded for by the IAV genome include non-structural protein 1 (NS1) and nuclear export protein (NEP), also called non-structural protein 2 (NS2). NS1 is crucial for dampening the host immune response that is triggered by the viral infection and excessive production of viral proteins [31]. It does this by – among others – limiting the production of interferons. More recently however, NS1 has also been shown to affect viral replication by modulating various processes of the viral replication cycle [32]. NEP facilitates the export of vRNPs from the nucleus into the cytosol, but has also been implicated in the regulation of viral mRNA transcription and replication [33, 34].

The process of infection with IAV consist of a series of interplays between virus and host that determine whether infection is successful. The first step of infection is transmission of infectious IAV particles between hosts. This can be mediated by small droplets (originating from sneezing/coughing) or (in)direct contact with contaminated surfaces [35]. After transmission, the virion needs to transverse the innate barriers of the respiratory tract. NA plays an important role in this step by cleaving sialylated glycoproteins in the mucus that obstruct IAV particles [36]. After migrating through the mucus, the virion attaches to the host cell. This is mediated by HA, which contains a receptor binding site for sialic acids (SA) that are often present as terminal residues of glycoproteins or glycolipids [37]. HA specifically binds to α2,3- or α2,6-linked SA, although the exact binding mechanism of HA might be more complex than what is currently understood [9].

Box 1: IAV replication cycle (continued)

Before HA is functional, is has to be cleaved into its active fragments HA1 and HA2 by proteases that reside in the respiratory tract. HA1 binds to SA after which the virion is endocytosed. Due to acidification of the endosome, HA changes conformation. This exposes the fusion peptide of HA2 which is inserted into the endosomal membrane and drives the fusion of the viral membrane with the endosomal membrane. Additionally, the low pH in the endosome activates the ion channel M2, which acidifies the internal environment of the virion. The acidification releases the vRNPs from the M1-coating of the viral envelope and allows the vRNPs to diffuse into the cytoplasm.

The released vRNPs are shuttled into the nucleus by host proteins, after which the viral polymerase complex transcribes the viral RNA (vRNA) into mRNA and additional vRNA molecules. From the viral mRNA, new viral proteins are translated by the host ribosomal complex in the cytoplasm or endoplasmic reticulum. NA, HA and M2 proteins are transported from the ER via the Golgi to the cell membrane, where they start forming a new virion. This causes the membrane to start budding and M1 proteins are recruited to line the interior of the vesicle in formation. Simultaneously, vRNPs are formed by packaging vRNA around NP with a cap of viral polymerase. These are then delivered to the budding vesicle in which vRNPs are incorporated in a 7+1 structure (one vRNP is surrounded by 7 others). When the budding has completed, the vesicle is released from the host membrane by NA molecules that cleave SA from N-linked glycans, thereby removing the interaction between HA and the host membrane.

Influenza virus vaccines – there is room for improvement

The first influenza virus vaccines were developed and tested in the 1930s and 40s [38]. Whole inactivated virus (WIV) influenza vaccines were prepared from virus grown in fertilized chicken eggs, which was inactivated by formalin treatment. WIV vaccines are a predecessor of the inactivated influenza vaccines (IIVs) that we are still using today, although the production methods of IIVs has been further refined. For example, split vaccines are a type of IIV that is created by disrupting the viral envelope with a solvent, thereby inactivating the virus. This process can be followed by further purification of HA by removing other influenza virus proteins, which then results in a so-called subunit vaccine. Due to their lower reactogenicity compared to WIV vaccines, split and subunit vaccines are currently the most commonly used influenza virus vaccines in the Western world [39, 40] (see Box 2). Importantly, all types of IIVs focus on HA content [41] and therefore levels of other influenza virus proteins are often unknown and may vary between vaccine production methods. A significant proportion of the IIV-

Box 2: influenza virus vaccines in the Netherlands

The Netherlands started their national influenza virus vaccination program in 1993 [60, 61]. Influenza virus vaccines are supplied by different manufacturers and can vary slightly in their production method, but all vaccines are based on haemagglutinin proteins. Until 2018, all vaccines were trivalent, meaning they contained HA proteins of two circulating influenza A viruses (H1N1, H3N2) and one influenza B virus (either Victoria or Yamagata lineage). From 2019 onwards, the Netherlands has switched to quadrivalent influenza virus vaccines that should offer increased protection by including both influenza B virus lineages (in addition to H1N1 and H3N2 influenza A viruses). Seasonal influenza virus vaccination is primarily offered to healthcare workers and risk groups, which includes persons with certain chronic illnesses (e.g. asthma), morbid obesity (BMI >40) and people of older age (>60 years). The Ministry of Public Health (Dutch: Ministerie van Volksgezondheid, Welzijn & Sport) decides which groups are offered vaccination based on advice from The Health council of the Netherlands (Dutch: Gezondheidsraad).

production is still egg-based due to the extensive experience with this method. Egg-based production of IIVs does have some severe drawback however (reviewed in [42]), which includes the introduction of 'egg-adaptation' mutations in the HA-sequence. For this reason, other production methods for influenza viruses or recombinant HA have also been developed.

A second type of licensed influenza virus vaccines are recombinant HA vaccines, which consist of HA proteins produced on cell-lines (often mammalian or insect). The formulation of this type of vaccine closely resembles that of sub-unit vaccines, as they solely contain HA. However, recombinant vaccines differ in the aspect that they do not require live influenza virus for their production [39]. Due to this, no mutations can occur in the HA protein and no other influenza virus proteins are present in the vaccine. Like traditional IIVs, recombinant HA vaccines are injected i.m. and primarily induce humoral responses [43].

As an alternative to IIVs, live attenuated influenza vaccines (LAIVs) have been developed separately in the US and Russia [44, 45]. These LAIV viruses have been made temperature-sensitive by cold adaptation to efficiently replicate at 33°C and less efficiently at higher temperatures found in the lower respiratory tract. This restricts their replication to the upper respiratory tract, thereby simulating an influenza virus infection without risk for complications due to lower respiratory tract infections. While LAIVs have been used since the 1980s in Russia [46], it was not until 2003 and 2011 that the first LAIVs were approved for use in the USA [47, 48] and

Europe [49] respectively. There are some benefits to the use of LAIVs. First, they can be administered intranasally, which helps induce local immunity where it is most needed: at the site of infection [50-52]. Secondly, LAIVs are replication competent and by infecting cells they activate immune mechanisms that are not triggered by traditional IIVs. This includes T cells, which are only effectively induced if host cells are infected and proteins are produced. Thirdly, LAIVs possess all influenza virus proteins due to which they can induce a broader immune response that targets not only HA, but also other influenza virus proteins [53]. These advantages have, however, not yet translated to a higher vaccine effectiveness. Multiple studies have compared LAIVs and IIVs and found that in most years LAIVs performed similar or worse than IIVs [54-59]. LAIVs are more often used in (young) children though and this might have introduced some bias in the interpretation of vaccine effectiveness.

Despite the availability of different types of vaccines, they all suffer from the same problem: vaccine strains need to be updated every few years to adjust to mutations in circulating strains. Additionally, IIVs and recombinant HA vaccines are administered i.m., which does not induce immune responses in the respiratory tract. With the exception of LAIV, influenza virus vaccines are also not capable of evoking robust cellular responses as they are replication incompetent. While LAIVs can induce T-cell immunity, the vaccine can be neutralized by pre-existing HA-antibodies before it infects cells, thereby preventing the induction of robust T-cell responses. Existing influenza virus vaccines thus primarily induce neutralizing antibodies that can prevent infection with homologous strains, but are often too strains-specific to protect against heterologous (same subtype, different strain) or heterosubtypic (different subtype) influenza virus infections. Hence, the scientific community is trying to improve influenza virus vaccines so that they induce a broader and more robust protection against viral influenza infections [62]. This might be achieved by steering the immune response towards more conserved influenza virus epitopes.

Adaptive immunity against IAV – antibodies

All IAV proteins are potential targets for the humoral immune response. However, some proteins are more likely to induce a protective antibody response. This mainly entails the HA and NA proteins that make up the virion exterior. As these proteins are displayed on the virion and cell-surface of infected cells, they are easily accessible and can induce potent antibody responses [19]. Importantly, due to the role of HA in infecting cells, HA-antibodies are seen as the most important antibodies to mediate neutralizing immunity – which is defined as a reduction of viral infectivity by binding of antibodies to surface proteins [63, 64]. For this reason, most IAV vaccines solely focus on inducing HA-antibodies [43].

The IAV HA protein is a homotrimer that consist of three identical HA molecules. Each HA molecule can be distinguished into its active HA1 and HA2 fragments (see Box 1). The globular head domain of HA is formed by HA1, while the stalk (or stem) domain of HA is formed by HA2. The majority of the vaccine-induced HA antibody response is centered around several immunodominant epitopes in the head domain of HA. Antibodies that bind to the HA-head can effectively 'neutralize' infectious IAV virions by blocking the interaction between HA and sialic acids, which prevents IAV infection [65]. The epitopes in the HA-head domain are however prone to mutations (antigenic drift) and hence the antibody response targeting these epitopes is often very specific for one or several closely related IAV strains. To achieve a broadly-reactive antibody response, it is thus necessary to target more conserved epitopes.

More conserved epitopes are present in the stalk-domain of HA [43]. Unfortunately, seasonal IAV vaccines hardly boost stalk-binding antibodies since the head-domain is immunodominant [66]. Furthermore, high pre-existing levels of antibodies against the HA-head domain can prevent the induction of HA-stalk antibodies [67]. Still, natural infections can induce stalk-binding antibodies, but their levels are lower than head-antibodies [68, 69]. To induce higher HA-stalk antibody levels, specific vaccination strategies have been developed [70]. These strategies differ to some extent but are based on the same principle: avoid repeated boosting of HA head-antibodies and enable boosting of stalk-antibodies. This can be achieved by creating modified or chimera HAs in which the head domain is absent or replaced by alternative head domains. For example, vaccination with H7/H1 chimera (H7-head, H1-stalk), followed by vaccination with H5/H1 (H5 head, H1 stalk) primarily boosts the stalk-specific antibodies against H1 as the head domain differs between the prime and boost vaccines. By using such – or similar – techniques, high levels of HA-stalk binding antibodies can be induced. Pre-clinical studies have shown that stalk-antibodies can reduce viral transmission and disease [71-75], and the first stalk-antibody-inducing vaccine is currently being evaluated in clinical trials [76].

Stalk-binding antibodies can be both neutralizing and non-neutralizing ([77-82], reviewed in [83]). Non-neutralizing antibodies do not prevent infection, but reduce the impact of IAV infections. This can be achieved by activating effector functions of the (innate) immune system (reviewed in [65]). One example of this is antibody-dependent cell-cytotoxicity (ADCC). Infected cells express HA, NA and M2 IAV proteins on their cell membrane for the production of new virus particles (see Box 2). Antibodies bind to these membrane-bound proteins and in turn, the Fc-part of the antibody is recognized by innate immune cells via the Fc-receptor (FcR). If the innate immune cell is triggered by recognition of antibodies in this way, it can initiate a cytotoxic process to kill the infected cell, hence the term 'antibody-dependent cell-cytotoxicity'.

After HA, NA is probably the best studied IAV protein in the context of antibody responses due to its abundance on the outside of the virion and its importance for transmission. NA is involved in migration through the mucus and release of new virus particles from infected cells (Box 1). NA-binding antibodies can interfere with these processes, thereby inhibiting viral replication and transmission [84]. It is thus not surprising that high anti-NA antibody titers are associated with reduced disease symptoms [85]. Hence, inclusion of NA in vaccines might offer a more robust protection, although – like HA – also the response against NA is limited by the high mutation rate of NA [84].

Besides HA and NA, other IAV proteins can also induce antibody responses, of which M1, M2 and NP are the most prominent. The M2 protein is an interesting target for vaccine development since it is present on both the virion surface and on the cell membrane of infected cells. While M2 is not very immunodominant, it is very conserved and several vaccines in pre-clinical development aim to induce protective levels of M2-antibodies [86, 87]. High antibody responses have also been measured against NP and M1 in humans [88, 89] and NP-antibodies have been shown to be protective in animal models [90, 91]. In contrast, not much is known about the protective effect of M1-antibodies. The mode of action of NP- and M1-antibodies is also not entirely clear, as NP and M1 are not – or only briefly – exposed on the cell membrane of infected cells.

Adaptive immunity against IAV – T cells are associated with protection in humans

T cells recognize antigens in a different manner than antibodies, which enables the T-cell response to target conserved regions in both surface and internal IAV proteins. Every cell – healthy or infected – cleaves a part of the proteins they produce into smaller peptides (8-14 amino acids in length, reviewed in [92]). These peptides can then be presented on the cell membrane via major histocompatibility complex (MHC) molecules, which are scanned by T cells with their T-cell receptor (TCR) to identify a possible infection. For a cell to present IAV peptides and activate T cells, it first has to become infected or take up IAV proteins. Due to this, T cells are not able to prevent infection, but can limit further spread by killing infected cells and recruiting other components of the immune system [93]. Two types of T cells are involved in this response: $CD4^+$ T cells and $CD8^+$ T cells. They recognize epitopes in the context of two different MHC proteins. $CD4^+$ T cells recognize epitopes presented on MHC class II (MHC-II) molecules, while $CD8^+$ T cells bind to MHC class I (MHC-I).

$CD4^+$ T cells have a wide range of effector functions. They can assist and drive B-cell and $CD8^+$ T-cell responses, thereby optimizing the immune responses to IAV infection (reviewed in [92]). For this reason, $CD4^+$ T cells are also called ‘helper T cells’.

Additionally, $CD4^+$ T cells can secrete inflammatory cytokines with which they steer and recruit other components of the immune system. $CD4^+$ T cells have also been shown to be cytolytic [94] – meaning they kill virus infected cells – but this is more the specialty of $CD8^+$ T cells. The $CD8^+$ T cell is also called 'cytotoxic T cell' for its role in the killing of infected cells. When an infected cell presents pathogen-derived epitopes via MHC-I, the $CD8^+$ T cell can initiate killing of the infected cell upon recognition of the epitope. $CD8^+$ T cells have multiple mechanism to achieve this [95]. Firstly, the $CD8^+$ T cell can induce apoptosis by direct cell-cell contact via CD95/CD95L (Fas/FasL), TRAIL/DR4 or DR5. Secondly, the $CD8^+$ T cell can secrete perforin and granzymes that cause membrane pore formation, which in turn can lead to apoptosis. Thirdly, inflammatory cytokines such as TNF and IFNγ can be secreted by activated $CD8^+$ T cells that enhance the inflammatory environment and can lead to (in)direct cell death. These pathways are partially redundant as $CD8^+$ T cells can still protect against IAV disease after removing one of these pathways [96].

Decades of research have shown that T cells can play a vital role in the protection against IAV. Evidence for this in humans is however largely restricted to associations and correlations. The unknown infection history of subjects and often uncontrolled environment results in experimental setups where the disease outcome is influenced by multiple factors. Despite these limitations, the accumulated research of the past decades convincingly illustrates the importance of T-cell immunity in the protection against heterosubtypic IAV infections in humans.

The Cleveland studies carried out during the H2N2 pandemic are probably one of the first documented indications that T cells can reduce IAV disease in humans. The investigators found that previous exposure to H1N1 influenza virus offered some protection against disease caused by the pandemic H2N2 influenza virus in 1957, which could not be explained by neutralizing antibodies [97, 98]. The authors could not investigate if T cells were involved, as T cells had not yet been discovered at that time [99, 100]. A controlled challenge study in 1983 provided additional evidence for the protective effect of T cells. McMichael and colleagues infected volunteers with H1N1 influenza virus and found that higher cytotoxic T-cell responses correlated with reduced viral shedding [101]. Later, the H1N1 pandemic of 2009 offered another rare chance to investigate the T-cell response in humans. T-cell epitopes were much more conserved than the B cell epitopes between the pandemic H1N1 virus (pH1N1) and the previous circulating H1N1 virus, indicating that pre-existing influenza-specific T-cell immunity might enhance protection against pH1N1 influenza virus [102]. In line with this, Sridhar *et al.* used the absence of neutralizing HA-antibodies against pH1N1 to show that high levels of pre-existing IAV-specific $CD8^+$ T cells correlated with decreased disease burden during the 2009 H1N1 pandemic [103]. Similarly, upon infection with the avian H7N9 influenza virus, $CD8^+$ T cells seemed to contribute to recovery of patients [104]. In a human IAV-challenge study where Wilkinson et al.

selected participants with low pre-existing antibody titers, they found that IAV-specific memory $CD4^+$ T cells were associated with lower viral shedding and reduced disease after H1N1 or H3N2 infection [105].

In the absence of (neutralizing) antibodies, T cells thus seem to reduce disease in IAV-infected patients. As mentioned above, T cells can recognize conserved epitopes, which enables them to respond to a wide range of influenza A viruses. This is illustrated by the observation that healthy human blood donors possessed $CD4^+$ and $CD8^+$ T-cell responses against H5N1 influenza virus [106]. These donors had no known exposure to H5N1, which is as expected since H5N1 strains are not circulating among humans. Similarly, others have shown that IAV-specific T cells from healthy blood donors cross-react with H7N9 influenza virus, even when these donors had never been exposed to H7N9 influenza virus [107]. This means that the T-cell responses observed against H5N1 and H7N9 were induced by infections with other IAV subtypes, likely either seasonal H1N1 or H3N2 influenza virus. Although this explanation is theoretically sound, it remains difficult to provide direct evidence that T cells induced by IAV infection can also protect against infection with other IAV subtypes in humans. For this reason, animal models have been – and will continue to be – instrumental in revealing the intricacies of T cells in IAV disease.

T cells in IAV – protection against heterosubtypic disease in animal models

Much of what we know regarding T cells and IAV originates from murine models. The large palette of techniques and reagents available for mice allows a more in-depth investigation of T-cell immunity. By using cell depletion, knock-out models, adoptive transfer experiments and T cells specific for single IAV epitopes, it has been shown that T cells are essential for increased survival and reduced disease upon (heterosubtypic) infection in the absence of (neutralizing) antibodies [108-116]. Depletion of $CD8^+$ and/or $CD4^+$ T cells in PR8-immunized (H1N1) mice reduced protection against a X31 (H3N2) infection [108], yielding strong evidence that T cells – and not antibodies – are essential for protection against heterosubtypic IAV infections. In line with this, transfer of IAV-specific $CD8^+$ effector T cells into naïve B cell-deficient mice increased survival after IAV infection [109]. Of note, $CD4^+$ T cell transfer only partially protected mice in this experiment, but others have shown an equally important role of $CD4^+$ and $CD8^+$ T cells. In one such experiment, IAV-immunized antibody-deficient mice ($Ig^{-/-}$) were protected against a heterosubtypic IAV infection, but not after depletion of either $CD4^+$ or $CD8^+$ T cells [110]. These findings are convincing evidence that – at least in the mouse model – T cells are crucial for protection against heterosubtypic IAV infections.

Until a few years ago, most studies focused on T-cell responses in the blood or spleen, because they are easily isolated and yield large numbers of lymphocytes. More

recently, scientists have also been investigating T cells residing in the respiratory tract, a subset called tissue-resident memory T (T_{RM}) cells. T_{RM} cells are a population of non-circulating memory T cells that reside in the tissue [117]. Due to their location – close to the possible site of infection – T_{RM} cells can rapidly respond to reinfections with pathogens by producing cytokines or killing infected cells. T_{RM} cells have been described in humans [118-122], but the difficulty of obtaining material limits an in-depth investigation of T_{RM} cells in humans. Most of our knowledge regarding the role of T_{RM} in influenza virus infection thus stems from experiments with animal models, predominantly mice.

Respiratory T_{RM} cells have been found to be essential for the protection against heterosubtypic IAV infections [111-113, 123-125]. Among others, the group of John Harty has shown that loss of respiratory T cells can result in reduced protection against heterosubtypic IAV infections [111-113]. Inversely, boosting of respiratory T cells enhanced protection. Unfortunately, lung-T_{RM} cells have a short half-life and regular boosting might be required to maintain a protective level of T_{RM} cells. In mice that were primed by a single IAV infection, lung-T_{RM} cell levels kept declining even though systemic memory T cells had long reached stable levels [113, 124]. This coincided with a loss of heterosubtypic immunity. Fortunately, repeated antigen boosting can extent the survival of $CD8^+$ lung-T_{RM} cells in mice [111]. This is also in agreement with the finding that donor-derived T_{RM} cells can be found back up to a year later in human recipients of a lung transfer [119]. Although more research is required to fully understand how and for which duration lung-T_{RM} cells are maintained, these findings indicate that repeated boosting contributes to the longevity of the lung T_{RM} response. It would be wise if during the development of IAV vaccines, the possible benefit of inducing T_{RM} cells in the respiratory tract is taken into account.

While the murine model has allowed us to unravel many of the mysteries surrounding T cells and their response to IAV, we should keep in mind that mice significantly differ from humans in many aspects. Mice are not a natural host for IAV and most IAV strains need to be adapted before they can infect mice [126]. Hence, findings in mice might be difficult to extrapolate to humans. This also means that mice are not suited for transmission studies as most wild-type (WT) IAV strains do not naturally infect mice and need to be adapted become infectious in mice. Even with adaptation of IAV strains, mice do not display the typical clinical symptoms of IAV infection. IAV-infected humans can suffer from fever, sneezing, coughing etc. Mice in contrast display hypothermia [127] and do not present nasal discharge or coughing [128]. In addition to the lack of IAV disease symptoms, mice are generally housed in a sterile environment to reduce environmental bias, which does not really model the human situation [129, 130]. These circumstances mean that the murine immune response towards an IAV infection is not easily translatable to the human situation.

Since mice have some inherent disadvantages when studying IAV, other animal models have been used. These include ferrets, guinea pigs, hamster, chickens, pigs, cats, dogs and non-human primates [128]. Among these, the ferret (*Mustela putorius furo*) is often regarded as the preferred model when studying IAV disease. IAV-infected ferrets develop human-like influenza disease and are highly susceptible to a wide range of influenza viruses, including human and avian IAV strains. The symptoms these strains induce in ferrets – fever, sneezing, coughing – are often similar to that of a human infection, including the lung pathology [128]. Ferrets are also specifically used to investigate the transmission of IAV strains as they can be an indication of how easily the virus will transmit between humans [13, 14, 73, 131-135]. As with all animal models, the ferret model also has its disadvantages. While ferrets are relatively low-cost compared to non-human primates, they are still significantly more expensive than mice which limits their use to labs with sufficient financial leeway. In addition, ferret-specific reagents are scarce compared to the murine model. However, recently new assays and reagents have been developed, which have improved the ability to measure cellular and humoral responses in the ferret model [136-138]. With this progress and the inherent benefits of the ferret model, it can be regarded as a very potent pre-clinical model for the further development and testing of new universal influenza virus vaccines.

As ferrets very well represent human influenza disease, new influenza virus vaccines are usually tested in the ferret-model before clinical trials are initiated. This includes IIV [139-144], LAIV [145-150], vector [151, 152], peptide [153], single replication cycle [154, 155], mRNA [72] and DNA vaccines [152, 156]. In the majority of these studies the vaccinated ferrets were naïve, meaning they had never been exposed to influenza virus infections before. This does not resemble the human population, of which the majority has already overcome several influenza virus infections. Therefore, a few research groups actually started pre-exposing ferrets to influenza viruses, followed by vaccination to evaluate the vaccine in an influenza virus-immune population [142, 148, 154]. Vaccination tended to be more effective in pre-exposed ferrets compared to naïve ferrets, which might be due to the induction of local immunity and/or T cells. Unfortunately, most ferret vaccination studies focus on antibody responses and neglect T-cell immunity. It is thus often unknown to which extent T cells contribute to the protection induced by vaccination in the ferret model.

While vaccination studies rarely report on T-cell immunity in ferrets, there are several publications that specifically investigated the role of T cells in protection against heterosubtypic IAV infections. Prior exposure to IAV – by either vaccination or infection – protected against a heterosubtypic IAV infection with H1N1 [155], H3N2 [157] or H5N1 [158-160]. In these experiments, ferrets displayed reduced weight loss, lower and shorter viral replication and less severe fever upon a heterosubtypic challenge if they were pre-immunized (e.g. by vaccination or infection). This protection was associated

with the induction of broadly-reactive T-cell responses [157-159]. No antibodies against HA of the challenge strain were detected by hemagglutination inhibition (HI) or virus neutralization (VN) assay, although this does not take into account the possible effect of antibodies against other IAV proteins. It remains challenging to completely distinguish between the contribution of cellular and humoral responses in the ferret model due to a lack of reagents and techniques. Hence, the pre-clinical development and validation of new influenza virus vaccines will ultimately depend on multiple animal models that complement each other.

How to improve influenza vaccines – switching vaccine formats

The induction of immune responses against (additional) conserved influenza virus proteins is essential for vaccines to offer better, broader and longer-lasting protection. This requires novel vaccine concepts that are capable of inducing broadly-reactive immune responses, including T-cell immunity. Traditional IIVs hardly induce cellular immunity because IIVs do not infect cells and proteins are not effectively presented to T cells. While LAIVs do not have this drawback as they can infect cells, they still do not perform much better than IIVs. This has driven the scientific community to investigate other vaccine formats for the induction of protective immune responses against influenza viruses.

One possibility to improve vaccine effectiveness is by optimizing existing LAIVs. The licensed LAIVs are typically based on the cold-adapted A/AnnArbor/6/1960 and A/Leningrad/134/17/57 strains, which circulated over 60 years ago. Due to antigenic drift, the backbone of these strains that contain the conserved T-cell epitopes might not accurately resemble the currently circulating influenza A viruses. To remedy this, Korenkov *et al*. updated the A/Leningrad/134/17/57 strain by replacing the original NP-sequence with a NP-sequence of a more recent isolate [161]. Although overall not much difference in the protection induced by original and updated LAIVs was detected in ferret experiments [149, 150], this line of investigation might be promising for the improvement of LAIVs.

Beside improving existing influenza virus vaccines, another option would be to use a different vaccine platform to deliver influenza virus antigens. Vector vaccines are based on other viruses (vectors) that are genetically engineered to display influenza virus antigens to the immune system. Vectors are usually attenuated, meaning that they do infect cells but their replication is reduced or even completely defective [162]. This makes vector vaccines relatively safe, while still inducing potent humoral and cellular immune responses. In this aspect, vector vaccines are relatively similar to LAIVs. The additional benefits of vector vaccines are that they can be produced in high concentrations and are not hampered by pre-existing influenza virus antibodies that prevent delivery of the antigen. Unfortunately, HA-expressing vectors suffer from

the same disadvantages as traditional vaccines: the induced antibody response is limited to specific influenza virus strains – or in the best case – a single influenza virus subtype. For this reason, vectors have also been made to express NA, NP, M1, M2, PB2 or a combination of these proteins (reviewed in [162]). These vector vaccines showed mixed results, with some inducing heterosubtypic immunity in one animal model, but not in others.

Some groups have also investigated peptide vaccines as a way to induce immune responses against conserved epitopes. Upon infection or vaccination, the majority of antibody responses are targeting immunodominant, but non-conserved epitopes in the head-domain of HA. In contrast, conserved epitopes are often less immunogenic, as is the case of M2e and HA-stalk. Peptide vaccines seek to mitigate this by limiting the available targets to a few selected, highly conserved peptides. These peptides can contain both T and B cell epitopes (reviewed in [163]). Although the immune response against these peptides might be immunosubdominant under normal conditions, by presenting only a few selected epitopes in combination with adjuvants, the induced immune response is no longer overtaken by responses against non-conserved immunodominant epitopes. Additionally, peptide sequences can be slightly altered to enhance uptake and binding to MHC molecules, thereby further strengthening the immune response [164]. The advantages of peptide vaccination are however also their disadvantage. By including only a few immunosubdominant epitopes, the induced immune response is also limited in its magnitude and breadth. It is thus not surprising that most studies show only a modest effect of peptide vaccination in mice and ferrets [153, 165-167].

Another class of potential vaccine concepts are based on direct delivery of genetic material in the form of DNA or RNA (reviewed in [168, 169]). The genetic material – coding for one or more proteins – is taken up by cells after which they express the protein of interest. This can effectively induce both humoral and cellular immune responses. DNA/RNA-based vaccines are not only relevant for a universal vaccine, but also for seasonal influenza virus vaccinations as they can be rapidly adapted to changes in the circulating viruses. Whereas it takes approximately 6 months from strain identification to vaccination for IIVs, DNA/RNA vaccines can be produced (and administered) much more rapidly. Pre-clinical models have already shown that the DNA/RNA-based vaccine platform is very promising for future influenza virus vaccines. Vaccination with DNA plasmids coding for NP, M1, M2 or PB1 (or a combination) induced potent humoral and cellular responses that protected against heterosubtypic infections in mice [152, 170], ferrets [152] and non-human primates [171]. Similarly, RNA-vaccines have been shown to protect against homosubtypic and heterosubtypic influenza virus infections [172-174] and multiple HA-encoding mRNA vaccines have recently entered clinical trials [175]. In addition, the rapid development and production of mRNA-based SARS-CoV-2 vaccines during the pandemic has

demonstrated the potential of RNA-based vaccines. These vaccines have been shown to induce robust humoral and cellular immune responses [176-180] and RNA-based vaccines are therefore an interesting vaccine concept for future influenza virus vaccines.

Besides the vaccine format, one should also take into account the administration route. Most vaccines are administered i.m. or intra dermal (i.d.), which primarily induces local immune responses at the site of administration. For respiratory viruses such as influenza virus however, it can be beneficial to specifically induce immune responses in the respiratory tract, including T_{RM} cells. The close distance between the site of infection and vaccine-induced immunity allows the host's immune system to rapidly respond upon encountering new infections. LAIVs and vector vaccines can already be administered i.n. and ongoing innovations might also allow other vaccine formats to do so.

Aim and scope of this thesis

The threat posed by IAV necessitates the development of new and improved influenza virus vaccines. T-cell immunity – which is not sufficiently induced by traditional IIVs – can be essential to improve vaccine effectiveness. While HA-antibodies are very strain-specific, T-cell immunity spans across influenza virus subtypes, thereby offering protection against heterosubtypic infections. However, future T-cell inducing vaccines need to be pre-clinically evaluated, which requires relevant animal models to measure both IAV pathogenesis and adaptive immunity. Mice are not entirely suited for this purpose, as they do not mimic the human influenza disease. In this regard, the ferret model is very promising, but much is still unknown regarding T-cell immunity in ferrets. In this thesis, we aim to remedy this knowledge gap. More specifically, we set-out to describe (respiratory) T-cell immunity against IAV in the ferret model and how this can be used to protect against disease caused by heterosubtypic IAV infections.

In **Chapter 2**, we describe how to set-up an infection model for H2N2 influenza virus in ferrets. H2N2 influenza virus started circulating in the human population in 1957, but was replaced by the H3N2 subtype in 1968. Since H2N2 influenza virus has infected humans before and H2-based influenza viruses are still present in avian reservoirs, there is a risk that H2N2 influenza virus will be reintroduced into the human population. In order to prepare for such an event and to accommodate the development and testing of vaccines, we developed a ferret model for H2N2 influenza virus infection. We investigated if virus replication and pathology in ferrets differed between inoculation routes (intranasal vs intratracheal) and between H2N2 virus isolates with different HA receptor binding affinities.

With the knowledge we gained in Chapter 2, we set-out to investigate the cross-reactive T-cell response after IAV infection in the ferret model in **Chapter 3**. Previously, not much was known about T-cell immunity in the ferret model and most studies are limited to analysis of lymphocytes derived from blood and spleen. We aimed to change this by measuring T-cell responses in the lung, nasal turbinates and bronchoalveolar lavage fluid after H2N2 influenza virus infection in naïve and H1N1 influenza-exposed ferrets. We also investigated if ferrets that were previously infected with H1N1 influenza virus developed broadly-reactive T-cell responses and if this lead to better protection against H2N2-induced disease.

Next, we wondered if the protection offered by broadly-reactive T-cell responses could be induced and enhanced by vaccination. In **Chapter 4**, we evaluated a new mRNA-based T-cell vaccine that encodes conserved internal proteins of H1N1 influenza virus. To mimic the human situation, we evaluated the vaccine in both naïve and influenza-experienced ferrets. We placed additional focus on T-cell immunity in the respiratory tract since the vaccine is administered i.m. and it is unknown if this vaccination route can induce or boost T-cell immunity in the respiratory tract. Most importantly, we evaluated the protective effect of vaccination by challenging ferrets with a heterosubtypic avian H7N9 influenza virus challenge.

In response to the SARS-CoV-2 pandemic, we utilized our experience to set-up a ferret model that could be utilized to evaluate SARS-CoV-2 vaccines in **Chapter 5**. In humans, hospitalization and mortality increases with age and is higher for males than females [181-185]. Furthermore, we know from influenza research that disease in the ferret model is dependent on the route of inoculation, with lower respiratory tract infection tending to lead to more severe disease [145, 186, 187]. Based on this knowledge, we studied if age and infection route could affect SARS-CoV-2 induced disease in the ferret model by infecting young and adult male ferrets via intranasal or intratracheal inoculation with SARS-CoV-2.

Finally, in **Chapter 6** we summarize and discuss our findings in the context of other published research. We also elaborate on future perspectives and describe what is required for a future universal influenza virus vaccine to offer protection against all influenza viruses.

References

1. Pappas, G., I.J. Kiriaze, and M.E. Falagas, *Insights into infectious disease in the era of Hippocrates.* Int J Infect Dis, 2008. **12**(4): p. 347-50.
2. Martin, P.M. and E. Martin-Granel, *2,500-year evolution of the term epidemic.* Emerg Infect Dis, 2006. **12**(6): p. 976-80.
3. *Etymologia: influenza.* Emerging Infectious Diseases, 2006. **12**(1): p. 179-179.
4. Smith, W., C.H. Andrewes, and P.P. Laidlaw, *A Virus Obtained from Influenza Patients.* The Lancet, 1933. **222**(5732): p. 66-68.
5. Wright, P.F., G. Neumann, and Y. Kawaoka, *Orthomyxoviruses*, in *Fields Virology*, D.M. Knipe and P.M. Howley, Editors. 2013, Wolters Kluwer Health/Lippincott Williams & Wilkins: Philadelphia.
6. Asha, K. and B. Kumar, *Emerging Influenza D Virus Threat: What We Know so Far!* J Clin Med, 2019. **8**(2).
7. Iuliano, A.D., et al., *Estimates of global seasonal influenza-associated respiratory mortality: a modelling study.* Lancet, 2018. **391**(10127): p. 1285-1300.
8. WHO, *A revision of the system of nomenclature for influenza viruses: a WHO memorandum.* Bull World Health Organ, 1980. **58**(4): p. 585-91.
9. Kosik, I. and J.W. Yewdell, *Influenza Hemagglutinin and Neuraminidase: Yin(-)Yang Proteins Coevolving to Thwart Immunity.* Viruses, 2019. **11**(4).
10. Krammer, F., et al., *Influenza.* Nat Rev Dis Primers, 2018. **4**(1): p. 3.
11. Kessler, S., et al., *Influenza A Viruses and Zoonotic Events-Are We Creating Our Own Reservoirs?* Viruses, 2021. **13**(11).
12. Mostafa, A., et al., *Zoonotic Potential of Influenza A Viruses: A Comprehensive Overview.* Viruses, 2018. **10**(9).
13. Herfst, S., et al., *Airborne transmission of influenza A/H5N1 virus between ferrets.* Science, 2012. **336**(6088): p. 1534-41.
14. Imai, M., et al., *Experimental adaptation of an influenza H5 HA confers respiratory droplet transmission to a reassortant H5 HA/H1N1 virus in ferrets.* Nature, 2012. **486**(7403): p. 420-8.
15. Nobusawa, E. and K. Sato, *Comparison of the mutation rates of human influenza A and B viruses.* J Virol, 2006. **80**(7): p. 3675-8.
16. Wong, K.K., et al., *Correlation of polymerase replication fidelity with genetic evolution of influenza A/Fujian/411/02(H3N2) viruses.* J Med Virol, 2011. **83**(3): p. 510-6.
17. Pauly, M.D., M.C. Procario, and A.S. Lauring, *A novel twelve class fluctuation test reveals higher than expected mutation rates for influenza A viruses.* Elife, 2017. **6**.
18. te Velthuis, A.J.W. and E. Fodor, *Influenza virus RNA polymerase: insights into the mechanisms of viral RNA synthesis.* Nature Reviews Microbiology, 2016. **14**: p. 479-493.
19. Altman, M.O., D. Angeletti, and J.W. Yewdell, *Antibody Immunodominance: The Key to Understanding Influenza Virus Antigenic Drift.* Viral Immunol, 2018. **31**(2): p. 142-149.
20. Heiny, A.T., et al., *Evolutionarily conserved protein sequences of influenza a viruses, avian and human, as vaccine targets.* PLoS One, 2007. **2**(11): p. e1190.
21. Wu, N.C. and I.A. Wilson, *A Perspective on the Structural and Functional Constraints for Immune Evasion: Insights from Influenza Virus.* J Mol Biol, 2017. **429**(17): p. 2694-2709.
22. Okoli, G.N., et al., *Variable seasonal influenza vaccine effectiveness across geographical regions, age groups and levels of vaccine antigenic similarity with circulating virus strains: A systematic review and meta-analysis of the evidence from test-negative design studies after the 2009/10 influenza pandemic.* Vaccine, 2021. **39**(8): p. 1225-1240.
23. Skowronski, D.M., et al., *Influenza vaccine effectiveness by A(H3N2) phylogenetic sub-cluster and prior vaccination history: 2016-17 and 2017-18 epidemics in Canada.* J Infect Dis, 2020.

24. Zimmerman, R.K., et al., *2014-2015 Influenza Vaccine Effectiveness in the United States by Vaccine Type.* Clin Infect Dis, 2016. **63**(12): p. 1564-1573.
25. Garten, R.J., et al., *Antigenic and genetic characteristics of swine-origin 2009 A(H1N1) influenza viruses circulating in humans.* Science, 2009. **325**(5937): p. 197-201.
26. Smith, G.J.D., et al., *Origins and evolutionary genomics of the 2009 swine-origin H1N1 influenza A epidemic.* Nature, 2009. **459**: p. 1122-1125.
27. Scholtissek, C., et al., *On the origin of the human influenza virus subtypes H2N2 and H3N2.* Virology, 1978. **87**(1): p. 13-20.
28. Kawaoka, Y., S. Krauss, and R.G. Webster, *Avian-to-human transmission of the PB1 gene of influenza A viruses in the 1957 and 1968 pandemics.* J Virol, 1989. **63**(11): p. 4603-8.
29. Schafer, J.R., et al., *Origin of the pandemic 1957 H2 influenza A virus and the persistence of its possible progenitors in the avian reservoir.* Virology, 1993. **194**(2): p. 781-8.
30. Taubenberger, J.K. and D.M. Morens, *Influenza: the once and future pandemic.* Public Health Rep, 2010. **125 Suppl 3**: p. 16-26.
31. Krug, R.M., et al., *Intracellular warfare between human influenza viruses and human cells: the roles of the viral NS1 protein.* Virology, 2003. **309**(2): p. 181-189.
32. Hale, B.G., et al., *The multifunctional NS1 protein of influenza A viruses.* J Gen Virol, 2008. **89**(Pt 10): p. 2359-2376.
33. O'Neill, R.E., J. Talon, and P. Palese, *The influenza virus NEP (NS2 protein) mediates the nuclear export of viral ribonucleoproteins.* EMBO J, 1998. **17**(1): p. 288-96.
34. Paterson, D. and E. Fodor, *Emerging roles for the influenza A virus nuclear export protein (NEP).* PLoS Pathog, 2012. **8**(12): p. e1003019.
35. Killingley, B. and J. Nguyen-Van-Tam, *Routes of influenza transmission.* Influenza Other Respir Viruses, 2013. **7 Suppl 2**: p. 42-51.
36. Cohen, M., et al., *Influenza A penetrates host mucus by cleaving sialic acids with neuraminidase.* Virol J, 2013. **10**: p. 321.
37. Weis, W., et al., *Structure of the influenza virus haemagglutinin complexed with its receptor, sialic acid.* Nature, 1988. **333**(6172): p. 426-31.
38. Barberis, I., et al., *History and evolution of influenza control through vaccination: from the first monovalent vaccine to universal vaccines.* Journal of preventive medicine and hygiene, 2016. **57**(3): p. E115-E120.
39. Huber, V.C., *Influenza vaccines: from whole virus preparations to recombinant protein technology.* Expert Rev Vaccines, 2014. **13**(1): p. 31-42.
40. Parkman, P.D., et al., *Summary of clinical trials of influenza virus vaccines in adults.* J Infect Dis, 1977. **136 Suppl**: p. S722-30.
41. Gerdil, C., *The annual production cycle for influenza vaccine.* Vaccine, 2003. **21**(16): p. 1776-1779.
42. Trombetta, C.M., et al., *Challenges in the development of egg-independent vaccines for influenza.* Expert Rev Vaccines, 2019. **18**(7): p. 737-750.
43. Krammer, F. and P. Palese, *Advances in the development of influenza virus vaccines.* Nat Rev Drug Discov, 2015. **14**(3): p. 167-82.
44. Alexandrova GI and S. AA., *Obtaining of an additionally attenuated vaccinating cryophilic influenza strain.* Revue Roumaine d'Inframicrobiologie, 1965. **2**: p. 179-186.
45. Maassab, H.F., *Adaptation and growth characteristics of influenza virus at 25 degrees c.* Nature, 1967. **213**(5076): p. 612-4.
46. Alexandrova, G.I., et al., *Study of live recombinant cold-adapted influenza bivalent vaccine of type A for use in children: an epidemiological control trial.* Vaccine, 1986. **4**(2): p. 114-118.
47. Belshe, R.B., et al., *Safety, efficacy, and effectiveness of live, attenuated, cold-adapted influenza vaccine in an indicated population aged 5-49 years.* Clin Infect Dis, 2004. **39**(7): p. 920-7.

48. Treanor, J., *History of Live, Attenuated Influenza Vaccine.* J Pediatric Infect Dis Soc, 2020. **9**(Supplement_1): p. S3-S9.
49. Agency, E.M., *Fluenz: EPAR - Public assessment report*. 2011: London. p. 85.
50. Mohn, K.G., et al., *Live Attenuated Influenza Vaccine in Children Induces B-Cell Responses in Tonsils.* J Infect Dis, 2016. **214**(5): p. 722-31.
51. Clements, M.L. and B.R. Murphy, *Development and persistence of local and systemic antibody responses in adults given live attenuated or inactivated influenza A virus vaccine.* J Clin Microbiol, 1986. **23**(1): p. 66-72.
52. Gustin, K.M., et al., *Comparative immunogenicity and cross-clade protective efficacy of mammalian cell-grown inactivated and live attenuated H5N1 reassortant vaccines in ferrets.* J Infect Dis, 2011. **204**(10): p. 1491-9.
53. Hoft, D.F., et al., *Live and Inactivated Influenza Vaccines Induce Similar Humoral Responses, but Only Live Vaccines Induce Diverse T-Cell Responses in Young Children.* The Journal of Infectious Diseases, 2011. **204**(6): p. 845-853.
54. Chung, J.R., et al., *Live Attenuated and Inactivated Influenza Vaccine Effectiveness.* Pediatrics, 2019. **143**(2).
55. Monto, A.S., et al., *Comparative efficacy of inactivated and live attenuated influenza vaccines.* N Engl J Med, 2009. **361**(13): p. 1260-7.
56. Fleming, D.M., et al., *Comparison of the efficacy and safety of live attenuated cold-adapted influenza vaccine, trivalent, with trivalent inactivated influenza virus vaccine in children and adolescents with asthma.* Pediatr Infect Dis J, 2006. **25**(10): p. 860-9.
57. DiazGranados, C.A., M. Denis, and S. Plotkin, *Seasonal influenza vaccine efficacy and its determinants in children and non-elderly adults: a systematic review with meta-analyses of controlled trials.* Vaccine, 2012. **31**(1): p. 49-57.
58. Gilbert, P.B., et al., *HAI and NAI titer correlates of inactivated and live attenuated influenza vaccine efficacy.* BMC Infect Dis, 2019. **19**(1): p. 453.
59. Krishnan, A., et al., *Efficacy of live attenuated and inactivated influenza vaccines among children in rural India: A 2-year, randomized, triple-blind, placebo-controlled trial.* PLoS Med, 2021. **18**(4): p. e1003609.
60. Environment, D.I.f.P.H.a.t. *Achtergrondinformatie griepprik*. 2021 21-10-2021 25-10-2021]; Available from: https://www.rivm.nl/griep-griepprik/griepprik/nationaal-programma-griep preventie.
61. Environment, D.I.f.P.H.a.t. *Influenzavaccinatie buiten het NPG*. 2019 29-9-2021 25-10-2021]; Available from: https://lci.rivm.nl/richtlijnen/influenzavaccinatie-buiten-het-npg#2-geregistreerde-vaccins.
62. Yamayoshi, S. and Y. Kawaoka, *Current and future influenza vaccines.* Nat Med, 2019. **25**(2): p. 212-220.
63. Klasse, P.J., *Neutralization of Virus Infectivity by Antibodies: Old Problems in New Perspectives.* Adv Biol, 2014. **2014**.
64. Padilla-Quirarte, H.O., et al., *Protective Antibodies Against Influenza Proteins.* Front Immunol, 2019. **10**: p. 1677.
65. Sicca, F., S. Neppelenbroek, and A. Huckriede, *Effector mechanisms of influenza-specific antibodies: neutralization and beyond.* Expert Rev Vaccines, 2018. **17**(9): p. 785-795.
66. Ellebedy, A.H., et al., *Induction of broadly cross-reactive antibody responses to the influenza HA stem region following H5N1 vaccination in humans.* Proc Natl Acad Sci U S A, 2014. **111**(36): p. 13133-8.
67. Andrews, S.F., et al., *Immune history profoundly affects broadly protective B cell responses to influenza.* Sci Transl Med, 2015. **7**(316): p. 316ra192.
68. Margine, I., et al., *H3N2 influenza virus infection induces broadly reactive hemagglutinin stalk antibodies in humans and mice.* J Virol, 2013. **87**(8): p. 4728-37.

69. Sui, J., et al., *Wide prevalence of heterosubtypic broadly neutralizing human anti-influenza A antibodies.* Clin Infect Dis, 2011. **52**(8): p. 1003-9.
70. Bullard, B.L. and E.A. Weaver, *Strategies Targeting Hemagglutinin as a Universal Influenza Vaccine.* Vaccines (Basel), 2021. **9**(3).
71. Liu, W.C., et al., *Sequential Immunization With Live-Attenuated Chimeric Hemagglutinin-Based Vaccines Confers Heterosubtypic Immunity Against Influenza A Viruses in a Preclinical Ferret Model.* Front Immunol, 2019. **10**: p. 756.
72. Pardi, N., et al., *Nucleoside-modified mRNA immunization elicits influenza virus hemagglutinin stalk-specific antibodies.* Nat Commun, 2018. **9**(1): p. 3361.
73. Nachbagauer, R., et al., *Hemagglutinin Stalk Immunity Reduces Influenza Virus Replication and Transmission in Ferrets.* J Virol, 2015. **90**(6): p. 3268-73.
74. Krammer, F., et al., *Assessment of influenza virus hemagglutinin stalk-based immunity in ferrets.* J Virol, 2014. **88**(6): p. 3432-42.
75. Krammer, F., et al., *H3 stalk-based chimeric hemagglutinin influenza virus constructs protect mice from H7N9 challenge.* J Virol, 2014. **88**(4): p. 2340-3.
76. Nachbagauer, R., et al., *A chimeric hemagglutinin-based universal influenza virus vaccine approach induces broad and long-lasting immunity in a randomized, placebo-controlled phase I trial.* Nat Med, 2021. **27**(1): p. 106-114.
77. Sui, J., et al., *Structural and functional bases for broad-spectrum neutralization of avian and human influenza A viruses.* Nat Struct Mol Biol, 2009. **16**(3): p. 265-73.
78. Leon, P.E., et al., *Optimal activation of Fc-mediated effector functions by influenza virus hemagglutinin antibodies requires two points of contact.* Proc Natl Acad Sci U S A, 2016. **113**(40): p. E5944-E5951.
79. Terajima, M., et al., *Complement-dependent lysis of influenza a virus-infected cells by broadly cross-reactive human monoclonal antibodies.* J Virol, 2011. **85**(24): p. 13463-7.
80. Mullarkey, C.E., et al., *Broadly Neutralizing Hemagglutinin Stalk-Specific Antibodies Induce Potent Phagocytosis of Immune Complexes by Neutrophils in an Fc-Dependent Manner.* mBio, 2016. **7**(5).
81. Henry Dunand, C.J., et al., *Both Neutralizing and Non-Neutralizing Human H7N9 Influenza Vaccine-Induced Monoclonal Antibodies Confer Protection.* Cell Host Microbe, 2016. **19**(6): p. 800-13.
82. DiLillo, D.J., et al., *Broadly neutralizing hemagglutinin stalk-specific antibodies require FcgammaR interactions for protection against influenza virus in vivo.* Nat Med, 2014. **20**(2): p. 143-51.
83. Krammer, F., *The human antibody response to influenza A virus infection and vaccination.* Nat Rev Immunol, 2019.
84. Krammer, F., et al., *NAction! How Can Neuraminidase-Based Immunity Contribute to Better Influenza Virus Vaccines?* mBio, 2018. **9**(2).
85. Murphy, B.R., J.A. Kasel, and R.M. Chanock, *Association of Serum Anti-Neuraminidase Antibody with Resistance to Influenza in Man.* New England Journal of Medicine, 1972. **286**(25): p. 1329-1332.
86. Tompkins, S.M., et al., *Matrix protein 2 vaccination and protection against influenza viruses, including subtype H5N1.* Emerg Infect Dis, 2007. **13**(3): p. 426-35.
87. Mytle, N., et al., *Influenza Antigens NP and M2 Confer Cross Protection to BALB/c Mice against Lethal Challenge with H1N1, Pandemic H1N1 or H5N1 Influenza A Viruses.* Viruses, 2021. **13**(9).
88. Jegaskanda, S., et al., *Induction of H7N9-Cross-Reactive Antibody-Dependent Cellular Cytotoxicity Antibodies by Human Seasonal Influenza A Viruses that are Directed Toward the Nucleoprotein.* J Infect Dis, 2017. **215**(5): p. 818-823.

89. Vanderven, H.A., et al., *What Lies Beneath: Antibody Dependent Natural Killer Cell Activation by Antibodies to Internal Influenza Virus Proteins.* EBioMedicine, 2016. **8**: p. 277-290.
90. Carragher, D.M., et al., *A novel role for non-neutralizing antibodies against nucleoprotein in facilitating resistance to influenza virus.* J Immunol, 2008. **181**(6): p. 4168-76.
91. LaMere, M.W., et al., *Contributions of antinucleoprotein IgG to heterosubtypic immunity against influenza virus.* J Immunol, 2011. **186**(7): p. 4331-9.
92. Murphy, K., C. Weaver, and C. Janeway, *Janeway's immunobiology*. 9th ed. 2017.
93. Jansen, J.M., et al., *Influenza virus-specific CD4+ and CD8+ T cell-mediated immunity induced by infection and vaccination.* J Clin Virol, 2019. **119**: p. 44-52.
94. Brown, D.M., A.T. Lampe, and A.M. Workman, *The Differentiation and Protective Function of Cytolytic CD4 T Cells in Influenza Infection.* Front Immunol, 2016. **7**: p. 93.
95. Schmidt, M.E. and S.M. Varga, *The CD8 T Cell Response to Respiratory Virus Infections.* Front Immunol, 2018. **9**: p. 678.
96. Hamada, H., et al., *Multiple redundant effector mechanisms of CD8+ T cells protect against influenza infection.* J Immunol, 2013. **190**(1): p. 296-306.
97. Jordan, W.S., Jr., et al., *A study of illness in a group of Cleveland families. XVII. The occurrence of Asian influenza.* Am J Hyg, 1958. **68**(2): p. 190-212.
98. Epstein, S.L., *Prior H1N1 influenza infection and susceptibility of Cleveland Family Study participants during the H2N2 pandemic of 1957: an experiment of nature.* J Infect Dis, 2006. **193**(1): p. 49-53.
99. Miller, J.F. and G.F. Mitchell, *Cell to cell interaction in the immune response. I. Hemolysin-forming cells in neonatally thymectomized mice reconstituted with thymus or thoracic duct lymphocytes.* J Exp Med, 1968. **128**(4): p. 801-20.
100. Roitt, I.M., et al., *The Cellular Basis of Immunological Responses.* The Lancet, 1969. **294**(7616): p. 367-371.
101. McMichael, A.J., et al., *Cytotoxic T-cell immunity to influenza.* N Engl J Med, 1983. **309**(1): p. 13-7.
102. Greenbaum, J.A., et al., *Pre-existing immunity against swine-origin H1N1 influenza viruses in the general human population.* Proc Natl Acad Sci U S A, 2009. **106**(48): p. 20365-70.
103. Sridhar, S., et al., *Cellular immune correlates of protection against symptomatic pandemic influenza.* Nat Med, 2013. **19**(10): p. 1305-12.
104. Wang, Z., et al., *Recovery from severe H7N9 disease is associated with diverse response mechanisms dominated by CD8(+) T cells.* Nat Commun, 2015. **6**: p. 6833.
105. Wilkinson, T.M., et al., *Preexisting influenza-specific CD4+ T cells correlate with disease protection against influenza challenge in humans.* Nat Med, 2012. **18**(2): p. 274-80.
106. Lee, L.Y., et al., *Memory T cells established by seasonal human influenza A infection cross-react with avian influenza A (H5N1) in healthy individuals.* J Clin Invest, 2008. **118**(10): p. 3478-90.
107. van de Sandt, C.E., et al., *Human cytotoxic T lymphocytes directed to seasonal influenza A viruses cross-react with the newly emerging H7N9 virus.* J Virol, 2014. **88**(3): p. 1684-93.
108. Liang, S., et al., *Heterosubtypic immunity to influenza type A virus in mice. Effector mechanisms and their longevity.* The Journal of Immunology, 1994. **152**(4): p. 1653.
109. Graham, M.B. and T.J. Braciale, *Resistance to and Recovery from Lethal Influenza Virus Infection in B Lymphocyte–deficient Mice.* The Journal of Experimental Medicine, 1997. **186**(12): p. 2063.
110. Benton, K.A., et al., *Heterosubtypic immunity to influenza A virus in mice lacking IgA, all Ig, NKT cells, or gamma delta T cells.* J Immunol, 2001. **166**(12): p. 7437-45.
111. Van Braeckel-Budimir, N., et al., *Repeated Antigen Exposure Extends the Durability of Influenza-Specific Lung-Resident Memory CD8(+) T Cells and Heterosubtypic Immunity.* Cell Rep, 2018. **24**(13): p. 3374-3382 e3.

112. Slütter, B., et al., *Lung airway-surveilling CXCR3(hi) memory CD8(+) T cells are critical for protection against influenza A virus.* Immunity, 2013. **39**(5): p. 939-48.
113. Slütter, B., et al., *Dynamics of influenza-induced lung-resident memory T cells underlie waning heterosubtypic immunity.* Sci Immunol, 2017. **2**(7).
114. Dong, W., et al., *Cross-Protective Immune Responses Induced by Sequential Influenza Virus Infection and by Sequential Vaccination With Inactivated Influenza Vaccines.* Front Immunol, 2018. **9**: p. 2312.
115. Eickhoff, C.S., et al., *Highly conserved influenza T cell epitopes induce broadly protective immunity.* Vaccine, 2019. **37**(36): p. 5371-5381.
116. McKinstry, K.K., et al., *Memory CD4+ T cells protect against influenza through multiple synergizing mechanisms.* J Clin Invest, 2012. **122**(8): p. 2847-56.
117. Rosato, P.C., L.K. Beura, and D. Masopust, *Tissue resident memory T cells and viral immunity.* Curr Opin Virol, 2017. **22**: p. 44-50.
118. de Bree, G.J., et al., *Selective accumulation of differentiated CD8+ T cells specific for respiratory viruses in the human lung.* J Exp Med, 2005. **202**(10): p. 1433-42.
119. Snyder, M.E., et al., *Generation and persistence of human tissue-resident memory T cells in lung transplantation.* Sci Immunol, 2019. **4**(33).
120. Pizzolla, A., et al., *Influenza-specific lung-resident memory T cells are proliferative and polyfunctional and maintain diverse TCR profiles.* J Clin Invest, 2018. **128**(2): p. 721-733.
121. Hombrink, P., et al., *Programs for the persistence, vigilance and control of human CD8(+) lung-resident memory T cells.* Nat Immunol, 2016. **17**(12): p. 1467-1478.
122. Thome, J.J., et al., *Spatial map of human T cell compartmentalization and maintenance over decades of life.* Cell, 2014. **159**(4): p. 814-28.
123. Pizzolla, A., et al., *Resident memory CD8(+) T cells in the upper respiratory tract prevent pulmonary influenza virus infection.* Sci Immunol, 2017. **2**(12).
124. Wu, T., et al., *Lung-resident memory CD8 T cells (TRM) are indispensable for optimal cross-protection against pulmonary virus infection.* J Leukoc Biol, 2014. **95**(2): p. 215-24.
125. Zens, K.D., J.K. Chen, and D.L. Farber, *Vaccine-generated lung tissue–resident memory T cells provide heterosubtypic protection to influenza infection.* JCI Insight, 2016. **1**.
126. Bouvier, N.M. and A.C. Lowen, *Animal Models for Influenza Virus Pathogenesis and Transmission.* Viruses, 2010. **2**: p. 1530-1563.
127. Yang, Y.T. and C.A. Evans, *Hypothermia in mice due to influenza virus infection.* Proc Soc Exp Biol Med, 1961. **108**: p. 776-80.
128. Nguyen, T.Q., R. Rollon, and Y.K. Choi, *Animal Models for Influenza Research: Strengths and Weaknesses.* Viruses, 2021. **13**(6).
129. Rosshart, S.P., et al., *Wild Mouse Gut Microbiota Promotes Host Fitness and Improves Disease Resistance.* Cell, 2017. **171**(5): p. 1015-1028 e13.
130. Rosshart, S.P., et al., *Laboratory mice born to wild mice have natural microbiota and model human immune responses.* Science, 2019. **365**(6452).
131. Buhnerkempe, M.G., et al., *Mapping influenza transmission in the ferret model to transmission in humans.* Elife, 2015. **4**.
132. Frise, R., et al., *Contact transmission of influenza virus between ferrets imposes a looser bottleneck than respiratory droplet transmission allowing propagation of antiviral resistance.* Scientific Reports, 2016. **6**.
133. Karlsson, E.A., et al., *Visualizing real-time influenza virus infection, transmission and protection in ferrets.* Nat Commun, 2015. **6**: p. 6378.
134. Oh, D.Y., et al., *Evaluation of oseltamivir prophylaxis regimens for reducing influenza virus infection, transmission and disease severity in a ferret model of household contact.* J Antimicrob Chemother, 2014. **69**(9): p. 2458-69.

135. Pappas, C., et al., *Assessment of transmission, pathogenesis and adaptation of H2 subtype influenza viruses in ferrets.* Virology, 2015. **477**: p. 61-71.
136. Rutigliano, J.A., et al., *Screening monoclonal antibodies for cross-reactivity in the ferret model of influenza infection.* Journal of immunological methods, 2008. **336**: p. 71-7.
137. Music, N., et al., *Influenza vaccination accelerates recovery of ferrets from lymphopenia.* PLoS One, 2014. **9**(6): p. e100926.
138. DiPiazza, A., et al., *Flow Cytometric and Cytokine ELISpot Approaches To Characterize the Cell-Mediated Immune Response in Ferrets following Influenza Virus Infection.* J Virol, 2016. **90**(17): p. 7991-8004.
139. Govorkova, E.A., et al., *Immunization with reverse-genetics-produced H5N1 influenza vaccine protects ferrets against homologous and heterologous challenge.* J Infect Dis, 2006. **194**(2): p. 159-67.
140. Baras, B., et al., *Cross-protection against lethal H5N1 challenge in ferrets with an adjuvanted pandemic influenza vaccine.* PLoS One, 2008. **3**(1): p. e1401.
141. de Jonge, J., et al., *H7N9 influenza split vaccine with SWE oil-in-water adjuvant greatly enhances cross-reactive humoral immunity and protection against severe pneumonia in ferrets.* NPJ Vaccines, 2020. **5**(1): p. 38.
142. Reneer, Z.B., et al., *Broadly Reactive H2 Hemagglutinin Vaccines Elicit Cross-Reactive Antibodies in Ferrets Preimmune to Seasonal Influenza A Viruses.* mSphere, 2021. **6**(2).
143. Stadlbauer, D., et al., *AS03-adjuvanted H7N9 inactivated split virion vaccines induce cross-reactive and protective responses in ferrets.* NPJ Vaccines, 2021. **6**(1): p. 40.
144. Bodewes, R., et al., *A single immunization with CoVaccine HT-adjuvanted H5N1 influenza virus vaccine induces protective cellular and humoral immune responses in ferrets.* J Virol, 2010. **84**(16): p. 7943-52.
145. de Jonge, J., et al., *H7N9 Live Attenuated Influenza Vaccine Is Highly Immunogenic, Prevents Virus Replication, and Protects Against Severe Bronchopneumonia in Ferrets.* Mol Ther, 2016. **24**(5): p. 991-1002.
146. Yeolekar, L.R., et al., *Immunogenicity and efficacy comparison of MDCK cell-based and egg-based live attenuated influenza vaccines of H5 and H7 subtypes in ferrets.* Vaccine, 2020. **38**(40): p. 6280-6290.
147. Dibben, O., et al., *Defining the root cause of reduced H1N1 live attenuated influenza vaccine effectiveness: low viral fitness leads to inter-strain competition.* NPJ Vaccines, 2021. **6**(1): p. 35.
148. Liu, W.C., et al., *Chimeric Hemagglutinin-Based Live-Attenuated Vaccines Confer Durable Protective Immunity against Influenza A Viruses in a Preclinical Ferret Model.* Vaccines (Basel), 2021. **9**(1).
149. Korenkov, D.A., et al., *Safety, immunogenicity and protection of A(H3N2) live attenuated influenza vaccines containing wild-type nucleoprotein in a ferret model.* Infect Genet Evol, 2018. **64**: p. 95-104.
150. Isakova-Sivak, I., et al., *Sequential Immunization with Universal Live Attenuated Influenza Vaccine Candidates Protects Ferrets against a High-Dose Heterologous Virus Challenge.* Vaccines (Basel), 2019. **7**(3).
151. Demminger, D.E., et al., *Adeno-associated virus-vectored influenza vaccine elicits neutralizing and Fcgamma receptor-activating antibodies.* EMBO Mol Med, 2020. **12**(5): p. e10938.
152. Price, G.E., et al., *Vaccination focusing immunity on conserved antigens protects mice and ferrets against virulent H1N1 and H5N1 influenza A viruses.* Vaccine, 2009. **27**(47): p. 6512-21.

153. Rosendahl Huber, S.K., et al., *Synthetic Long Peptide Influenza Vaccine Containing Conserved T and B Cell Epitopes Reduces Viral Load in Lungs of Mice and Ferrets.* PLoS One, 2015. **10**(6): p. e0127969.
154. Hatta, Y., et al., *Novel influenza vaccine M2SR protects against drifted H1N1 and H3N2 influenza virus challenge in ferrets with pre-existing immunity.* Vaccine, 2018. **36**(33): p. 5097-5103.
155. Holzer, B., et al., *Comparison of Heterosubtypic Protection in Ferrets and Pigs Induced by a Single-Cycle Influenza Vaccine.* J Immunol, 2018. **200**(12): p. 4068-4077.
156. Guilfoyle, K., et al., *Protective efficacy of a polyvalent influenza A DNA vaccine against both homologous (H1N1pdm09) and heterologous (H5N1) challenge in the ferret model.* Vaccine, 2021. **39**(34): p. 4903-4913.
157. Gooch, K.E., et al., *Heterosubtypic cross-protection correlates with cross-reactive interferon-gamma-secreting lymphocytes in the ferret model of influenza.* Sci Rep, 2019. **9**(1): p. 2617.
158. Bodewes, R., et al., *Vaccination against seasonal influenza A/H3N2 virus reduces the induction of heterosubtypic immunity against influenza A/H5N1 virus infection in ferrets.* J Virol, 2011. **85**(6): p. 2695-702.
159. Park, S.J., et al., *Evaluation of heterosubtypic cross-protection against highly pathogenic H5N1 by active infection with human seasonal influenza A virus or trivalent inactivated vaccine immunization in ferret models.* Journal of General Virology, 2014. **95**: p. 793-798.
160. Bissel, S.J., et al., *H1N1, but Not H3N2, Influenza A Virus Infection Protects Ferrets from H5N1 Encephalitis.* Journal of Virology, 2014. **88**: p. 3077-3091.
161. Korenkov, D., et al., *Live Attenuated Influenza Vaccines engineered to express the nucleoprotein of a recent isolate stimulate human influenza CD8+T cells more relevant to current infections.* Human Vaccines and Immunotherapeutics, 2018.
162. de Vries, R.D. and G.F. Rimmelzwaan, *Viral vector-based influenza vaccines.* Hum Vaccin Immunother, 2016. **12**(11): p. 2881-2901.
163. Rosendahl Huber, S., et al., *T cell responses to viral infections - opportunities for Peptide vaccination.* Front Immunol, 2014. **5**: p. 171.
164. Rosendahl Huber, S.K., et al., *Chemical Modification of Influenza CD8+ T-Cell Epitopes Enhances Their Immunogenicity Regardless of Immunodominance.* PLoS One, 2016. **11**(6): p. e0156462.
165. Mozdzanowska, K., et al., *Induction of influenza type A virus-specific resistance by immunization of mice with a synthetic multiple antigenic peptide vaccine that contains ectodomains of matrix protein 2.* Vaccine, 2003. **21**(19-20): p. 2616-2626.
166. Herrera-Rodriguez, J., et al., *A novel peptide-based vaccine candidate with protective efficacy against influenza A in a mouse model.* Virology, 2018. **515**: p. 21-28.
167. Wang, T.T., et al., *Vaccination with a synthetic peptide from the influenza virus hemagglutinin provides protection against distinct viral subtypes.* Proceedings of the National Academy of Sciences of the United States of America, 2010. **107**: p. 18979-84.
168. Lee, L.Y.Y., L. Izzard, and A.C. Hurt, *A Review of DNA Vaccines Against Influenza.* Front Immunol, 2018. **9**: p. 1568.
169. Scorza, F.B. and N. Pardi, *New Kids on the Block: RNA-Based Influenza Virus Vaccines.* Vaccines (Basel), 2018. **6**(2).
170. Wang, W., et al., *Protective Efficacy of the Conserved NP, PB1, and M1 Proteins as Immunogens in DNA- and Vaccinia Virus-Based Universal Influenza A Virus Vaccines in Mice.* Clin Vaccine Immunol, 2015. **22**(6): p. 618-30.
171. Koday, M.T., et al., *Multigenic DNA vaccine induces protective cross-reactive T cell responses against heterologous influenza virus in nonhuman primates.* PLoS One, 2017. **12**(12): p. e0189780.

172. Freyn, A.W., et al., *A Multi-Targeting, Nucleoside-Modified mRNA Influenza Virus Vaccine Provides Broad Protection in Mice.* Mol Ther, 2020. **28**(7): p. 1569-1584.
173. Magini, D., et al., *Self-Amplifying mRNA Vaccines Expressing Multiple Conserved Influenza Antigens Confer Protection against Homologous and Heterosubtypic Viral Challenge.* PLoS One, 2016. **11**(8): p. e0161193.
174. Petsch, B., et al., *Protective efficacy of in vitro synthesized, specific mRNA vaccines against influenza A virus infection.* Nat Biotechnol, 2012. **30**(12): p. 1210-6.
175. Dolgin, E., *mRNA flu shots move into trials.* Nature Reviews Drug Discovery, 2021. **20**(11): p. 801-803.
176. Oberhardt, V., et al., *Rapid and stable mobilization of CD8(+) T cells by SARS-CoV-2 mRNA vaccine.* Nature, 2021. **597**(7875): p. 268-273.
177. Wang, Z., et al., *mRNA vaccine-elicited antibodies to SARS-CoV-2 and circulating variants.* Nature, 2021. **592**(7855): p. 616-622.
178. Amanat, F., et al., *SARS-CoV-2 mRNA vaccination induces functionally diverse antibodies to NTD, RBD, and S2.* Cell, 2021. **184**(15): p. 3936-3948 e10.
179. Sahin, U., et al., *COVID-19 vaccine BNT162b1 elicits human antibody and TH1 T cell responses.* Nature, 2020. **586**(7830): p. 594-599.
180. Zollner, A., et al., *B and T cell response to SARS-CoV-2 vaccination in health care professionals with and without previous COVID-19.* EBioMedicine, 2021. **70**: p. 103539.
181. Cdc Weekly, C., *The Epidemiological Characteristics of an Outbreak of 2019 Novel Coronavirus Diseases (COVID-19) — China, 2020.* China CDC Weekly, 2020. **2**(8): p. 113-122.
182. Karagiannidis, C., et al., *Case characteristics, resource use, and outcomes of 10 021 patients with COVID-19 admitted to 920 German hospitals: an observational study.* The Lancet Respiratory Medicine, 2020. **8**(9): p. 853-862.
183. Verity, R., et al., *Estimates of the severity of coronavirus disease 2019: a model-based analysis.* Lancet Infect Dis, 2020. **20**(6): p. 669-677.
184. Du, Y., et al., *Clinical Features of 85 Fatal Cases of COVID-19 from Wuhan. A Retrospective Observational Study.* Am J Respir Crit Care Med, 2020. **201**(11): p. 1372-1379.
185. Zhou, F., et al., *Clinical course and risk factors for mortality of adult inpatients with COVID-19 in Wuhan, China: a retrospective cohort study.* Lancet, 2020. **395**(10229): p. 1054-1062.
186. Kreijtz, J.H., et al., *Low pathogenic avian influenza A(H7N9) virus causes high mortality in ferrets upon intratracheal challenge: a model to study intervention strategies.* Vaccine, 2013. **31**(43): p. 4995-9.
187. Bodewes, R., et al., *Pathogenesis of Influenza A/H5N1 virus infection in ferrets differs between intranasal and intratracheal routes of inoculation.* Am J Pathol, 2011. **179**(1): p. 30-6.

2

Varying viral replication and disease profiles of H2N2 influenza in ferrets is associated with virus isolate and inoculation route

Koen van de Ven[1], Harry van Dijken[1], Wenjuan Du[2], Femke de Heij[1], Justin Mouthaan[1], Sanne Spijkers[1], Sharon van den Brink[1], Paul Roholl[3], Cornelis A.M. de Haan[2], Jørgen de Jonge[1]

[1]Centre for Infectious Disease Control, National Institute for Public Health and the Environment (RIVM), Bilthoven, the Netherlands
[2]Section Virology, Division Infectious Diseases & Immunology, Department Biomolecular Health Sciences, Faculty Veterinary Medicine, Utrecht University, the Netherlands
[3]Microscope Consultancy, Weesp, the Netherlands

Manuscript submitted at Journal of Virology

Abstract

H2N2 influenza virus, the causative agent of the 1957 ‘Asian flu’ pandemic, has disappeared from circulation. However, H2-influenza viruses are still circulating in avian reservoirs. Combined with the waning of H2N2-specific immunity in the human population, there is a risk of reintroduction of H2N2 influenza virus. Vaccines could help in preventing a future pandemic, but to assess their efficacy animal models are required. We therefore set out to develop a ferret model for H2N2 influenza disease. We infected ferrets intranasally or intratracheally with four different H2N2 viruses to investigate their influence on the severity of disease. The H2N2 viruses were collected either during the pandemic or near the end of H2N2 circulation and covered both clade I and clade II viruses. Infection of ferrets with the different viruses showed that viral replication, disease and pathology, differed markedly between virus isolates and infection route. Intranasal inoculation induced a severe to mild rhinitis, depending on the virus isolate, and did not lead to lung infection or pathology. When administered intratracheally, isolates that successfully replicated in the lower respiratory tract (LRT) induced a non-lethal disease that resembles that of a moderate pneumonia in humans. Differences in viral replication and disease between viruses could be associated with their binding preference for α2,3- and α2,6-sialic acid. The model presented here could facilitate the development of a new generation of H2N2 influenza vaccines.

Introduction

In 1957 the 'Asian flu' became the second influenza pandemic of the 20th century. The cause of the pandemic was an H2N2 influenza A virus, which resulted from a reassortment between avian influenza H2, N2 and PB1 genes with human H1N1 influenza gene segments [1-4]. The virus quickly spread throughout the immune-naïve population, leading to an estimated 1-2 million deaths during the pandemic [5, 6]. After its introduction, H2N2 remained circulating as a seasonal influenza virus until it was replaced by H3N2 in 1968. Despite its disappearance, we are not safeguarded against a new introduction as genetically similar strains are still circulating in birds [7, 8] and people born after 1968 do not possess H2-neutralizing antibodies [6]. With the pandemic track record of H2N2, this poses a risk now that humoral immunity against H2N2 on the population level is rapidly declining [6, 9].

Mutations in the receptor binding domain of haemagglutinin (HA) can affect its binding affinity to the receptor on cells. Avian-originating HA-proteins are more likely to bind to α2,3-linked sialic acid (SA), while HA from human-adapted influenza strains prefer α2,6-SA (reviewed in [10]). In the adaptation from avian to human hosts, binding-preference switching from α2,3-SA to α2,6-SA is likely an essential process for avian derived influenza viruses. Not surprisingly, most pandemic influenza A viruses with an HA of avian origin started circulating among humans with a mixed α2,3-SA and α2,6-SA binding preference (reviewed in [11]). Continued circulation of these strains in the human population lead to a gradual increase in their binding preference for α2,6-SA. Importantly, α2,3-SA is mainly present on alveolar cells in the lower respiratory tract (LRT) of humans, while cells expressing α2,6-SA are primarily present in the upper respiratory tract (URT; reviewed in [10]). URT infections are usually limited to symptoms of a common cold, while LRT infections can lead to severe pneumonia. A switch in binding affinity from α2,3- to α2,6-SA is thus often accompanied by lower disease burden. Hence, the binding preference of individual H2N2 strains might also influence their pathogenesis.

With the looming threat of a next H2N2 pandemic, we set out to develop an animal model to be able to assess the efficacy of H2N2 vaccines. In general, the ferret is considered the best small animal model to study protection against influenza due to its similarities to human influenza disease [12]. This resemblance might be partly explained by the distribution of α2,6-SA, which is similar between ferrets and humans [13]. Others have already shown that ferrets are effectively infected upon intranasal (i.n.) inoculation with H2N2 influenza [14-17], but not how disease and pathology is affected by intratracheal (i.t.) inoculation. By depositing influenza virus into the lungs i.t. inoculation, more severe influenza disease can be modelled [18-20]. We infected ferrets i.n. or i.t. with various pandemic and seasonal human H2N2 virus isolates and found that there were clear differences in infectiousness and pathology

between H2N2 isolates and infection routes. Importantly, the differences between H2N2 isolates in infectiousness and pathology might be due to their varying binding preference for α2,3- and α2,6-SA.

Materials & Methods

Ethical statement

All animal experiments were approved by the Animal Welfare Body of Poonawalla Science Park – Animal Research Center (Bilthoven, The Netherlands) under permit number AVD326002018-4765 of the Dutch Central Committee for Animal experiments. All procedures were conducted according to EU legislation. Animals were examined for general health on a daily basis and after infection, ferrets were scored daily for activity and impaired breathing. The following scoring system was used for activity: 0=active; 1=active when stimulated; 2=inactive and 3=lethargic; and for respiratory distress: 0=normal breathing; 1=fast breathing and 2=heavy and stomach breathing. If animals showed severe disease according to the defined end points (lethargic or heavy breathing and inactive or more than 20% weight loss) prior to scheduled termination, they would be euthanized by cardiac bleeding under anesthesia with ketamine (5 mg/kg; Alfasan, Woerden, The Netherlands) and medetomidine (0.1 mg/kg; Orion Pharma, Espoo, Finland).

Viruses

Wild-type egg-grown H2N2 influenza viruses (A/Singapore/1/57, A/Leningrad/134/57, A/California/1/66 and A/Tokyo/3/67) with an unknown passage history were obtained from the influenza strain repository of the Institute of Experimental Medicine (IEM, St Petersburg, Russia). Live attenuated H2N2 viruses (A/Leningrad/134/17/57, A/17/California/66/395 and A/17/Tokyo/67/326 were likewise supplied by the IEM. The A/Singapore/1/57 reassortant (NIBRG-147, NIBSC code 09/306) virus was obtained from the National Institute for Biological Standards and Control (NIBSC, Hertfortshire, UK). All experiments involving wild-type H2N2 virus were carried out under BSL-3 conditions. Influenza viruses were grown on MDCK cells in MEM medium (Gibco; Thermo Fisher Scientific, Waltham, MA) supplemented with 40µg/ml gentamycin, 0.01M Tricin and 2µg/ml TPCK treated trypsin (all from Sigma-Aldrich, Saint Louis, MO). At >90% cytopathic effect (CPE), the suspension was collected and spun down (4000x g for 10 minutes) to remove cell debris and stored at -80°C. HA sequences of attenuated reassortant viruses were sequenced at Baseclear (Leiden, the Netherlands) and sequences are deposited in GISAID (identifiers in Table 1).

Virus sequencing & alignment

HA and NA segments of H2N2 influenza viruses were amplified by PCR with the MBTuni-12 [5′-ACGCGTGATCAGRAAAAGCAGG] and MBTuni-13 [5′-ACGCGTGATCAGTAGAAACAAGG]) primers [21]. Sequencing was performed with

the MinION (Nanopore technologies, Oxford, UK) and sequence data was analyzed using an inhouse pipeline. HA sequences of wild-type human and avian influenza virus isolates were extracted from GISAID and Genbank (identifiers in Fig. 1A) [22, 23]. Wild-type and reassortant H2N2 virus sequences were aligned by the MUSCLE algorithm using MEGA11 software [24]. Aligned wild-type human H2N2 viruses were color-coded according to the Clustal X color scheme in Jalview 2.11.1.4 [25]. These HA sequences are displayed according to H3-numbering [26]. HA protein sequences of avian and human wild-type H2N2 viruses were used to construct a maximum likelihood phylogenetic tree in MEGA11. For all viruses depicted in the phylogenetic tree, HA protein sequences were derived from GISAID with the exception of A/California/1/66 and A/Tokyo/3/67, for which no full-length HA sequence has been deposited. Instead, the full-length HA sequences reported in this paper have been used.

Animal handling

Female ferrets (*Mustela putorius furo*) supplied by Schimmel BV (The Netherlands) aged 4-8 months were tested for prior influenza and Aleutian disease infections and only negative animals were selected. Upon arrival at the animal facility, ferrets were allocated into groups based on weight and housed by group in open cages. From the moment of infection, all procedures were carried-out in BSL-3 certified isolators. A 'DST micro T' temperature transponder (Star-Oddi, Garðabær, Iceland) was implanted intra-abdominally 14 days prior to commencement of the experiment to measure body temperature. For this procedure, animals were anesthetized with ketamine (5 mg/kg) and medetomidine (0.1 mg/kg). Buprenodale (0.2 ml; AST Farma, Oudewater, The Netherlands) was administered as a post-operative analgesic. Anesthesia by medetomidine was antagonized with atipamezole (0.25 mg/kg; Orion Pharma). Blood collection and infections were carried out with the same anesthetics, but for the latter atipamezole treatment was delayed by 30 minutes to avoid excretion of the inoculum by sneezing and coughing. Weight determinations and swabbing on days without other treatments (e.g. infection/blood draws) occurred under anesthesia with ketamine alone. The ferrets received food and water *ad libitum*. At scheduled termination, ferrets were euthanized by cardiac bleeding under anesthesia with ketamine and medetomidine.

Study design

The data presented here originated from three independent ferret experiments (1 = Sin/57; 2 = Tok/67, 3 = Len/57 and Cal/66). In each experiment, ferrets were infected intranasally (0.5 mL) or intratracheally (3 mL) with 10^6 $TCID_{50}$ of one of the four selected H2N2 influenza viruses. Three, five and seven days after infection with A/Tokyo/3/67 and A/Singapore/1/57, animals were sacrificed in order to study pathology and virology. For experiments with A/Leningrad/134/57 and A/California/1/66 animals were euthanized five days post infection only. Groups consisted of three animals per condition (route of infection and day of termination).

On 2, 3 and 5 days after infection nasal and throat swabs were collected and bodyweight was measured. For A/Tokyo/3/67 and A/Singapore/1/57 infections, additional swabs and weight measurements were taken on days 1, 4, 6 and 7 post infection. Nose and throat swabs were collected in 2 ml transport medium containing 15% sucrose (Merck, Kenilworth, NJ), 2.5µg/ml Amphotericin B, 100 U/ml penicillin, 100µg/ml streptomycin and 250µg/ml gentamycin (all from Sigma) and stored at -80°C. At pre-determined time-points, animals were dissected as described before [20]. In short, animals were sedated (ketamine and medetomidine) and exsanguinated after which the trachea was clamped off and the inflated lungs were isolated, weighed and examined for gross pathology. The middle section of the trachea (~1cm), sections of the three right lung lobes and the accessory lobe along the proximodistal axis (~1 cm by 3mm) and the right nasal turbinates were isolated and stored in Lysing Matrix A tubes (MP Biomedicals, Irvine, CA) at -80°C for later virological analysis. The left cranial and caudal lung lobes and the left nasal turbinates were fixed in 10% buffered formalin for histopathological analysis.

Animal temperature, bodyweight and lung weight

Temperature data were retrieved from the implanted temperature loggers and consisted of measurements taken every 30 minutes. Baseline temperature was calculated as the average temperature in the 4 days before infection. The change in temperature was calculated as deviation from baseline (ΔT). The area under the curve (AUC) was calculated as the total ΔT up till 5 dpi. Values smaller than 'baseline-2*standard deviation of baseline' were excluded as these often occur due to anesthesia. Relative bodyweight and relative lung weight are expressed as a percentage of bodyweight or ratio on the day of infection.

Virus quantification

Thawed lung, trachea and nasal turbinate samples were homogenized in Lysing Matrix A tubes using FastPrep (MP Biomedicals) and clarified by centrifugation for 5 minutes at 4000x g. Nasal and throat swabs were thawed and vortexed. All samples for virus quantification were serially diluted and tested in sextuplicate (6-plo) on MDCK cells in infection medium (MEM + 40µg/ml gentamycin, 0.01M Tricin and 2µg/ml TPCK treated trypsin). CPE was scored after 6 days of culturing and $TCID_{50}$ values were calculated using the Reed & Muench method.

Pathology

Pathology scoring was performed as described before [27, 28]. In brief, the left cranial and caudal lung lobes were inflated with, and stored in, 10% formaldehyde. After fixation, the lung lobes were embedded in paraffin and sliced into 5µm thick sections. Slides were stained with hematoxylin and eosin and microscopically examined at 50x or 100x magnification. For each lung lobe, at least 6 microscopic fields were scored. Pathological scoring distinguished between the categories 'epithelial damage' and

'inflammation'. Damage related parameters included hypertrophy, hyperplasia, flattened or pseudo squamous epithelia, necrosis and denudation of bronchi(oli) epithelium, hyperemia of septa and alveolar emphysema and hemorrhages. Inflammation related parameters included (peri)bronchi(oli)tis, interstitial infiltrate, alveolitis and (peri)vasculitis characterized by polymorphonuclear (PMN) cells, macrophages and lymphocytic infiltrate. Pathological findings were scored on a scale of 0 (no aberrations) to 5 (severe damage) and were summarized in two 'end scores' for the categories 'epithelial damage' and 'inflammation'. The percentage affected lung tissue was estimated at 20x magnification.

Nasal turbinates were fixated and stained similar to lung tissue and analyzed as reported before [29]. Slides were examined microscopically and a summary score (on a scale of 0-5) based on the severity and percentage of tissue affected by different histopathological parameters was determined. Histopathological parameters consisted of damage to the epithelial linings, presence of inflammatory cells, and the presence of exudate and/or hemorrhages. All microscopic slides were randomized and scored blindly.

Receptor binding

The binding activities of H2N2 viruses were analyzed by biolayer interferometry using the Octet RED348 (Fortebio, Fremont, CA), similarly as described previously [30, 31]. Briefly, streptavidin sensors were loaded to saturation with biotinylated synthetic glycans 2,3-sialyl-N-acetyllactosamine-N-acetyllactosamine (3'SLNLN, referred to as α2,3-SA) or 2,6-sialyl-N-acetyllactosamine-N-acetyllactosamine (6'SLNLN, referred to as α2,6-SA). Synthetic glycans were synthesized at the Department of Chemical Biology and Drug Discovery, Utrecht University, Utrecht, the Netherlands. Subsequently, the sensors were moved to virus-containing wells in the presence of NA inhibitor oseltamivir carboxylate (OC) for 15-30 min to achieve virus binding curves, which were used for the determination of the virus initial binding rates (referring to vobs=dB/dT in nm/min) as described previously [31]. All the experiments were conducted in PBS with calcium and magnesium at 30 ° with sensor shaking at 1000 rpm. Initial binding rates were normalized for virus particle numbers, which were determined by nanoparticle tracking analysis using a NanoSight NS300 instrument (Malvern Panalytical, Malvern, UK) as described previously [30]. The virus preparations were prediluted with Ultra Pure PBS (Merck) to reach a concentration suitable for analysis with NTA. All measurements were carried out at 19 °. The NanoSight NS300 recorded five 60s sample videos per analysis, which were then used for the analysis with the Nanoparticle Tracking analysis 3.0 software, generating the quantitative information on particle numbers. Particle numbers were used to determine the initial binding rate per particle.

Data analysis, statistical testing and data availability

Data analysis and visualization was performed using R software (v4.0.2) [32] with the packages tidyverse [33], ggpubr [34] and ggplot2 [35]. Virus titers were log_{10}-transformed for visualization. Sialic acid binding data was compared using 1-way ANOVA, followed by Tukey multiple comparisons test in GraphPad Prism software (v9.1.0). No statistical testing was performed for ferret experiments as group numbers (n = 3) were insufficient for reliable statistical testing. Some data was excluded from analysis, which included temperature transponders that malfunctioned and shut down before the defined termination point. Lung weight was not measured for one A/Singapore/1/57-infected ferret at 3 dpi. No other data was excluded from analysis. Virus HA sequences are available from GISAID. Data supporting the main figures is available as upon request to the corresponding author.

Results

HA sequence correlates with binding to α2,3- or α2,6-sialic acid

We selected two early and two late human H2N2 viruses for the infection of ferrets (Fig. 1a). A/Singapore/1/57 (Sin/57) and A/Leningrad/134/57 (Len/57) were both isolated during the pandemic in 1957. A/California/1/66 (Cal/66) and A/Tokyo/3/67 (Tok/67) are seasonal isolates from the end of H2N2 circulation and can be classified as clade I and II respectively [4]. These viruses display slight amino acid differences in their HA sequence that might affect their binding and replication properties. Due to this, these viruses may induce divergent pathological changes in the ferret model.

The binding preference of HA to sialic acid is primarily determined by the receptor binding pocket of HA, which is made up of the 130-loop, the 190-helix and the 220-loop [36]. We sequenced the HA segments of the H2N2 isolates to investigate their binding preference. HA of Len/57 contains a Gln226 and Gly228 in the 220-loop (H3 numbering; Fig. 1b), which corresponds with the residues found in H2 derived from avian viruses. H2 HAs with these residues are predicted to bind to both avian-type α2,3-SA and human-type α2,6-SA [36]. In contrast, Sin/57 and Tok/67 are probably better adapted to the human host as they contain Gln226Leu and Gly228Ser substitutions, which are known to result in strong preferential binding to α2,6-SA. While Cal/66 is similar to the latter two isolates in that it contains Ser228, it deviates with its Phe226. In addition, the H2 HAs of these viruses differ to some extent in their 130-loop and 190-helix, which is also likely to affect receptor binding specificity and/or affinity (Fig. 1b).

As binding preference markedly influences viral replication and consequently pathology and disease, we set out to confirm and further analyze the predicted binding properties of the selected viruses by biolayer interferometry. As this binding-assay could only be performed under BSL-2 conditions, we used attenuated reassortant vaccine viruses of the respective BSL-3 classified original viruses.

Sequence analyses of the vaccine viruses showed that while some mutations have arisen compared to wild-type viruses, none of these mutations are present in the HA-binding pocket (Table 1). The four viruses could all bind to α2,3-SA (Fig. 1c), although they differed to some extent in their initial binding rate. Most viruses – the exception being Len/57 with its avian-like HA (Gln226/Gly228) – also bound to α2,6-SA (Fig. 1c). Sin/57 and Tok/67 preferentially bound to α2,6-SA, in agreement with their human-like HA signature (Leu226/Ser228; Fig. 1d). While Cal/66 (Phe226/Ser228) was able to bind α2,6-SA, it preferred binding to α2,3-SA, just as Len/57, which did not display any binding to α2,6-SA. We conclude that the SA binding preferences of the different viruses largely correspond with their predicted preference based on the identity of the residues on position 226 and 228. Interestingly, while the Cal/66 virus was isolated many years after the start of the pandemic, it nevertheless prefers binding to avian-type receptors.

Table 1: Mutations in HA of vaccine strain versus respective wild-type virus

Wild-type virus[1]	Vaccine virus[2]	Reference strain (HA accession #)[3]	Difference wild-type virus with vaccine virus (H3-numbering)	Difference wild-type virus with reference strain (H3-numbering)
A/Singapore/1/57	NIBRG-147	A/Singapore/1/57 (GISAID: EPI160146)	G158E	-
A/Tokyo/3/67	A/17/Tokyo/67/326	A/Tokyo/3/67 (Genbank: AY209987.1[4])	G126E	R81S; K93R; Y94D; S95G; G126R; K131T; D133T; K137R; Q145P; K259Q; I268M; C281F; N289K
		A/Netherlands/ B2/1968 (GISAID: EPI545874)		P159Q; K186N; E193A; I436T
A/Leningrad/ 134/57	A/Leningrad/ 134/17/57	A/Leningrad/134/57 (GISAID: EPI555074)	V182M; N186T; V202I; I347V	I347V
A/California/1/66	A/17/California/ 66/395	A/California/1/66 (Genbank: AAO46291.1[4])	-	A19S; M268L

1 = BSL-3 viruses used for ferret infections in this study.
2 = BSL-2 viruses used for biolayer interferometry in this study.
3 = Reference strain (same isolate or most-closely related) derived from online depository to compare HA sequences with in-house HA sequence results of 'Wild-type virus'.
4 = Only partial reference sequence of HA is available.

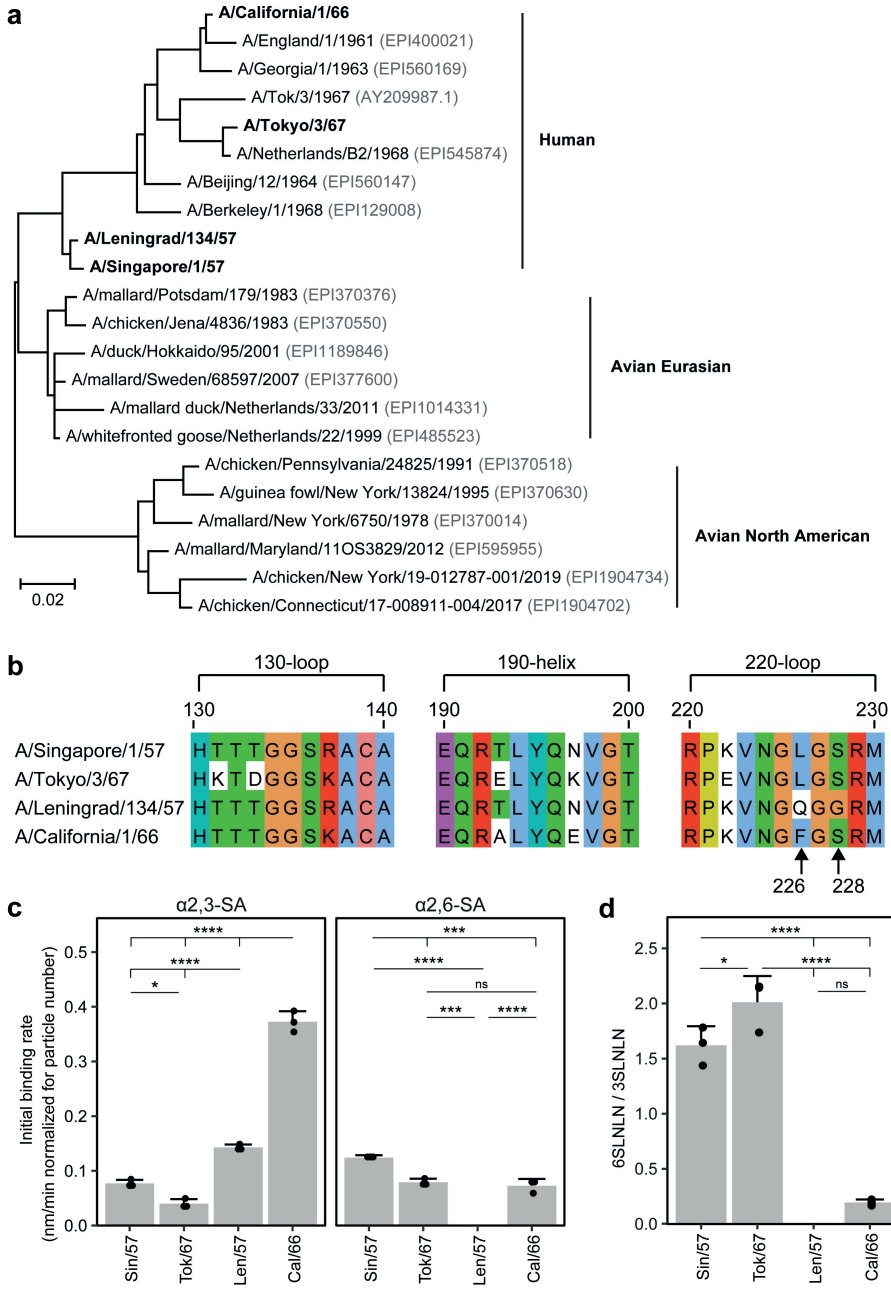
a
A/California/1/66
A/England/1/1961 (EPI400021)
A/Georgia/1/1963 (EPI560169)
A/Tok/3/1967 (AY209987.1)
A/Tokyo/3/67
A/Netherlands/B2/1968 (EPI545874)
A/Beijing/12/1964 (EPI560147)
A/Berkeley/1/1968 (EPI129008)
A/Leningrad/134/57
A/Singapore/1/57
Human
A/mallard/Potsdam/179/1983 (EPI370376)
A/chicken/Jena/4836/1983 (EPI370550)
A/duck/Hokkaido/95/2001 (EPI1189846)
A/mallard/Sweden/68597/2007 (EPI377600)
A/mallard duck/Netherlands/33/2011 (EPI1014331)
A/whitefronted goose/Netherlands/22/1999 (EPI485523)
Avian Eurasian
A/chicken/Pennsylvania/24825/1991 (EPI370518)
A/guinea fowl/New York/13824/1995 (EPI370630)
A/mallard/New York/6750/1978 (EPI370014)
A/mallard/Maryland/11OS3829/2012 (EPI595955)
A/chicken/New York/19-012787-001/2019 (EPI1904734)
A/chicken/Connecticut/17-008911-004/2017 (EPI1904702)
Avian North American
0.02
b
130-loop
190-helix
220-loop
130
140
190
200
220
230
A/Singapore/1/57 HTTTGGSRACA EQRTLYQNVGT RPKVNGLGSRM
A/Tokyo/3/67 HKTDGGSKACA EQRELYQKVGT RPEVNGLGSRM
A/Leningrad/134/57 HTTTGGSRACA EQRTLYQNVGT RPKVNGQGGRM
A/California/1/66 HTTTGGSKACA EQRALYQEVGT RPKVNGFGSRM
226
228
c
α2,3-SA
α2,6-SA
Initial binding rate
(nm/min normalized for particle number)
0.0
0.1
0.2
0.3
0.4
0.5
****
****
*
***
****
ns
***
****
Sin/57
Tok/67
Len/57
Cal/66
d
6SLNLN / 3SLNLN
0.0
0.5
1.0
1.5
2.0
2.5
****
*
****
ns
Sin/57
Tok/67
Len/57
Cal/66

Figure 1: Binding of H2N2 strains to α2,3- and α2,6-sialic acid. a) Phylogenetic tree of human and avian H2 sequences. The tree was constructed based on HA protein sequences by the maximum likelihood method. The four human H2N2 isolates used in this study are depicted in bold and the GISAID (or Genbank for A/Tokyo/3/67) HA protein identifiers are written in grey. A/Tokyo/3/67 is depicted twice, once with the full-length HA sequence reported in this study (no protein identifier) and once with the truncated HA sequence found in Genbank. Scale bar depicts genetic distance. **b)** Amino acid sequence alignment of the three sites involved in the binding to sialic acid (SA) [36] of H2 of the four human H2N2 influenza viruses used in this study. Colors indicate the (conservation of) amino acid profile based on the Clustal X color scheme. HA sequences are displayed according to H3-numbering [26]. **c**) Binding of H2N2 virus strains to α2,3- and α2,6-SA and **d**) the binding ratio between α2,6- and α2,3-SA as determined by biolayer interferometry. The ratio of Leningrad could not be determined as binding to α2,6-SA was zero. Data is visualized as mean ± SD with n = 3. Binding rate of viruses in panels c and d was compared using 1-way ANOVA, followed by Tukey multiple comparisons test. * = $p < 0.05$; ** = $p < 0.01$; *** = $p < 0.001$; **** = $p < 0.0001$.

We additionally investigated if the HA and NA protein sequences of the H2N2 isolates used in this study are identical to known reference sequences since repeated passaging might have introduced mutations. No differences were detected in NA protein sequence and no (Sin/57) or few mutations (Len/57 = 1; Cal/66 = 2) were present in the HA sequence of Sin/57, Len/57 and Cal/66 (Table 1). These mutations where however not present in the receptor binding pocket of HA and it is therefore unlikely that this influenced binding to sialic acid much. In the case of Tok/67, we found multiple differences between our virus isolate and the reference sequence (Table 1). However, according to a protein blast, the reference sequence is not similar to other (late) H2N2 Clade II sequences and does not group together. In contrast, the Tok/67 HA protein sequence reported here is 99.12% similar to A/Netherlands/B2/1968 and clusters together with other H2N2 viruses (Table 1 and Fig. 1a). It is therefore plausible that the reference sequence is incorrect, while the Tok/67 sequence we report here is representative of late circulating Clade II viruses given the high similarity to A/Netherlands/B2/1968.

Viral replication and tissue distribution differs between H2N2 isolates and route of infection

Next, we performed a series of independent animal experiments in which we infected ferrets with the four H2N2 viruses and assessed the influence of i.n. versus i.t. inoculation on viral replication and pathology. We first infected ferrets with H2N2 isolates Sin/57 or Tok/67 and euthanized animals on 3, 5 and 7 days post infection (dpi) to determine the kinetics of virus replication and development of pathology (Fig. 2a). Based on these experiments we found that viral replication and pathology could be best assessed 5 dpi. Subsequent experiments with Len/57 and Cal/66 thus only assessed pathology and viral replication on 5 dpi.

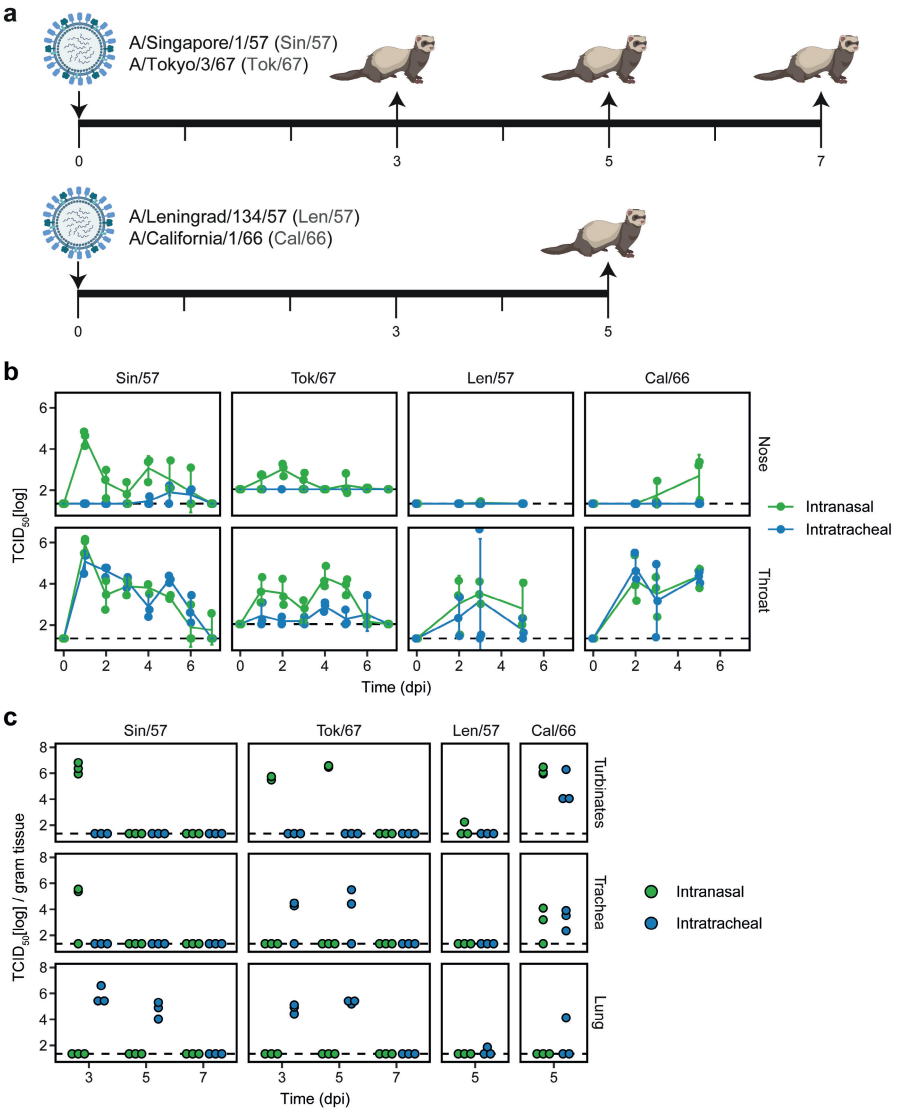

Figure 2: Virus tissue distribution and replication kinetics depend on the route of infection and virus isolate. a) Female ferrets of 4-8 months old were infected with 10^6 $TCID_{50}$ influenza virus via intranasal or intratracheal inoculation on day 0. Animals were then euthanized on day 3, 5, 7 (Sin/57 and Tok/67) or only on day 5 (Len/57 and Cal/66) after infection to study viral replication and pathology. N = 3 per inoculation route and dissection day. Infections with Sin/57 and Tok/67 were carried out in separate experiments while Len/57 and Cal/66 infections were performed within one experiment. **b, c**) Viral load in (b) nasal and throat swabs and (c) respiratory tissues was measured by $TCID_{50}$-assay on MDCK cells. Dotted lines represent the limit of detection. Data is visualized as (b) mean ± SD (c) or individual values where each dot represents a ferret. dpi = days post infection. **a** was created using BioRender.

We assessed viral replication in the respiratory tract by $TCID_{50}$ determination in nose and throat swabs. Similar to earlier reports for other H2N2 influenza viruses [15, 17], Sin/57 and Tok/67 replicated for approximately 6 days as most animals tested negative (below detection limit) on 7 dpi (Fig. 2b). Animals infected i.n. with Sin/57 clearly displayed higher viral titers in the nose than ferrets inoculated i.t., but no such difference was seen in the throat. In contrast, viral titers of i.t. infected animals with Tok/67 were lower in throat swabs and below detection limit in nasal swabs. Inoculation route did not influence the viral titers of Len/57 and Cal/66 in throat swabs, but viral titers in the nose did increase from 3 dpi onwards in ferrets infected i.n. with Cal/66. Importantly, no infectious virus could be detected in the nasal swabs of animals infected i.n. or i.t. with Len/57. In conclusion, with the exception of Len/57, viral replication in the nose was higher in i.n. infected animals for the isolates we investigated. The inefficient replication of Len/57 in the nose may be explained by the inability to bind to α2,6-SA (Fig. 1c). Viral replication in the throat was comparable between i.n. and i.t. infected animals with the exception of the Tok/67 virus.

To investigate the URT and LRT in more detail, we homogenized nasal, trachea and lung tissue on days 3, 5 and 7 after infection and determined the viral load by $TCID_{50}$-assays. In agreement with the nasal swabs, i.t. infected animals mostly tested negative for influenza in the nasal turbinates (Fig. 2c). This was however not the case for Cal/66, as virus was also found in the nasal turbinates and trachea of both i.n. and i.t. infected animals. For other viruses, viral replication in the trachea was limited to i.n. (Sin/57) or i.t. (Tok/67) inoculated ferrets. Len/57 hardly replicated in any of the tissues, with a viral load just above detection level in a few animals. As expected, viral replication in the lung was only observed in i.t. infected animals, showing that i.n. inoculation is insufficient to establish a LRT infection with the H2N2 viruses tested. While Sin/57 and Tok/67 efficiently replicated in the lungs after i.t. inoculation, this was not the case for Len/57 and Cal/66.

Fever and weight loss differ between virus isolates and inoculation routes

The clinical symptoms we observed were generally mild with only a few Sin/57-infected animals displaying a minor reduction in activity and increased difficulty breathing. No pronounced clinical symptoms were observed for the infections with other virus isolates. We additionally measured fever as this is an unbiased measure for disease severity. In general, LRT infections are more severe [18-20] and this might thus affect the duration or height of fever. Tok/67 and Sin/57 both replicated in the LRT and i.t. infection led to earlier onset of fever (Fig. 3a). Especially in the case of Sin/57, fever was longer-lasting for i.t. infected animals. Cal/66 infection induced a minor fever, but there was no strong difference between i.n. and i.t. infected animals. This is in agreement with the observed restriction of virus replication to the URT and failure to establish a LRT infection (Fig. 2b). Animals infected with Len/57 did not show any fever, independent of route of infection, which is also in line with the absence of an established infection.

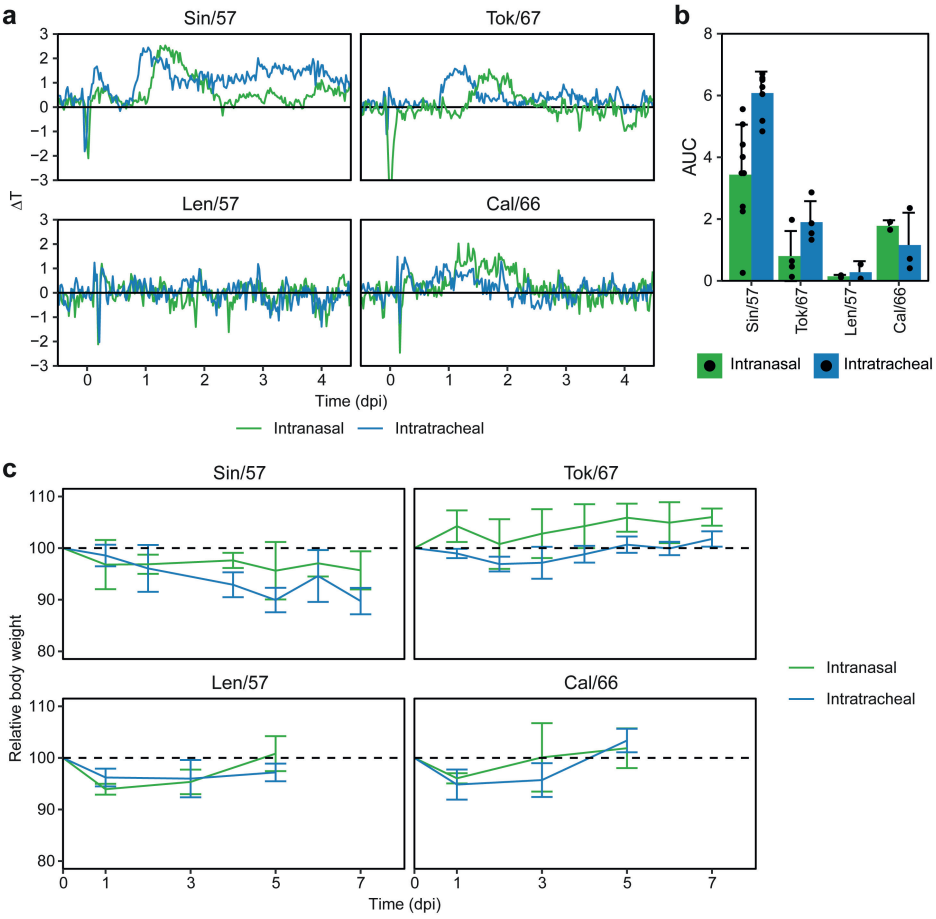

Figure 3: Fever and weight loss is dependent on virus isolate and route of infection. a) Body temperature was measured in 30-minute intervals via an abdominal transponder. Data is visualized as deviation from baseline (ΔT), with lines indicating the mean per group. **b**) Area under the curve (AUC) of data from 'A' up to 5 days post infection (dpi). Temperatures more than 2x SD below baseline were excluded as these are often due to anesthesia. Data is visualized as mean ± SD and individual values (black dots). N = 8-9 for Sin/57; 4 for Tok/67; 2 for Len/57; and 2-3 for Cal/66. **c**) Body weight during infection relative to body weight at the day of infection. Data is presented as mean ± SD, with n = 3-6 for Sin/57 and Tok/67; n = 3 for Len/57 and Cal/66.

The area under the curve (AUC) – which is a derivative of the sum of fever episodes within a certain timespan – confirmed that i.t. inoculation induced more severe fever for the preferentially α2,6-binding viruses Sin/57 and Tok/67 (Fig. 3b). This was not the case for Cal/66 or Len/57. These findings are corroborated by bodyweight data. For both Len/57 and Cal/66 viruses, weight decrease is similar between i.n. and i.t. infection (Fig. 3c). In contrast, Tok/67 and Sin/57 infections lead to a more severe

decline in weight when they are administered i.t., although the within-group variation is relatively high. Weight loss was much more pronounced upon Sin/57 infection compared to Tok/67 infection.

Pathology in the respiratory tract is influenced by the route of inoculation and virus isolate

We observed that the virus isolate and route of infection affected the site of viral replication and clinical disease. In order to determine whether this also led to differences in pathological aberrations, we analyzed hematoxylin & eosin-stained slides of nasal turbinates and lung tissue at 5 dpi. The different pathology parameters scored in the nasal turbinates were summarized in a final pathology severity score on a scale of 0-5. As expected, the nasal turbinates were more severely affected in i.n. inoculated ferrets (score 1-5), as pathology was absent or mild in i.t. infected animals (score 0-1; Fig. 4a, b). I.n. infection resulted in aberrations of the naso- and maxilloturbinates, whereas the ethmoid (olfactory) turbinates were largely unaffected. At 5 dpi, a severe rhinitis was present in Sin/57 i.n. inoculated ferrets accompanied by hypertrophy of the goblet cells, pseudo squamous epithelium and a severe (sub)mucosal inflammation. Together this resulted in a pathology score of 5. Tok/67 infection was milder with a mild to moderate rhinitis and a minor inflammation of the submucosa. The respiratory epithelium was moderately affected over a large surface with hypertrophy and loss of cilia, resulting in a maximum score of 3. Ferrets infected i.n. with Cal/66 scored 2-3 and displayed aberrations in the surface of the respiratory epithelium ranging from minimal disturbances of the mucosa to pseudo desquamation of the epithelial lining. Inflammation and hyperemia were present in the submucosa. In contrast to the three other viruses, Len/57 did not cause much pathology in ferrets. Only slight disturbances and inflammation in the (sub)mucosa were observed, leading to a maximum score of 1 in both i.n. and i.t. Len/57 infected ferrets.

In the lungs, the infection induced a slight to moderate multifocal broncho-interstitial pneumonia of which the severity depended on the route of infection and virus isolate. The main pathological observations made throughout the groups are characterized by a multifocal inflammation around the terminal and respiratory bronchioles (peribronchiolitis) and ranges from a score 0-3 on a scale of 0-5 (Fig. 4c). The inflammation included lymphocytes, macrophages and polymorphonuclear cells. In some cases, bronchiolar lumina were filled, but not obstructed, with mononuclear and polymorphonuclear infiltrate and some necrotic cellular debris. Disturbances to the epithelial lining of the bronchioli was restricted to a slight to moderate hypertrophy and hyperplasia. Sporadically necrosis of bronchiolar epithelium and inflammation of the interstitium and hyperemia of the alveolar septa was observed. Alveolitis, alveolar hemorrhages and perivasculitis were sometimes present. Sporadic aberrations were seen in the bronchi and the bronchus was unaffected.

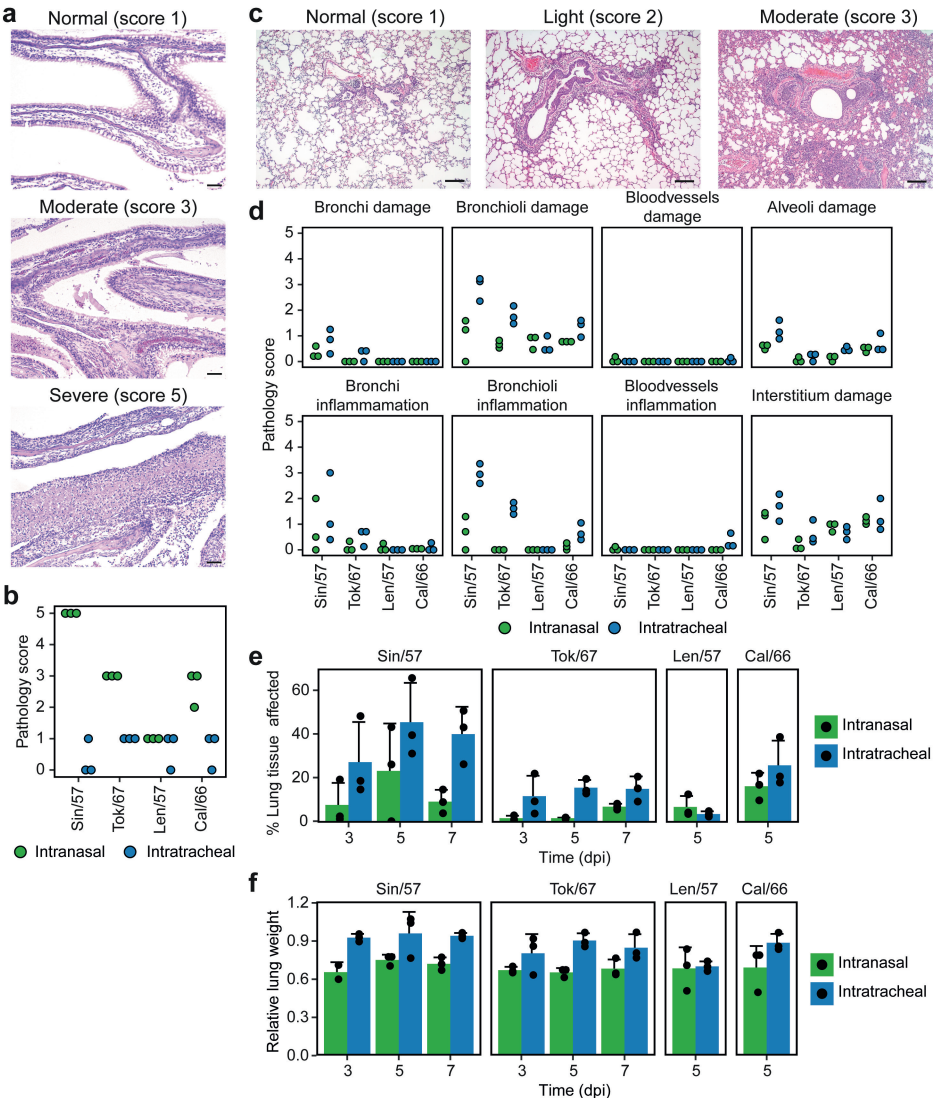

Figure 4: Pathology in respiratory tract is determined by virus isolate and route of inoculation. a) Haematoxylin & eosin staining of representative nasal turbinate slides with different pathological severities at 100x magnification. Bars represent 50 µm. **b**) Pathological summary score (scale 0-5) of nasal turbinates 5 days post infection (dpi). **c**) Haematoxylin & eosin staining of representative lung slides with different pathological severities at 50x magnification. Bars represent 200 µm. **d**) Pathological scoring (scale 0-5) for damage and inflammation parameters of different segments of the lung at 5 dpi. **e**) Percentage of lung tissue affected by pathology scored in 'd'. **f**) Lung weight after infection relative to body weight at the day of infection. Data is presented as individual values (a, c-e) with mean ± SD (d and e only). N = 3 for all plots, with the exception of Sin/57 in panel e (n = 2-3).

Multiple lung segments were scored for pathological parameters related to damage and inflammation on a scale of 0-5. Differences between infection routes and viruses were most prominent in the damage and inflammation of the bronchioli (Fig. 4d). As expected, lung pathology was more severe after i.t. inoculation, which was especially the case for Sin/57 and Tok/67. Little to no aberrations were detected in the bronchi and bronchioli of Len/57 and Cal/66-infected animals, reflecting the absence of clinical disease and viral replication in the LRT by these viruses. For all virus isolates except Len/57, we observed a trend that i.t. inoculation resulted in a higher percentage of affected lung tissue (Fig. 4e). We additionally determined the relative lung-to-body weight after H2N2 infection as an unbiased analysis of tissue inflammation and edema formation. The increased relative lung weights confirm that i.t. infection leads to more severe LRT pathology compared to i.n. inoculation (Fig. 4f). As expected, this was not the case for Len/57 which did not replicate in the LRT.

Discussion

Here we report our efforts to establish a ferret model for H2N2 influenza infection and disease for vaccine evaluation purposes. Of the four viruses we investigated, infection with Sin/57 and Tok/67 – both of which prefer binding to α2,6-SA – lead to consistent high viral replication and disease symptoms. In contrast, Cal/66 replication was restricted to the upper respiratory tract and induced only mild disease. Len/57 infection hardly induced disease, reflecting the absence of an established infection. The site of replication for Sin/57 and Tok/67 was clearly dictated by the inoculation route, as virus deposited in the LRT did not infect the URT and vice versa. This in contrast to Cal/66 where both URT and LRT inoculation resulted in replication only in the URT. Thus, for two viruses the site of replication was dictated by inoculation route while for one virus the binding preference likely restricted replication to the URT. The site of replication also affected disease severity as a LRT-infection via i.t. inoculation lead to more severe clinical disease and pathology when compared to i.n. inoculation.

Of the four H2N2 viruses that we tested, all infections were sub-lethal in ferrets similar to the other (seasonal) human H1N1 and H3N2 viruses [37, 38]. In contrast, infections with avian-derived H5N1 and H7N9 isolates are – depending on the strain and route of inoculation – lethal in ferrets [18, 19]. The absence of mortality in this H2N2 influenza ferret model reflects the human situation during the H2N2 pandemic, which was not excessively deadly when compared to the 1918 pandemic or zoonotic infections with H5N1 and H7N9 [39, 40]. Early reports indicated that the clinical symptoms of pandemic H2N2 disease did not differ much from regular seasonal influenza (reviewed in [41]). Above all, most H2N2 pandemic deaths occurred in the very young, very old or those with comorbidities [42]. The most accurate representation of H2N2 infection should thus manifest itself as a mild, sublethal disease. In that aspect, the H2N2 infection ferret model we established accurately mimics a human H2N2 infection.

It is difficult to compare the pathology in the H2N2 influenza ferret model with human cases, as pathology reports only document lethal H2N2 cases [41, 43, 44]. However, based on these reports we found that the pathological facets in ferrets were similar to human cases, albeit less extensive. In both humans and ferrets, H2N2 infection could result in multifocal pneumonia [43]. Hyperemia was present in ferrets, but seemed more severe in humans [43]. The epithelial lining of the bronchioli was damaged in both humans [44] and ferrets, although for ferrets signs of damage were limited to hypertrophy and hyperplasia. Severe hyperemia, alveolar hemorrhage and capillary thrombosis are indicative of a lethal infection and were only observed in human cases [43]. The (severity of) pathology in ferrets was clearly influenced by the route of inoculation. In general, i.n. inoculation induced mild disease representative of a standard seasonal infection, while i.t. administration induced a moderate pneumonia. This was primarily the case for Sin/57 and Tok/67, which both replicated efficiently in the URT and LRT. Similar, but less severe pathology was seen for Cal/66. In contrast, Len/57 replication in the LRT was below detection and similar to i.n. administration, i.t. inoculation did not induce disease or pathology.

Other groups have infected ferrets with H2 influenza virus before. Chen et al. inoculated ferrets i.n. and found that all viruses investigated replicated in both nasal turbinates and lung, despite i.n. administration [16]. It is unlikely that this is due to differences in inoculation volume, but a higher infectious dose might have played a role. While Chen et al. used a higher infectious those compared to us (10^7 vs 10^6 $TCID_{50}$), their inoculation volume was smaller (0.2 vs 0.5 mL). Similarly, Moore et al. have shown that intranasal inoculation with 10^6 $TCID_{50}$ H1N1 or H3N2 influenza virus in a volume of 0.5 mL is sufficient to introduce virus into the lungs [45]. Alternatively, the virus isolates tested by Chen et al. might have different SA-binding preferences or the viruses are less restricted by the inoculation route. Pappas *et al.* showed that H2N2 viruses with a preference for α2,3-SA transmit less efficient in ferrets [15]. For one virus, a Gln226Leu substitution naturally occurred in infected ferrets. This mutation is associated with enhanced binding affinity for α2,6-SA [46] and substantially improved transmission between ferrets [15, 17]. This is likely a direct effect of the distribution of α2,3- and α2,6-SA in the ferret respiratory tract, where α2,6-SA is more abundantly expressed throughout the respiratory tract [47, 48]. These studies and our results from the binding analysis offer some explanation as to why the α2,3-SA-binding Len/57 hardly replicates in ferrets and does not cause observable disease and pathology. Similarly, the α2,6-SA-prefering Sin/57 and Tok/67 are able to readily infect the ferret respiratory tract, leading to high viral titers and subsequent pathology. Cal/66 prefers α2,3-SA but can also still bind to α2,6-SA. Nevertheless, replication of Cal/66 in the lungs was much reduced compared the α2,6-SA preferring viruses. Possibly, Cal/66 has adapted to replication at lower temperatures in the URT, which limits its replication in the warmer LRT. More research is needed to elucidate the molecular basis of this difference in replication.

Viral replication, disease and histopathology differed with inoculation route and virus. Clearly, Len/57 is not suitable to model H2N2 disease in ferrets due to the absence of productive viral replication and disease. Cal/66 in contrast did replicate and caused mild disease, although it was unable to infect the LRT. For a future ferret model our preference would thus be to use either Sin/57 or Tok/67. Both viruses could replicate in the URT and LRT and were restricted by the inoculation route, which can be utilized to tweak the severity of disease. LRT infections induced by intratracheal inoculation tended to be more severe than intranasally-induced URT infections. In our opinion, intratracheal inoculation is therefore preferred for vaccine-challenge models assessing severity of disease, while intranasal administration would be more suitable to assess reduction of transmission by vaccine induced immunity.

With the study presented here, we show that ferrets are a representative model for human H2N2 influenza. The induced severity of disease and pathology can be altered by the route of infection and strain selection, enabling us to model both mild and moderate H2N2 disease. Together with the development of tools and reagents to study cellular and humoral immunity in ferrets [37, 49], we now have a working model to study vaccine-induced immune responses in the context of protection against influenza infection. These developments can further facilitate the research of new, improved influenza vaccines.

References

1. Gething, M.J., et al., *Cloning and DNA sequence of double-stranded copies of haemagglutinin genes from H2 and H3 strains elucidates antigenic shift and drift in human influenza virus.* Nature, 1980. **287**(5780): p. 301-6.
2. Kawaoka, Y., S. Krauss, and R.G. Webster, *Avian-to-human transmission of the PB1 gene of influenza A viruses in the 1957 and 1968 pandemics.* J Virol, 1989. **63**(11): p. 4603-8.
3. Scholtissek, C., et al., *On the origin of the human influenza virus subtypes H2N2 and H3N2.* Virology, 1978. **87**(1): p. 13-20.
4. Lindstrom, S.E., N.J. Cox, and A. Klimov, *Genetic analysis of human H2N2 and early H3N2 influenza viruses, 1957-1972: evidence for genetic divergence and multiple reassortment events.* Virology, 2004. **328**(1): p. 101-19.
5. Viboud, C., et al., *Global Mortality Impact of the 1957-1959 Influenza Pandemic.* J Infect Dis, 2016. **213**(5): p. 738-45.
6. Reneer, Z.B. and T.M. Ross, *H2 influenza viruses: designing vaccines against future H2 pandemics.* Biochem Soc Trans, 2019. **47**(1): p. 251-264.
7. Munster, V.J., et al., *Spatial, temporal, and species variation in prevalence of influenza A viruses in wild migratory birds.* PLoS Pathog, 2007. **3**(5): p. e61.
8. Jones, J.C., et al., *Risk assessment of H2N2 influenza viruses from the avian reservoir.* J Virol, 2014. **88**(2): p. 1175-88.
9. Babu, T.M., et al., *Population Serologic Immunity to Human and Avian H2N2 Viruses in the United States and Hong Kong for Pandemic Risk Assessment.* J Infect Dis, 2018. **218**(7): p. 1054-1060.
10. de Graaf, M. and R.A. Fouchier, *Role of receptor binding specificity in influenza A virus transmission and pathogenesis.* EMBO J, 2014. **33**(8): p. 823-41.
11. Thompson, A.J. and J.C. Paulson, *Adaptation of influenza viruses to human airway receptors.* J Biol Chem, 2021. **296**: p. 100017.
12. Belser, J.A., J.M. Katz, and T.M. Tumpey, *The ferret as a model organism to study influenza A virus infection.* Dis Model Mech, 2011. **4**(5): p. 575-9.
13. Jayaraman, A., et al., *Decoding the distribution of glycan receptors for human-adapted influenza A viruses in ferret respiratory tract.* PLoS One, 2012. **7**(2): p. e27517.
14. Chen, G.L., et al., *Evaluation of replication and cross-reactive antibody responses of H2 subtype influenza viruses in mice and ferrets.* J Virol, 2010. **84**(15): p. 7695-702.
15. Pappas, C., et al., *Receptor specificity and transmission of H2N2 subtype viruses isolated from the pandemic of 1957.* PLoS One, 2010. **5**(6): p. e11158.
16. Chen, G.L., et al., *Evaluation of three live attenuated H2 pandemic influenza vaccine candidates in mice and ferrets.* J Virol, 2014. **88**(5): p. 2867-76.
17. Pappas, C., et al., *Assessment of transmission, pathogenesis and adaptation of H2 subtype influenza viruses in ferrets.* Virology, 2015. **477**: p. 61-71.
18. Bodewes, R., et al., *Pathogenesis of Influenza A/H5N1 virus infection in ferrets differs between intranasal and intratracheal routes of inoculation.* Am J Pathol, 2011. **179**(1): p. 30-6.
19. Kreijtz, J.H., et al., *Low pathogenic avian influenza A(H7N9) virus causes high mortality in ferrets upon intratracheal challenge: a model to study intervention strategies.* Vaccine, 2013. **31**(43): p. 4995-9.
20. de Jonge, J., et al., *H7N9 Live Attenuated Influenza Vaccine Is Highly Immunogenic, Prevents Virus Replication, and Protects Against Severe Bronchopneumonia in Ferrets.* Mol Ther, 2016. **24**(5): p. 991-1002.

21. Zhou, B., et al., *Single-reaction genomic amplification accelerates sequencing and vaccine production for classical and Swine origin human influenza a viruses.* J Virol, 2009. **83**(19): p. 10309-13.
22. Shu, Y. and J. McCauley, *GISAID: Global initiative on sharing all influenza data - from vision to reality.* Euro Surveill, 2017. **22**(13): p. 30494.
23. *Fludb*. 18-10-2021]; Available from: www.fludb.org.
24. Tamura, K., G. Stecher, and S. Kumar, *MEGA11: Molecular Evolutionary Genetics Analysis Version 11.* Mol Biol Evol, 2021. **38**(7): p. 3022-3027.
25. Waterhouse, A.M., et al., *Jalview Version 2--a multiple sequence alignment editor and analysis workbench.* Bioinformatics, 2009. **25**(9): p. 1189-91.
26. Burke, D.F. and D.J. Smith, *A recommended numbering scheme for influenza A HA subtypes.* PLoS One, 2014. **9**(11): p. e112302.
27. de Jonge, J., et al., *H7N9 influenza split vaccine with SWE oil-in-water adjuvant greatly enhances cross-reactive humoral immunity and protection against severe pneumonia in ferrets.* NPJ Vaccines, 2020. **5**(1): p. 38.
28. van de Ven, K., et al., *Pathology and Immunity After SARS-CoV-2 Infection in Male Ferrets Is Affected by Age and Inoculation Route.* Frontiers in Immunology, 2021. **12**.
29. Isakova-Sivak, I., et al., *Development and pre-clinical evaluation of two LAIV strains against potentially pandemic H2N2 influenza virus.* PLoS One, 2014. **9**(7): p. e102339.
30. Du, W., et al., *The 2nd sialic acid-binding site of influenza A virus neuraminidase is an important determinant of the hemagglutinin-neuraminidase-receptor balance.* PLoS Pathog, 2019. **15**(6): p. e1007860.
31. Guo, H., et al., *Kinetic analysis of the influenza A virus HA/NA balance reveals contribution of NA to virus-receptor binding and NA-dependent rolling on receptor-containing surfaces.* PLoS Pathog, 2018. **14**(8): p. e1007233.
32. R Core Team, *R: A Language and Environment for Statistical Computing*. 2021, R Foundation for Statistical Computing.
33. Wickham, H., et al., *Welcome to the Tidyverse.* Journal of Open Source Software, 2019. **4**(43): p. 1686.
34. Kassambara, A., *ggpubr: 'ggplot2' Based Publication Ready Plots*. 2020, CRAN.
35. Wickham, H., *ggplot2: Elegant Graphics for Data Analysis*. 2016, Springer-Verlag New York.
36. Liu, J., et al., *Structures of receptor complexes formed by hemagglutinins from the Asian Influenza pandemic of 1957.* Proc Natl Acad Sci U S A, 2009. **106**(40): p. 17175-80.
37. van de Ven, K., et al., *Systemic and respiratory T-cells induced by seasonal H1N1 influenza protect against pandemic H2N2 in ferrets.* Commun Biol, 2020. **3**(1): p. 564.
38. Bodewes, R., et al., *Infection of the upper respiratory tract with seasonal influenza A(H3N2) virus induces protective immunity in ferrets against infection with A(H1N1)pdm09 virus after intranasal, but not intratracheal, inoculation.* J Virol, 2013. **87**(8): p. 4293-301.
39. Ke, C., et al., *Human Infection with Highly Pathogenic Avian Influenza A(H7N9) Virus, China.* Emerg Infect Dis, 2017. **23**(8): p. 1332-1340.
40. WHO. *Cumulative number of confirmed human cases of avian influenza A(H5N1) reported to WHO*. 2020 [cited 2021 25-5-2021]; Available from: https://www.who.int/influenza/human_animal_interface/H5N1_cumulative_table_archives/en/.
41. Louria, D.B., et al., *Studies on influenza in the pandemic of 1957-1958. II. Pulmonary complications of influenza.* J Clin Invest, 1959. **38**(1 Part 2): p. 213-65.
42. Davenport, F.M. and A.V. Hennessy, *The clinical epidemiology of Asian influenza.* Ann Intern Med, 1958. **49**(3): p. 493-501.
43. Hers, J.F. and J. Mulder, *Broad aspects of the pathology and pathogenesis of human influenza.* Am Rev Respir Dis, 1961. **83(2)Pt 2**(2P2): p. 84-97.

44. Hers, J.F., N. Masurel, and J. Mulder, *Bacteriology and histopathology of the respiratory tract and lungs in fatal Asian influenza.* Lancet, 1958. **2**(7057): p. 1141-3.
45. Moore, I.N., et al., *Severity of clinical disease and pathology in ferrets experimentally infected with influenza viruses is influenced by inoculum volume.* J Virol, 2014. **88**(23): p. 13879-91.
46. Connor, R.J., et al., *Receptor specificity in human, avian, and equine H2 and H3 influenza virus isolates.* Virology, 1994. **205**(1): p. 17-23.
47. Xu, Q., et al., *Influenza H1N1 A/Solomon Island/3/06 virus receptor binding specificity correlates with virus pathogenicity, antigenicity, and immunogenicity in ferrets.* J Virol, 2010. **84**(10): p. 4936-45.
48. Jia, N., et al., *Glycomic characterization of respiratory tract tissues of ferrets: implications for its use in influenza virus infection studies.* J Biol Chem, 2014. **289**(41): p. 28489-504.
49. DiPiazza, A., et al., *Flow Cytometric and Cytokine ELISpot Approaches To Characterize the Cell-Mediated Immune Response in Ferrets following Influenza Virus Infection.* J Virol, 2016. **90**(17): p. 7991-8004.

3

Systemic and respiratory T-cells induced by seasonal H1N1 influenza protect against pandemic H2N2 in ferrets

Koen van de Ven[1], Femke de Heij[1], Harry van Dijken[1], José A. Ferreira[2], Jørgen de Jonge[1]

[1]Centre for Infectious Disease Control, National Institute for Public Health and the Environment (RIVM), Bilthoven, the Netherlands
[2]Department of Statistics, Informatics and Modelling, National Institute for Public Health and the Environment (RIVM), Bilthoven, The Netherlands.

Communications biology - 2020
https://doi.org/10.1038/s42003-020-01278-5

Abstract

Traditional influenza vaccines primarily induce a narrow antibody response that offers no protection against heterosubtypic infection. Murine studies have shown that T cells can protect against a broad range of influenza strains. However, ferrets are a more potent model for studying immune correlates of protection in influenza disease. We therefore set out to investigate the role of systemic and respiratory T cells in the protection against heterosubtypic influenza A infections in ferrets. H1N1-priming induced systemic and respiratory T cells that responded against pandemic H2N2 and correlated with reduced viral replication and disease. Especially CD8 T cell responses in the upper and lower respiratory tract were exceptionally high. We additionally confirmed that H2N2-responsive T cells are present in healthy human blood donors. These findings underline the importance of the T cell response in influenza immunity and prove that T cells are a potent target for future universal influenza vaccines.

Introduction

Influenza A virus (IAV) remains a threat to human health despite the availability of vaccines [1]. Traditional influenza vaccines mainly activate the humoral immune response against the surface proteins haemagglutinin (HA) and neuraminidase (NA; reviewed in [2]). However, HA and NA can mutate over time (antigenic drift) and multiple influenza strains can reassort to establish a new virus with altered HA and/or NA composition (antigenic shift; reviewed in [3]). Both antigenic drift and shift can lead to evasion of the antibody response. In contrast to surface proteins, the internal influenza proteins are far less subject to change and are highly conserved between influenza subtypes. Epitopes of internal IAV proteins can be recognized by T cells that can either kill virus-infected cells or assist in the development of adaptive immune responses (reviewed in [4, 5]).

The impact of influenza strains evading the human immune response is illustrated by the pandemic of H2N2 in 1957. After introduction into the human population the virus spread rapidly, leading to approximately 1-2 million deaths worldwide [6, 7]. Although H2N2 disappeared from the human population in 1968, there is a risk of reintroduction as associated-H2N2 strains still circulate in birds [8, 9]. Moreover, persons born after 1968 have not encountered H2N2 and will likely have no neutralizing antibodies against H2N2 [7, 10]. With the pandemic history of H2N2, a possible reemergence in humans should be taken into account.

T cells might offer protection if H2N2 reemerges. The Cleveland Family study already reported in 1958 that prior exposure to H1N1 influenza resulted in reduced disease in participants infected with H2N2 [11, 12]. This was independent of neutralizing antibodies, hinting towards a role for T cells. Later studies provided more evidence that T cells can protect against heterosubtypic IAV infections. Pre-existing influenza-specific CD8 T cells correlated with decreased disease burden during the H1N1 pandemic of 2009 [13] and were also found to contribute to recovery from H7N9 infection [14]. In a human challenge study, pre-existing CD4 T cells responding to internal influenza proteins were associated with reduced virus shedding and disease upon infection with seasonal H1N1 and H3N2 [15].

Animal studies provided additional proof that T cells are essential for heterosubtypic immunity. In ferrets, prior exposure to influenza protected against heterosubtypic infections with H1N1 [16], H3N2 [17] or H5N1 [18], which was likely mediated by T cells. Murine research demonstrated that T cells in general (reviewed in [19]) – and especially tissue-resident memory T cells (Trm) [20-23] – are crucial for protection against heterosubtypic IAV infections. Trm is a population of non-circulating T cells that is located near the site of infection and can respond rapidly upon (recurring) infections with the production of cytokines and killing of infected cells (reviewed

in [24]). Trm have also been identified in human lungs [25-29], but the availability of tissue and ethical concerns are hindering a more in-depth investigation.

The role of T cells in influenza infections is often studied in murine models, which offer a wide variety of techniques and reagents but are limited as an influenza model. Mice do not display the traditional disease symptoms (fever, sneezing, etc.) of an influenza infection and virus strains often require adaptation to increase virulence in mice [30]. Hence extrapolation to humans is difficult and it is unknown how well the findings from murine studies translate to humans. In contrast, ferrets show typical symptoms of influenza disease and are susceptible to both avian and human influenza strains. Ferrets are therefore considered the best small animal model for predicting IAV disease outcome in humans [31]. Elucidating influenza T cell responses in the ferret model can bridge the gap between murine and human research, thereby facilitating the development of improved influenza vaccines.

Although reagents for the ferret model are still scarce, we recently developed techniques to study (respiratory) T cell responses in IAV infections. Due to this we had the unique opportunity to investigate the role of systemic and respiratory T cells in the protection against H2N2 infection in ferrets. We show that priming with seasonal influenza H1N1 (A/California/07/2009) induced a T cell response that could reduce H2N2 (A/Singapore/1/57) viral replication and disease. H1N1-induced T cells responded to H2N2 and both systemic and respiratory T cell responses were boosted by heterosubtypic H2N2 infection. Respiratory CD8 T cell responses were especially high, even without prior H1N1-priming. Importantly, a group of healthy human donors that was too young to have been into contact with H2N2, displayed responses to H2N2 peptide pools. Together, these results argue that T cells induced by infections with seasonal influenza strains can contribute to protection against pandemic H2N2 infections. Future influenza vaccination strategies should take into account that inducing or boosting T cell responses can protect against heterosubtypic influenza infections.

Materials & Methods

Ethical statement

The experiment was approved by the local Authority for Animal Welfare of the Antonie van Leeuwenhoek terrain (Bilthoven, The Netherlands) under permit number AVD3260020184765 of the Dutch Central Committee for Animal experiments. All procedures were conducted according to EU legislation. Ferrets were examined for general health on a daily basis. If animals showed severe disease according to the defined end points prior to scheduled termination they would be euthanized by cardiac bleeding under anesthesia with ketamine (5 mg/kg; Alfasan) and medetomidine (0.1 mg/kg; Orion Pharma). Endpoints were scored based on clinical

parameters for activity (0 = active; 1 = active when stimulated; 2 = inactive and 3 = lethargic) and impaired breathing (0 = normal; 1 = fast breathing; 2 = heavy/stomach breathing). Animals were euthanized when they reached score 3 on activity level (lethargic) or when the combined score of activity and breathing impairment reached 4.

Viruses

A/California/07/2009 (H1N1) and A/Switzerland/97-15293/2013 (H3N2) influenza viruses were obtained from the National Institute for Biological Standards and Control (NIBSC, London, England). A/Singapore/1/57 (H2N2) influenza virus was kindly donated by the Institute of Experimental Medicine (IEM, St Petersburg, Russia). All experiments involving H2N2 virus were carried out under BSL-3 conditions. Influenza viruses were grown on MDCK cells in MEM medium (Gibco; Thermo Fisher Scientific) supplemented with 40µg/ml gentamicin, 0.01M Tricine and 2µg/ml TPCK treated trypsin (all from Sigma-Aldrich). At >90% cytopathic effect (CPE), the suspension was collected and spun down (4000x g for 10 minutes) to remove cell debris. H1N1 and H3N2 viruses were sucrose purified on a discontinuous 10-50% sucrose gradient. Due to restrictions inherent with the BSL-3 regime, H2N2 virus suspension was not sucrose purified. Instead, virus suspensions were washed twice on Amicon 100kD Ultra-15 filter units (Merck) with MEM medium. Wild-type mumps virus (MuVi/Utrecht.NLD/40.10; genotype G) [32] was multiplied on Vero cells in DMEM (Gibco) with 2% fetale bovine serum (FBS; HyClone, GE Healthcare). Supernatant of the infected Vero cells was centrifuged at 500x g and subsequently filtered (5um pore size). All virus aliquots were stored at -80°C.

Animal handling

Animals were housed by subgroup in open cages. From the moment of infection till 14 days after, all groups were housed in BSL-3 level isolators. Animals were visually inspected each day and received food and water *ad libitum*. For the placement of temperature transponders animals were anesthetized with ketamine (5 mg/kg) and medetomidine (0.1 mg/kg) with 0.2 ml Buprenodale (AST Farma) as a post-operative analgesic. Anaesthesia was antagonized with atipamezole (0.25 mg/kg; Orion Pharma). Blood collection from the vena cava on days 0, 14 and 28 happened under similar conditions but without post-operative analgesic. For (mock)-infections, anaesthesia likewise consisted of ketamine and medetomidine, but atipamezole administration was delayed by 30 minutes to avoid excretion of the inoculum by sneezing and coughing. Weight determinations and swabbing occurred under anaesthesia with ketamine alone and did not require an antagonist.

Study design

Outbred female ferrets (Schimmel b.v.) aged 18-20 months arrived at the Animal Research Centre (Bilthoven, The Netherlands) at least three weeks before

commencement of the study for acclimatization. Each treatment/control group consisted of six animals. For practical reasons the experiment was divided into two sub-experiments – named 'A' and 'B' – with each three animals per group. The animals were semi-randomly distributed by weight. Although there were no evident differences between results of the experiments A and B, the statistical analyses used blocking by experiments in order to correct for possible time effects (see 'Statistics' section below).

Animals received temperature transponders (Star Oddi) in the intra peritoneal cavity two weeks before start of the experiment, which recorded body temperature every 30 minutes. On day 0, two groups were mock-primed intra nasally (i.n.) with PBS ('control' and 'non-primed' groups). A third group was primed with 10^6 $TCID_{50}$ H1N1 i.n. ('H1N1-primed' group). After four weeks, non-primed and primed groups were infected i.n. with 10^6 $TCID_{50}$ H2N2 while the control group received a mock-infection i.n. with PBS. For both H1N1 and H2N2 infections, inoculum was administered in 0.1 ml. Prior to infection and on days 2, 4, 7 and 14 after infection, viral nose and throat swabs were collected and animal weight was measured. At the end of the experiment, animals were euthanized by heart puncture and heparin blood and serum was collected. The lungs were then perfused and broncho-alveolar lavage (BAL) was collected by flushing the lungs twice with 30ml of room temperature RPMI1640 (Gibco, Thermo Fisher). Heparin blood and BAL were used the same day. The spleen, lungs and nasal turbinates were collected in RPMI1640 and stored overnight at 4°C. Serum was isolated by centrifugation of clotted blood at 2000x g for 10 minutes and stored at -20°C until further use.

Lung perfusion

Tubing for manual artificial breathing was inserted via an incision in the trachea followed by opening of the chest. A cannula was inserted into the pulmonary artery via an incision in the right ventricle. The abdominal aorta was cut below the junction with the hepatic aorta to allow flushing of the cardiovascular system. Via the cannula the lungs were perfused with physiological saline (B Braun) until the lungs appeared white and a colorless liquid ran from the abdominal aorta.

Lymphocyte isolation

Blood was collected in sodium-heparin coated Vacutainers (BD) and diluted 1:1 with PBS (Gibco) for density centrifugation on a 1:1 mixture of LymphoPrep (1.077 g/ml, Stemcell) and Lympholyte-M (1.0875 g/ml, Cedarlane). Cells were spun down for 30 minutes at 800x g (RT) and the interphase was washed twice using washing medium (RPMI1640 + 1%FBS). The cells were collected in stimulation medium (RPMI1640 + 10% FBS + 1x penicillin-streptomycin-glutamine [Gibco]) and counted using a hemocytometer.

Spleens were homogenized in a sieve using the plunger of a 10mL syringe after which the suspension was collected in a 50 ml tube. The tube was gently inverted to mix the suspension after which the tube was left for 1-2 minutes to let the larger debris sink. The upper 40ml of cell suspension was transferred to another tube and centrifuged for 5 min at 500x g. The pellet was resuspended in EDTA-supplemented washing medium (RPMI1640 + 1% FBS + 2mM EDTA (Invitrogen)) and put over a 100µm cell strainer. The resulting suspension was layered on top of Lympholyte-M and density centrifugation was performed in a similar manner as described for blood. All washing steps were performed with EDTA-supplemented medium to prevent agglutination of cells.

BAL was washed twice with washing medium and resuspended in stimulation medium for further use. Lungs were processed into small cubes of approximately 5mm^3 and digested in 12ml of collagenase I (2.4mg/ml, Merck) and DNase I (1mg/ml, Novus Biologicals) for 30 minutes at 37°C while rotating. Following this, samples were further homogenized in a sieve using a 10 mL plunger and subsequently washed with EDTA-supplemented washing medium. The suspension was then filtered over a 70µm cell strainer and used for density centrifugation similar to the spleen.

Nasal turbinates (NT) were gently mashed in a sieve and subsequently filtered over a 70µm cell strainer. The resulting suspension was rested for 1 minute to allow the cartilage fragments to sediment. The suspension – excluding the sedimented cartilage fragments – was transferred to another tube and washed twice with EDTA-supplemented washing medium. The cells were then resuspended in 40% Percoll (GE Healthcare) and layered on top of 70% Percoll. Samples were centrifuged for 20 minutes at 500x g after which the interphase was collected and washed twice with EDTA-supplemented washing medium. Lymphocytes were resuspended in stimulation medium for further use.

H2N2 peptide pools

PepMix™ peptide pools for T cell stimulation assays were obtained from JPT Peptide Technologies GmbH. Each pool contained 15 amino acids long peptides with an overlap of 11 amino acids spanning an entire protein of the internal influenza proteins of the H2N2 A/Leningrad/134/17/1957 strain. The sequence identity between A/Leningrad/134/17/1957 and A/Singapore/1/57 is ≥ 98% for all proteins, excluding NA and HA. The peptides were synthesized by FMOC-chemistry using a peptide synthesizer and analyzed by LC-MS. Before use, freeze-dried peptide pools were dissolved in DMSO, aliquoted and stored at -20°C. On the day of use, peptide pool aliquots were thawed and diluted with stimulation medium. The peptide pool suspension was added to cells such that a final peptide concentration of 1µg/ml per peptide with a DMSO concentration of less than 0.2% was achieved.

IFNγ responses by flow cytometry

1-3 million lymphocytes were stimulated with virus at MOI 1 for 24 hours or H2N2 peptide pools for 8 hours. For the last 6 hours of stimulation, Brefeldin A (Golgiplug, BD) was added to the cells, followed by storage o/n at 4°C. The next day, cells were washed twice with FACS buffer (2mM EDTA, 0.5% BSA in PBS) and extracellular staining was performed in 100µl FACS buffer with live-dead aqua (Invitrogen), α-CD4-APC (02, Sino Biological) and α-CD8a-eFluor450 (OKT8, eBioscience) for 30 minutes at 4°C. After washing, cells were fixated and permeabilised with Foxp3/Transcription factor staining buffer set (eBioscience) according to the manufacturers protocol. Cells were then stained intracellularly with α-CD3e-FITC (CD3-12, Biorad), α-CD79a-APC/eFluor780 (eBioscience) and α-IFNγ-PE (CC302, Bioconnect) for 30 minutes at 4°C. After washing twice, the pellet was resuspended in FACS buffer and measured on a LSR Fortessa X-20 (BD). Data was analyzed using FlowJo™ Software V10 (BD) and an example of the gating strategy is presented in Supplemental Fig. 4a.

Cell counts by flow cytometry

To reduce cell loss inherent to washing and centrifugation steps during staining, NT and BAL samples were stained using the non-centrifugation PerFix-NC kit (Beckman Coulter) according to the manufacturers protocol. In brief, cells were stained with α-CD4-APC, α-CD8a-eFluor450, and α-CD14-PE (Tük4; Thermo Fisher) for 30 minutes at RT. Subsequently, cells were fixated with 25µl Fixative Reagent for 15 minutes followed by permeabilization by the addition of 300µl of Permeabilizing Reagent containing α-CD3e-FITC and α-CD79a-APC/eFluor780. Cells were intracellularly stained for 30 minutes at RT, after which 3ml of Final Reagent was added to each tube. To concentrate the cells the tube was spun down (500x g, 5 min) and 2.5ml of the liquid was discarded while the pellet was resuspended in the remaining volume. 50µl of Coulter Flow-Count Fluorospheres (Beckman Coulter) was added to each sample and the sample was vortexed just before measurement on a LSR Fortessa X-20. Data was analyzed using FlowJo™ Software V10 (BD) and an example of the gating strategy is presented in Supplemental Fig. 4b.

ELISpot

Pre-coated Ferret IFNγ-ELISpot (ALP) plates (Mabtech) were used according to the manufacturers protocol. Lymphocytes were stimulated with live virus (MOI 1 or 0.1) or H2N2 peptide pools in ELISpot plates at 37°C. Per well, 250K cells (PBMC, splenocytes), 125K cells (nasal turbinates), 62.5K cells (lung lymphocytes) or undiluted cell suspension (BAL) was added. After 20 hours the plates were developed according to the manufacturers protocol, with the modification that the first antibody staining was performed overnight at 4°C. Plates were left to dry for 2-3 days after which they were packaged under BSL-3 conditions and heated to 65°C for 3 hours to inactivate any remaining infectious influenza particles. Analysis of ELISpot plates was performed using the ImmunoSpot® S6 CORE (CTL, Cleveland, OH).

Virus titer analysis
Nose and throat swabs were collected in 2 ml transport medium containing 15% sucrose (Merck), 2.5µg/ml Amphotericin B, 100 U/ml penicillin, 100µg/ml streptomycin and 250µg/ml gentamicin (all from Sigma) and stored at -80°C. For analysis, swabs were thawed, vortexed, serially diluted and tested in 6-plo on MDCK cells. CPE was scored after 5 days of culturing and $TCID_{50}$ values were calculated using the Reed & Muench method.

ELISA
Immulon 2 HB 96-well plates (Thermo Fisher) were coated overnight at RT with 100µl/well recombinant H2-protein of A/Singapore/1/57 (0.5µg/ml; BEI Resources; NR-2668). Sera were 2-fold serially diluted in PBS supplemented with 0.1% Tween-80, incubated on the coated plates for 60 minutes at 37°C and subsequently washed thrice with 0.1% Tween-80. HRP-conjugated goat anti-ferret IgG (Alpha Diagnostic) was diluted 1:5000 in PBS containing 0.1% Tween-80 and 0.5% Protivar (Nutricia) and used to stain H2 bound antibodies for 60 minutes at 37°C. Plates were then washed thrice with 0.1% Tween-80 to remove residual antibodies and once with normal PBS to remove Tween-80. Plates were developed for 10 minutes with SureBlue™ TMB (KPL) substrate, after which development was stopped by the addition of 100µl 2M H_2SO_4 per well. OD_{450}-values were determined on the EL808 absorbance reader (Bio-Tek Instruments) and individual curves were visualized using local polynomial regression fitting with R software [33].

Serological analysis
Hemagglutination inhibition (HAI) titers in ferret sera were determined according to WHO guidelines [34]. In brief, sera were heat-inactivated at 56°C for 30 minutes, treated with receptor destroying enzyme (Sigma) and tested in duplicate against four hemagglutinating units of H1N1 or H2N2 using 1% turkey red blood cells (bioTRADING Mijdrecht).

Human blood donors
Buffy coats from healthy individuals born after 1968 were obtained from the Dutch blood bank (Sanquin, Netherlands). Donors provided written informed consent and the study was approved by the Medical Ethics Committee of Sanquin Blood Supply. PBMCs were isolated by density centrifugation as described before [35] and stored at -135°C till further use. Samples were thawed, resuspended in stimulation medium and rested for 3 hours at 37°C. ELISpot plates were coated with the Human IFN-γ ELISpot^{BASIC} kit (Mabtech) and stimulations were performed as described above with 400K PBMCs per stimulus.

Influenza A sequence and epitope analysis

Protein sequences of influenza A subtypes were retrieved from the GISAID database [36] (www.gisaid.org [accessed 9-4-2019]) and aligned against A/California/07/2009 using the online NIH protein blast tool. For the epitope analysis, influenza A epitopes were retrieved from the Immune Epitope Database and Analysis Resource [37] (IEDB; www.iedb.org [accessed on 25-9-2019]). A search for linear, MHC class-I restricted and assay-confirmed epitopes yielded a total of 849 epitopes for all influenza A proteins. After exclusion of non-unique epitopes and alignment against A/California/07/2009 using R software [33], a total of 343 epitopes was found to be present in proteins of A/California/07/2009. These 343 epitopes were subsequently mapped against the proteins of A/Singapore/1/57 to determine if these epitopes were conserved between strains.

Statistics and Reproducibility

The experiment was divided into two subgroups, A and B, for practical reasons. Although we did not see evident differences between experiments A and B, we included the experimental subgroup as a blocking factor in our analysis. In brief, differences between groups were analyzed using R software [33] and images were visualized with the R package ggplot2 [38]. Treatment groups, namely H1N1-primed and Non-primed, were compared by means of the permutation test for differences in group averages with experiment (time) as block implemented in the R package coin [39], with p-values estimated by 10,000,000 simulations. Assays analyzed by this method include $TCID_{50}$ determinations on MDCK cells sampled from the throat and from the nose at days 30 and 32, and with respect to weight at days 30, 32, 35 and 42. The same test was used to compare the two treatment groups and each treatment group with the placebo group with respect to the following endpoints: maximum temperature between days 28-38, infiltration of CD8 T cells in the BAL and NT, percent IFNγ+ cells within CD4 and in CD8 T cell population sampled from spleen, lungs and PBMC, IFNγ-spot counts for lungs and PBMC. The results of the tests were corrected for multiple testing by using the Benjamini-Hochberg method [40] at a nominal false discovery rate (FDR) of 10%. Only the results that passed the correction have been reported as findings in the results section, which, roughly speaking, means that at most 10% of our findings are likely to be spurious. Associations between IFNγ-spot count and CD8 T cell numbers were tested by using Pearson's correlation coefficient.

Results

H1N1 immunity reduces H2N2 viral replication and disease

Infection with circulating IAV might partially protect against H2N2 influenza strains by inducing T cells that recognize shared epitopes (hereafter called 'cross-reactive T cells'). To estimate the likelihood of shared epitopes, we first assessed the level of protein identity between IAV subtypes.

Viral protein sequences from early human and recent avian H2N2 isolates were retrieved from influenza database GisAid [36] and aligned against recently circulating A/California/07/2009 (hereafter called H1N1). While HA (<65%) and NA (<44%) are poorly conserved, most internal proteins retain >90% sequence identity (Fig. 1a). We then determined how many human CD4 and CD8 T cell epitopes were conserved

a

Type	Host	Virus	HA	NA	NP	NS1	NEP	PA	PB1	PB2	M1	M2
H1N1	Human	A/California/07/2009	100	100	100	100	100	100	100	100	100	100
H3N2	Human	A/Switzerland/9715293/2013	42.8	43.2	89.8	77.6	89.3	93.0	97.1	94.1	92.1	84.5
H2N2	Human	A/Singapore/1/57	63.6	42.9	91.8	82.2	89.3	94.8	96.8	95.7	94.8	85.6
H2N2	Human	A/Korea/426/1968	63.6	43.1	91.0	80.8	89.3	94.6	96.0	95.3	94.4	85.6
H2N2	Human	A/Victoria/5/1968	63.4	43.1	91.2	81.3	89.3	94.7	96.2	94.9	94.0	84.5
H2N2	Avian	A/mallard/Iowa/10OS2721/2010	64.9	42.9	94.4	84.0	90.9	97.1	97.1	97.5	96.4	94.8
H2N2	Avian	A/mallard_duck/Netherlands/33/2011	64.8	43.5	94.4	68.5	78.5	97.1	96.7	97.5	96.4	92.8
H2N2	Avian	A/turkey/Connecticut/15-009905-1/2015	64.6	42.5	94.0	67.6	81.0	96.4	96.2	97.5	96.8	89.7
H2N2	Avian	A/quail/Connecticut/16-016726-1/2016	64.8	42.5	93.4	67.1	81.0	96.0	96.2	97.4	96.4	90.7

b

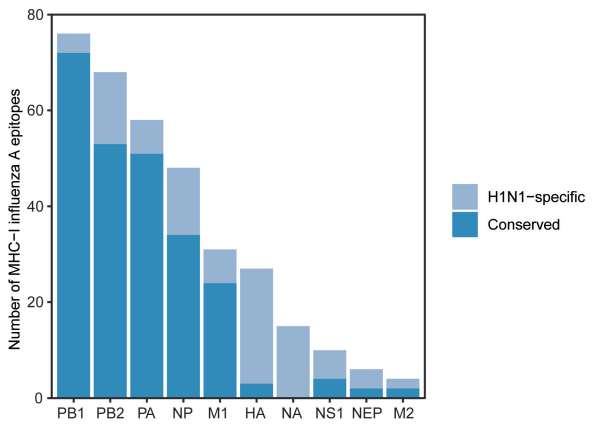

Figure 1: Epitopes are conserved between H1N1 and H2N2 influenza A subtypes. a) Sequence identity of influenza A proteins between different H1N1, H2N2 and H3N2 strains. Sequence identity is expressed as per cent amino acid overlap with A/California/07/2009 (H1N1). As H1N1 does not express PB1-F2, all PB1-F2 sequences have been excluded from analysis. **b)** Influenza epitopes presented by human MHC class I were mapped against the protein sequence of H1N1 and A/Singapore/1/57 (H2N2). Conserved epitopes (dark blue) are present in both H1N1 and H2N2, while H1N1-specific epitopes (light blue) are only present in H1N1.

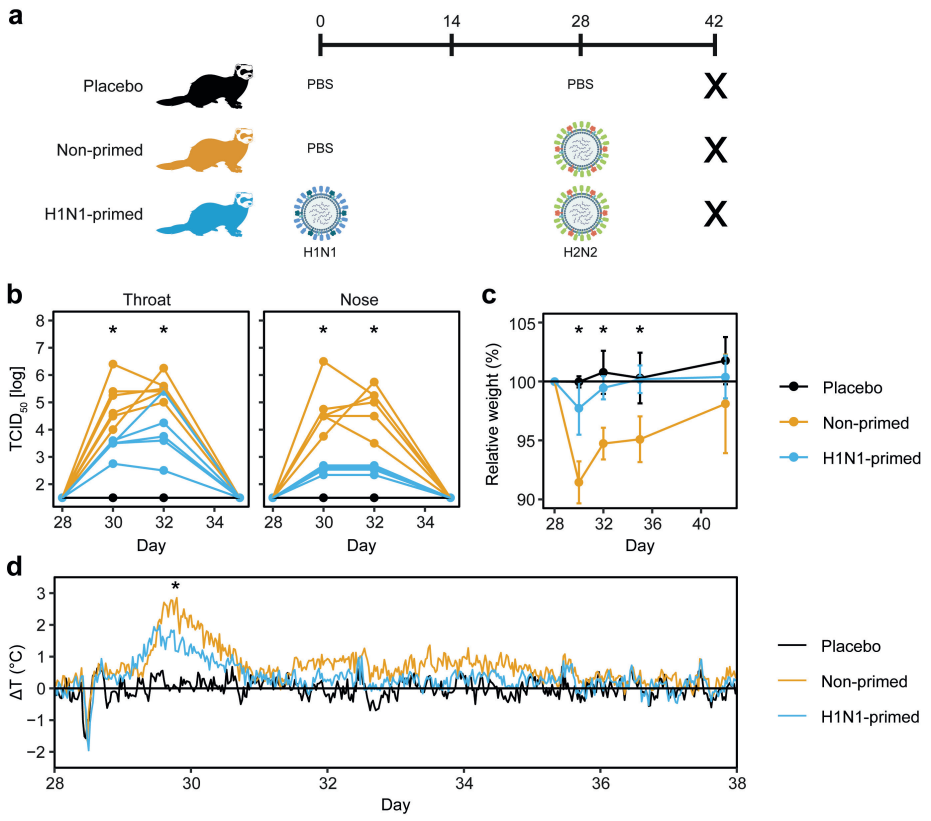

Figure 2: H2N2 viral replication and disease manifestation are reduced by prior H1N1 priming. a) Outline of the study. Ferrets were primed with H1N1 (A/California/07/2009) or received PBS on day 0. Subsequently, both primed and non-primed animals were infected with H2N2 (A/Singapore/1/57) on day 28. The placebo group received PBS on both occasions. All animals were euthanized on day 42 to analyze T cell responses. **b)** Viral replication in throat and nose of H2N2-infected ferrets prior to infection (day 28) and 2, 4 and 7 days after infection (days 30, 32 and 35 respectively). Lines depict individual ferrets (n = 6). **c)** Relative changes in weight from the moment of H2N2 infection until the end of the experiment (n = 6). Data are displayed as mean ± SD. **d)** Temperature displayed as mean deviation from baseline in 30 minute intervals from the day of H2N2 infection until day 38 (n = 5-6). Baseline temperature was calculated as the average temperature over 4 days prior to H2N2 infection. * indicates significant differences ($p < 0.05$) between non-primed and H1N1-primed groups after correction for multiple testing. Panel A was created using Biorender.

between H1N1 and a pandemic H2N2 strain (A/Singapore/1/57; hereafter called H2N2) using the Immune Epitope Database [37]. Corresponding with the sequence identity, epitopes were relatively well conserved for internal IAV proteins, but not for HA and NA (Fig. 1b).

Based on the sequence identity between H1N1 and H2N2, we expect that cellular immunity induced by H1N1 priming can protect against H2N2 infection. To confirm this in a relevant influenza model, we intranasally primed six female ferrets with H1N1 or administered ferrets with PBS as a treatment control (day 0; Fig. 2a and Supplemental Fig. 1). When four weeks later both groups were infected with H2N2, animals primed with H1N1 showed decreased viral replication in the throat and nose (Fig. 2b). Correspondingly, weight loss and fever was less severe in primed animals (Fig. 2c, d). A control group that received PBS on both occasions showed baseline weight and temperature and no detectable viral replication. Together, these results confirm that immunity induced by H1N1 priming can protect against heterosubtypic H2N2 infection, as seen by reduced disease symptoms and viral replication.

H1N1-priming induces cross-reactive T cell responses

Next, we examined the role of humoral and cellular responses in the protection against H2N2 infection. H1N1-priming did not raise detectable hemagglutination inhibition (HI) or virus neutralisation (VN) titres against H2N2 (Fig. 3a, b). This shows that disease was not reduced by neutralization of virus particles. However, we did detect low levels of binding to recombinant H2-protein by ELISA, indicating that there was cross-reactivity of H1N1-induced antibodies with H2-protein (Supplemental Fig. 2). Importantly, the level of H2-binding antibodies after a single H1N1 infection was relatively low when compared to after H2N2 infection. When we measured IFNγ-responses in PBMCs by ELISpot prior to H2N2 infection, we observed not only responses to H1N1, but also against H2N2 in primed animals (Fig. 3c). PBMCs from these animals additionally responded against H3N2 influenza (A/Switzerland/97/15293/2013), but not against a nonspecific viral control (mumps), proving the observed responses were influenza-specific. These results are in agreement with prior findings that T cells respond to multiple influenza subtypes by recognizing conserved epitopes [41-43].

To determine the target-proteins of the T cell response, we stimulated PBMCs with peptide pools spanning the internal proteins of H2N2 and assessed IFNγ-responses by ELISpot. Following H1N1-priming, most responses were observed against NP (59% ± 26) and NS1 (22% ± 22) H2N2 peptide pools (Fig 3d, e). Virtually no responses against M2, NEP or PB-F2 were detected. Naïve animals did not respond to any of the H2N2 peptide pools (Supplemental Fig. 3).The high variability in responses between animals is likely in part due to MHC diversity in outbred ferrets. Despite this variation it is clear that H1N1-priming induced T cells that respond to internal proteins of H2N2.

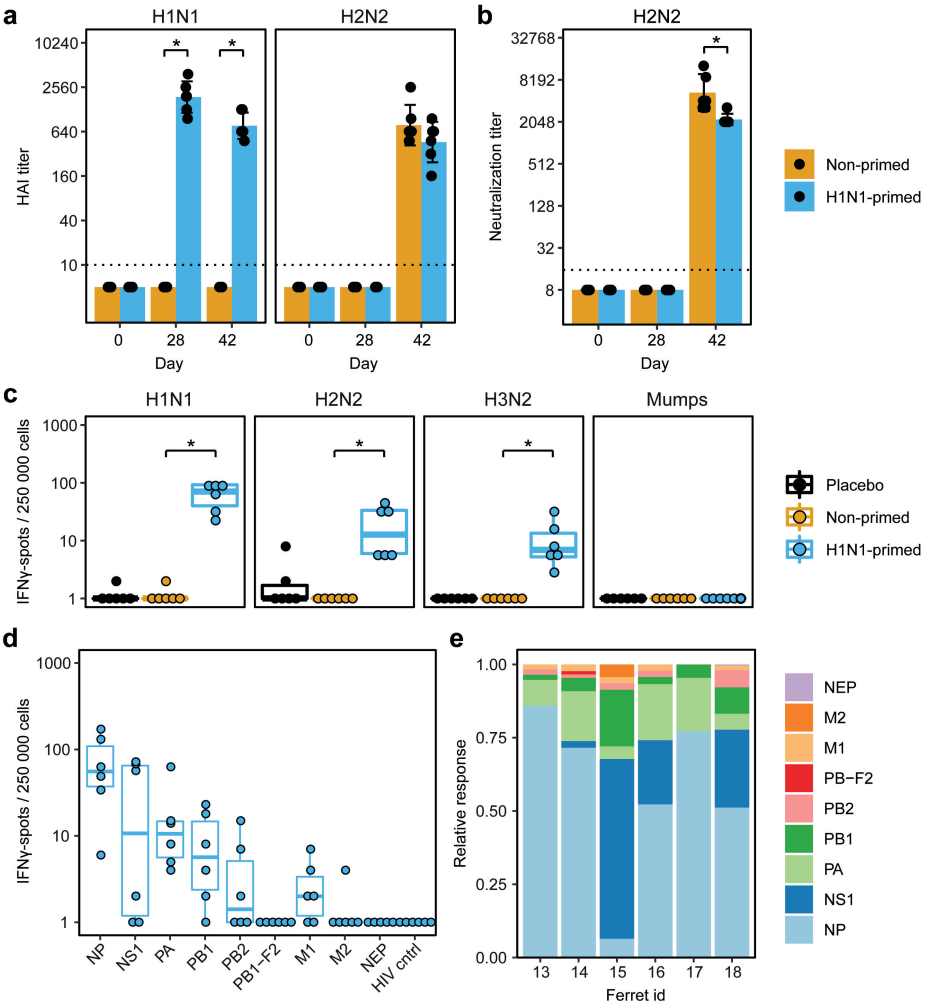

Figure 3: H1N1-priming induced H2N2-reactive T cells but no H2N2-neutralizing antibodies. a, b) Sera from primed and non-primed ferrets was tested for antibody responses against A/California/07/2009 (H1N1) and A/Singapore/1/57 (H2N2) before H1N1 priming (day 0), before H2N2 infection (day 28) and two weeks after H2N2 infection (day 42). Bars depict mean ± SD. **a)** Hemagglutination-inhibition (HAI) titers against H1N1 and H2N2. **b)** Virus neutralization titer against H2N2. **c, d, e)** IFNγ-responses by ELISpot after *ex-vivo* stimulation of PBMCs obtained 28 days after H1N1-priming. Responses are corrected for background signals (minus medium stimulation). **c)** Responses against H1N1, H2N2, A/Switzerland/97/2013 (H3N2) and mumps virus. **d)** Responses of H1N1-primed animals to peptide pools spanning the internal proteins of H2N2 and the control HIV gag protein. Non-primed and placebo animals were negative for all peptide pools tested but were left out for visualization purposes. **e)** For each ferret shown in d), relative responses against the different influenza proteins was calculated. Boxplots depict the median, 25% and 75% percentile, where the upper and lower whiskers extend to the smallest and largest value respectively within 1.5* the inter quartile ranges. In all plots n=6. * indicates significant differences ($p < 0.05$) between non-primed and H1N1-primed groups after correction for multiple testing.

H1N1 immunity results in higher CD8 T cell numbers in the airways upon heterosubtypic infection

Previous studies have shown that T cells residing in the respiratory tract are essential for the protection against heterosubtypic influenza infections [20, 21]. To assess whether respiratory T cells contributed to protection against H2N2 infection, we first determined absolute T cell numbers in the bronchoalveolar lavage (BAL) two weeks after H2N2 infection. Using a non-centrifugation staining protocol for flow cytometry, we found no difference in absolute CD4 T cell counts (Fig. 4a). However, CD8 T cell counts were significantly increased after H2N2 infection with the largest increase seen in primed animals (Fig. 4a, b).

We also investigated T cell numbers in nasal turbinates (NT), but due to the large variation in absolute cell counts that is inherent with creating a single cell suspension from tissue we could only analyse relative T cell numbers for NT. Similar to BAL, the NT of placebo animals contained few CD8 T cells (~3% of lymphocytes) and relative numbers were increased after H2N2 infection in non-primed ferrets (~12.5%; Fig. 4c). Again, we observed that the response in primed animals was substantially higher (~29.7%). Relative CD4 T cell numbers remained similar between groups (Fig. 4a).

Infiltrating T cells might be attracted due to inflammation without being responsive to IAV. By plotting the number of infiltrating CD8 T cells versus the number of IAV responsive cells determined by IFNγ-ELISpot, we can derive whether those infiltrating T cells are also IAV-responsive. As expected, increased CD8 T cell numbers in the BAL correlated with higher IFNγ-responses against IAV (Fig. 4d). Importantly, responses against H1N1, H2N2 and H3N2 all correlated with CD8 T cell influx, demonstrating that the infiltrating CD8 T cell population recognizes a broad range of IAV subtypes. Although we did not investigate the presence of T cells in the respiratory tract of H1N1-primed animals before H2N2 infection, we did find that a single influenza infection (with H2N2; Fig. 4b) is sufficient to induce respiratory T cells. Furthermore, respiratory T cell numbers were increased in H1N1-primed ferrets after H2N2 infection. This suggests that these T cells were at least in part induced by primary H1N1 infection, and that they responded to secondary H2N2 infection and likely contributed to reduced disease severity.

T cell responses in the lung are high but not boosted by heterosubtypic infection

To further dissect the T cell response in lung, we measured IFNγ-production in CD4 and CD8 T cells by flow cytometry after *ex vivo* stimulation with IAV. As lung tissue is rich in vasculature, we perfused the lungs with saline solution to reduce contamination by blood lymphocytes. After stimulation with H1N1, H2N2 or H3N2, CD8 T cells from infected animals responded strongly with up to 40% of all CD8 T cells being positive for IFNγ (Fig. 5a, b).

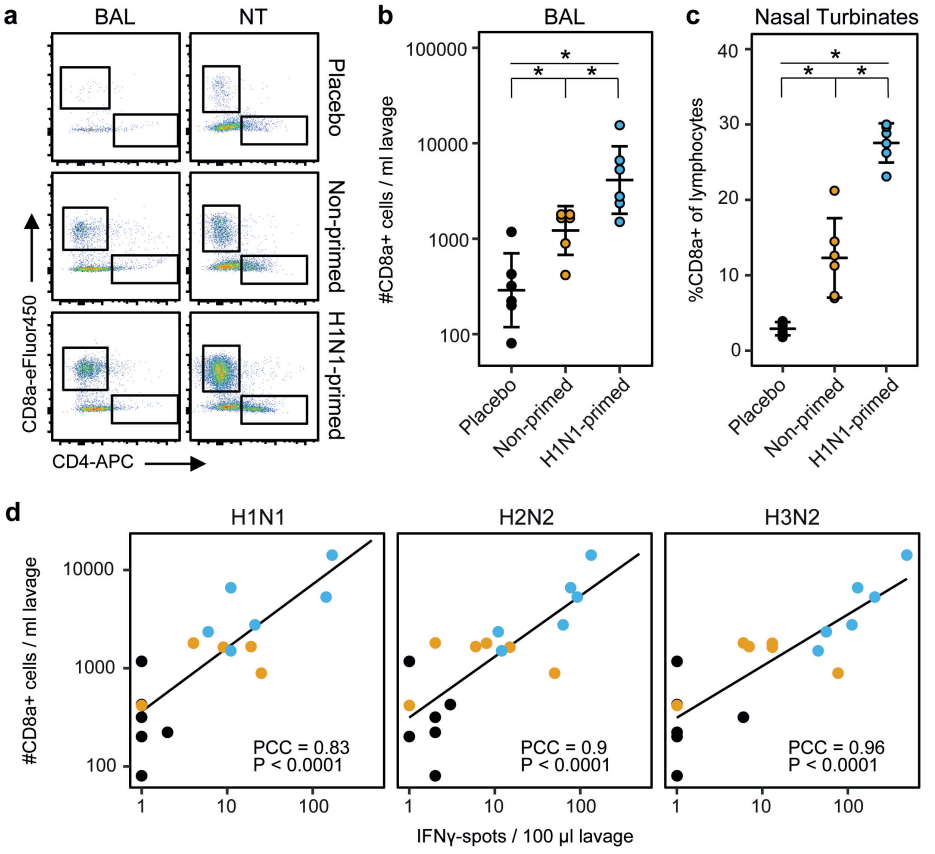

Figure 4: Pre-existing T cell immunity leads to increased infiltration of CD8 T cells into the respiratory tract upon heterologous influenza infection. a) Representative flow cytometry plots depicting the infiltration of CD4 and CD8 T cells in the BAL and nasal turbinates in ferrets two weeks after H2N2 infection (day 42). Cells were gated on lymphocytes; singlets; CD3+ and plotted as CD4-APC vs CD8a-eFluor450. **b)** Summary of absolute CD8 T cell numbers in the bronchoalveolar lavage (BAL) after H2N2 infection, displayed as geometric mean ± relative SD. **c)** Relative CD8 T cell number in the nasal turbinates two weeks after H2N2 infection. Percentages were calculated as number of CD8a+ cells within all lymphocyte singlets and are displayed as mean ± SD. **d)** Correlation between influenza-responsive lymphocytes and the influx of CD8 T cells in BAL on day 42. Absolute CD8a+ T cell numbers and IFNγ-responses towards several virus stimulations were assessed by flow cytometry and ELISpot respectively. The PCC indicates Pearson's correlation coefficient between spot count and number of CD8a+ T cells in BAL. * $p < 0.05$ after correction for multiple testing.

Interestingly, responses were similar between primed- and non-primed animals. As CD8 T cell responses in the lung are high even after primary infection, further boosting of the response might be inhibited to prevent excessive immunopathology. In comparison to the CD8 T cell compartment, CD4 T cell IFNγ-responses were smaller but noteworthy, with up to 10% of lung-derived CD4 T cells producing IFNγ. As virus stimulations induced some nonspecific IFNγ-responses in placebo animals, we also stimulated lung-derived T cells with a cocktail of peptide pools spanning NP, PA and NS1 proteins of H2N2 that elicited high responses in ELISpot assays (Fig. 3d). Stimulation with this peptide cocktail induced a clean T cell response with hardly any responses in placebo animals (Fig. 5c). The majority of responses was seen in the CD8 T cell compartment, with relatively few CD4 T cell responders.

In order to compare T cell responses between respiratory and systemic tissues, we additionally measured T cell response in blood and spleen. In contrast to the lung, average CD8 T cell responses after viral restimulation were clearly increased in the spleen of H1N1-primed animals compared to non-primed animals (Fig. 5d). Similar findings were seen for CD4 and CD8 T cells in the blood, but results were not significant due to the small group size (n = 3). Additionally, after stimulation with the H2N2 peptide cocktail, H1N1-primed animals displayed significantly increased CD4 and CD8 T cell responses in the spleen, with a similar trend for CD8 T cells in the blood (Fig. 5e). CD4 T cells hardly responded to peptide cocktail stimulation by producing IFNγ. Importantly, CD4 T cells might respond by producing other cytokines that we were unable to measure. Hence, we are likely underestimating the true contribution of the CD4 T cell compartment. These results suggest that a boost shortly after priming can improve systemic T cell responses, but hardly leads to increased T cells responses in lung tissue. Interestingly, CD8 T cells numbers were increased in the BAL and NT after heterosubtypic infection, indicating that there might be differences between the different sites of the respiratory system.

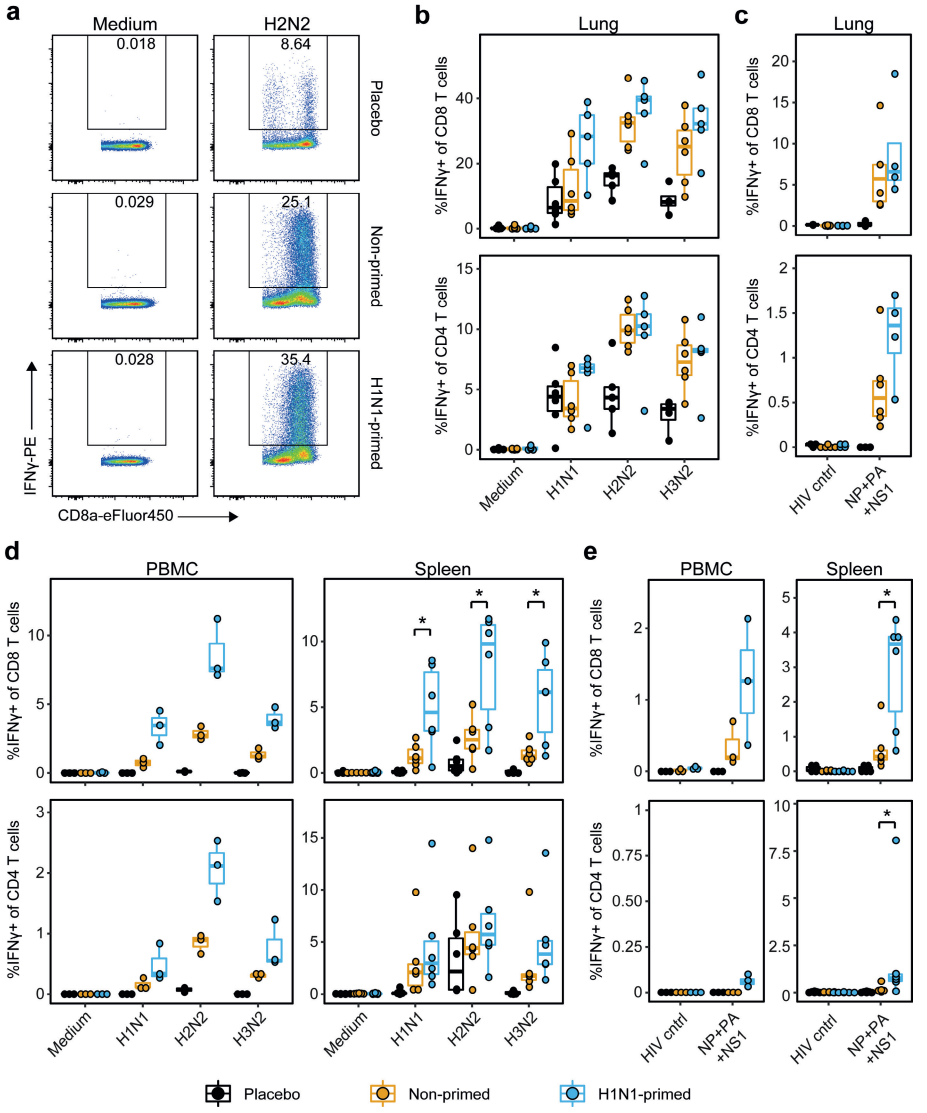

Figure 5: IFNγ-responses in the lung are high and only systemic responses are boosted by heterosubtypic H2N2 infection. Lymphocytes were isolated from blood, spleen and perfused lungs 14 days after H2N2 infection and stimulated for 6 (peptides) or 24 (viruses) hours. IFNγ-responses were then quantified by intracellular cytokine staining. **a)** Flow cytometry plot depicting IFNγ-responses in CD8 T cells after medium and H2N2 stimulation of lung lymphocytes. **b, c)** Percentage IFNγ-producing cells within the CD8 and CD4 T cell population after stimulation with (b) respective viruses or (c) a peptide cocktail spanning the NP, PA and NS1 proteins of H2N2 or HIV gag. **d, e)** Percentage IFNγ producing cells after stimulation of PBMCs or splenocytes with (d) virus or (e) H2N2 peptide cocktail. In panels b-e n = 3 for PBMC, n = 6

for spleen and n = 4-6 for lung. Boxplots depict the median, 25% and 75% percentile, where the upper and lower whiskers extend to the smallest and largest value respectively within 1.5* the inter quartile ranges. * indicates significant differences ($p < 0.05$) between non-primed and H1N1-primed groups after correction for multiple testing.

Pre-existing H1N1 immunity slightly alters the immune hierarchy of an H2N2 infection

As some internal IAV proteins are more conserved than others (Fig. 1a, b) we wondered whether priming could affect the response to individual H2N2 proteins after an H2N2 challenge. To test this, we measured the IFNγ-responses of primed and non-primed animals to IAV and H2N2 peptide pools by ELISpot. In agreement with our flow cytometric analysis, responses toward IAV stimulations were higher in the blood of primed animals, but not in the lungs (Fig. 6a). However, when we investigated responses to individual influenza proteins, differences between primed and non-primed animals were marginal (Fig. 6b). Out of all H2N2 peptide pools tested, only responses towards NS1 and possibly NP (n.s.) were higher in H1N1-primed animals. Interestingly, primed animals actually responded less well to PB1 and M2 peptide pools compared to non-primed animals. Although PB1-responses detected after H1N1-priming were boosted by H2N2 infection (Supplemental Fig. 3), the boost was minor and did not exceed the primary PB1-response seen upon a single H2N2 infection. H1N1-priming did not raise any responses to H2N2 M2 peptide pool (Fig. 3d, Supplemental Fig. 3) and while H2N2 infection induced responses to M2 peptide pool in non-primed animals, this was not the case for primed animals (Fig. 6b and Supplemental Fig. 3). Although most responses towards H2N2 peptide pools are similar between primed and non-primed animals, these results suggest that T cell responses can be skewed towards certain antigens by previous infections.

H2N2 cross-reactive T cells are present in human blood donors

We have shown that H1N1-priming can induce H2N2 cross-reactive T cells in an animal model. However, this is no guarantee that similar cross-reactivity exists in humans. To investigate whether cross-reactivity to H2N2 is also present in the human population, we measured IFNγ-responses to H2N2 peptide pools in PBMCs of 18 healthy donors (8 male, 10 female). All donors were born after 1968, when the H2N2 influenza subtype was no longer circulating. Strikingly, almost all donors responded to stimulations with NP, M1 and PB1 peptide pools, with some individuals additionally reacting to PA, PB2 and NS1 (Fig. 7). These findings show that H2N2 cross-reactive T cells are present in the human population. Based on earlier studies and our findings in the ferret model, these T cells have the potential to reduce H2N2 spread and disease, although their numbers may be too low in the general population. Boosting the responses by vaccination could therefore be a strategy to limit the consequences of newly introduced influenza subtypes such as H2N2.

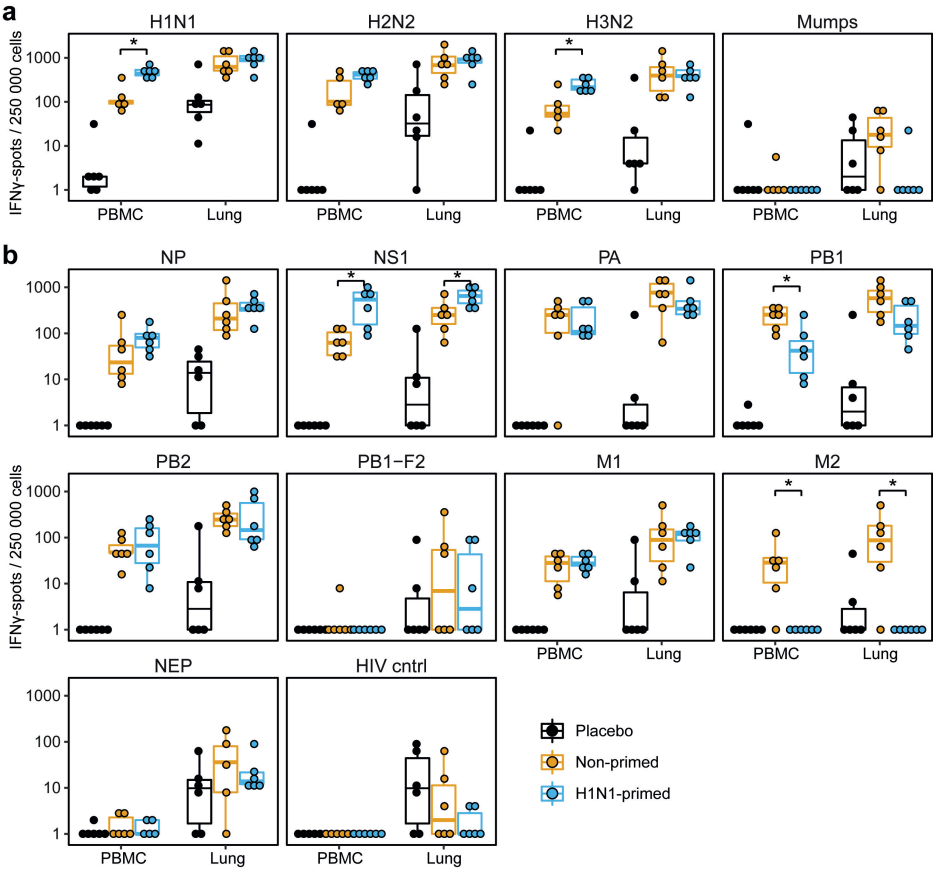

Figure 6: Primed animals show increased responses to influenza A virus. a, b) Lymphocytes isolated from blood or lung were stimulated with multiple influenza virus subtypes (a) or H2N2 peptide pools (b) in an ELISpot assay for 20 hours. Responses are corrected for background signals (minus medium stimulation). In all panels, n=5-6. Boxplots depict the median, 25% and 75% percentile, where the upper and lower whiskers extend to the smallest and largest value respectively within 1.5* the inter quartile ranges. * indicates significant differences ($p < 0.05$) between non-primed and H1N1-primed groups after correction for multiple testing.

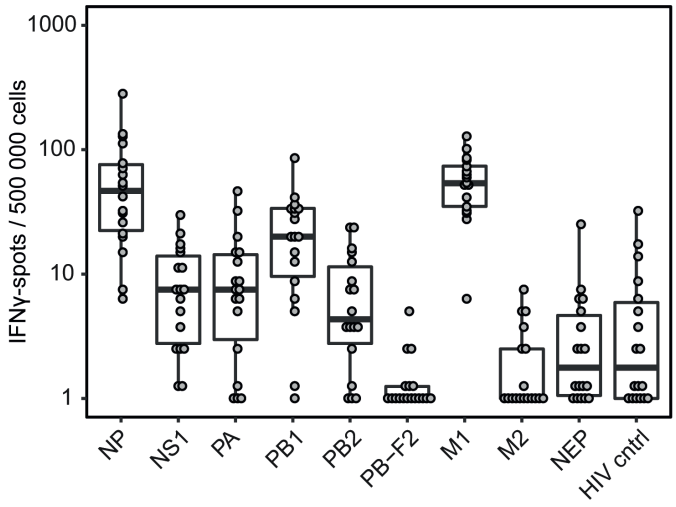

Figure 7: H2N2 cross-reactive T cells are present in human blood donors that were born after H2N2 stopped circulating. Frozen PBMCs from healthy human donors (n=18) were thawed and stimulated with peptide pools coding for the internal proteins of H2N2 or HIV gag in an ELISpot assay. Responses are corrected for background signal (minus medium stimulation). Boxplots depict the median, 25% and 75% percentile, where the upper and lower whiskers extend to the smallest and largest value respectively within 1.5* the inter quartile ranges.

Discussion

With this study we confirmed prior murine work in a more relevant model for influenza disease. We present evidence that (respiratory) T cells can protect against heterosubtypic influenza infection in the ferret model. Priming with H1N1 lead to reduced viral replication and disease upon H2N2 infection, which was associated with the presence of cross-reactive influenza-specific T cells in the blood before H2N2 infection. Correspondingly, H2N2 infection boosted the T cell responses that were evoked by H1N1-priming. This was illustrated by increased CD8 T cell numbers in the respiratory tract of primed animals and higher IFNγ-responses in spleen and blood. Importantly, we could confirm the finding that infection with other influenza subtypes can induce T cell responses to pandemic H2N2 in healthy human blood donors. By using both the ferret model and human blood donors, we partly mitigated the shortcomings that are associated with murine and human influenza studies.

The Cleveland Family study which ran from 1947-1957 reported that adults pre-exposed to H1N1 displayed reduced H2N2 disease [11, 12]. With our study we have clearly shown that H1N1 priming induces cross-reactive T cells and that they are associated with protection against H2N2 infection in ferrets. H2N2-responsive T cells are also present in our selection of human blood donors and it is thus likely that T cells

played a role in the protection against H2N2 observed in the Cleveland study. This stresses the importance of the T cell response in heterosubtypic influenza infections. Later studies with influenza-infected individuals extended the initial findings of the Cleveland Family study by showing that high numbers of IAV cross-reactive T cells in the blood correlate with improved clinical outcome in H1N1 [13, 15], H3N2 [15] and H7N9 [14] infections. Like the Cleveland study, these studies are however limited by the availability of tissue (mainly PBMCs) and the unknown infection history of subjects. The more fundamental questions regarding T cell immunity in influenza infections can therefore only be investigated in animal models.

Earlier ferret studies have shown that prior exposure to IAV can protect against heterosubtypic IAV infection [16-18, 44-49]. While some studies especially investigated the role of T cells in this protection, thus far none have addressed the involvement of CD4 and CD8 populations in multiple compartments of the respiratory tract in ferrets. This is especially important as tissue resident memory T cells (Trm) – a subset of T cells that are non-circulating and respond rapidly upon a (recurring) infection [21, 22] – can reduce disease severity and duration upon heterosubtypic infections [20, 21, 50, 51]. In order to study respiratory T cells, we set up a lung perfusion model, which enabled us to analyze a relatively pure population of lung-derived lymphocytes. Additionally, we developed techniques to isolate T cells from the upper respiratory tract (nasal turbinates), which have recently been attributed an important role in blocking dissemination of IAV infection to the lower respiratory tract [23]. These techniques allowed us to investigate the T cell response in respiratory tissues, although we lacked the reagents to determine whether these cells were also truly tissue-resident.

Unfortunately we could not investigate T cells in respiratory tissues of H1N1-primed animals before H2N2 infection. However, as a single H2N2 influenza infection induced a strong T cell response in the respiratory tract (Fig. 5), it is very likely that this was also the case for the H1N1 infection. Moreover, CD8 T cell numbers and T cell responses to H2N2 were higher in the respiratory tract of primed animals compared to non-primed animals (Fig. 4), indicating that T cells induced by H1N1 were boosted by H2N2 infection. These findings suggest that influenza-specific T cells were present in respiratory tissues of H1N1-primed ferrets at the time of H2N2 infection and that these cells are associated with reduced H2N2 disease severity.

We also investigated whether humoral immunity could have contributed to reduced H2N2 disease. HAI and VN assays did not indicate the presence of H2N2-neutralizing antibodies, although it is possible that H1N1-priming induced antibodies which protected against H2N2 by other modes of action. Indeed, in ELISA assays we found that H1N1-induced antibodies could bind to H2N2, albeit at low levels. The antibodies that we detected by ELISA might bind conserved domains in the HA head or stalk,

which can mediate protection against heterosubtypic influenza infections [52, 53]. However, others have shown that broadly-reactive HA-stalk targeting antibodies attain sufficiently high levels only after repeated vaccination or infection [54].

Although the ferret model is less cost-efficient than mice and is hampered by a lack of reagents, the strong resemblance to human influenza infection and disease is a strong motivation to develop the model further for performing studies on correlates of protection. This requires a more thorough understanding of how well the influenza-specific T cell response in ferrets resembles that of humans. In this study we showed that both H1N1-primed ferrets and healthy human donors display high responses against NP and intermediate responses against PA and NS1 H2N2 peptide pools. Responses against PB-F2, M2 and NEP were absent or very low in both ferrets and humans. M1 responses were high in human samples but low in H1N1-primed ferrets, although H2N2 infection did lead to higher responses (Fig. 6, Supplemental Fig. 3). This discrepancy might be caused by differences in infection history and/or MHC alleles. Improved understanding of ferret MHC composition and diversity is essential for understanding such similarities and differences between ferret and human T cell responses.

The current generation of influenza vaccines is focused on inducing HA-neutralizing antibodies. Subunit vaccines contain only HA and NA, while split vaccines additionally contain unknown or small amounts of other influenza A proteins [55, 56]. Whole inactivated virus (WIV) vaccines do contain a broader range of influenza proteins. However, inactivated vaccines in general do not infect cells or induce expression of viral proteins, which likely leads to a lower presentation of T cell epitopes and a reduced T-cell response. With rapid mutations in IAV surface proteins and the threat of pandemics, the use of vaccines that solely focus on humoral responses is an unviable approach. In addition, vaccination of children without prior exposure to influenza might hinder the development of heterosubtypic immunity when traditional inactivated influenza vaccines are used [18, 57]. Live attenuated influenza vaccine (LAIV) does infect cells and induce expression of viral proteins [56], but in recent years LAIV vaccination has yielded mixed results (reviewed in [58]). Hence, despite these developments we are still in dire need of improved influenza vaccines.

In the end, a successful influenza response requires both the humoral and cellular immune response, in which tissue-residency is an important factor. These branches of the immune system play different roles in the response against influenza and complement each other. As the main line of defense, neutralizing antibodies can prevent infection. Cross-reactive antibodies might additionally limit disease upon heterosubtypic infections. If an influenza strain still manages to escapes the humoral immune response, the cellular response can prevent severe disease and reduce viral replication by recognition of conserved epitopes. However, care should be taken to

prevent excessive immune activation which could lead to immunopathology [59]. Vaccines that support the interplay of cellular and humoral immunity while preventing excessive immune responses, could help us in reducing future morbidity, mortality and spread of seasonal and pandemic influenza infections.

Supplemental Tables & Figures

Supplemental data 1 and 2 can be accessed digitally at https://www.nature.com/articles/s42003-020-01278-5#Sec28

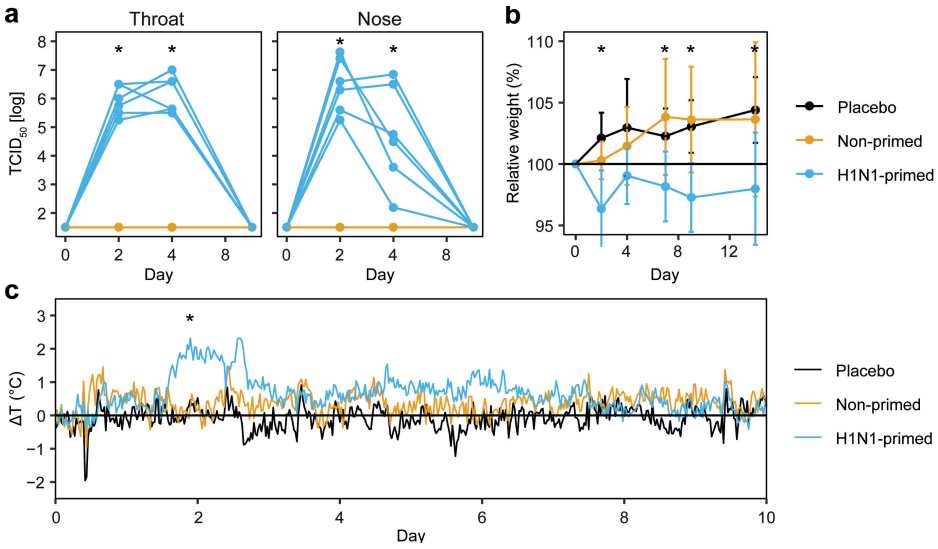

Supplemental Figure 1: H1N1 viral replication and disease manifestation. a) Viral replication in throat and nose prior to infection (day 0) and 2, 4 and 7 days after infection with A/California/07/2009 (H1N1). Lines depict individual ferrets (n = 6). **b)** Relative changes in weight from the moment of H1N1 infection until day 14 (n = 6). Data are displayed as mean ± SD. **c)** Temperature displayed as mean deviation from baseline in 30 minute intervals from the day of H1N1 infection until day 10 (n = 5-6). Baseline temperature was calculated as the average temperature over 4 days prior to H1N1 infection. * indicates significant differences ($p < 0.05$) between non-primed and H1N1-primed groups after correction for multiple testing.

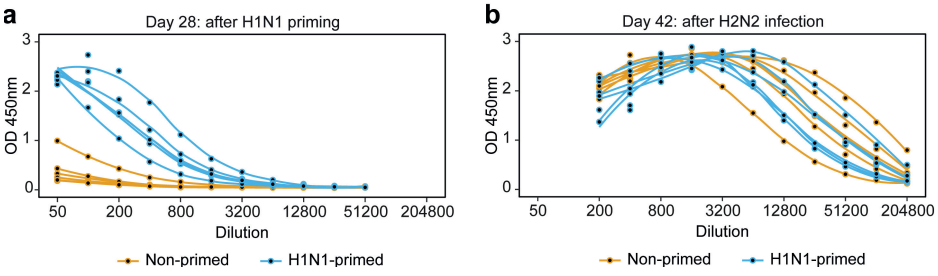

Supplemental Figure 2: H1N1-priming induces low levels of H2-cross reactive antibodies. Sera from ferrets collected at **a)** day 28 (after H1N1 priming) and **b)** day 42 (14 days after H2N2 infection) were tested by ELISA for the presence of H2-binding IgG. Lines depict the smoothed curves of individual animals, which were calculated with Local Polynomial Regression Fitting. Points depict the actual measurements per individual animal.

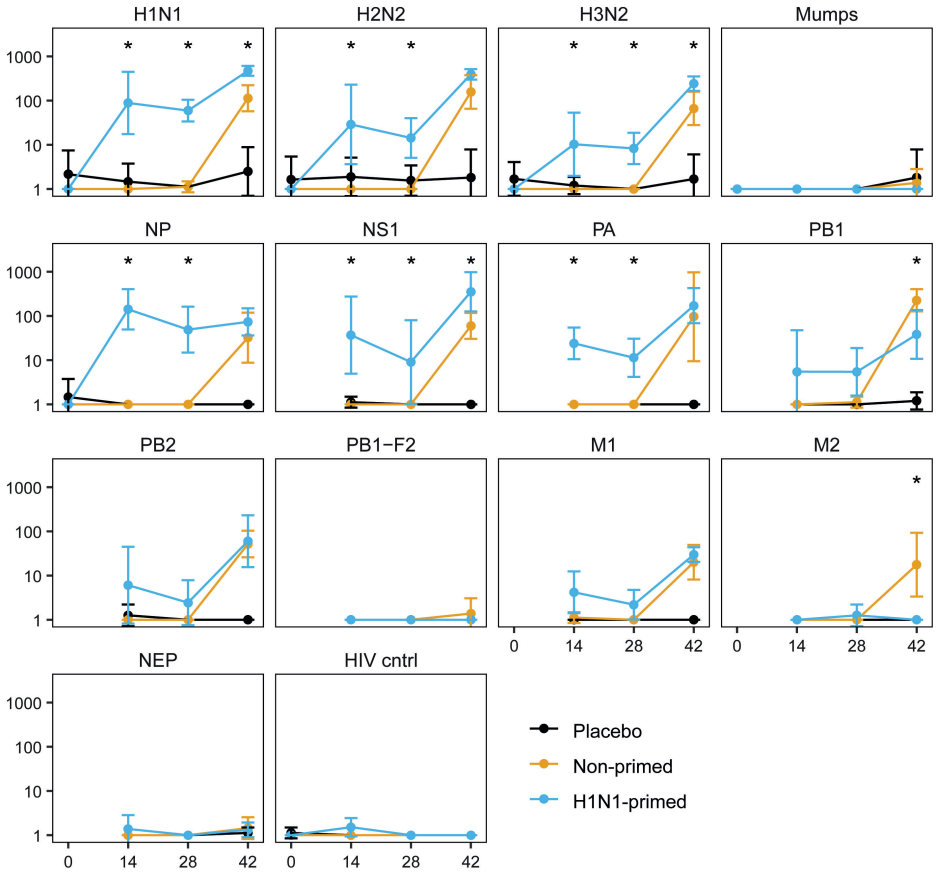

Supplemental Figure 3: IFNγ responses to influenza peptide stimulations, measured in PBMCs by ELISpot over time. Blood samples were taken before (day 0) and two weeks after (day 14) H1N1 priming and before (day 28) and two weeks after (day 42) H2N2 infection. Lines represent means per groups of 5-6 animals ± SD. * indicates significant differences ($p < 0.05$) between non-primed and H1N1-primed groups after correction for multiple testing.

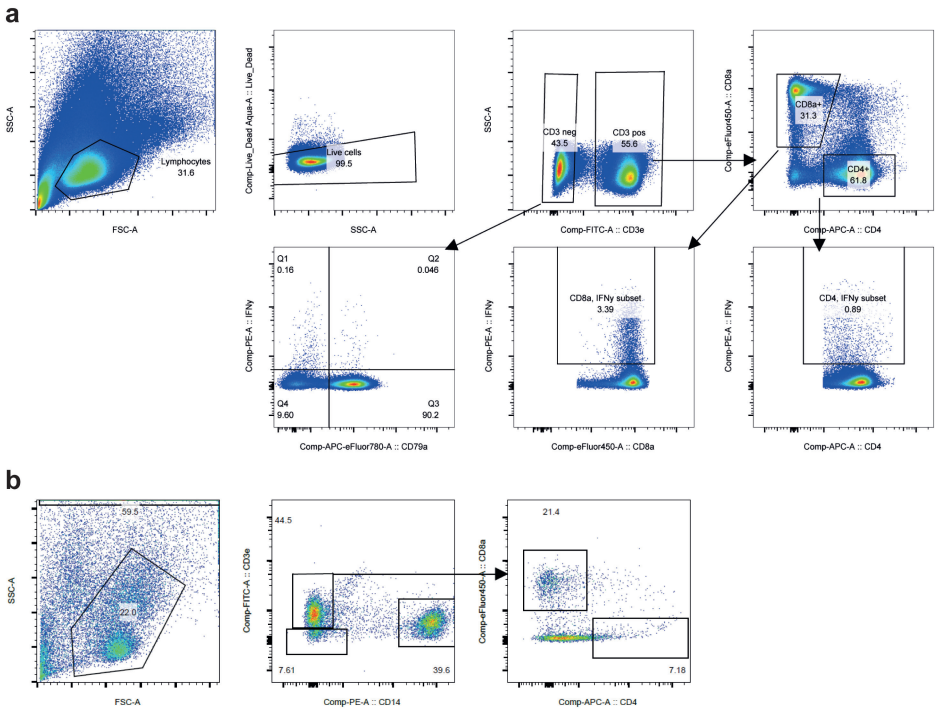

Supplemental Figure 4: Gating strategy for flow cytometric analysis. a) Gating strategy for analysis of IFNγ responses. Plots show PBMCs stimulated with H2N2 influenza (A/Singapore/1/57) and are representative for other stimulations and tissues. **b)** Gating strategy of CD4 and CD8 T cells for Trucount analysis of broncho alveolar lavage (BAL) and nasal turbinates. The plots displayed are from the BAL of one animal, but are representative for other animals and tissues.

References

1. Cassini, A., et al., *Impact of infectious diseases on population health using incidence-based disability-adjusted life years (DALYs): results from the Burden of Communicable Diseases in Europe study, European Union and European Economic Area countries, 2009 to 2013.* Euro Surveill, 2018. **23**(16).
2. Keshavarz, M., et al., *Influenza vaccine: Where are we and where do we go?* Rev Med Virol, 2019. **29**(1): p. e2014.
3. Taubenberger, J.K. and J.C. Kash, *Influenza virus evolution, host adaptation, and pandemic formation.* Cell Host Microbe, 2010. **7**(6): p. 440-51.
4. Clemens, E.B., et al., *Harnessing the Power of T Cells: The Promising Hope for a Universal Influenza Vaccine.* Vaccines (Basel), 2018. **6**(2): p. 18.
5. Jansen, J.M., et al., *Influenza virus-specific CD4+ and CD8+ T cell-mediated immunity induced by infection and vaccination.* J Clin Virol, 2019. **119**: p. 44-52.
6. Viboud, C., et al., *Global Mortality Impact of the 1957-1959 Influenza Pandemic.* J Infect Dis, 2016. **213**(5): p. 738-45.
7. Reneer, Z.B. and T.M. Ross, *H2 influenza viruses: designing vaccines against future H2 pandemics.* Biochem Soc Trans, 2019. **47**(1): p. 251-264.
8. Munster, V.J., et al., *Spatial, temporal, and species variation in prevalence of influenza A viruses in wild migratory birds.* PLoS Pathog, 2007. **3**(5): p. e61.
9. Jones, J.C., et al., *Risk assessment of H2N2 influenza viruses from the avian reservoir.* J Virol, 2014. **88**(2): p. 1175-88.
10. Babu, T.M., et al., *Population Serologic Immunity to Human and Avian H2N2 Viruses in the United States and Hong Kong for Pandemic Risk Assessment.* J Infect Dis, 2018. **218**(7): p. 1054-1060.
11. Epstein, S.L., *Prior H1N1 influenza infection and susceptibility of Cleveland Family Study participants during the H2N2 pandemic of 1957: an experiment of nature.* J Infect Dis, 2006. **193**(1): p. 49-53.
12. Jordan, W.S., Jr., et al., *A study of illness in a group of Cleveland families. XVII. The occurrence of Asian influenza.* Am J Hyg, 1958. **68**(2): p. 190-212.
13. Sridhar, S., et al., *Cellular immune correlates of protection against symptomatic pandemic influenza.* Nat Med, 2013. **19**(10): p. 1305-12.
14. Wang, Z., et al., *Recovery from severe H7N9 disease is associated with diverse response mechanisms dominated by CD8(+) T cells.* Nat Commun, 2015. **6**: p. 6833.
15. Wilkinson, T.M., et al., *Preexisting influenza-specific CD4+ T cells correlate with disease protection against influenza challenge in humans.* Nat Med, 2012. **18**(2): p. 274-80.
16. Bodewes, R., et al., *Infection of the upper respiratory tract with seasonal influenza A(H3N2) virus induces protective immunity in ferrets against infection with A(H1N1)pdm09 virus after intranasal, but not intratracheal, inoculation.* J Virol, 2013. **87**(8): p. 4293-301.
17. Gooch, K.E., et al., *Heterosubtypic cross-protection correlates with cross-reactive interferon-gamma-secreting lymphocytes in the ferret model of influenza.* Sci Rep, 2019. **9**(1): p. 2617.
18. Bodewes, R., et al., *Vaccination against seasonal influenza A/H3N2 virus reduces the induction of heterosubtypic immunity against influenza A/H5N1 virus infection in ferrets.* J Virol, 2011. **85**(6): p. 2695-702.
19. Altenburg, A.F., G.F. Rimmelzwaan, and R.D. de Vries, *Virus-specific T cells as correlate of (cross-)protective immunity against influenza.* Vaccine, 2015. **33**(4): p. 500-6.
20. Slütter, B., et al., *Lung airway-surveilling CXCR3(hi) memory CD8(+) T cells are critical for protection against influenza A virus.* Immunity, 2013. **39**(5): p. 939-48.

21. Slütter, B., et al., *Dynamics of influenza-induced lung-resident memory T cells underlie waning heterosubtypic immunity.* Sci Immunol, 2017. **2**(7).
22. Van Braeckel-Budimir, N., et al., *Repeated Antigen Exposure Extends the Durability of Influenza-Specific Lung-Resident Memory CD8(+) T Cells and Heterosubtypic Immunity.* Cell Rep, 2018. **24**(13): p. 3374-3382 e3.
23. Pizzolla, A., et al., *Resident memory CD8(+) T cells in the upper respiratory tract prevent pulmonary influenza virus infection.* Sci Immunol, 2017. **2**(12).
24. Rosato, P.C., L.K. Beura, and D. Masopust, *Tissue resident memory T cells and viral immunity.* Curr Opin Virol, 2017. **22**: p. 44-50.
25. de Bree, G.J., et al., *Selective accumulation of differentiated CD8+ T cells specific for respiratory viruses in the human lung.* J Exp Med, 2005. **202**(10): p. 1433-42.
26. Teijaro, J.R., et al., *Memory CD4 T cells direct protective responses to influenza virus in the lungs through helper-independent mechanisms.* J Virol, 2010. **84**(18): p. 9217-26.
27. Snyder, M.E., et al., *Generation and persistence of human tissue-resident memory T cells in lung transplantation.* Sci Immunol, 2019. **4**(33).
28. Pizzolla, A., et al., *Influenza-specific lung-resident memory T cells are proliferative and polyfunctional and maintain diverse TCR profiles.* J Clin Invest, 2018. **128**(2): p. 721-733.
29. Hombrink, P., et al., *Programs for the persistence, vigilance and control of human CD8(+) lung-resident memory T cells.* Nat Immunol, 2016. **17**(12): p. 1467-1478.
30. Oh, D.Y. and A.C. Hurt, *Using the Ferret as an Animal Model for Investigating Influenza Antiviral Effectiveness.* Front Microbiol, 2016. **7**: p. 80.
31. Enkirch, T. and V. von Messling, *Ferret models of viral pathogenesis.* Virology, 2015. **479-480**: p. 259-70.
32. Gouma, S., et al., *Mumps-specific cross-neutralization by MMR vaccine-induced antibodies predicts protection against mumps virus infection.* Vaccine, 2016. **34**(35): p. 4166-4171.
33. R Core Team, *R: A Language and Environment for Statistical Computing*. 2021, R Foundation for Statistical Computing.
34. WHO, *Manual for the laboratory diagnosis and virological surveillance of influenza*. 2011, World Health Organization: Geneva.
35. van de Garde, M.D.B., et al., *Prediction and Validation of Immunogenic Domains of Pneumococcal Proteins Recognized by Human CD4(+) T Cells.* Infect Immun, 2019. **87**(6).
36. Shu, Y. and J. McCauley, *GISAID: Global initiative on sharing all influenza data - from vision to reality.* Euro Surveill, 2017. **22**(13).
37. Vita, R., et al., *The Immune Epitope Database (IEDB): 2018 update.* Nucleic Acids Res, 2019. **47**(D1): p. D339-D343.
38. Wickham, H., *ggplot2: Elegant Graphics for Data Analysis*. 2016, Springer-Verlag New York.
39. Hothorn, T., et al., *Implementing a Class of Permutation Tests: ThecoinPackage.* Journal of Statistical Software, 2008. **28**(8).
40. Benjamini, Y. and Y. Hochberg, *Controlling the False Discovery Rate: A Practical and Powerful Approach to Multiple Testing.* Journal of the Royal Statistical Society. Series B (Methodological), 1995. **57**(1): p. 289-300.
41. Eickhoff, C.S., et al., *Highly conserved influenza T cell epitopes induce broadly protective immunity.* Vaccine, 2019. **37**(36): p. 5371-5381.
42. Belz, G.T., W. Xie, and P.C. Doherty, *Diversity of epitope and cytokine profiles for primary and secondary influenza a virus-specific CD8+ T cell responses.* J Immunol, 2001. **166**(7): p. 4627-33.
43. Koutsakos, M., et al., *Human CD8(+) T cell cross-reactivity across influenza A, B and C viruses.* Nat Immunol, 2019. **20**(5): p. 613-625.

44. Cheng, X., et al., *Evaluation of the humoral and cellular immune responses elicited by the live attenuated and inactivated influenza vaccines and their roles in heterologous protection in ferrets.* J Infect Dis, 2013. **208**(4): p. 594-602.
45. Rosendahl Huber, S.K., et al., *Synthetic Long Peptide Influenza Vaccine Containing Conserved T and B Cell Epitopes Reduces Viral Load in Lungs of Mice and Ferrets.* PLoS One, 2015. **10**(6): p. e0127969.
46. Holzer, B., et al., *Comparison of Heterosubtypic Protection in Ferrets and Pigs Induced by a Single-Cycle Influenza Vaccine.* J Immunol, 2018. **200**(12): p. 4068-4077.
47. Korenkov, D.A., et al., *Safety, immunogenicity and protection of A(H3N2) live attenuated influenza vaccines containing wild-type nucleoprotein in a ferret model.* Infect Genet Evol, 2018. **64**: p. 95-104.
48. Reber, A.J., et al., *Extensive T cell cross-reactivity between diverse seasonal influenza strains in the ferret model.* Sci Rep, 2018. **8**(1): p. 6112.
49. McMahon, M., et al., *Vaccination With Viral Vectors Expressing Chimeric Hemagglutinin, NP and M1 Antigens Protects Ferrets Against Influenza Virus Challenge.* Front Immunol, 2019. **10**: p. 2005.
50. McMaster, S.R., et al., *Pulmonary antigen encounter regulates the establishment of tissue-resident CD8 memory T cells in the lung airways and parenchyma.* Mucosal Immunol, 2018. **11**(4): p. 1071-1078.
51. McMaster, S.R., et al., *Airway-Resident Memory CD8 T Cells Provide Antigen-Specific Protection against Respiratory Virus Challenge through Rapid IFN-gamma Production.* J Immunol, 2015. **195**(1): p. 203-9.
52. Liu, W.C., et al., *Sequential Immunization With Live-Attenuated Chimeric Hemagglutinin-Based Vaccines Confers Heterosubtypic Immunity Against Influenza A Viruses in a Preclinical Ferret Model.* Front Immunol, 2019. **10**: p. 756.
53. Gostic, K.M., et al., *Potent protection against H5N1 and H7N9 influenza via childhood hemagglutinin imprinting.* Science, 2016. **354**(6313): p. 722-726.
54. Nachbagauer, R., et al., *Hemagglutinin Stalk Immunity Reduces Influenza Virus Replication and Transmission in Ferrets.* J Virol, 2015. **90**(6): p. 3268-73.
55. Sridhar, S., K.A. Brokstad, and R.J. Cox, *Influenza Vaccination Strategies: Comparing Inactivated and Live Attenuated Influenza Vaccines.* Vaccines (Basel), 2015. **3**(2): p. 373-89.
56. Korenkov, D., I. Isakova-Sivak, and L. Rudenko, *Basics of CD8 T-cell immune responses after influenza infection and vaccination with inactivated or live attenuated influenza vaccine.* Expert Rev Vaccines, 2018. **17**(11): p. 977-987.
57. Bodewes, R., et al., *Annual influenza vaccination affects the development of heterosubtypic immunity.* Vaccine, 2012. **30**(51): p. 7407-10.
58. Matrajt, L., M.E. Halloran, and R. Antia, *Successes and Failures of the Live-attenuated Influenza Vaccine: Can We Do Better?* Clin Infect Dis, 2020. **70**(6): p. 1029-1037.
59. Damjanovic, D., et al., *Immunopathology in influenza virus infection: uncoupling the friend from foe.* Clin Immunol, 2012. **144**(1): p. 57-69.

A universal influenza mRNA vaccine candidate boosts T-cell responses and reduces zoonotic influenza virus disease in ferrets

4

Koen van de Ven[1], Josien Lanfermeijer[1,2], Harry van Dijken[1], Hiromi Muramatsu[3], Caroline Vilas Boas de Melo[1], Stefanie Lenz[1], Florence Peters[1], Mitchell B Beattie[4], Paulo J C Lin[4], José A. Ferreira[5], Judith van den Brand[6], Debbie van Baarle[1,7], Norbert Pardi[3], Jørgen de Jonge[1]

[1] Centre for Infectious Disease Control, National Institute for Public Health and the Environment (RIVM), Bilthoven, the Netherlands
[2] Center for Translational Immunology, University Medical Center Utrecht, Utrecht, Netherlands
[3] Department of Microbiology, University of Pennsylvania, Philadelphia, PA, USA
[4] Acuitas Therapeutics, Vancouver, BC V6T 1Z3, Canada.
[5] Department of Statistics, Informatics and Modelling, National Institute for Public Health and the Environment (RIVM), Bilthoven, The Netherlands.
[6] Division of Pathology, Faculty of Veterinary Medicine, Utrecht University, Utrecht, Netherlands.
[7] Department of Medical Microbiology and Infection prevention, Virology and Immunology research Group, University Medical Center Groningen, Groningen, Netherlands

Manuscript submitted

Abstract

Universal influenza vaccines have the potential to protect against continuously evolving and newly emerging influenza viruses. T cells may be an essential target of such vaccines as they can clear infected cells through recognition of conserved influenza virus epitopes. We evaluated a novel T cell-inducing nucleoside-modified mRNA vaccine that encodes the conserved nucleoprotein, matrix protein 1 and polymerase basic protein 1 of an H1N1 influenza virus. To mimic the human situation, we applied the mRNA vaccine as a prime-boost regimen in naïve ferrets (mimicking young children) and as a booster in influenza-experienced ferrets (mimicking adults). The vaccine induced and boosted broadly-reactive T cells in the circulation, bone marrow and respiratory tract. Booster vaccination enhanced protection against heterosubtypic infection with potential pandemic H7N9 influenza virus in influenza-experienced ferrets. Our findings show that mRNA vaccines encoding internal influenza virus proteins are a promising strategy to induce broadly-protective T-cell immunity against influenza viruses.

Introduction

Influenza viruses infect 5-15% of the world population annually, resulting in approximately 290-650 thousands of deaths worldwide [1, 2]. While vaccines mitigate influenza virus-induced morbidity and mortality, the effectiveness of inactivated influenza virus vaccines is insufficient [3-5]. These vaccines mainly induce strain-specific immunity and are therefore limited in their ability to protect against mutated or newly introduced influenza virus strains. Animal-to-human transmissions of influenza A viruses pose a particular risk, as seasonal influenza vaccination does not offer protection against these strains. There are ample examples of influenza viruses crossing the species barrier and causing a pandemic, with the Spanish flu of 1918 as the most dramatic known example [6, 7]. Recent zoonotic transmissions of highly pathogenic avian influenza virus – like H5N1 and H7N9 – have occurred frequently and are associated with high mortality rates [8, 9]. Especially alarming is the recent rise in outbreaks of these viruses on poultry farms and among migrating birds in Europe and other parts of the world [10]. Although human-to-human transmission of these viruses has been limited so far, experimental work indicates that only a few mutations are required to enhance transmission among humans, highlighting their pandemic potential [11-13]. This emphasizes the ongoing threat posed by influenza viruses and the requirement for a broadly-reactive influenza vaccine that protects against all influenza subtypes.

The narrow protection of inactivated influenza virus vaccines is mainly due to the induction of strain-specific antibodies against the highly variable globular head domain of influenza virus hemagglutinin (HA) [14]. New vaccine concepts strive to provide a wider range of protection by inducing responses against more conserved protein domains [15]. One way to achieve this is by inducing T-cell responses, as they can recognize epitopes derived from conserved influenza proteins such as nucleoprotein (NP), matrix protein 1 (M1) and polymerase basic protein 1 (PB1) [16-18]. T-cells can clear infected cells and T-cell immunity is associated with improved influenza disease outcome in humans [19-23]. In addition, animal models have confirmed that T cells can protect against heterosubtypic influenza virus infections [24-30]. For these reasons, various new influenza vaccine concepts focus on inducing protective T-cell immunity [14].

In recent years, lipid nanoparticle (LNP)-encapsulated nucleoside-modified mRNA (mRNA-LNP) has shown to be a potent novel vaccine format against influenza and other infectious diseases [31, 32]. The potency of the mRNA-LNP platform has been demonstrated by the rapid development and successful world-wide use of mRNA-LNP-based SARS-CoV-2 vaccines [33]. mRNA-LNP induces both T-cell and antibody responses [34-38] and is therefore an interesting platform for novel influenza vaccines. Additionally, mRNA-LNP vaccines can be rapidly produced and are easily adjusted to

new emerging viral variants [39]. Multiple influenza vaccines based on mRNA-LNP are currently in development, with promising early results [40-43]. These vaccines, however, primarily focus on inducing humoral responses against HA, without utilizing the potential of T-cell immunity against conserved internal influenza proteins.

There is still very limited information about the potential of mRNA-LNP vaccines for inducing broadly-protective T-cell responses against influenza virus infections. We set out to remedy this knowledge-gap by evaluating the immunogenicity and protective efficacy of a novel mRNA-LNP influenza vaccine in a highly relevant ferret model. We have previously shown in ferrets that circulating and respiratory T cells recognize conserved influenza virus epitopes and can protect against heterosubtypic influenza virus infection [25]. Here, we investigated if we could induce and enhance this protective immunity by vaccination with nucleoside-modified mRNA-LNP encoding for three conserved internal proteins of H1N1 influenza virus, NP, M1 and PB1 (mRNA-Flu). To mimic the human situation – which consists of both naïve young children and influenza-experienced individuals – we evaluated mRNA-Flu as a prime-boost regimen in naïve ferrets (a model for naïve children) and as a booster in influenza-experienced ferrets (a model for influenza-experienced individuals). Both strategies successfully induced and boosted systemic and respiratory T-cell responses, but mRNA-Flu vaccination in influenza-experienced ferrets resulted in higher and broader responses. Moreover, mRNA-Flu booster immunization reduced disease severity in influenza-experienced ferrets after challenge with a potential pandemic avian H7N9 influenza virus, whereas mock-boosted influenza-experienced ferrets were not protected. Our results demonstrate that broadly-reactive T-cell immunity is boosted by a nucleoside-modified mRNA-LNP vaccine that encodes several internal influenza virus proteins. This mRNA-LNP vaccine enhanced protection against heterosubtypic influenza infection and is a promising strategy for the development of a universal influenza vaccine.

Materials & Methods

Ethics statement

The experiment was approved by the Animal Welfare Body of Poonawalla Science Park – Animal Research Center (Bilthoven, The Netherlands) under permit number AVD3260020184765 of the Dutch Central Committee for Animal experiments. All procedures were conducted according to EU legislation. Ferrets were examined for general health on a daily basis. If animals showed severe disease according to the defined end points prior to scheduled termination they would be euthanized by cardiac bleeding under anesthesia with ketamine (5 mg/kg; Alfasan, Woerden, The Netherlands) and medetomidine (0.1 mg/kg; Orion Pharma, Espoo, Finland). Endpoints were scored based on clinical parameters for activity (0 = active; 1 = active when stimulated; 2 = inactive and 3 = lethargic) and impaired breathing (0 = normal;

1 = fast breathing; 2 = heavy/stomach breathing). Animals were euthanized when they reached score 3 on activity level (lethargic), when the combined score of activity and breathing impairment reached 4 or if their body weight decreased by more than 20%.

Cell & virus culture

MDCK cells were grown in MEM (Gibco, Thermo Fisher Scientific, Waltham, MA) supplemented with 10% fetal bovine serum (FBS; HyClone, GE Healthcare, Chicago, IL), 40 µg/ml gentamicin and 0.01M Tricin (both from Sigma-Aldrich, Saint Louis, MO). VERO E6 cells were cultured in DMEM (Gibco) supplemented with 10% FBS and 1x penicillin-streptomycin-glutamine (Gibco). A/California/07/2009 (H1N1), A/Switzerland/97-15293/2013 (H3N2), A/Vietnam/1203/2004 WT (H5N1), A/Anhui/1/2013 (H7N9) and H7N9/PR8 reassortant (NIBRG-268, NIBSC code 13/250) influenza viruses were obtained from the National Institute for Biological Standards and Control (NIBSC, Hertfordshire, England). Influenza virus was grown on MDCK cells in MEM medium supplemented with 40 µg/ml gentamicin, 0.01M Tricine and 2 µg/ml TPCK treated trypsin (Sigma-Aldrich). At >90% cytopathic effect (CPE), the suspension was collected and spun down (4000x g for 10 minutes) to remove cell debris. H1N1 and H3N2 virus was sucrose purified on a discontinuous 10-50% sucrose gradient. Due to BSL-3 classification of H7N9 and H5N1, the virus was not purified. All virus aliquots were snap-frozen and stored at -80 °C.

mRNA production

NP, M1 and PB1 mRNAs are based on the A/Michigan/45/2015 H1N1pdm virus, which is nearly identical to A/California/07/2009 (NP = 99.2%, M1 = 98.4% and PB1 = 99.6% conserved). Production of mRNAs was performed as described earlier [40, 44]. Briefly, codon-optimized NP, M1, and PB1 genes were synthesized (Genscript, Piscataway, NJ) and cloned into an mRNA production plasmid. T7-driven in vitro transcription reactions (Megascript, Ambion, Thermo Fisher) using linearized plasmid templates were performed to generate mRNAs with 101 nucleotide long poly(A) tails. Capping of mRNAs was performed in concert with transcription through addition of a trinucleotide cap1 analog, CleanCap (TriLink, San Diego, CA) and m1Ψ-5'-triphosphate (TriLink) was incorporated into the reaction instead of UTP. Cellulose-based purification of mRNAs was performed as described [45]. mRNAs were then tested on an agarose gel before storing at -20 °C.

Lipid nanoparticle formulation of mRNA

Purified mRNAs were formulated into lipid nanoparticle using a self-assembly process wherein an ethanolic lipid mixture of an ionizable cationic lipid, phosphatidylcholine, cholesterol, and polyethylene glycol-lipid was rapidly combined with an aqueous solution containing mRNA at acidic pH as previously described [46]. The ionizable cationic lipid (pKa in the range of 6.0-6.5, proprietary to Acuitas Therapeutics, Vancouver, Canada) and LNP composition are described in the patent application WO

2017/004143. The average hydrodynamic diameter was ~80 nm with a polydispersity index of 0.02-0.06 as measured by dynamic light scattering using a Zetasizer Nano ZS (Malvern Instruments Ltd, Malvern, UK) and an encapsulation efficiency of ~95% as determined using a Ribogreen assay.

Animal handling

63 female ferrets (*Mustela putorius furo*) aged 12-13 months (Euroferret, Copenhagen, Denmark) were delivered three weeks before commencement of the study and were semi-randomly distributed by weight. Ferret throat swabs were screened for SARS-CoV-2 by RT-qPCR as described before [47] and ferret sera was screened for influenza exposure by NP ELISA (Innovate Diagnostics, Grabels, France) and HI. Additionally, ferret sera (ELISA) and swabs (RT-qPCR) were screened for other corona viruses, canine distemper virus and Aleutian disease by the European Veterinary Laboratory (EVL, Woerden, the Netherlands). All ferrets tested negative for influenza and SARS-CoV-2; four animals displayed low antibody titers against Aleutian disease; all animals possessed titers for CDV-antibodies but tested negative for active infection by RT-qPCR. Ferrets were housed per 3 or 4 animals in open cages and received pelleted food (Altromin 5539) and water *ad libitum*. Animals were visually inspected daily and weighed at least once per 7 days. Light was adjusted to 9.5 hours per day to prevent the ferrets from going into estrous. For influenza infections animals were moved to BSL-3 level isolators. Due to a limited number of isolators, groups that did not receive an infection were kept housed in regular open cages. 14 days after infection the animals were confirmed to be negative for infectious influenza and moved back to regular housing.

Ferrets that received a (mock) infection were swabbed and weighed at 0, 2, 4, 7, 9 and 14 days after the first and second infection. Vaccinated animals were only swabbed at days 0 and 14 and weighed on days 0, 7 and 14. Blood was collected from the vena cava at 0, 14, 28, 42, 56 and 71 days post priming (dpp). These handlings were performed under anesthesia with ketamine (5 mg/kg). Blood was collected by heart puncture on 70 and 76 dpp. Infections, vaccinations, temperature transponder implantation and euthanasia were performed after anaesthetization with ketamine and medetomidine (0.1 mg/kg). Animals that received a temperature transponder (Star Oddi, Garðabær, Iceland) abdominally received 0.2 ml Buprenodale (AST Farma, Oudewater, The Netherlands) as a post-operative analgesic. Anesthesia with medetomidine was antagonized with atipamezole (0.25 mg/kg; Orion Pharma), but was delayed by 30 minutes in case of infection/vaccination to prevent sneezing and coughing.

Study outline

The study consisted of five experimental groups: 1) placebo; 2) mRNA/mRNA; 3) H1N1/mock; 4) H1N1/mRNA; and 5) H1N1/H3N2. Each experimental group consisted of 14 (group 1-4) or 7 (group 5) ferrets. For practical reasons the experiment was split

into three sub experiments (A, B and CD). All sub-experiments followed the same regime up to day 70 of the experiment, but were started 8 days after each other. Sub-experiments A and B both contained groups 1-5 with 3-4 animals/group and were terminated 70 dpp to study the immune response. Sub-experiment CD contained groups 1-4 with 7 animals/group, split over 2 cages. Sub-experiment CD was again dived into two smaller sub-experiments (C and D) on 71 dpp, which were challenged with H7N9 on 71 and 72 dpp respectively. Data from the different sub-experiments were visualized and analyzed together.

On day 0, groups 3-5 were inoculated intranasally (i.n.) with 10^6 $TCID_{50}$ H1N1 in 0.1 ml inoculum. Group 1 received PBS in the same manner. Group 2 was administered 250 µl of mRNA vaccine – containing 50 µg of NP, M1 and PB1 – in their left or right hindleg. On 42 dpp, animals received a booster treatment. Group 5 was inoculated i.n. with 10^6 $TCID_{50}$ H3N2 in 0.1 ml inoculum. Group 1 was treated similarly but received PBS instead of H3N2 virus. Groups 2-4 were injected with 250 µl of influenza-mRNA vaccine (groups 2, 4) or Luciferase-mRNA (group 3; 50 µg) in their left or right hindleg. At 70 dpp, seven ferrets of each group were euthanized to study the immune response in the respiratory tract. The other seven animals (excluding group 5) were challenged intratracheally (i.t.) with 10^6 $TCID_{50}$ H7N9 in 3ml inoculum at 71 or 72 dpp. Five days later, ferrets were euthanized to study viral titers and pathology.

Animals were euthanized by heart puncture and blood and serum was collected. For ferrets in sub-experiments A and B, the lungs were perfused as described before [25] and broncho-alveolar lavage (BAL) was collected by flushing the lungs twice with 30ml of room temperature (RT) RMPI1640 (Gibco). The BAL fluid was then kept on ice till processing. Lungs, spleen, femur (right leg) and nasal turbinates (NT) were collected in cold RMPI1640 supplemented with 10% FBS and 1x penicillin-streptomycin-glutamine and stored at +4 °C until processing. For ferrets in sub-experiments C and D, lungs were weighed before the left cranial and caudal lobes were inflated with and stored in 10% formaldehyde for later pathological analysis. Small slices of the right cranial, middle and caudal lobes were put in Lysing matrix A tubes (MP Biomedicals, Irvine, CA) and stored at -80 °C until later virological analysis. The lower part of the trachea was stored in 10% formaldehyde for pathology and 1 cm of the middle part of the trachea was stored in Lysing matrix A tubes.

Tissue processing

Blood was collected in 3.5 ml VACUETTE tubes with clot activator (Greiner, Merck, Kenilworth, NJ) and spun down at 4000x g for 10 minutes to isolate serum. Heparin blood was collected in 9 ml sodium-heparin coated VACUETTE tubes (Greiner) and diluted 1:1 with PBS (Gibco) for density centrifugation on a 1:1 mixture of LymphoPrep (1.077 g/ml, Stemcell, Vancouver, Canada) and Lympholyte-M (1.0875 g/ml, Cedarlane, Burlington, Canada). Cells were spun for 30 minutes at 800x g, after which the

interphase was collected and washed thrice with washing medium (RPMI1640 + 1% FCS + 1x penicillin-streptomycin-glutamine). Next, cells were resuspended in stimulation medium (RPMI1640 + 10% FCS + 1x penicillin-streptomycin-glutamine) and counted using a hemocytometer.

Spleen, lung and NT tissue were processed as detailed before [25]. In brief, spleens were homogenized in a sieve using the plunger of a 10 ml syringe. The resulting suspension was collected while excluding the larger debris and pelleted by centrifugation for 10 minutes at 500x g. The pellet was resuspended in 50 ml EDTA-supplemented (2mM) washing medium and transferred over a 100 µm SmartStrainer (Miltenyi Biotec, Bergisch Gladbach, Germany). The cell suspension was then diluted to 90 ml, which was divided into 3x 30 ml and layered on top of 15 ml Lympholyte-M for density centrifugation similar to that of blood. All washing steps were performed with EDTA-supplemented medium to prevent agglutination of cells.

Lungs were cut into 5 mm^3 cubes and digested in 12 ml of collagenase I (2.4 mg/ml, Merck) and DNase I (1 mg/ml, Novus Biologicals, Centennial, CO) for 60 minutes at 37 °C while rotating. Samples were homogenized in a sieve using a plunger, spun down for 10 minutes at 500x g and resuspended in washing medium. This suspension was transferred over a 70 µm cell strainer (Greiner) and used for density centrifugation similar to that of the spleen.

Nasal turbinates were mashed on a sieve using a plunger and pelleted by spinning for 5 minutes at 500x g. The pellet was resuspended in 3 ml collagenase/DNAse solution (similar to lung) and incubated for 30 minutes at 37 °C while rotating. Next, the suspension was directly mashed over a 70 µm cell strainer (Greiner) with a plunger and washed twice with 10 ml washing medium. The resulting pellet was resuspended in 6 ml of 40% Percoll (GE Healthcare) and layered on top of 70% Percoll to isolate leukocytes. Samples were spun for 20 minutes at 500x g after which the interphase was collected and washed twice with washing medium. After the final wash, cells were resuspended in stimulation medium and used for ELISpot and FACS.

After collection, 3 ml BAL was used for ELISpot without further processing. The remaining volume was spun down at 500x g for 5 minutes and resuspended in 12 ml FACS buffer (PBS [Gibco]+ 0.5% BSA [Merck] + 2mM EDTA). The suspension was transferred over a 70 µm SmartStrainer (Miltenyi Biotec), spun down at 500x g for 5 minutes and resuspended in FACS buffer. This suspension was used for FACS.

Femurs were cleaned from residual tissues and briefly decontaminated with 70% ethanol. The femur was then cut on both sides so that the shaft could be flushed with 15 ml of ice-cold RPMI washing medium. The suspension was transferred over a 70 µm cell strainer and pelleted by centrifugation for 7 minutes at 500xg at

4 °C. Erythrocytes were lysed with ACK lysis buffer after which the suspension was spun down, resuspended in washing medium and again transferred over a 70 µm cell strainer. The resulting suspension was spun down, resuspended in stimulation medium and used for ELISpot and FACS.

Peptide pools

NP (NR-18976), M1 (NR-21541) and PB1 (NR-18981) H1N1 peptide arrays were obtained through BEI Resources, NIAID, NIH. Peptides were supplied as individual aliquots and were pooled in-house after dissolving in H_2O, 50% acetonitrile or DMSO depending on the solvability. The merged peptide-suspension was then aliquoted and speed-vacced for 48 hours to reduce the volume. Vials were stored at -80 °C.

H2N2 peptide pools were based on A/Leningrad/134/17/1957 and were custom ordered from JPT Peptide Technologies GmbH (Berlin, Germany). Each pool contained 15 amino acid long peptides with an overlap of 11 amino acids spanning the entire protein of NP, M1 or PB1. Peptides were synthesized as reported before [25]. HIV-1 Con B gag motif peptide pool (JPT) served as a negative control for our assays and was handled in the same way as the H2N2 peptide pools.

Before use, H1N1 and H2N2 peptide pools were dissolved in DMSO, aliquoted and stored at -20 °C. On the day of use, peptide pool aliquots were thawed and diluted with stimulation medium. The peptide pool suspension was added to cells, such that a final peptide concentration of 1 µg/ml per peptide with a DMSO concentration of less than 0.2% was achieved.

ELISpot

Pre-coated Ferret IFNγ ELISpot (ALP) plates (Mabtech, Nacka Strand, Sweden) were used according to the manufacturers protocol. Lymphocytes were stimulated with live virus (MOI 100 for H3N2; MOI 1 for H5N1; MOI 0.1 for H1N1 and H7N9) or peptide pools (1 µg/ml) in ELISpot plates at 37 °C. Per well, 250K cells (PBMC), 400K cells (BM), 62.5K cells (lung lymphocytes) or undiluted cell suspension (BAL, nasal turbinates) was added. On day 56 – 2 weeks after booster vaccination – 125K PBMCs were used for viral stimulations due to high cellular responses. After 20 hours the plates were developed according to the manufacturers protocol, with the modification that the first antibody staining was performed overnight at 4 °C. Plates were left to dry for 2-3 days after which they were packaged under BSL-3 conditions and heated to 65 °C for 3 hours to inactivate any remaining infectious influenza particles. Analysis of ELISpot plates was performed using the ImmunoSpot® S6 CORE (CTL, Cleveland, OH).

Flow cytometry – cell counts

BAL and NT samples were stained in 96-wells plates using the FoxP3 / Transcription factor staining buffer set (eBioscience, Thermo Fisher). Cells were stained with α-CD4-

APC (02, Sino biological, Beijing, China), α-CD8a-eFluor450 (OKT8, eBioscience), α-CD14-PE (Tük4; Thermo Fisher) and Fixable Viability Stain 780 (BD, Franklin Lakes, NJ) in 100 µl for 30 minutes at 4°C. Samples were then washed twice with 150 µl FACS buffer, followed by fixation with 100 µl fixative from the FoxP3 staining kit for 20 minutes at RT. Next, samples were washed twice with 150 µl 1x permeabilization buffer (FoxP3 staining kit). After the second wash, samples were stained with 100 µl permeabilization buffer containing α-CD3e-FITC (CD3-12, Bio-Rad, Hercules, CA) for 30 minutes at 4 °C. Samples were then washed twice with 150 µl 1x permeabilization buffer and once with 150 µl FACS buffer. After the last wash, samples were resuspended in 180 µl FACS buffer after which 50 µl precision count beads (Biolegend, San Diego, CA) were added to BAL and NT samples. Samples were measured in plates using the high-throughput system of a Symphony A3 system (BD). Data was analyzed using FlowJo™ Software V10.6 (BD).

Flow cytometry – intracellular cytokine staining

Lymphocytes derived from blood, lung or BM were stimulated in U-bottom plates with 1-3 million cells/well. Stimulations consisted of medium, H1N1 live virus (MOI 1), H3N2 live virus (MOI 10), an H1N1 peptide cocktail containing peptide pools of NP, M1 and PB1 (1 µg/peptide/ml), and a HIV peptide pool (1 µg/peptide/ml) serving as a negative control. Cells were stimulated for 20 (virus, medium) or 6 hours (peptide pools) at 37 °C. During the last 5 hours of stimulation, 1x brefeldin A (Biolegend) was added to each well. Plates were then stored at 4 °C until they were stained the following morning. Staining and acquisition followed the same procedure as detailed above, with the exception that α-CD14-PE was absent in the extracellular staining and instead, α-IFNγ-RPE (CC302, MyBioSource, San Diego, CA) was added to the intracellular staining.

TCID50 determination

Nose and throat swabs were collected in 2 ml transport medium containing 15% sucrose (Merck), 2.5 µg/ml Amphotericin B, 100 U/ml penicillin, 100 µg/ml streptomycin and 250 µg/ml gentamicin (all from Sigma) and stored at -80 °C. For analysis, swabs were thawed, vortexed, serially diluted and tested in sextuplicate on MDCK cells. Trachea and lung samples stored in Matrix A tubes were thawed and 750 µl of DMEM infection medium (DMEM containing 2% FBS and 1x penicillin-streptomycin-glutamine) was added. Tissues were then dissociated in a FastPrep-24™ by shaking twice for 1 minute after which the samples were spun down for 5 minutes at 4000x g. To determine viral titers, the supernatant was serially diluted in sextuplicate on MDCK cells. Cytopathic effect (CPE) was scored after 6 days of culturing and $TCID_{50}$ values were calculated using the Reed & Muench method. Viral titers in virus stocks were similarly tested, but in octuplicate.

ELISA

Immulon 2 HB 96-well plates (Thermo Fisher) were coated overnight at RT with 100 µl/well recombinant HA (0.5 µg/ml), NP (0.5 µg/ml) or M1 (0.25 µg/ml) protein of A/Anhui/1/2013 (Sino biologicals). The next day, plates were washed thrice with PBS + 0.1% Tween-80 before use. Sera were diluted 1:100 in PBS + 0.1% Tween-80 and then 2-fold serially diluted. Per well, 100 µl of diluted sera was added and plates were incubated for 60 minutes at 37 °C. After washing thrice with 0.1% Tween-80, plates were incubated for 60 minutes at 37 °C with HRP-conjugated goat anti-ferret IgG (Alpha Diagnostic), diluted 1:5000 in PBS containing 0.1% Tween-80 and 0.5% Protivar (Nutricia, Hoofddorp, The Netherlands). Plates were then washed trice with PBS + 0.1% Tween-80 and once with PBS, followed by development with 100 µl SureBlue™ TMB (KPL, Gaithersburg, MD) substrate. Development was stopped after 10 minutes by addition of 100 µl 2M H_2SO_4 and OD_{450}-values were determined on the EL808 absorbance reader (Bio-Tek Instruments). Individual curves were visualized using local polynomial regression fitting with R software v4.1.1 [48]. Antibody titers were determined as the dilution at which antibody responses dropped below background. This background was calculated as the 'mean + 3 * standard deviation' of the OD_{450} at a 200x (HA, M1) or 1600x (NP) serum-dilution of placebo animals.

Hemagglutination inhibition assay

Hemagglutination inhibition (HI) titers in ferret sera were determined in duplicate according to WHO guidelines [49]. In brief, sera were heat-inactivated at 56 °C for 30 minutes and treated with receptor destroying enzyme (Sigma) in a 1:4 mixture (5x dilution of sera). Sera were then two-fold serially diluted in PBS with and mixed 1:1 with four hemagglutinating units of H1N1 or H7N9 in 96 wells plates (starting dilution = 1:10). The serum-virus mixture was incubated for 20 minutes at RT, followed by the addition of 0.5% turkey red blood cells (bioTRADING) in a 1:1 mixture. Samples were incubated for 45 minutes at RT after which agglutination was scored.

Virus neutralization assay

Virus neutralizing (VN) titers were determined as described previously [50] and according to WHO guidelines [49]. Sera were inactivated (30 minutes at 56 °C) and two-fold serially diluted in virus growth medium using a starting dilution of 1:8. Virus at a concentration of 100 $TCID_{50}$ was added and the mixture was incubated for 2 hours at 37 °C. Next, the virus-serum mixture was transferred to 96 wells plates containing confluent MDCK cells and incubated for another 2 hours at 37 °C after which the medium was refreshed. Plates were incubated until a back titration plate reached CPE at a titer of 100 $TCID_{50}$ (4-5 days). The 50% virus neutralization titers per ml serum was calculated by the Reed and Muench method [51].

Pathology

Tissues harvested for histological examination (trachea, bronchus and left lung) were fixed in 10% neutral-buffered formalin, embedded in paraffin, sectioned at 4 mm and stained with hematoxylin and eosin (HE) for examination by light microscopy. Semiquantitative assessment of influenza virus-associated inflammation in the lung (four slides with longitudinal section or cross-section of cranial or caudal lobes per animal) was performed on every slide as reported earlier [52] with few modifications: for the extent of alveolitis and alveolar damage we used: 0, 0%; 1, 1–25%; 2, 25–50%; 3, >50%. For the severity of alveolitis, bronchiolitis, bronchitis, and tracheitis we scored: 0, no inflammatory cells; 1, few inflammatory cells; 2, moderate numbers of inflammatory cells; 3, many inflammatory cells. For the presence of alveolar edema and type II pneumocyte hyperplasia we scored: 0, 0%, 1, <25%, 2, 25-50%, 3, >50%. The presence of alveolar hemorrhage we scored: 0, no; 1, yes. For the extent of peribronchial/perivascular edema we scored: 0, no, 1, yes. Finally, for the extent of peribronchial, peribronchiolar, and perivascular infiltrates we scored: 0, none; 1, one to two cells thick; 2, three to ten cells thick; 3, more than ten cells thick. Slides were examined without knowledge of the treatment allocation of the animals.

Body temperature, body weight and lung weight

Temperature data were retrieved from the implanted temperature loggers and consisted of measurements taken every 30 minutes. Baseline temperature was calculated as the average temperature in the 5 days before infection. The change in temperature was calculated as deviation from baseline (ΔT). The area under the curve (AUC) was calculated as the total ΔT up till 5 dpi. Values smaller than 'baseline - 2*standard deviation of baseline' were excluded as these often occur due to anesthesia. Relative bodyweight and relative lung weight are expressed as a percentage of bodyweight or ratio on the day of infection.

Data analysis

All the statistical tests carried out aimed at detecting differences between the distributions of responses in two treatment groups (e.g. H1N1/mRNA and placebo), each response pertaining to a given stimulus (or measured variable, e.g. body weight) on a given tissue on a given day. The tests are based on the 'sum statistic' [53] as implemented in the R package 'coin' [54], in the guise of the function 'independence_test', possibly with blocking in the event that some experiments were done on different days (in which case the data from the same experiment are collected in the same block), and with the (exact) p-values estimated by random permutations. The tests were grouped into various themes based on tissue and assay (e.g. all stimulations for lung IFNγ ELISpot), and the Benjamini-Hochberg (BH) method [55] was used separately per theme to control the false discovery rate (FDR) at the level of 10%. Only the results of the tests that passed through the BH method are reported and commented upon in the results section. The overall proportion of spurious results

(over all the themes) is expected to be at most 10% of all those reported. Tables with the complete results of the tests and multiple testing corrections are available as Supplementary data file 1. The results reported are illustrated by graphs (e.g. box plots) in the main text or in the online supplemental material.

IFNγ-ELISpot spot counts, viral titers, serum titers and cell counts were log-transformed for statistical testing. We excluded two datapoints of flow cytometry data from data visualization and analysis. These datapoints (one in PBMC, one in lung) refer to the percentage $IFNγ^+$ within $CD4^+$ T cells and were at least two-times higher than the nearest datapoint. No other data was excluded from analysis.

Results

Study set-up

We designed the mRNA vaccine based on the NP, M1, and PB1 proteins of H1N1 influenza virus (mRNA-Flu) since these proteins are highly conserved (Supplemental Table 1) and immunogenic in humans [25, 56]. To model mRNA-Flu vaccination in both naïve and influenza-experienced humans, we followed a prime-boost strategy with different regimens (Fig. 1a). Naïve ferrets were prime-boosted by intramuscular (i.m.) mRNA-Flu vaccination on days 0 and 42, modelling naïve individuals (group mRNA/mRNA). Another group of ferrets was primed on day 0 by intranasal (i.n.) infection with 10^6 $TCID_{50}$ A/California/07/2009 (H1N1) influenza virus followed by booster vaccination with mRNA-Flu on day 42 to mimic vaccination of influenza virus-experienced individuals (group H1N1/mRNA). As a control for this treatment, another group of ferrets received the same priming (H1N1 infection), but a mock booster with mRNA-LNP encoding for firefly luciferase (group H1N1/mock) on day 42. A placebo group that received only phosphate-buffered saline (PBS) as a prime-boost served as a negative control. The positive control consisted of ferrets that were primed by H1N1 infection and boosted with 10^6 $TCID_{50}$ A/Uruguay/217/2007 (H3N2) influenza virus, as a secondary heterosubtypic influenza infection is a very potent booster of T-cell responses (group H1N1/H3N2) [25]. Blood was collected at 0, 14, 42, 56 and 70 days post priming (dpp). Four weeks after the booster (70 dpp), ferrets were euthanized to study systemic and local T-cell responses.

An mRNA-based T-cell vaccine induces and boosts systemic cellular responses against conserved influenza virus proteins

We evaluated the cellular responses induced by mRNA-Flu vaccination by stimulation of peripheral blood mononuclear cells (PBMCs) from immunized ferrets with overlapping peptide pools of H1N1 NP, M1 and PB1 in IFNγ ELISpot assays. A single dose of mRNA-Flu induced cellular responses against NP, but not to M1 and PB1 at 14 dpp (Fig. 1b and Supplemental Fig. 1a). Responses were stronger and broader in H1N1 influenza virus-primed ferrets as they displayed responses against NP, M1 and PB1.

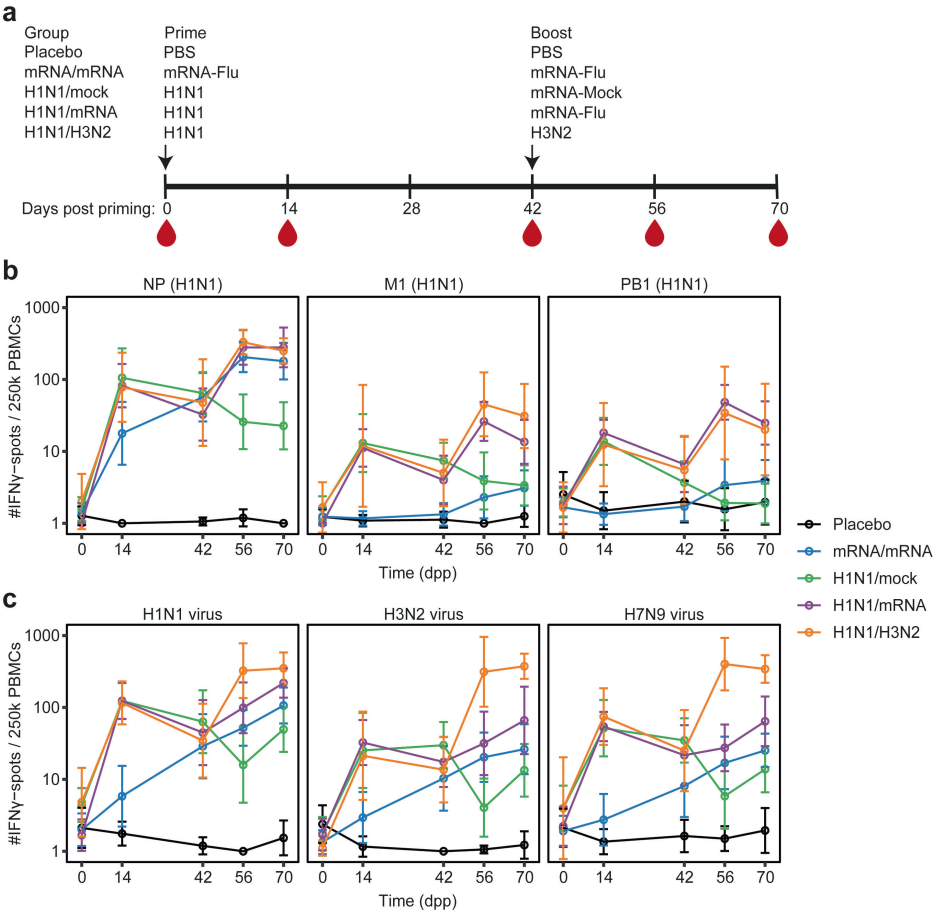

Figure 1: Cellular responses in blood after prime-boost immunization with mRNA-Flu. a) Study layout depicting the prime-boost strategy. On day 0, ferrets were primed intranasally with PBS, 10^6 $TCID_{50}$ H1N1 influenza virus (A/California/07/2009) or primed intramuscularly with mRNA-LNPs encoding for NP, M1 and PB1 (50 µg per mRNA-LNP; mRNA-Flu). Ferrets primed with PBS (group placebo) or mRNA-Flu (group mRNA/mRNA) received the same treatment as booster 42 days post priming (dpp). H1N1-primed ferrets were boosted intramuscularly with mRNA-Flu (H1N1/mRNA-Flu), mRNA-LNP encoding firefly luciferase (50 µg; H1N1/mock) or boosted intranasally with 10^6 $TCID_{50}$ H3N2 influenza virus (H1N1/H3N2; A/Uruguay/217/2007). Blood was collected on 0, 14, 42, 56 and 70 dpp. Ferrets were euthanized 70 dpp to study cellular responses in tissues. **b, c)** Cellular responses measured by IFNγ ELISpot after 20 hours stimulation of PBMCs with **b)** H1N1 NP, M1 and PB1 overlapping peptide pools or **c)** live influenza viruses H1N1, H3N2 or H7N9 (A/Anhui/1/2013). Data were corrected for medium background and are visualized as geometric mean + geometric standard deviation. n = 7 for H1N1/H3N2 and n = 12-14 for all other groups. Statistics are detailed in Supplemental data file 1.

The cellular response against NP in mRNA-primed ferrets increased further between 14 and 42 dpp, while this response was already contracting in H1N1-primed ferrets. This might be due to the long availability of influenza antigens produced from the mRNA-LNP vaccines after i.m. immunization [46].

mRNA-Flu vaccination at 42 dpp boosted existing cellular responses, irrespective of whether ferrets were initially primed with mRNA-Flu or H1N1 influenza (Fig. 1b). At 56 and 70 dpp, NP-specific responses were similar between mRNA/mRNA and H1N1/mRNA ferrets. Responses against M1 and PB1 were still weaker in the mRNA/mRNA group, although they were clearly boosted as approximately half of the animals developed cellular responses after the second vaccination (Fig. 1b and Supplemental Fig. 1b). Importantly, NP-specific cellular responses in mRNA/mRNA and H1N1/mRNA ferrets were similarly robust to that measured in H1N1-experienced ferrets boosted with H3N2 influenza virus infection. This finding indicates that nucleoside-modified mRNA-LNP vaccination can be as effective in boosting existing T-cell responses as a heterosubtypic influenza infection.

Based on the high level of protein conservation of internal influenza virus proteins (>90%; Supplemental Table 1), T cells induced by mRNA-Flu or H1N1-priming should respond against a wide range of influenza viruses. Indeed, cellular responses measured in PBMCs after stimulation with H1N1 peptide pools correlated strongly with responses obtained with peptide pools specific for H2N2 influenza virus (A/Leningrad/134/17/57; Supplemental Fig. 1c). Live virus stimulations confirmed these findings as we observed substantial responses against heterosubtypic influenza viruses H3N2, H5N1 (A/Vietnam/1204/2004) and H7N9 (A/Anhui/1/2013) (Fig. 1c and Supplemental Fig. 1d). In conclusion, immunization with mRNA-Flu induces and boosts a cellular response that is cross-reactive with a wide range of influenza viruses due to targeting conserved influenza virus epitopes.

The mRNA-based T-cell vaccine induces and boosts cellular responses in the respiratory tract and bone marrow

T cells located in the respiratory tract are essential for protection against heterosubtypic influenza virus infections [28, 57]. To determine if mRNA-Flu vaccination is also able to induce and boost T-cell responses in the respiratory tract, we assessed cellular immune responses in the bronchoalveolar lavage (BAL) fluid and nasal turbinates (NT) of immunized ferrets by IFNγ ELISpot at 70 dpp. Despite i.m. administration, mRNA-Flu induced robust cellular responses against NP in the NT, but not in the BAL fluid of mRNA/mRNA ferrets (Fig. 2a, supplemental Fig. 1d). The effect of mRNA-Flu vaccination was even more potent in H1N1-primed ferrets. Vaccination effectively increased NP-, M1- and PB1-specific T-cell responses in the NT of H1N1/mRNA ferrets relative to H1N1/mock and mRNA/mRNA ferrets. NP-responses in the BAL fluid of H1N1/mRNA ferrets also demonstrated an increase compared to H1N1/mock ferrets.

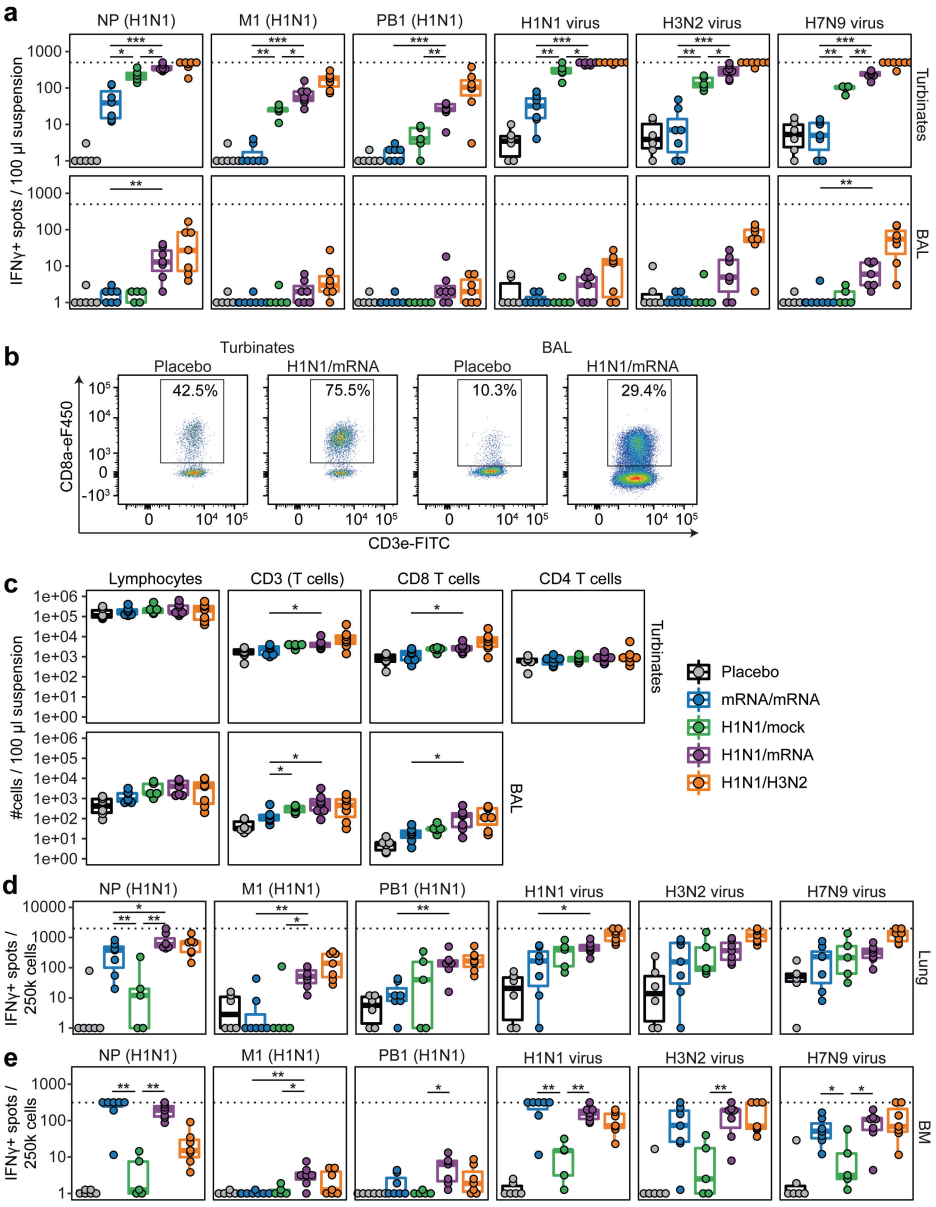

Figure 2: Cellular responses and counts in respiratory compartments and bone marrow of immunized ferrets. a) Cellular responses measured by IFNγ ELISpot after 20 hours stimulation with overlapping H1N1 peptide pools or live influenza virus using cells derived from nasal turbinates and bronchoalveolar lavage (BAL) fluid. **b, c)** Cell counts in nasal turbinates and BAL as measured by flow cytometry. **b)** FACS plot displaying the $CD8^+$ T cell population in representative turbinate and BAL samples. **c)** Count of different cell populations per 100 µl of suspension. $CD4^+$ T cell counts are not displayed for BAL as the αCD4-APC staining was not

consistent between BAL samples. **d, e)** Cellular responses measured by IFNγ ELISpot after 20 hours stimulation with overlapping H1N1 peptide pools or live influenza virus of cells derived from **d**) lung or **e**) bone marrow (BM). ELISpot data were corrected for medium background. Boxplots depict the median, 25% and 75% percentile, where the upper and lower whiskers extend to the smallest and largest value respectively within 1.5* the inter quartile ranges. In panels a and c-e, each dot represents one animal and n = 5-7. For visualization purposes, only comparisons between groups mRNA/mRNA, H1N1/mock and H1N1/mRNA are shown. An overview of all statistical comparisons is detailed in Supplemental data file 1. * = $p < 0.05$, ** = $p < 0.01$, *** = $p < 0.001$.

Responses against homologous (H1N1) and heterosubtypic (H3N2, H5N1, H7N9) influenza viruses were also higher in the NT (significant) and BAL (trend) of H1N1/mRNA ferrets compared to mRNA/mRNA and H1N1/mock ferrets. All groups that were initially primed intranasally with H1N1 influenza virus displayed stronger cellular responses in the NT than the mRNA/mRNA group, irrespective of whether they received a booster, suggesting that the site of priming dictates the response.

To determine whether mRNA-Flu vaccination also increased absolute T-cell numbers in the respiratory tract, we measured cell counts in the NT and BAL by flow cytometry. Compared to placebo ferrets, T-cell counts ($CD3^+$) in the NT were only significantly increased in H1N1/mRNA and H1N1/H3N2 ferrets (Fig. 2b, c and Supplemental Fig. 2a, b). This was primarily due to an increase in $CD8^+$ T cells, since $CD4^+$ T-cell counts did not significantly differ from placebo animals. In BAL, mRNA/mRNA treatment enhanced both $CD3^+$ and $CD8^+$ T-cell counts compared to placebo ferrets. The effect of prime-boost with mRNA-Flu vaccination on T cell numbers in the BAL was less effective compared to a single influenza virus infection, as H1N1/mock-treated ferrets displayed higher $CD3^+$ numbers compared to mRNA/mRNA ferrets. To determine if the increased T-cell counts correlated with increased IFNγ-responses, we performed a correlation analysis between population counts and IFNγ-ELISpot counts induced by H1N1 peptide pool stimulation. $CD8^+$ T cell counts showed the strongest correlation with IFNγ-ELISpot responses, indicating that the IFNγ-response in the BAL and NT was mainly mediated by $CD8^+$ T cells (Supplemental Fig. 3a, b).

We additionally investigated cellular responses by IFNγ ELISpot in lungs that were perfused with a saline solution to reduce contamination of lung-derived lymphocytes with circulating lymphocytes. Remarkably, we observed robust cellular responses against NP, but not to M1 and PB1 in the lungs of mRNA/mRNA ferrets (Fig. 2d). Responses in the lung of mRNA/mRNA ferrets exceeded those measured in the blood, indicating that it is unlikely that the increase is due to contamination with circulating lymphocytes. In H1N1-primed ferrets, mRNA-Flu vaccination significantly boosted cellular responses against NP and M1 in the lung (group H1N1/mRNA vs H1N1/mock), to levels similar as achieved by a secondary natural infection with influenza virus (group H1N1/H3N2).

Cellular responses against heterosubtypic virus stimulations (H3N2, H7N9, H5N1) were however similar between the H1N1/mRNA and mRNA/mRNA groups, indicating that mRNA/mRNA ferrets were not severely hampered by low responses against M1 and PB1 (Fig. 2d and Supplemental Fig. 1d).

Next, we investigated the presence of T-cell responses in the bone marrow (BM) since it is a reservoir for memory T cells [58]. mRNA/mRNA-treatment induced strong T-cell responses against NP in the BM (Fig. 2e and Supplemental Fig. 1d). Responses were similarly robust in H1N1/mRNA ferrets, while they were modest in H1N1/mock and H1N1/H3N2 ferrets. M1 and PB1 peptide pool responses were low for all groups in the BM, even though these responses were present in other tissues (Supplemental Fig. 4). The response to homologous (H1N1) and heterosubtypic (H3N2 [not significant for mRNA/mRNA], H5N1, H7N9) viruses was increased in both the mRNA/mRNA and H1N1/mRNA groups compared to H1N1/mock ferrets (Fig. 2e and Supplemental Fig. 1d). Together, these findings clearly demonstrate that the nucleoside-modified mRNA-LNP influenza T-cell vaccine is able to boost influenza virus-specific T-cell responses in the blood, respiratory tract and BM. Overall, compared to mRNA/mRNA ferrets, cellular responses were broader in H1N1/mRNA ferrets since they displayed robust M1 and PB1 responses in addition to NP (Supplemental Fig. 4).

The mRNA-based T-cell vaccine induces and boosts both CD4+ and CD8+ T-cell responses in PBMC, spleen, lung and bone marrow.

To study the T-cell response in more detail, we measured IFNγ production of $CD4^+$ and $CD8^+$ T cells at 70 dpp by flow cytometric analysis. We stimulated lymphocytes derived from blood, spleen, lung and BM with an H1N1 peptide cocktail consisting of NP, M1 and PB1 peptide pools. mRNA/mRNA and H1N1/mRNA ferrets possessed significantly more $CD8^+IFN\gamma^+$ T cells in all tissues investigated relative to the placebo and H1N1/mock animals (Fig. 3a, b and Supplemental Fig. 5a, b). In PBMC and lung, H1N1/mRNA ferrets demonstrated significantly stronger $CD8^+$ T-cell responses compared to mRNA/mRNA ferrets. Interestingly, the opposite was observed in the BM where mRNA/mRNA ferrets showed the most robust IFNγ-response, although this was not significantly stronger compared to H1N1/mRNA ferrets. Importantly, the H1N1 peptide cocktail-induced IFNγ-responses in PBMC, spleen and BM of H1N1/mRNA ferrets even exceeded those measured in ferrets boosted by a secondary infection (H1N1/H3N2 ferrets), further demonstrating the potency of the mRNA-Flu vaccine. In comparison to $CD8^+$ T cells, $CD4^+$ T-cell responses were weaker in most cases and differences between groups were slightly smaller (Fig. 3a, c and Supplemental Fig. 5a, c). Still, mRNA-Flu vaccination induced $CD4^+$ T-cell responses in all investigated compartments of mRNA/mRNA ferrets and significantly boosted $CD4^+$ T-cell responses in the blood and BM of H1N1/mRNA ferrets compared to H1N1/mock ferrets.

Stimulations with live H1N1 or H3N2 influenza virus yielded similar results to H1N1 peptide cocktail stimulations. However, there was a trend that $CD8^+$ T-cell responses in PBMC and lungs of H1N1/H3N2 ferrets were slightly stronger than in H1N1/mRNA ferrets (Fig. 3d). This is in part due to T cells that recognize conserved epitopes in proteins other than NP, M1 and PB1. $CD4^+$ T-cell responses after virus stimulation were comparable to their $CD8^+$ T cell counterparts, although $CD4^+$ T-cell responses in the lung could not be interpreted because of high IFNγ background-responses in placebo animals (Supplemental Fig. 5d). Stimulations with H3N2 virus resulted in weaker $CD4^+$ and $CD8^+$ T cell responses compared to H1N1 virus stimulations (Fig. 3d and Supplemental Fig. 5d), which was not observed in the ELISpot assays (Fig. 2). This is likely due to a lower virus-to-cells ratio used for H3N2 stimulation in flow cytometry assays.

To investigate if mRNA-Flu vaccination leads to skewing of the T-cell response towards a $CD4^+$ or $CD8^+$ T-cell phenotype, we calculated the $CD8^+/CD4^+$-ratio within the $CD3^+IFN\gamma^+$ population after H1N1 peptide cocktail or H1N1 virus stimulation.In the tissues investigated, H1N1/mock and H1N1/H3N2 ferrets tended to have an average ratio of 1, demonstrating that IFNγ responses were approximately evenly distributed between $CD4^+$ and $CD8^+$ T cells (Fig. 3e and Supplemental Fig. 5e). Interestingly, in all tissues there was a clear skewing towards a $CD8^+$ T-cell response in groups that received mRNA-Flu vaccination. Given the robust $CD4^+$ T-cell responses in mRNA-Flu-immunized ferrets, skewing towards a $CD8^+$ T cell response is not caused by a low $CD4^+$ T-cell response, but by a very strong boosting of the $CD8^+$ T-cell response. mRNA-Flu is thus a potent booster of both $CD4^+$ and $CD8^+$ T-cell immunity.

H7N9 disease is reduced in influenza-experienced ferrets after booster vaccination

Next, we investigated whether mRNA-Flu vaccination could protect against severe disease caused by a heterosubtypic avian influenza virus infection. To this end, we immunized ferrets as described above with the exception of H1N1/H3N2 ferrets and challenged these animals intratracheally (i.t.) with a lethal dose of 10^6 $TCID_{50}$ H7N9 influenza virus four weeks after the booster vaccination (Fig. 4a). At this time, the boosted T-cell response is expected to be in its memory phase, similar to when (vaccinated) individuals are infected with influenza virus. Ferrets were euthanized five days post infection (dpi) to study viral replication and pathology. Importantly, mRNA-Flu vaccination enhanced protection against H7N9 disease in H1N1-primed ferrets.Weight loss of H1N1/mRNA ferrets was limited to 7% and stabilized 5 dpi, while placebo animals lost more than 17% of bodyweight on average and were still losing weight at 5 dpi (Fig. 4b).

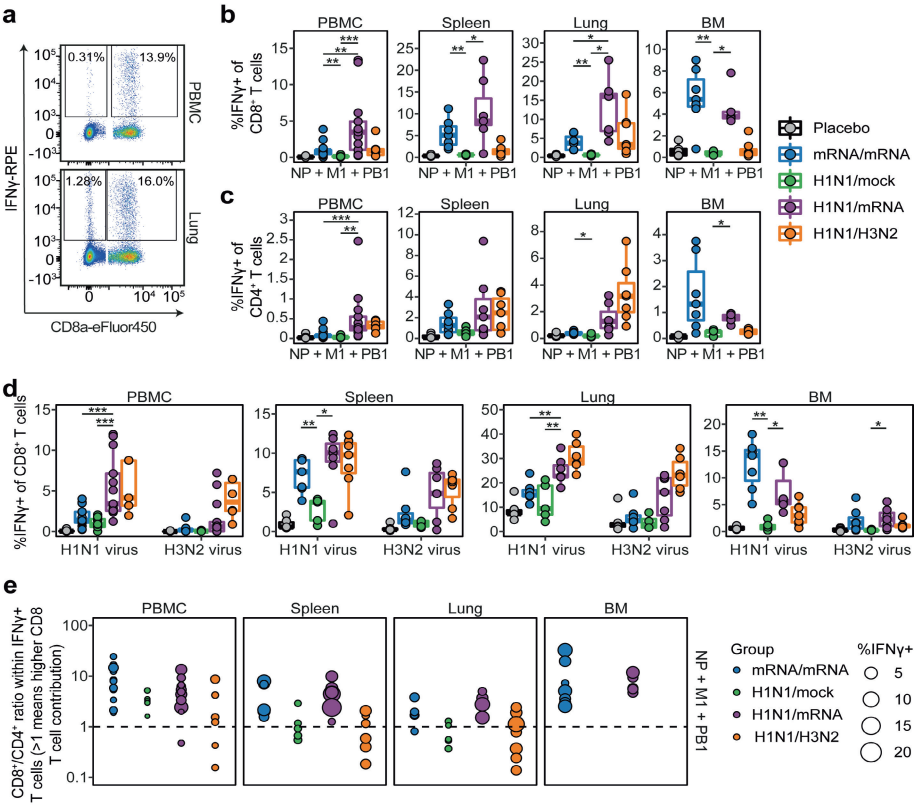

Figure 3: IFNγ responses of CD4⁺ and CD8⁺ T cells in PBMC, spleen, lung and bone marrow of immunized ferrets. Lymphocytes were stimulated with a peptide cocktail containing H1N1 NP, M1 and PB1 peptide pools or live influenza virus. Cells were stained for intracellular IFNγ and analyzed by flow cytometry. **a)** FACS plots depict representative CD4⁺ and CD8⁺ T-cell responses of H1N1/mRNA treated ferrets after peptide cocktail stimulation. Numbers indicate percentage of CD4⁺ or CD8⁺ T cells expressing IFNγ. **b, c)** IFNγ-positive CD8⁺ (B) and CD4⁺ (C) T cells after peptide cocktail stimulation. **d)** Percentage IFNγ-positive CD8⁺ T cells after stimulation with H1N1 (A/California/07/2009) or H3N2 (A/Uruguay/217/2007) influenza viruses. **e)** Ratio between CD8⁺ and CD4⁺ T cells within the CD3⁺ IFNγ⁺ T-cell population after peptide cocktail stimulation. Dotted line represents a ratio of 1 and samples with less than 50 CD3⁺ IFNγ⁺ cells were excluded from the analysis. Each dot represents one ferret and the dot size is relative to the total IFNγ response (%IFNγ⁺ of CD4⁺ and CD8⁺ T cells). Boxplots depict the median, 25% and 75% percentile, where the upper and lower whiskers extend to the smallest and largest value respectively within 1.5* the inter quartile ranges. In panels b-e, each dot represents one animal. n = 4-13 for PBMC and n = 4-7 for lung, spleen and BM. For visualization purposes, only comparisons between groups mRNA/mRNA, H1N1/mock and H1N1/mRNA are shown. No statistics were performed for panel e. An overview of all statistical comparisons is detailed in Supplemental data file 1. * = $p < 0.05$, ** = $p < 0.01$, *** = $p < 0.001$.

mRNA/mRNA ferrets showed mixed results, with weight loss in isolator 1 being similar to placebo (~15%) but less severe in isolator 2 (~11%). Of note, one (out of six) placebo ferrets and three (out of six) mRNA/mRNA ferrets displayed inactivity and severe impaired breathing at 4 dpi and needed to be euthanized due to reaching the human end-points. The mRNA/mRNA group was clearly affected by a cage-effect of unknown origin as all ferrets that reached the humane endpoints were housed in one of the two isolators. The cage effect could not be explained by pre-existing immunity or infection history with other viruses (e.g. influenza virus, Aleutian disease, ferret corona viruses), as these were similar between groups (Supplemental Table 2). The two mRNA/mRNA groups are therefore analyzed together but visualized separately. No cage-effect was present in other treatment groups.

Weight data were in line with clinical symptoms as H1N1/mRNA-treated ferrets had less difficulty with breathing and were more active compared to other groups at 4 and 5 dpi (Fig. 4c). The height and duration of fever was not influenced by prior treatment as all groups displayed similar increases in body temperature (Fig. 4d, Supplemental Fig. 6a). Three animals in the mRNA/mRNA group showed hypothermia starting from 2 dpi and were euthanized at 4 dpi. Viral titers in nose and throat swabs were similar between groups at 2 and 3 dpi (Fig. 4e). By 5 dpi however, viral titers were lower in both H1N1/mRNA and H1N1/mock ferrets when compared to placebo. mRNA/mRNA ferrets gave mixed results.

While viral titers in the nose were similar to placebo at all time-points investigated, viral titers in the throat at 5 dpi were significantly lower in surviving mRNA/mRNA ferrets compared to all other groups. We additionally measured viral titers in lung tissue. Differences were small, but H1N1/mRNA ferrets displayed significantly lower viral titers compared to all other groups (Fig. 4f). Viral titers in the trachea were low for all groups, except for the placebo group, indicating that all strategies limited viral replication to some extent.

Despite the reduced disease severity in H1N1/mRNA ferrets, the lungs showed moderate to severe broncho-interstitial pneumonia, often related to the bronchioles and bronchi which extended to the alveoli, irrespective of treatment (Fig. 4g, Supplemental Fig. 6b). However, alveolar edema, hyperplasia of Type II pneumocytes and alveolar damage was somewhat reduced in H1N1/mRNA-vaccinated ferrets. When we measured lung weight at 5 dpi as an independent measurement of lung pathology, H1N1/mRNA ferrets had significantly lower lung-weights (Fig. 4h). This indicates that inflammation and the resulting edema was less severe, which is in line with the less impaired breathing we observed in H1N1/mRNA ferrets. From these results, we conclude that nucleoside-modified mRNA-LNP influenza booster vaccination in H1N1-experienced ferrets was able to reduce H7N9 disease severity and virus replication.

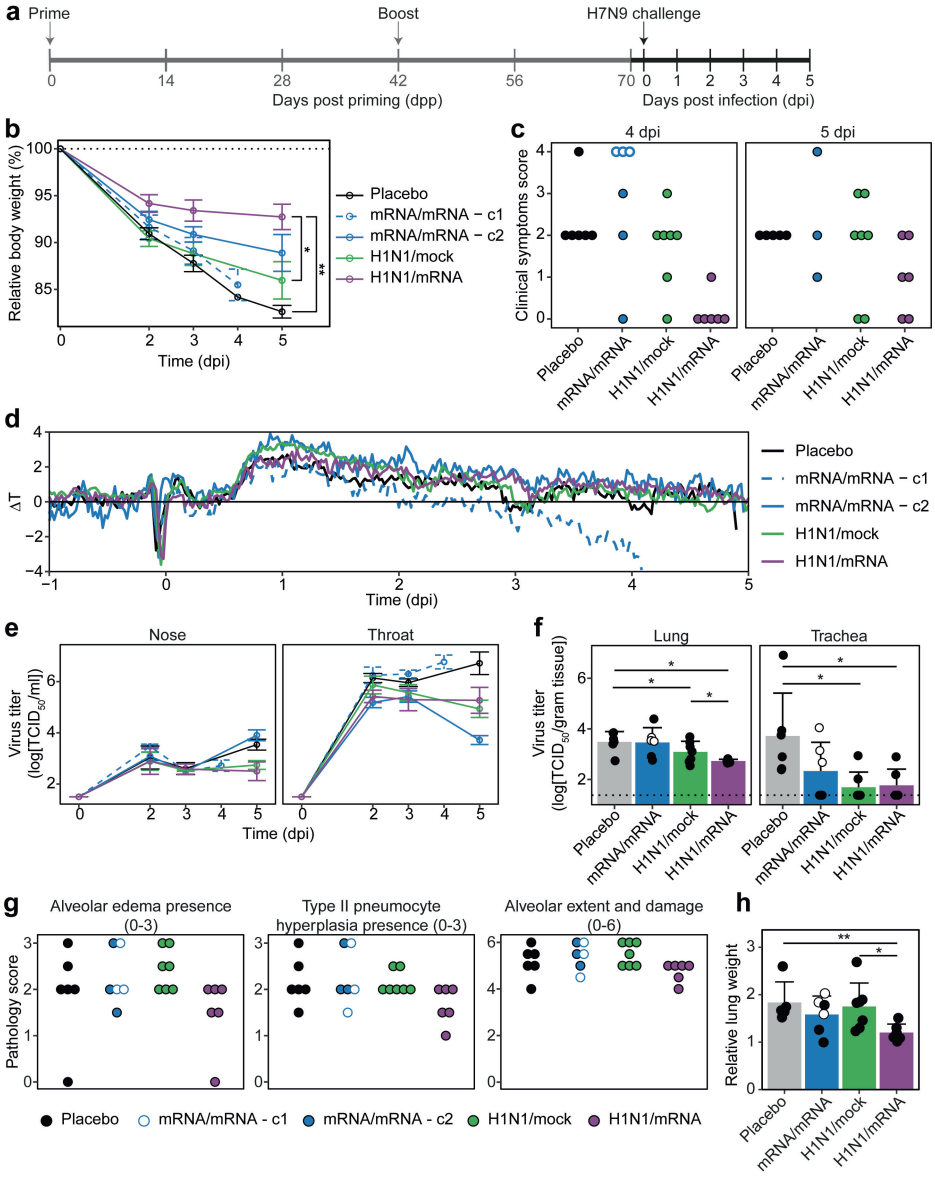

Figure 4: Boosting of existing immunity increases protection against H7N9 influenza virus challenge. a) Study layout depicting the H7N9 influenza virus challenge after different prime-boost regimens. Ferrets were challenged intratracheally with 10^6 $TCID_{50}$ A/Anhui/1/2013 (H7N9) influenza virus at 71 or 72 days post priming (dpp), which equals 0 days post infection (0 dpi). At 5 dpi, animals were euthanized after which pathology and virology was assessed. **b)** Decrease in body weight from 0 to 5 dpi. Body weight is depicted relative to body weight (%) on the day of challenge. **c)** Clinical scoring for parameters activity and breathing as detailed in the Materials & Methods. Ferrets reaching a combined score of 4 have reached the human end-

points and were euthanized. **d)** Fever depicted as temperature deviation from baseline. Baseline was determined as average body temperature from -5 to -1 dpi. **e, f)** Viral titers ($TCID_{50}$) in **e)** nose and throat swabs and **f)** homogenized lung and trachea tissue as determined by endpoint titration on MDCK cells. Dotted line in panel f indicates the limit of detection. **g)** Pathology scoring for selected parameters as detailed in the Materials & Methods. **h)** Lung weight 5 dpi relative to body weight on the day of infection. For all panels n = 6-7. In panels b, e, f, and h, data are visualized as mean ± SD. In panel d, data is shown as group mean. In panels c and f-h, dots represent individual observations of ferrets. One placebo ferret and three mRNA/mRNA treated ferrets needed to be euthanized 4 dpi due to reaching the humane endpoints. The mRNA/mRNA ferrets euthanized 4 dpi are visualized as separate groups or depicted by open symbols (instead of filled). For visualization purposes, only comparisons between groups placebo, H1N1/mock and H1N1/mRNA are shown. No statistics were performed for panels c and g, as these are nominal data. An overview of all statistical comparisons is detailed in Supplemental data file 1. * = $p < 0.05$, ** = $p < 0.01$, *** = $p < 0.001$.

Protection against H7N9 influenza virus is likely mediated by cellular responses

To assess whether enhanced cellular responses during H7N9 influenza virus infection are related to the observed disease outcomes, we collected PBMCs at 4 or 5 dpi (depending on when ferrets were euthanized) and stimulated cells with H1N1 peptide pools in an IFNγ ELISpot assay. Although cellular responses against M1 and PB1 were low before infection (Figure 1b), they became more substantial after infection (Supplemental Fig. 7), suggesting that M1- and PB1-specific T cells may play a role in the observed reduction in H7N9 disease parameters. Differences between groups were difficult to quantify due to the strong responses observed, which reached the upper limit of detection of the IFNγ ELISpot assay.

To exclude the possibility that antibodies against H7N9 influenza virus played a role in the protection against H7N9 infection we measured the level of antibodies in ferret sera before H7N9 infection (70 dpp). We did not detect H7N9-specific antibodies by hemagglutination inhibition (HI) and virus neutralization (VN) assays (Fig. 5a, b).

We additionally measured antibodies against H7N9 HA (H7), NP and M1 proteins by ELISA as not all influenza virus-specific antibodies can be detected by HI and VN assays. We did not find significant responses against H7, but we measured high antibody titers against NP and M1 (Fig. 5c). We could not investigate PB1-specific antibodies as the recombinant H7N9 PB1 protein was not commercially available. These findings indicate that HA-specific antibodies did not play a role in the disease reduction we observed, but the role of NP-, M1- and possibly PB1-specific antibodies remains to be investigated.

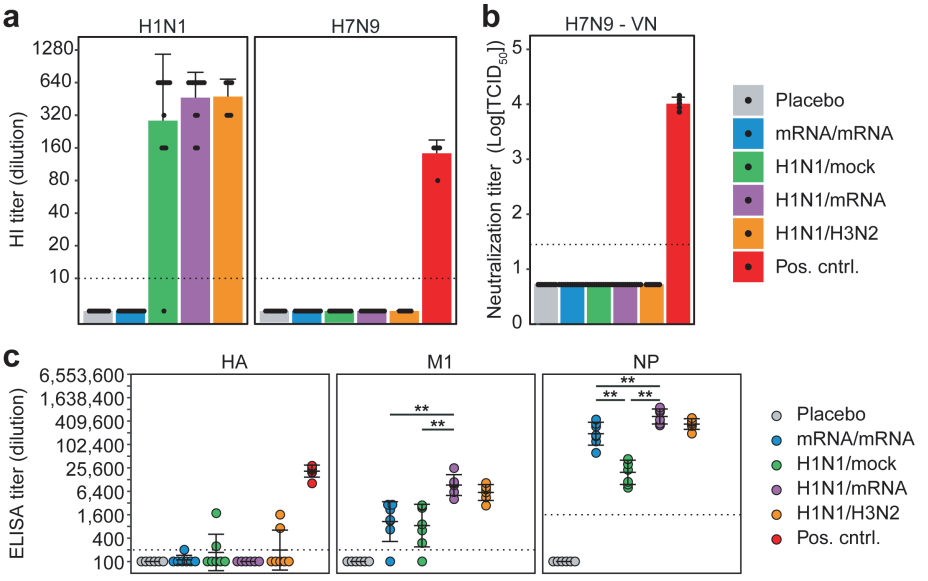

Figure 5: Antibody responses against H1N1 and H7N9 influenza viruses in sera obtained 70 days post priming (dpp). a) Antibodies against H1N1 (A/California/07/2009) or H7N9 (H7N9/PR8 reassortant) influenza virus, measured by hemagglutination inhibition (HI) assay. **b)** Virus neutralization titer against H7N9 influenza virus **c)** Antibodies binding to recombinant HA, M1 or NP of A/Anhui/1/2013 (H7N9) influenza virus measured by ELISA. The antibody titer is calculated as the extrapolated dilution of serum at which the OD 450 drops below background (mean of placebo animals + 3x SD). Positive control samples are sera from ferrets previously vaccinated twice with an H7N9 live attenuated virus [79]. Dotted line represents the lower limit of detection (a, b) or the background cut-off (c). In panels a-c, each dot represents one animal. For panels a and b, n = 7-14 (experimental groups) or n = 5 (positive control); for panel c, n = 6-7. For visualization purposes, only comparisons between groups mRNA/mRNA, H1N1/mock and H1N1/mRNA are shown in panel c. An overview of all statistical comparisons is detailed in Supplemental data file 1. * = $p < 0.05$, ** = $p < 0.01$, *** = $p < 0.001$.

Discussion

The COVID-19 pandemic has shown the enormous potential of the nucleoside-modified mRNA-LNP vaccine platform for inducing protective immune responses against SARS-CoV-2 infection in humans. This success is driving the development of mRNA-LNP vaccines against other infectious diseases, with influenza virus as a prime example. In fact, there are currently multiple mRNA-based influenza vaccines in the clinical phase of development [59]. Most of these vaccines are primarily focused on inducing neutralizing antibodies against the globular head domain of HA, which does not solve the problem of strain-specific immunity mediated by such antibodies. T cells could target a wider range of influenza viruses, but not much is known about the potential of mRNA-LNP vaccines to induce protective influenza-specific T-cell

immunity. Here, we utilized a unique ferret model in which we could measure systemic and respiratory T-cell responses to evaluate the protective capacity of a nucleoside-modified mRNA-LNP vaccine encoding three conserved influenza proteins (mRNA-Flu). To our knowledge, this is the first study that provides a detailed evaluation of an mRNA-based influenza vaccine in a relevant animal model of influenza virus infection.

To mimic the human situation, we tested a combined nucleoside-modified mRNA-LNP vaccine (mRNA-Flu) encoding the internal influenza proteins NP, M1 and PB1 as a prime-boost strategy in naïve ferrets or as a booster in influenza-experienced ferrets. Prime-boost vaccination with mRNA-Flu resulted in robust, broadly-reactive cellular responses in blood, spleen, lung, NT and BM, although responses were primarily targeted against NP. mRNA-Flu was even more effective as a booster vaccination in influenza-experienced ferrets as it enhanced T-cell responses in all tissues investigated – including the BAL – and also boosted responses against M1 and PB1. To test the protective effect of the induced immune response, we challenged ferrets with avian H7N9 influenza virus as this strain has repeatedly transmitted from birds to humans and is considered as potentially pandemic [60]. After challenge, influenza-experienced ferrets that were boosted with mRNA-Flu lost less weight, showed fewer clinical symptoms and their lungs contained less edema compared to ferrets that did not receive an mRNA-Flu booster vaccination. We did not observe a similar protection for ferrets prime-boosted with mRNA-Flu only, which might be due to less robust and broad T-cell responses in the respiratory tract. Still, these results show that our nucleoside-modified mRNA-LNP T-cell vaccine is a promising candidate to boost broadly-reactive cellular responses and can be used to enhance protection against heterosubtypic influenza viruses.

To induce a broadly-reactive T-cell response, we developed a vaccine targeting three immunogenic conserved influenza proteins. We have previously shown that both ferrets and healthy human blood donors possess clearly detectable NP-, M1- and PB1-reactive T-cells [25]. In our current experimental model, both a single mRNA-Flu vaccination and H1N1 influenza virus infection elicited NP-specific responses. Responses against M1 and PB1 were weaker, especially in mRNA-Flu-primed animals. However, booster vaccination increased M1- and PB1-specific responses in all H1N1-primed ferrets and approximately half of the mRNA/mRNA ferrets developed detectable M1 and PB1-specific responses. Although it is unclear why M1- and PB1-responses were weak initially, these responses substantially increased shortly after H7N9 influenza virus challenge, suggesting that M1- and PB1-specific T cells played a role in reducing H7N9 influenza disease. This indicates that it could be beneficial if future mRNA-based influenza vaccines targeted multiple relatively well-conserved internal proteins. This would also safeguard against influenza virus mutations as the virus is less likely to escape from a broad immune response.

The T cells induced by mRNA-Flu vaccination responded to a wide range of influenza viruses, including seasonal H3N2, pandemic H2N2 and avian H5N1 and H7N9 strains. Previous research has already shown that T cells are crucial for protection against heterosubtypic infections, especially lung resident memory T-cells (Trm) [57, 61]. We show that mRNA-LNP vaccination – in contrast to inactivated influenza vaccines [62] – is able to induce T cells residing in the respiratory tract, even when given i.m. Whether these T cells possess a Trm phenotype still remains to be elucidated due to a lack of ferret-specific reagents. The T-cell responses we found in NT and lung after mRNA-Flu prime-boost confirms a previous report of Lackzo et al. who found that i.m. administration of mRNA-LNP vaccines induced potent cellular responses in the lungs of mice [63]. The responses we found were not an artefact of circulating lymphocytes as lungs were perfused and cellular responses in the lung were higher than those in the blood, showing that influenza virus-specific T cells accumulated in the lung tissue. Still, responses in the BAL were absent in mRNA-Flu prime-boosted ferrets, indicating that local presentation of antigen and/or inflammation is required for extended tissue-residing cellular immunity. Intranasal administration of mRNA vaccines could potentially enhance protection by also inducing T cells in the BAL and increasing T-cell numbers in the NT, but additional research needs to be performed to overcome the epithelial barrier and to prevent excessive immune activation [64]. Remarkably, mRNA-Flu vaccination boosted cellular responses in the BAL, NT and lungs of H1N1-primed ferrets that reacted not only to NP, but also to M1 and PB1. This is a particularly relevant finding as a large part of the human population has already been naturally exposed to influenza virus. For this group, a single mRNA-LNP immunization administered i.m. might be sufficient to boost respiratory T-cell responses. These findings stress the importance of animal models that reflect the human infection history as pre-existing immunity can clearly influence vaccine responses.

mRNA-Flu also induced potent responses in the BM. This might be partly caused by the close proximity of mRNA-Flu administration (hind legs) and T-cell isolation from the BM (femur). In fact, T cells can be primed in the BM after local antigen presentation [65, 66]. This can be beneficial for the longevity of the cellular response as the BM serves as a reservoir for memory T cells [67, 68]. The observation that nucleoside-modified mRNA-LNP vaccination is a potent inducer of BM-residing T-cell immunity warrants further investigations into the longevity and importance of this response.

In our study, vaccine-induced T-cell responses consisted of both $CD4^+$ and $CD8^+$ T cells. Similarly, Freyn et al. found that a single dose of H1N1 NA- or NP-encoding mRNA-LNP induced robust $CD4^+$ and $CD8^+$ T-cell responses in mice [40]. In humans, SARS-CoV-2 mRNA-LNP vaccines also induced both $CD4^+$ and $CD8^+$ T cells, although the extent to which the vaccines induced $CD4^+$ and $CD8^+$ T cells differs between studies [34, 69, 70]. We found that the T-cell response after mRNA-Flu booster vaccination was

skewed towards a $CD8^+$ phenotype. This skewing might be beneficial, as clearing off virus-infected cells is primarily mediated by $CD8^+$ T cells [20]. It should be mentioned, however, that we could only measure IFNγ responses and we might have missed activated $CD4^+$ T cells that responded by producing other typical $CD4^+$ cytokines such as TNF-a and IL-2.

Besides T cells, the mRNA-Flu vaccine also induced humoral responses against NP, M1 and possibly PB1; antibodies against PB1 could not be measured due to the lack of reagents. We did not find any functional role for NP- and M1-antibodies by HI and VN assays, although these assays primarily detect (neutralizing) anti-HA antibodies. Still, in mice, vaccination with recombinant NP induced potent anti-NP antibodies that protected against severe disease after an influenza virus challenge, but only if these mice also possessed functional T cells [71, 72]. This protection might be mediated by antibody-dependent cell cytotoxicity (ADCC) activity, although it is still uncertain if NP- and M1-specific antibodies can facilitate ADCC [73, 74]. Whether ADCC or other effector mechanisms played a role in our study remains therefore unknown. Future serum transfer experiments in ferrets could help in clarifying the exact role of NP-, M1- and PB1-specific antibodies in the protection against influenza virus disease.

To evaluate the robustness of T-cell-mediated protective immunity, we utilized a ferret challenge model in which a lethal dose of H7N9 influenza virus was deposited directly into the lungs of animals by intratracheal inoculation. In this way, a large amount of pneumocytes become directly infected and T cells are only granted a short timeframe to become activated and prevent further disease. This robust challenge model is not representative of a normal human exposure. People typically encounter a lower viral load [75] and primarily in the upper respiratory tract, which affords T cells a longer time to establish protective immunity. We thus expect a greater protective effect of the T-cell response upon natural infection doses. The challenge model we used – while not utilizing a natural inoculation route and dose – very well represents the severe pneumonia observed in humans hospitalized with H7N9 influenza virus infection, which cannot be achieved with lower infection doses and other inoculation routes.

We could not clearly establish whether a prime-boost strategy with mRNA-Flu was protective likely due to a cage effect. Ferrets prime-boosted with mRNA-Flu housed in one isolator showed protection against H7N9 influenza disease similarly to mRNA-Flu-boosted influenza-experienced ferrets. Ferrets in the second isolator however showed more severe symptoms after infection than the placebo animals and needed to be euthanized one day prior to the scheduled termination of the experiment. We did not find differences between the two cages that explain this discrepancy. Both humoral and cellular immune responses were similar, ferrets tested negative for Aleutian disease and showed similar previous exposure to canine distemper virus

and ferret corona viruses. For practical reasons, the H7N9 influenza virus challenge was performed on two consecutive days with each treatment group split over both days (see Materials & Methods for details). It is unlikely that differences are due to separate preparation of the inoculum, as all other groups – which were also divided over two days – did not respond differently to the challenge. Additional experiments would be required to clarify if the influenza-specific T-cell response induced by prime-boost vaccination with mRNA-Flu is protective in naïve ferrets.

In contrast to traditional inactivated influenza virus vaccines, nucleoside-modified mRNA-LNP vaccines can induce both humoral and cellular immunity [34-38]. With the induction of a broadly-reactive T-cell response, these vaccines should be less sensitive to antigenic drift and shift that have hampered traditional HA-based vaccines. Furthermore, mRNA-LNP SARS-CoV-2 vaccines perform remarkably well in elderly people [76, 77], while inactivated influenza virus vaccines often have subpar performance with increasing age [78]. mRNA-based influenza vaccines might thus be especially suited to protect this group that is at high risk for influenza-related mortality and morbidity. For these reasons, the nucleoside-modified mRNA-LNP platform is a viable option for the improvement of seasonal influenza vaccination. The inclusion of conserved internal influenza virus proteins could additionally provide protection against potential pandemic influenza viruses, as demonstrated in the current study. To our best knowledge, this is the first study that provides a detailed evaluation of an mRNA-based combined influenza T-cell vaccine in a highly relevant ferret model. We postulate that the nucleoside-modified mRNA-LNP-based influenza vaccine can boost the number of broadly-reactive T-cells to a level that prevents severe disease and death, reducing the impact of future influenza epidemics and pandemics on the society.

Supplemental Tables & Figures

Supplemental Data File 1 and Supplemental Table 2 can be accessed online at https://doi.org/10.1101/2022.08.02.502529

Supplemental Table 1: Percentage amino acid identity of several proteins between influenza strains

Influenza virus	HA	NA	NP	M1	PB1
H1N1 (A/California/07/2009)	100	100	100	100	100
H2N2 (A/Leningrad/134/17/57)	63,43	43,49	91,77	94,05	96,3
H3N2 (A/Uruguay/716/2007)	43,01	44,03	89,56	92,46	97,49
H5N1 (A/Vietnam/1204/2004)	62,9	84,22	93,78	95,63	96,43
H7N9 (A/Anhui/1/2013)	41,12	45	92,97	92,46	95,77

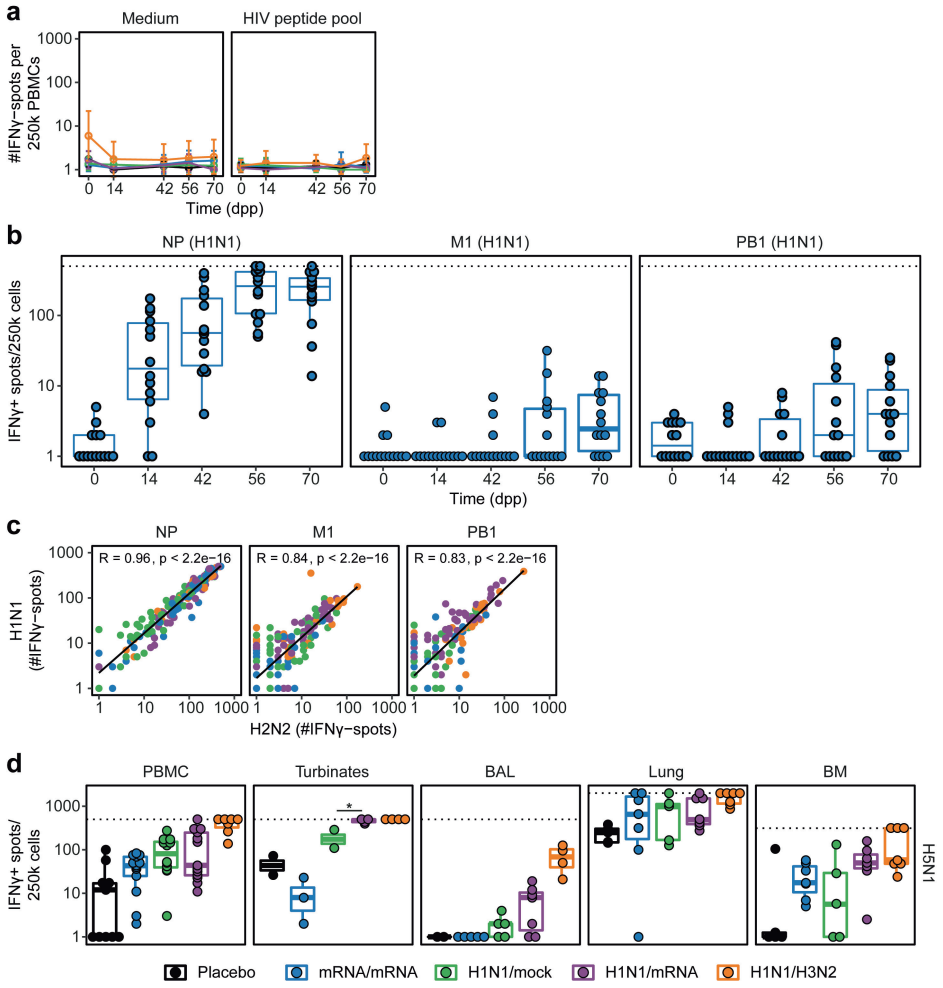

Supplemental Figure 1: Cellular responses measured by IFNγ ELISpot. a) Control stimulations for PBMC ELISpots performed 0, 14, 42, 56 and 70 days post priming (dpp). HIV responses were corrected for medium background responses. **b)** IFNγ responses in ferrets from mRNA/mRNA ferrets in time, showing that approximately half of the animals developed responses against M1 and PB1 after booster vaccination on 42 dpp. **c)** Correlation between peptide pool stimulations with NP, M1 and PB1 peptide pools of H1N1 (A/California/07/2009) and H2N2 (A/Leningrad/134/17/1957) influenza viruses. Data from ELISpots assays on 14, 42, 56 and 70 dpp are shown and correlation analysis was performed using the Pearson correlation coefficient (R). **d)** IFNγ responses measured by ELISpot after stimulation with H5N1 (A/Vietnam/1204/2004) influenza virus in various tissues 70 dpp. In panels b-d, each dot represents one animal, with n = 7-14 (PBMC), 2-4 (nasal turbinates) or 5-7 (BAL, lung, BM). For visualization purposes, only comparisons between groups mRNA/mRNA, H1N1/mock and H1N1/mRNA are shown. An overview of all statistical comparisons is detailed in Supplemental data file 1. * = $p < 0.05$, ** = $p < 0.01$, *** = $p < 0.001$.

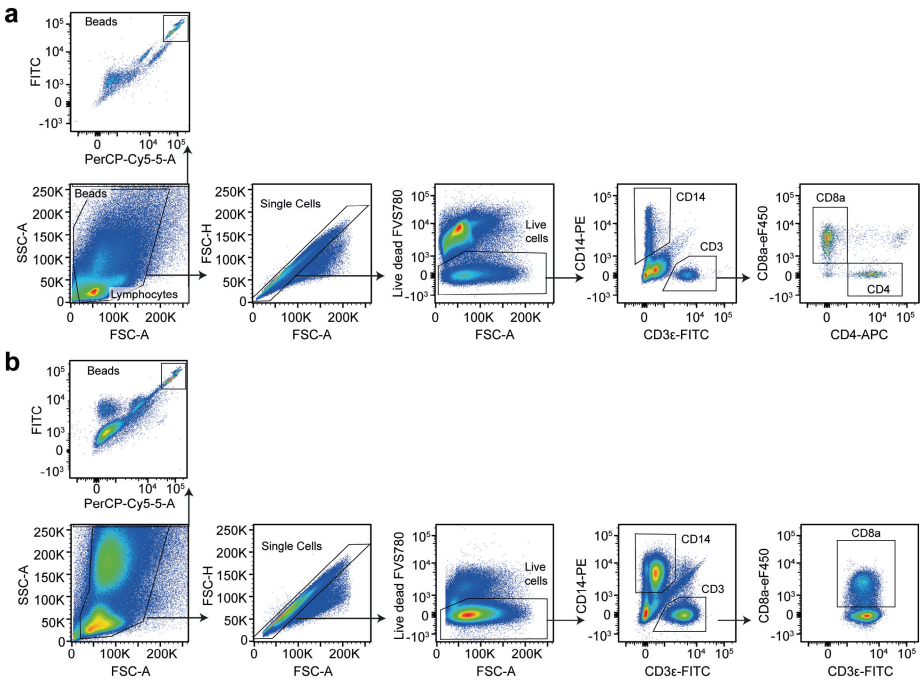

Supplemental Figure 2: FACS gating for cell counts in nasal turbinates and BAL. a, b) Gating strategy for cell populations in **a)** nasal turbinates and **b)** bronchoalveolar lavage (BAL). αCD4-APC staining was not consistent between BAL samples and was therefore excluded.

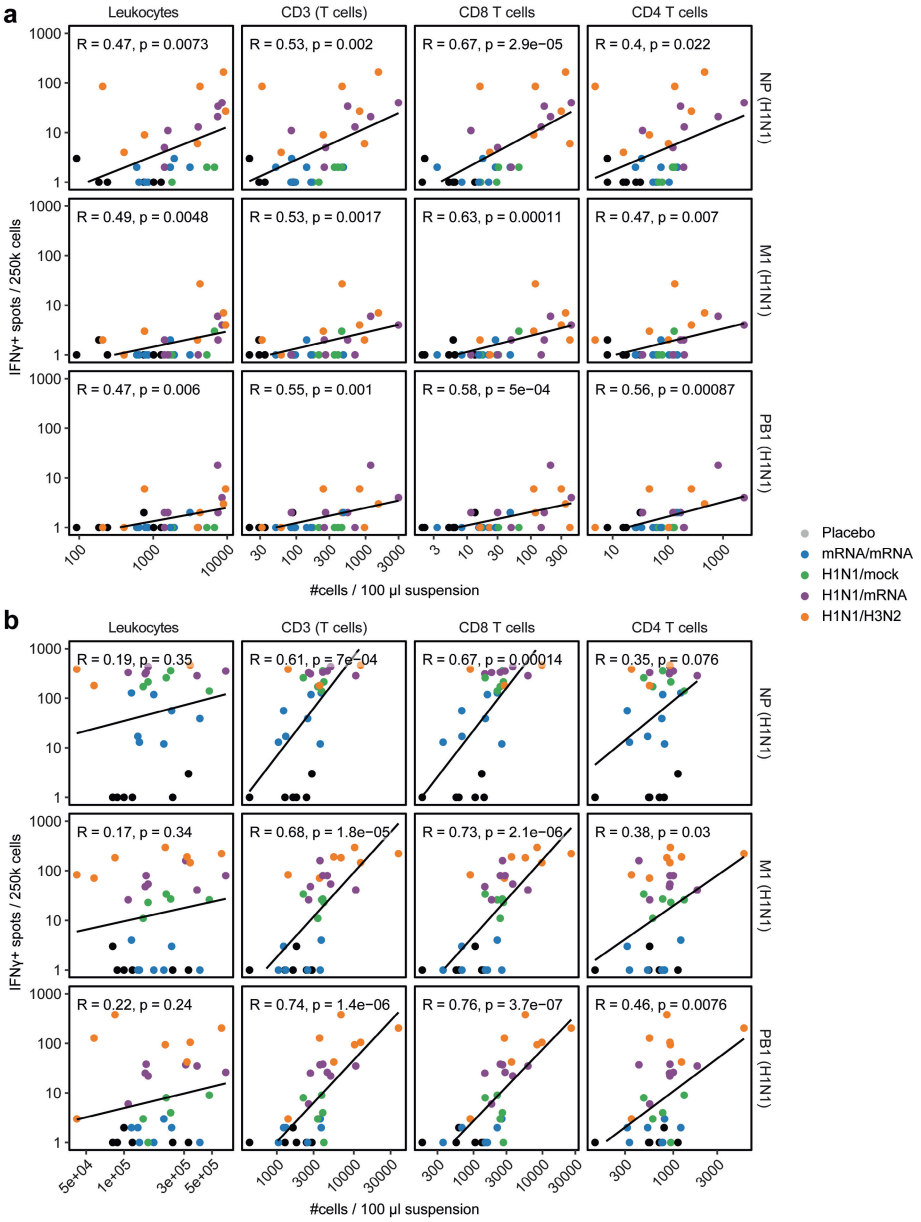

Supplementary Figure 3: Correlation between influx of cell populations and IFNγ spots in a) BAL fluid or b) nasal turbinates. Cell counts of different populations are plotted on the x-axis (data from Fig. 2c). IFNγ responses after H1N1 peptide pool stimulation are plotted on the y-axis (data from Fig. 2a). The correlation between cell counts and IFNγ responses is depicted by the black line and the correlation was calculated using the Pearson correlation coefficient (R). Each dot represents one animal with n = 5-7 per group.

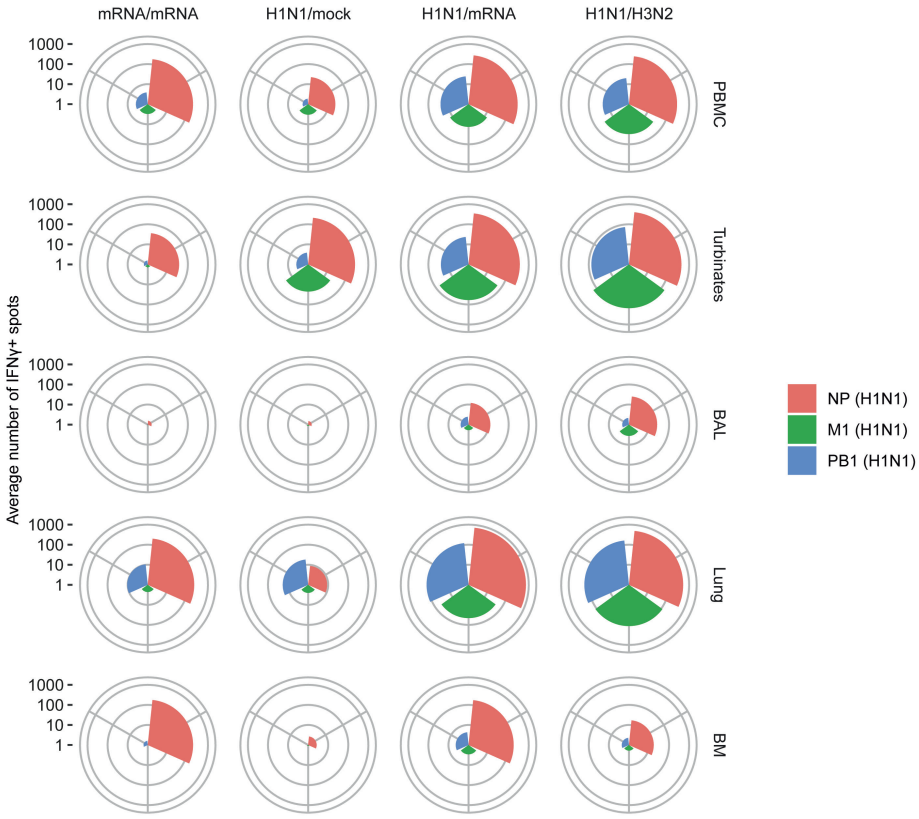

Supplemental Figure 4: Average cellular responses against NP, M1 and PB1 peptide pools of H1N1 influenza in different compartments at 70 days post priming. IFNγ ELISpot responses as depicted in Figure 1a and 2b,d,e were log-transformed and averaged per group for each response and tissue. Log-transformed means were transformed back to #spots per 250k cells and plotted per group and tissue. The size of each segment indicate the size of the average IFNγ response per group. For PBMCs, n = 12-14 for all groups except H1N1/H3N2 (n = 7). For all other tissues, n = 5-7.

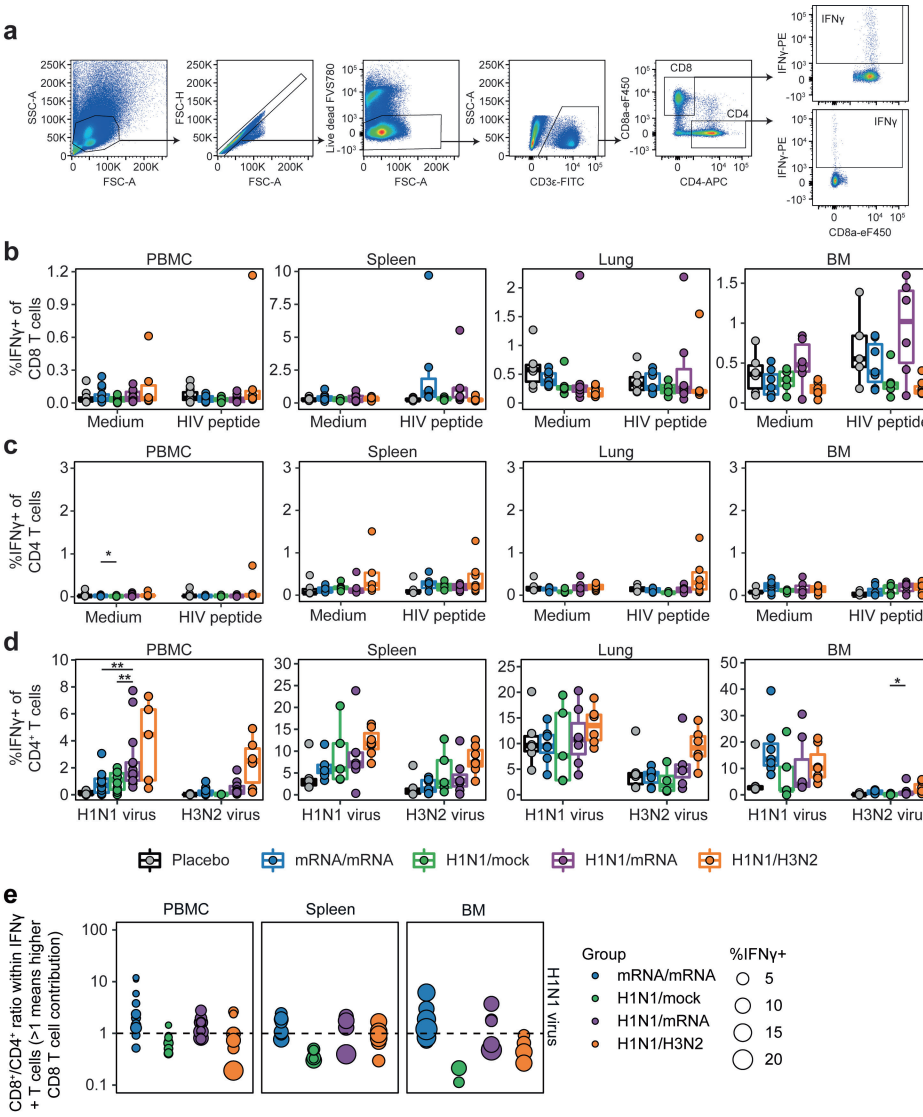

Supplemental Figure 5: IFNγ responses in CD8⁺ and CD4⁺ T cells measured by flow cytometry. a) Gating strategy for IFNγ⁺ cells within the CD8⁺ and CD4⁺ T cell populations. Example shown is from PBMCs of an H1N1/mRNA-treated ferret after peptide cocktail stimulation (NP, M1 and PB1 peptide pools), but is representative for other tissues and groups. **b, c)** Negative controls for stimulations depicted in Figure 3. IFNγ expression in **b)** CD8⁺ or **c)** CD4⁺ T cells after stimulation of lymphocytes derived from blood, spleen, lung and BM with medium or HIV peptide pool. **d)** Percentage IFNγ-positive CD4⁺ T cells after stimulation with H1N1 (A/California/07/2009) or H3N2 (A/Uruguay/217/2007) influenza viruses. **e)** Ratio between CD8⁺ and CD4⁺ T cells within the CD3⁺ IFNγ⁺ T-cell population after H1N1 influenza virus stimulation. Dotted line represents a ratio of 1 and samples with less than 50 CD3⁺ IFNγ⁺ cells were

excluded from the analysis. No ratio was calculated for lung after H1N1 virus stimulation as high background responses were present in the $CD4^+$ population of placebo animals. Boxplots depict the median, 25% and 75% percentile, where the upper and lower whiskers extend to the smallest and largest value respectively within 1.5* the inter quartile ranges. In panels b-f, each dot represents one animal. In panels b-d, for PBMC n = 6-13 and for lung, BM and spleen n = 4-7. For visualization purposes, only comparisons between groups mRNA/mRNA, H1N1/mock and H1N1/mRNA are shown. An overview of all statistical comparisons is detailed in Supplemental data file 1. * = p < 0.05, ** = p < 0.01, *** = p < 0.001.

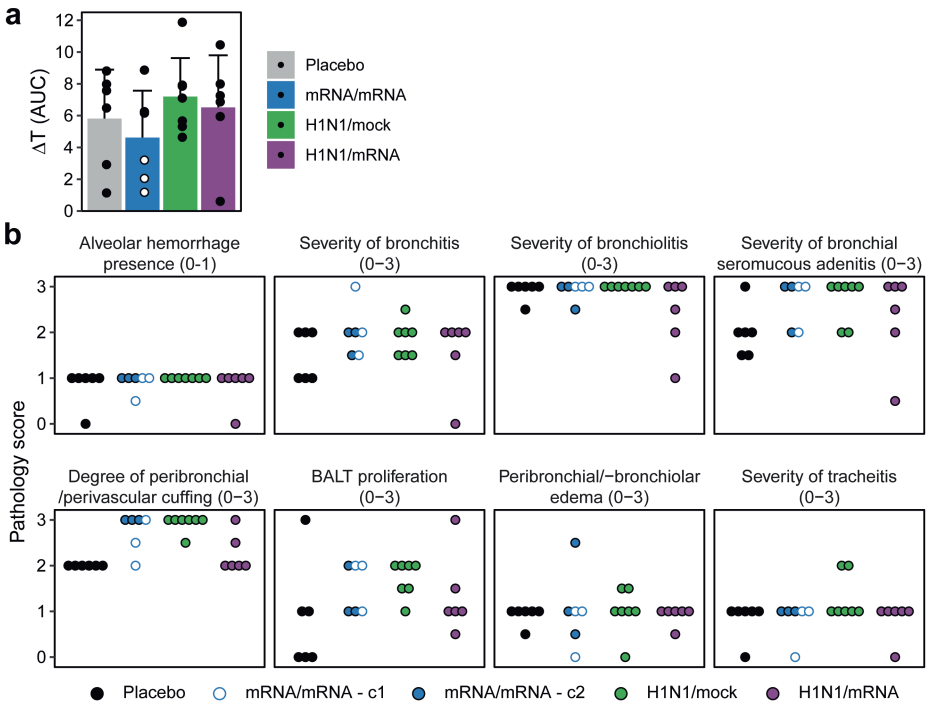

Supplemental Figure 6: Extended pathology during H7N9 influenza virus infection. a) Area under the curve (AUC) of body temperature, which was calculated from 0 to 5 days post infection (dpi) based on the data depicted in Fig. 4c. Values lower than mean + 2x SD were excluded as these are often due to anaesthesia. For one placebo ferret and three mRNA/mRNA ferrets (latter depicted in open circles), the AUC was only calculated up to 4 dpi due to these animals reaching the humane endpoints. Samples are depicted as mean ± SD with individual datapoints. **b)** Pathology scoring for various parameters. Each dot represents one animal. N = 6-7 for all panels. For visualization purposes, only comparisons between groups placebo, H1N1/mock and H1N1/mRNA are shown. No statistical testing was performed for panel b as these are nominal data. An overview of all statistical comparisons is detailed in Supplemental data file 1. * = p < 0.05, ** = p < 0.01, *** = p < 0.001.

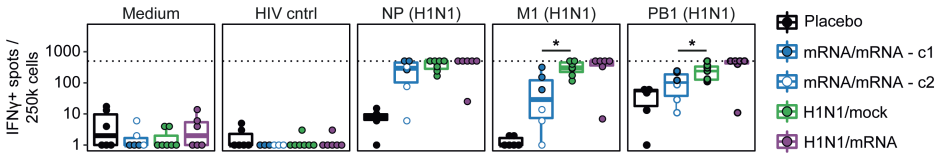

Supplemental Figure 7: Cellular responses during H7N9 influenza virus infection. PBMCs isolated 4 or 5 days post infection (dpi) with H7N9 (A/Anhui/1/2013) influenza virus were stimulated with medium, a HIV control peptide pool, or H1N1 peptide pools (NP, M1, PB1) in an IFNγ ELISpot assay. For one placebo ferret and three mRNA/mRNA ferrets, PBMCs were collected 4 dpi because these animals reached the humane endpoints and were sacrificed. For all other ferrets, blood was collected 5 dpi. Responses were corrected for medium background and data of 4 and 5 dpi were analysed together. Boxplots depict the median, 25% and 75% percentile, where the upper and lower whiskers extend to the smallest and largest value respectively within 1.5* the inter quartile ranges. Each dot represents one animal. In all panels, n = 6-7. For visualization purposes, only comparisons between groups placebo, H1N1/mock and H1N1/mRNA are shown. An overview of all statistical comparisons is detailed in Supplemental data file 1. * = $p < 0.05$, ** = $p < 0.01$, *** = $p < 0.001$.

References

1. Iuliano, A.D., et al., *Estimates of global seasonal influenza-associated respiratory mortality: a modelling study.* Lancet, 2018. **391**(10127): p. 1285-1300.
2. Paget, J., et al., *Global mortality associated with seasonal influenza epidemics: New burden estimates and predictors from the GLaMOR Project.* J Glob Health, 2019. **9**(2): p. 020421.
3. Ramsay, L.C., et al., *The impact of repeated vaccination on influenza vaccine effectiveness: a systematic review and meta-analysis.* BMC Med, 2017. **15**(1): p. 159.
4. Russell, K., et al., *Influenza vaccine effectiveness in older adults compared with younger adults over five seasons.* Vaccine, 2018. **36**(10): p. 1272-1278.
5. Osterholm, M.T., et al., *Efficacy and effectiveness of influenza vaccines: a systematic review and meta-analysis.* Lancet Infect Dis, 2012. **12**(1): p. 36-44.
6. Taubenberger, J.K., et al., *Characterization of the 1918 influenza virus polymerase genes.* Nature, 2005. **437**(7060): p. 889-93.
7. Worobey, M., G.Z. Han, and A. Rambaut, *Genesis and pathogenesis of the 1918 pandemic H1N1 influenza A virus.* Proceedings of the National Academy of Sciences, 2014. **111**(22): p. 8107-8112.
8. Ke, C., et al., *Human Infection with Highly Pathogenic Avian Influenza A(H7N9) Virus, China.* Emerg Infect Dis, 2017. **23**(8): p. 1332-1340.
9. WHO. *Cumulative number of confirmed human cases of avian influenza A(H5N1) reported to WHO*. 2020 [cited 2021 25-5-2021]; Available from: https://www.who.int/influenza/human_animal_interface/H5N1_cumulative_table_archives/en/.
10. OIE, *High Pathogenicity Avian Influenza (HPAI)- Situation Report*. 2022. p. 1-7.
11. Herfst, S., et al., *Airborne transmission of influenza A/H5N1 virus between ferrets.* Science, 2012. **336**(6088): p. 1534-41.
12. Linster, M., et al., *Identification, characterization, and natural selection of mutations driving airborne transmission of A/H5N1 virus.* Cell, 2014. **157**(2): p. 329-339.
13. Imai, M., et al., *Experimental adaptation of an influenza H5 HA confers respiratory droplet transmission to a reassortant H5 HA/H1N1 virus in ferrets.* Nature, 2012. **486**(7403): p. 420-8.
14. Krammer, F. and P. Palese, *Advances in the development of influenza virus vaccines.* Nat Rev Drug Discov, 2015. **14**(3): p. 167-82.
15. Nachbagauer, R. and P. Palese, *Is a Universal Influenza Virus Vaccine Possible?* Annu Rev Med, 2020. **71**: p. 315-327.
16. van de Sandt, C.E., et al., *Human cytotoxic T lymphocytes directed to seasonal influenza A viruses cross-react with the newly emerging H7N9 virus.* J Virol, 2014. **88**(3): p. 1684-93.
17. Tu, W., et al., *Cytotoxic T lymphocytes established by seasonal human influenza cross-react against 2009 pandemic H1N1 influenza virus.* J Virol, 2010. **84**(13): p. 6527-35.
18. Grant, E.J., et al., *Broad CD8(+) T cell cross-recognition of distinct influenza A strains in humans.* Nat Commun, 2018. **9**(1): p. 5427.
19. Koutsakos, M., K. Kedzierska, and K. Subbarao, *Immune Responses to Avian Influenza Viruses.* J Immunol, 2019. **202**(2): p. 382-391.
20. Jansen, J.M., et al., *Influenza virus-specific CD4+ and CD8+ T cell-mediated immunity induced by infection and vaccination.* J Clin Virol, 2019. **119**: p. 44-52.
21. Sridhar, S., et al., *Cellular immune correlates of protection against symptomatic pandemic influenza.* Nat Med, 2013. **19**(10): p. 1305-12.
22. Wilkinson, T.M., et al., *Preexisting influenza-specific CD4+ T cells correlate with disease protection against influenza challenge in humans.* Nat Med, 2012. **18**(2): p. 274-80.
23. Wang, Z., et al., *Recovery from severe H7N9 disease is associated with diverse response mechanisms dominated by CD8(+) T cells.* Nat Commun, 2015. **6**: p. 6833.

24. Bodewes, R., et al., *Infection of the upper respiratory tract with seasonal influenza A(H3N2) virus induces protective immunity in ferrets against infection with A(H1N1)pdm09 virus after intranasal, but not intratracheal, inoculation.* J Virol, 2013. **87**(8): p. 4293-301.
25. van de Ven, K., et al., *Systemic and respiratory T-cells induced by seasonal H1N1 influenza protect against pandemic H2N2 in ferrets.* Commun Biol, 2020. **3**(1): p. 564.
26. Gooch, K.E., et al., *Heterosubtypic cross-protection correlates with cross-reactive interferon-gamma-secreting lymphocytes in the ferret model of influenza.* Sci Rep, 2019. **9**(1): p. 2617.
27. Bodewes, R., et al., *Vaccination against seasonal influenza A/H3N2 virus reduces the induction of heterosubtypic immunity against influenza A/H5N1 virus infection in ferrets.* J Virol, 2011. **85**(6): p. 2695-702.
28. Van Braeckel-Budimir, N., et al., *Repeated Antigen Exposure Extends the Durability of Influenza-Specific Lung-Resident Memory CD8(+) T Cells and Heterosubtypic Immunity.* Cell Rep, 2018. **24**(13): p. 3374-3382 e3.
29. Slütter, B., et al., *Dynamics of influenza-induced lung-resident memory T cells underlie waning heterosubtypic immunity.* Sci Immunol, 2017. **2**(7).
30. Eickhoff, C.S., et al., *Highly conserved influenza T cell epitopes induce broadly protective immunity.* Vaccine, 2019. **37**(36): p. 5371-5381.
31. Pardi, N., et al., *mRNA vaccines - a new era in vaccinology.* Nat Rev Drug Discov, 2018. **17**(4): p. 261-279.
32. Scorza, F.B. and N. Pardi, *New Kids on the Block: RNA-Based Influenza Virus Vaccines.* Vaccines (Basel), 2018. **6**(2).
33. Hogan, M.J. and N. Pardi, *mRNA Vaccines in the COVID-19 Pandemic and Beyond.* Annu Rev Med, 2021.
34. Oberhardt, V., et al., *Rapid and stable mobilization of CD8(+) T cells by SARS-CoV-2 mRNA vaccine.* Nature, 2021. **597**(7875): p. 268-273.
35. Wang, Z., et al., *mRNA vaccine-elicited antibodies to SARS-CoV-2 and circulating variants.* Nature, 2021. **592**(7855): p. 616-622.
36. Amanat, F., et al., *SARS-CoV-2 mRNA vaccination induces functionally diverse antibodies to NTD, RBD, and S2.* Cell, 2021. **184**(15): p. 3936-3948 e10.
37. Sahin, U., et al., *COVID-19 vaccine BNT162b1 elicits human antibody and TH1 T cell responses.* Nature, 2020. **586**(7830): p. 594-599.
38. Zollner, A., et al., *B and T cell response to SARS-CoV-2 vaccination in health care professionals with and without previous COVID-19.* EBioMedicine, 2021. **70**: p. 103539.
39. Pardi, N., M.J. Hogan, and D. Weissman, *Recent advances in mRNA vaccine technology.* Curr Opin Immunol, 2020. **65**: p. 14-20.
40. Freyn, A.W., et al., *A Multi-Targeting, Nucleoside-Modified mRNA Influenza Virus Vaccine Provides Broad Protection in Mice.* Mol Ther, 2020. **28**(7): p. 1569-1584.
41. Feldman, R.A., et al., *mRNA vaccines against H10N8 and H7N9 influenza viruses of pandemic potential are immunogenic and well tolerated in healthy adults in phase 1 randomized clinical trials.* Vaccine, 2019. **37**(25): p. 3326-3334.
42. Bahl, K., et al., *Preclinical and Clinical Demonstration of Immunogenicity by mRNA Vaccines against H10N8 and H7N9 Influenza Viruses.* Mol Ther, 2017. **25**(6): p. 1316-1327.
43. Zhuang, X., et al., *mRNA Vaccines Encoding the HA Protein of Influenza A H1N1 Virus Delivered by Cationic Lipid Nanoparticles Induce Protective Immune Responses in Mice.* Vaccines (Basel), 2020. **8**(1).
44. Freyn, A.W., et al., *Antigen modifications improve nucleoside-modified mRNA-based influenza virus vaccines in mice.* Mol Ther Methods Clin Dev, 2021. **22**: p. 84-95.
45. Baiersdorfer, M., et al., *A Facile Method for the Removal of dsRNA Contaminant from In Vitro-Transcribed mRNA.* Mol Ther Nucleic Acids, 2019. **15**: p. 26-35.

46. Pardi, N., et al., *Expression kinetics of nucleoside-modified mRNA delivered in lipid nanoparticles to mice by various routes.* J Control Release, 2015. **217**: p. 345-51.
47. van de Ven, K., et al., *Pathology and Immunity After SARS-CoV-2 Infection in Male Ferrets Is Affected by Age and Inoculation Route.* Frontiers in Immunology, 2021. **12**.
48. R Core Team, *R: A Language and Environment for Statistical Computing*. 2021, R Foundation for Statistical Computing.
49. WHO, *Manual for the laboratory diagnosis and virological surveillance of influenza*. 2011, World Health Organization: Geneva.
50. de Jonge, J., et al., *H7N9 influenza split vaccine with SWE oil-in-water adjuvant greatly enhances cross-reactive humoral immunity and protection against severe pneumonia in ferrets.* NPJ Vaccines, 2020. **5**(1): p. 38.
51. Reed LJ, M.H., *A simple method of estimating fifty per cent endpoints.* The American Journal of Hygiene, 1938. **27**: p. 493–497.
52. van den Brand, J.M., et al., *Efficacy of vaccination with different combinations of MF59-adjuvanted and nonadjuvanted seasonal and pandemic influenza vaccines against pandemic H1N1 (2009) influenza virus infection in ferrets.* J Virol, 2011. **85**(6): p. 2851-8.
53. Rosenbaum, P.R., *Observational Studies*. Springer Series in Statistics. 2002.
54. Hothorn, T., et al., *Implementing a Class of Permutation Tests: ThecoinPackage.* Journal of Statistical Software, 2008. **28**(8): p. 23.
55. Benjamini, Y. and Y. Hochberg, *Controlling the False Discovery Rate: A Practical and Powerful Approach to Multiple Testing.* Journal of the Royal Statistical Society. Series B (Methodological), 1995. **57**(1): p. 289-300.
56. Hayward, A.C., et al., *Natural T cell-mediated protection against seasonal and pandemic influenza: Results of the flu watch cohort study.* American Journal of Respiratory and Critical Care Medicine, 2015. **191**: p. 1422-1431.
57. Pizzolla, A., et al., *Resident memory CD8(+) T cells in the upper respiratory tract prevent pulmonary influenza virus infection.* Sci Immunol, 2017. **2**(12).
58. Chang, H.D. and A. Radbruch, *Maintenance of quiescent immune memory in the bone marrow.* Eur J Immunol, 2021. **51**(7): p. 1592-1601.
59. Dolgin, E., *mRNA flu shots move into trials.* Nature Reviews Drug Discovery, 2021. **20**(11): p. 801-803.
60. Su, S., et al., *Epidemiology, Evolution, and Pathogenesis of H7N9 Influenza Viruses in Five Epidemic Waves since 2013 in China.* Trends Microbiol, 2017. **25**(9): p. 713-728.
61. Wu, T., et al., *Lung-resident memory CD8 T cells (TRM) are indispensable for optimal cross-protection against pulmonary virus infection.* J Leukoc Biol, 2014. **95**(2): p. 215-24.
62. Zens, K.D., J.K. Chen, and D.L. Farber, *Vaccine-generated lung tissue–resident memory T cells provide heterosubtypic protection to influenza infection.* JCI Insight, 2016. **1**.
63. Laczko, D., et al., *A Single Immunization with Nucleoside-Modified mRNA Vaccines Elicits Strong Cellular and Humoral Immune Responses against SARS-CoV-2 in Mice.* Immunity, 2020. **53**(4): p. 724-732 e7.
64. Li, M., et al., *Enhanced intranasal delivery of mRNA vaccine by overcoming the nasal epithelial barrier via intra- and paracellular pathways.* J Control Release, 2016. **228**: p. 9-19.
65. Feuerer, M., et al., *Bone marrow as a priming site for T-cell responses to blood-borne antigen.* Nat Med, 2003. **9**(9): p. 1151-7.
66. Duffy, D., et al., *Neutrophils transport antigen from the dermis to the bone marrow, initiating a source of memory CD8+ T cells.* Immunity, 2012. **37**(5): p. 917-29.
67. Di Rosa, F. and R. Pabst, *The bone marrow: a nest for migratory memory T cells.* Trends Immunol, 2005. **26**(7): p. 360-6.

68. Pascutti, M.F., et al., *Peripheral and systemic antigens elicit an expandable pool of resident memory CD8(+) T cells in the bone marrow.* Eur J Immunol, 2019. **49**(6): p. 853-872.
69. Naaber, P., et al., *Dynamics of antibody response to BNT162b2 vaccine after six months: a longitudinal prospective study.* Lancet Reg Health Eur, 2021. **10**: p. 100208.
70. Naranbhai, V., et al., *Comparative immunogenicity and effectiveness of mRNA-1273, BNT162b2 and Ad26.COV2.S COVID-19 vaccines.* J Infect Dis, 2021.
71. Carragher, D.M., et al., *A novel role for non-neutralizing antibodies against nucleoprotein in facilitating resistance to influenza virus.* J Immunol, 2008. **181**(6): p. 4168-76.
72. LaMere, M.W., et al., *Contributions of antinucleoprotein IgG to heterosubtypic immunity against influenza virus.* J Immunol, 2011. **186**(7): p. 4331-9.
73. Jegaskanda, S., et al., *Induction of H7N9-Cross-Reactive Antibody-Dependent Cellular Cytotoxicity Antibodies by Human Seasonal Influenza A Viruses that are Directed Toward the Nucleoprotein.* J Infect Dis, 2017. **215**(5): p. 818-823.
74. Vanderven, H.A., et al., *What Lies Beneath: Antibody Dependent Natural Killer Cell Activation by Antibodies to Internal Influenza Virus Proteins.* EBioMedicine, 2016. **8**: p. 277-290.
75. Oh, D.Y. and A.C. Hurt, *Using the Ferret as an Animal Model for Investigating Influenza Antiviral Effectiveness.* Front Microbiol, 2016. **7**: p. 80.
76. Polack, F.P., et al., *Safety and Efficacy of the BNT162b2 mRNA Covid-19 Vaccine.* N Engl J Med, 2020. **383**(27): p. 2603-2615.
77. Baden, L.R., et al., *Efficacy and Safety of the mRNA-1273 SARS-CoV-2 Vaccine.* N Engl J Med, 2021. **384**(5): p. 403-416.
78. Smetana, J., et al., *Influenza vaccination in the elderly.* Hum Vaccin Immunother, 2018. **14**(3): p. 540-549.
79. de Jonge, J., et al., *H7N9 Live Attenuated Influenza Vaccine Is Highly Immunogenic, Prevents Virus Replication, and Protects Against Severe Bronchopneumonia in Ferrets.* Mol Ther, 2016. **24**(5): p. 991-1002.

5

Pathology and immunity after SARS-CoV-2 infection in male ferrets is affected by age and inoculation route

Koen van de Ven[1], Harry van Dijken[1], Lisa Wijsman[1], Angéla Gomersbach[2], Tanja Schouten[2], Jolanda Kool[1], Stefanie Lenz[1], Paul Roholl[3], Adam Meijer[1], Puck B. van Kasteren[1], Jørgen de Jonge[1]

[1]Centre for Infectious Disease Control, National Institute for Public Health and the Environment (RIVM), Bilthoven, the Netherlands
[2]Animal Research Centre, Poonawalla Science Park, Bilthoven, The Netherlands
[3]Microscope Consultancy, Weesp, the Netherlands

Frontiers in Immunology - 2021
https://doi.org/10.3389/fimmu.2021.750229

Abstract

Improving COVID-19 intervention strategies partly relies on animal models to study SARS-CoV-2 disease and immunity. In our pursuit to establish a model for severe COVID-19, we inoculated young and adult male ferrets intranasally or intratracheally with SARS-CoV-2. Intranasal inoculation established an infection in all ferrets, with viral dissemination into the brain and gut. Upon intratracheal inoculation only adult ferrets became infected. However, neither inoculation route induced observable COVID-19 symptoms. Despite this, a persistent inflammation in the nasal turbinates was prominent in especially young ferrets and follicular hyperplasia in the bronchi developed 21 days post infection. These effects -if sustained- might resemble long-COVID. Respiratory and systemic cellular responses and antibody responses were induced only in animals with an established infection. We conclude that intranasally-infected ferrets resemble asymptomatic COVID-19 and possibly aspects of long-COVID. Combined with the increasing portfolio to measure adaptive immunity, ferrets are a relevant model for SARS-CoV-2 vaccine research.

Introduction

Severe acute respiratory syndrome coronavirus 2 (SARS-CoV-2) was first detected in patients near the end of 2019 and soon started a new pandemic [1]. As an intervention, effective SARS-CoV-2 vaccines were rapidly developed and implemented. Although many of these vaccines have proven to be effective in limiting mortality and morbidity [2], it remains a point of concern that SARS-CoV-2 mutants might escape vaccine-induced immunity [3]. Additionally, much remains unknown about the pathology and long-term effects of SARS-CoV-2 infection and protective immunity. Animal models are essential for investigating these issues and the scientific community has made unprecedented advances in their development since the outbreak [4, 5]. However, there are still some remaining knowledge gaps that limit the evaluation of outstanding questions.

SARS-CoV-2 spreads through direct contact, aerosols, or droplets [6-9]. Viral RNA has been detected in stool samples of infected individuals [10-12] and this has raised the question whether the fecal-oral route could also facilitate SARS-CoV-2 transmission [13]. The virus primarily replicates in respiratory tissue, but viral RNA has been detected in many other tissues including the brain, gut, heart, and endothelial lining of the vascular system [12, 14, 15]. SARS-CoV-2 infection usually induces mild disease (COVID-19), with symptoms limited to fever, dry cough, anosmia/ageusia, myalgia, fatigue, dyspnea, sputum production, headache, and occasionally diarrhea (reviewed in [16]). Fatal cases are marked by respiratory failure, arrhythmia, shock, and acute respiratory distress syndrome [15, 17, 18]. Mortality significantly increases with age and certain comorbidities such as cardiovascular disease and diabetes [15, 17, 19-21]. Despite similar infection rates between men and women, men are more likely to succumb to infection [17, 19, 20]. Some individuals additionally suffer from 'long-COVID' (post-acute COVID-19 syndrome) where they experience persisting symptoms long after initial SARS-CoV-2 infection [22].

As the ferret (*Mustela putorius furo*) is considered the best small animal model for respiratory disease caused by influenza virus [23, 24], multiple groups have investigated if ferrets are also suited to model COVID-19 [25-33]. From these studies, we know that SARS-CoV-2 efficiently replicates in the upper respiratory tract (URT) of ferrets upon intranasal (i.n.) inoculation, but replication in the lower respiratory tract (LRT) is limited [25]. There are however still many unknowns regarding the ferret model.

Here, we report our efforts to investigate the influence of both age and inoculation route on SARS-CoV-2 infection in the ferret model. As intratracheal (i.t.) inoculation with influenza virus induces more severe disease in ferrets [34-36], we wondered if we could model severe COVID-19 in ferrets by i.t. inoculation with SARS-CoV-2. In

addition, as advancing age is a risk factor for the development of severe disease [17, 19, 20], we investigated the role of age by infecting both young and adult ferrets. We found that SARS-CoV-2 infection was more efficient via the i.n. route and that i.t. inoculation and increased age did not result in more severe disease. Regardless of age and inoculation route, no clinical disease was observed. Despite the absence of symptoms, we did find pathological aberrations in the nasal turbinates and lungs that were more prominent in young ferrets and seemed to increase with time, potentially reflecting long-COVID in humans. We also report that humoral and cellular immune responses appear to depend on sufficient viral load during the acute phase of the infection. Together, our findings indicate that while ferrets might not be suited to study severe COVID-19, they can be used to model viral replication, adaptive immune responses, asymptomatic COVID-19 and possibly long-COVID.

Materials & Methods

Ethical statement

All animal experiments were conducted in line with EU legislation. The experiment was approved by the Animal Welfare Body of the Antonie van Leeuwenhoek terrain (Bilthoven, The Netherlands) under permit number AVD3260020184765 of the Dutch Central Committee for Animal experiments. Ferrets received food and water ad libitum and were inspected daily. If ferrets reached the pre-defined end points, they would be euthanized by cardiac bleeding under anesthesia with ketamine (5 mg/kg; Alfasan) and medetomidine (0.1 mg/kg; Orion Pharma). Endpoints were scored based on clinical parameters for activity (0 = active; 1 = active when stimulated; 2 = inactive and 3 = lethargic) and impaired breathing (0 = normal; 1 = fast breathing; 2 = heavy/stomach breathing). Ferrets were euthanized when they reached score 3 on activity level (lethargic) or when the combined score of activity and impaired breathing reached 4.

Cell and virus culture

VERO E6 cells were cultured in DMEM (Gibco; Thermo Fisher Scientific) supplemented with 1x penicillin-streptomycin-glutamine (Gibco) and 10% fetal bovine serum (FBS; HyClone, GE Healthcare). SARS-CoV-2 virus was originally isolated from a Dutch patient (hCoV-19/Netherlands/ZuidHolland_10004/2020) and grown on VERO E6 cells in infection medium consisting of DMEM, 1x penicillin-streptomycin-glutamine and either 0% or 2% FBS. When >90% cytopathic effect (CPE) was observed, the suspension was spun down for 10 minutes at 4000x g to pellet cell debris. The remaining suspension was aliquoted and stored at -80°C. Sequencing of virus stock used for infection revealed that no mutations had occurred compared to the primary isolate (GISAID accession ID: EPI_ISL_454753) and that the furin cleavage site was maintained. Wild-type mumps virus (MuVi/Utrecht.NLD/40.10; genotype G) was grown on Vero cells in DMEM (Gibco) with 2% FBS. Upon >90% CPE, the supernatant of the

infected Vero cells was centrifuged at 500x g, filtered (5um pore size) and aliquots were stored at -80°C.

Animal handling

Young (9-10 months) and adult (36-48 months) outbred male ferrets (Schimmel b.v., The Netherlands) arrived at the animal research facility (ARC, Bilthoven, The Netherlands) at least one week before commencement of the study. From arrival till the day of infection, ferrets were housed in open cages per group. Animals with confirmed exposure to Aleutian disease or NL63 were housed in a separate chamber. Infections were carried out in BSL-3 classified isolators where the ferrets remained till the end of the experiment. Placement of temperature transponders and infections were carried out under anesthesia with ketamine (5 mg/kg) and medetomidine (0.1 mg/kg). Buprenodale (0.2ml; AST Farma) was administered after transponder placement as a post-operative analgesic. Anesthesia was antagonized with atipamezole (0.25 mg/kg; Orion Pharma), which was delayed by 30 minutes in case of infections to prevent secretion of the inoculum by sneezing or coughing. Weight determinations and swabbing occurred under anesthesia with ketamine alone.

Study design

The study was split into three experiments (A, B and C) that were infected separately with SARS-CoV-2. Ferrets in the A, B and C experiments were respectively dissected 5, 14 and 21 days after infection. Each experiment consisted of 4-5 groups with 3 ferrets each. Groups were defined by their age (young vs adult) and infection route (intra nasal vs intra tracheal). Due to a shortage of adult ferrets, experiment B did not contain a group with i.n. infected adult ferrets. An additional mock-infected group to control for immunological assays and pathology was added to experiments B (young ferrets) and C (adult ferrets).

On day 0, ferrets were infected i.t. or i.n. with 10^7 $TCID_{50}$ SARS-CoV-2 diluted in PBS. Mock-infected ferrets received PBS i.n. alone. Virus was administered in 0.1ml for i.n. and 3ml for i.t administration. Prior to infection and on every-other day starting from day 3, bodyweight was measured and nasal, throat and rectal swabs were collected. At the end of the experiment, animals were euthanized by bleeding via heart puncture under anesthesia with ketamine and medetomidine. Prior to heart puncture, bodyweight was measured and swabs were taken.

Importantly, this study had several complicating factors. At the supplier, males were housed in groups of 3 animals. Due to strict hierarchy present in male ferret groups, we were unable to randomly allocate individual animals to treatment groups. Instead, whole cages (with 3 animals) were randomly allocated to a certain treatment. Before arrival at the animal facility, ferret sera were screened by the European Veterinary Laboratory (EVL, The Netherlands) for prior infections with Aleutian disease, human

corona NL63, canine distemper virus (CDV), feline corona virus (FCoV) and canine enteric corona virus (CCoV). FCoV and CCoV are representative for systemic and enteric ferret corona viruses respectively. Almost all animals displayed prior exposure against CDV and multiple animals tested positive for antibodies against NL63, FCoV, CCoV, influenza and Aleutian disease before start of the experiment (Supplementary table 1). Ferrets that tested positive for antibodies against influenza or Aleutian disease were allocated to placebo groups.

Sample collection

During the experiment, blood was collected from the cranial vena cava and stored in either sodium-heparin coated VACUETTE tubes (Greiner) for cellular assays or in CAT serum separator clot activator VACUETTE tubes (Greiner) to isolate serum. Blood was kept at RT and analyzed the same day. At the end of the experiment, blood was collected by heart puncture after which groups B and C received a lung perfusion to remove the majority of lymphocytes in the circulation that might affect cellular assays. The lower 4cm of the trachea was stored in formalin to study pathology while the middle 1.5cm was used to determine viral load. Lungs were weighed and the left cranial lobe was inflated with formalin and stored in 10% buffered formalin for histopathological analysis. To assess viral RNA and $TCID_{50}$-titers, 0.5cm slices of the right cranial, middle and caudal lobe were collected in Lysing Matrix A tubes (MP Biomedicals, Germany). Samples in Lysing Matrix A tubes were stored at -80°C until analysis. The rest of the lungs were used for immunological analysis and were kept cold (4°C) o/n until processing the next day.

Of the intestine, 1.5cm parts of the ileum and upper colon were collected in Lysing Matrix A tubes and formalin to assess viral RNA and pathology respectively. Next, the cranium was bisected with an oscillating blade moving from the caudal to the rostral position to prevent contamination of brain tissue by any particles from URT. The nasal turbinates on the left of the septum were used for pathology while the right side was used for virology and immunology. Finally, the olfactory bulb (OB) and sections of the cerebrum and cerebellum were collected for virology and pathology. Samples for pathology, virology and immunology were stored respectively in formalin, Lysing Matrix A tubes and RPMI1640 supplemented with 1x penicillin-streptomycin-glutamine.

Nasal and throat swabs were collected in 2ml transport buffer consisting of 15% sucrose (Merck), 2.5µg/ml Amphotericin B, 100 U/ml penicillin, 100µg/ml streptomycin and 250µg/ml gentamicin (all from Sigma). Rectal swabs were stored in 1ml S.T.A.R. buffer (Roche). After collection, all swabs were vortexed, aliquoted under BSL-3 conditions and stored at -80 °C until further analysis. Of each sample, 200µl was directly added to MagNA Pure External Lysis Buffer (Hoffmann-La Roche, Basel, Switzerland), vortexed and stored at -20 °C for RT-qPCR. Samples stored in Matrix A

tubes were thawed and 750µl of DMEM infection medium (DMEM containing 2% FBS and 1x penicillin-streptomycin-glutamine) was added. Tissues were then dissociated in a FastPrep-24™ by shaking twice for 1 minute after which the samples were spun down for 5 minutes at 4000x g. Of the supernatant, 200µl was used for RT-qPCR analysis as detailed above and 250µl was used for $TCID_{50}$-determination.

The dissection of SARS-CoV-2 infected animals occurred under BSL-3 conditions and all materials from swabs, samples in Lysing Matrix A tubes and nasal turbinates were handled under BSL-3 conditions. Blood was handled under BSL-2 conditions as blood was shown to be PCR-negative for SARS-Cov-2. Spleen and lung dissected 14 and 21 dpi were processed under BSL-2+ conditions as lung tissue did not contain infectious virus 5 d.p.i. as shown by $TCID_{50}$ analysis.

Temperature logging

In experiments B and C, animals received temperature probes (Star Oddi, Iceland) two weeks before the infection. These probes recorded temperature every 30 minutes from 7 days before infection till the end of the experiment. Fever was calculated as deviation from baseline (ΔT), where the baseline refers to the mean temperature over 5 days prior to SARS-CoV-2 infection.

Pathology

Pathology scoring was performed as described before [16, 28]. After fixation, the lung lobes were embedded in paraffin and sliced into 5µm thick sections. Slides were stained with haematoxylin and eosin and microscopically examined at 50x or 100x magnification. For each tissue, at least 20 microscopic fields were scored. Pathological scoring distinguished between the categories 'epithelial damage' and 'inflammation'. Damage related parameters included hypertrophy, hyperplasia, flattened or pseudo squamous epithelia, necrosis and denudation of bronchi(oli) epithelium, hyperemia of septa and alveolar emphysema and haemorrhages. Inflammation related parameters included (peri)bronchi(oli)tis, interstitial infiltrate, alveolitis and (peri)vasculitis characterized by polymorphonuclear (PMN) cells, macrophages and lymphocytic infiltrate. Pathological findings were scored on a scale of 0 (no aberrations) to 5 (severe damage) and were summarized in two 'end scores' for the categories 'epithelial damage' and 'inflammation'. Microscopic slides were randomized and scored blindly by an experienced pathologist.

Lymphocyte isolation

Blood collected in sodium-heparin tubes was diluted 1:1 with PBS (Gibco) and layered on top of a 1:1 mixture of Lymphoprep (1.077 g/ml, Stemcell) and Lymphoyte-M (1.0875 g/ml, Cedarlane). The gradient was spun at 800x g for 30 minutes and the interface containing PBMCs was collected. The cells were subsequently washed twice with washing medium (RPMI1640 + 1% FBS) and spun down at 500x g for 10 minutes (first

wash) or 5 minutes (second wash). After the final washing step, cells were resuspended in stimulation medium (RPMI1640 + 10% FBS + 1x penicillin-streptomycin-glutamine).

On days 14 and 21 after infection, the lungs of euthanized animals were perfused with saline to remove circulating lymphocytes from the lungs as described before [37]. Lymphocytes from the lung were isolated using enzymatic digestion. Lungs were first processed into small dices of approximately 5mm^3 using scissors. The diced tissue was then digested for 60 minutes at 37°C in 12ml of a pre-heated suspension of collagenase I (2.4mg/ml, Merck) and DNase I (1mg/ml, Novus Biologicals) in RPMI1640 while rotating. Tissue was further homogenized by gently pressing the tissue over a sieve using the plunger of a 10ml syringe. The resulting suspension was diluted with EDTA-supplemented washing medium (RPMI1640 + 1% FBS + 2mM EDTA (Invitrogen)) and filtered over a 70µm cell strainer. This suspension was layered on top of 15ml Lympholyte-M in a 50ml tube. Density centrifugation and washing steps were performed as described above, with the exception that washing medium was supplemented with EDTA to prevent agglutination of cells

SARS-CoV-2 peptide pools

PepMix™ peptide pools for T cell stimulation assays were obtained from JPT Peptide Technologies GmbH. Each pool contained 15 amino acids long peptides with an overlap of 11 amino acids spanning an entire protein of SARS-CoV-2. Due to the length of the spike protein, the spike PepMix™ was distributed over two separate vials containing peptides 1-158 and 159-315.

ELISpot

Pre-coated Ferret IFNγ-ELISpot (ALP) plates (Mabtech) were used according to the manufacturers protocol. Per well, 250K PBMCs or 31.25K lung lymphocytes were stimulated with live virus (MOI 1) or SARS-CoV-2 peptide pools (1µg/peptide/ml) in ELISpot plates for 20 hours at 37°C. Plates were then washed and developed according to the manufacturers protocol, with the modification that incubation with the first antibody occurred o/n at 4°C instead of 2 hours at RT. After the final washing step, plates were left to dry for >2 days. Plates were then packaged under BSL-3 conditions and heated to 65°C for 3 hours to inactivate any remaining SARS-CoV-2 particles. Plates were analyzed on the ImmunoSpot® S6 CORE (CTL, Cleveland, OH). Spot counts were corrected for background signals by subtracting the number of spots in the medium condition from all other conditions. Data were visualized on a log-scale, so the minimum spot count was set to '1' for visualization purposes.

Trucount

Of each animal, 50µl of heparin-blood was used for trucount analysis with the non-centrifugation PerFix-NC kit (Beckman Coulter). Cells were first stained extracellular with α-CD4-APC (02, Sino Biological), α-CD8a-eFluor450 (OKT8, eBioscience), and

α-CD14-PE (Tük4; Thermo Fisher) for 15 minutes at RT. Cells were then fixated with 5µl Fixative Reagent for 15 minutes after which 300µl Permeabilizing reagent was added. The subsequent intracellular staining consisted of α-CD3e-FITC (CD3-12, Biorad) and α-CD79a-APC/eFluor780 (eBioscience). After 15 minutes incubation at RT, 3ml of Final reagent was added to each sample. To decrease measurement time, samples were spun down for 5 minutes at 500x g and 2.8ml suspension was removed. The pellet was resuspended in the remaining volume and 50µl of Precision Count beads (Biolegend) was added to each sample to calculate the absolute number of cells. Samples were measured on a FACSymphony A3 (BD) and analysed using FlowJo™ Software V10.6.2 (BD). An example of the gating strategy is present in Supplemental figure 1.

Virus titer analysis

Virus stocks were titrated in octuplicate on VERO E6 cells in 96-wells plates. Samples were titrated in DMEM medium containing 2% FBS and 1x penicillin-streptomycin-glutamine. After 6 days, CPE was scored and $TCID_{50}$ values were calculated using the Reed & Muench method. Nose and throat swabs were similarly tested, but in sextuplicate with 8 dilutions. For swabs, 2.5µg/ml Amphotericin B and 250µg/ml gentamicin was added to the titration medium.

RT-qPCR

Lysis buffer was spiked with equine arteritis virus (EAV) as an internal RT-qPCR control and stored at -20°C until sample material was added. Total nucleic acid was extracted from samples with the MagNA Pure 96 system using the MagNA Pure 96 DNA and Viral NA Small Volume Kit and eluted in a volume of 50µl Roche Tris-HCl elution buffer. A 20µl Real-time Reverse-Transcription PCR (RT-qPCR) reaction contained 5µl of sample nucleic acid, 7µl of 4x Taqman Fast Virus Master Mix (Thermo Fisher), 5µl of DNAse/RNAse free water and 3µl of primers and probe mix (sequences shown in Table 1). The in-house SARS-CoV-2 detection assay was performed using E-gene primers and probe specific for SARS-related betacoronaviruses as described by Corman et al. [39] and the equine arteritis virus (EAV) internal control primers and probe as described by Scheltinga et al. [40]. This E-gene RT-qPCR detects genomic and subgenomic SARS-CoV-2 RNA molecules. The in-house subgenomic mRNA E-gene assay was performed using the E-gene reverse primer and probe and the forward primer as described by Zhang et al. [41]. All tests were performed on a Light Cycler 480 I (LC480 I, Roche) according to the cycling protocol detailed in table 2. Cycle threshold (Ct) values were recorded.

Total nucleic acid extracted with the MagNA Pure 96 system was used to determine ACE2 and TMPRSS2 expression in a separate reaction. First, cDNA was synthesized from the isolated RNA with the iScript™ cDNA synthesis kit (Bio-Rad) according to the manufacturers protocol using a StepOnePlus RT-PCR system (Thermo Fisher).

Table 1. Primers and probes used in this study

Oligonucleotide	Sequence	Type	Annealing temperature	Label
E_Sarbeco_F	ACAGGTACGTTAATAGTTAATAGCGT	forward	60°C	
E_Sarbeco_R	ATATTGCAGCAGTACGCACACA	reverse	60°C	
E_Sarbeco_P1	ACACTAGCCATCCTTACTGCGCTTCG	probe	60°C	FAM-BHQ1
EAV-2043F	CTGTCGCTTGTGCTCAATTTAC	forward	60°C	
EAV-2193R	AGCGTCCGAAGCATCTC	reverse	60°C	
EAV 2102P-2	TGCAGCTTATGTTCCTTGCACTGTGTTC	probe	60°C	TXR-BHQ2
Leader_Sars2	CCCAGGTAACAAACCAACCAAC	forward	60°C	
Cyclophilin_A_F	GGTGGTAAGTCCATCTACGG	forward	54°C	
Cyclophilin_A_R	ACTCTGAGATCCAGCTAGGC	reverse	54°C	
ACE2_F	TTGTATCTGTTGGCCTTCCC	forward	53°C	
ACE2_R	TCTTGATCCTGAAGTCACGC	reverse	53°C	
TMPRSS2_F	TGGGTTGAGTCAAATCTGCC	forward	55°C	
TMPRSS2_R	CTACAGTTTACCTGCTGGCC	reverse	55°C	
Beta-actin_F	TGACCGGATGCAGAAGGA [38]	forward	51°C	
Beta-actin_R	CCGATCCACACCGAGTACTT [38]	reverse	51°C	

Table 2. Cycling and temperature protocol for SARS-CoV-2 E-gene RT-qPCR

PCR Program	Segment number	Temp Target (°C)	Hold Time (sec.)	Slope (°C/sec.)	Acquisition mode	
Reverse Transcription	1	50	900	EXTERNAL*		
Denaturation/Inactivation	1	95	120	EXTERNAL*		
Denaturation	1	95	60	4.4	None	LC 480
Amplification	1	95	10	4.4	None	
(cycles:50)	2	60	30	2.2	Single	
Cooling	1	40	30	4.4	None	

* cDNA was synthesized on a thermal block after which the reactions were transferred to the LC480 thermal cycler.

RT-qPCR was performed using 1x Maxima SYBR Green/ROX qPCR Master Mix (Thermo Fisher) on the StepOnePlus with primers for Cyclophilin A, ACE2, TMPRSS2 and Beta-actin (Isogen Life Science, Netherlands; Table 1). RT-qPCR was performed for 10 minutes at 95°C, followed by 40 cycles of 95°C for 30 seconds and primer-specific annealing temperatures (see above) for 45 seconds. This was followed by 95°C for 15 seconds, 53°C for 60 seconds and 95°C for 15 seconds. A pooled reference sample consisting of 5-fold dilutions of cDNA of the nasal turbinates of 6 animals was taken along in duplicate with each RT-qPCR to create a standard curve. RNA concentrations (in arbitrary units) of test samples were interpolated from the standard curve. The relative mRNA expression of target genes ACE2 and TMPRSS2 was calculated by dividing the interpolated arbitrary RNA unit of the target genes by the geometric mean of the endogenous control genes (Cyclophilin A and Beta-actin).

ELISA

Immulon 2 HB 96-well plates (Thermo Fisher) were coated overnight at RT with 100µl/well 0.25µg/ml recombinant SARS-CoV-2 Spike or Spike receptor binding domain protein (Sino biological, China) and washed thrice with PBS + 0.1% Tween-80 before use. Sera were first diluted 1:100 in PBS + 0.1% Tween-80 and then 2-fold serially diluted. Per well, 100µl of diluted sera was added and plates were incubated for 60 minutes at 37°C. After washing thrice with 0.1% Tween-80, plates were incubated for 60 minutes at 37°C with HRP-conjugated goat anti-ferret IgG (Alpha Diagnostic), diluted 1:5000 in PBS containing 0.1% Tween-80 and 0.5% Protivar (Nutricia). Plates were then washed trice with PBS + 0.1% Tween-80 and once with PBS, followed by development with 100µl SureBlue™ TMB (KPL) substrate. Development was stopped after 10 minutes by addition of 100µl 2M H_2SO_4 and OD_{450}-values were determined on the EL808 absorbance reader (Bio-Tek Instruments). Individual curves were visualized using local polynomial regression fitting with R software [42]. Antibody titers were determined as the dilution at which antibody responses dropped below background. This background was calculated as the 'mean + 3 * standard deviation' of the OD_{450} at a 400x serum-dilution of all animals tested before SARS-CoV-2 infection.

Data analysis & Statistics

All raw data was analyzed with the software detailed above. These data were then exported to Excel and loaded into R software [42]. Data analysis and visualization of data was carried out using the R packages ggplot2 [43], tidyverse [44] and ggpubr [45]. Due to the exploratory goal and small group numbers of this study, statistical analysis was limited. For most assays, groups consisted of 3 ferrets, which we deemed insufficient for statistical testing. In case of blood cell counts, groups could be combined into young and adult animals. These groups were sufficiently large for statistical comparison, which was performed in R using the Wilcoxon signed-rank test and a correction for multiple testing by the Holm-Bonferroni method [46].

Results

Study outline

In this study we assessed the role of age and infection route on SARS-CoV-2 disease and immunity in ferrets, in an attempt to model the (severe) COVID-19 observed in humans. We infected young (9-10 months) and adult (36-48 months) male ferrets with SARS-CoV-2 through either intranasal (i.n.) or intratracheal (i.t.) inoculation (Fig. 1A). To show that adult ferrets differed from young ferrets immunologically, we performed baseline whole blood trucounts. Compared to young ferrets, B and T cell numbers were lower in adult ferrets (Fig. 1B and Supplemental Fig. 1), which has also been described for older humans [47]. Ferrets were then inoculated with a dose of 10^7 $TCID_{50}$ as others have reported that a low dose is insufficient to establish infection [32]. On 5, 14, and 21 days post infection (dpi), three animals per group were euthanized to study viral replication, pathology, and immune responses. Due to a limited supply of ferrets, no adult i.n. inoculated animals were euthanized on 14 dpi. Mock-infected young and adult ferrets inoculated i.n. with PBS were only euthanized on 14 and 21 dpi respectively.

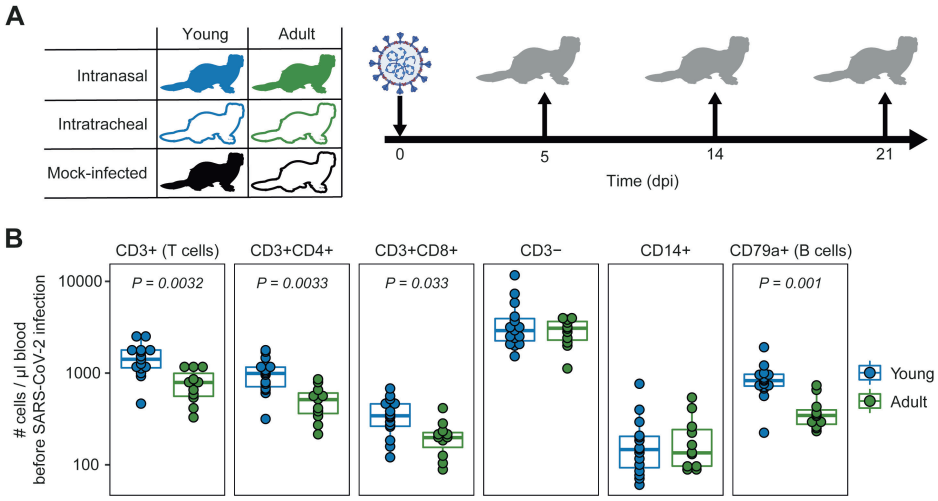

Figure 1: study outline and immunological profile of young and adult ferrets. A) Young and adult ferrets were inoculated intranasally or intratracheally with 10^7 $TCID_{50}$ SARS-CoV-2 on day 0. On 5, 14 and 21 days post infection (dpi), 3 ferrets were euthanized per group. Mock-infected ferrets were euthanized on 14 dpi (young) and 21 dpi (adult). No intranasally inoculated adult ferrets were euthanized at 14 dpi due to limited availability of adult ferrets. **B**) Cell counts in blood of uninfected young and adult ferrets. N = 15 for young animals and n = 11 for adult animals. Boxplots depict the median with the first and third quartiles. Differences between young and adult ferrets were tested via a two-sample Wilcoxon test and corrected for multiple testing using the Holm method. Panel A was created using BioRender.

Viral load is higher after i.n. inoculation

After i.n. SARS-CoV-2 infection, viral RNA was high in nose, throat, and rectal swabs, with no difference between ages (Fig. 2A). In contrast, i.t. inoculation led to reduced viral loads and was clearly influenced by age as less viral RNA was measured in young animals. Viral RNA detected by RT-qPCR does not necessarily equal the presence of infectious virus, so we determined the amount of replication-competent virus in the nose and throat by $TCID_{50}$-assay. Although viral RNA could be detected by RT-qPCR as late as 21 dpi (Fig. 2A), infectious virus was no longer detectable by 9 dpi (Fig. 2B). I.n. infection resulted in the highest viral titer in nose and throat. Viral titers were lower for i.t. infected ferrets, especially for young ferrets where almost all samples were below the detection limit.

Next, we measured viral RNA in various tissues on 5, 14, and 21 dpi. Similar to the swabs, viral RNA was higher in almost all tissues of i.n. inoculated ferrets at 5 dpi, independent of age (Fig. 2C). For i.n. infected ferrets, viral RNA was high in the nasal turbinates and low in the lung. Contrary to our expectations, i.t. inoculation did not lead to more viral RNA in the LRT (lungs and trachea). Viral RNA was also detected in the gut (ileum and colon) and disseminated from the initial site of infection to the olfactory bulb, cerebrum and even into the cerebellum. In these tissues, more viral RNA was detected in ferrets infected i.n. From day 5 onwards, viral RNA declined and was only sporadically detectable at 21 dpi.

To test whether the detected viral RNA was a result from an active infection at the site of sampling, we performed both a $TCID_{50}$-assay and an RT-qPCR specific for viral subgenomic mRNA. The presence of viral subgenomic mRNA is indicative of previous or current viral transcription in infected cells and was detected in most tissues 5 dpi (Fig. 2D), but declined afterwards. By 14 dpi viral subgenomic mRNA was only detected in the nasal turbinates of young i.n. inoculated ferrets and at 21 dpi all tissues tested negative (data not shown). Interestingly, while the presence of subgenomic mRNA indicates that SARS-CoV-2 infected multiple tissues 5 dpi, this did not result in the production of detectable infectious viral particles. Analysis by $TCID_{50}$ showed that infectious virus was only produced in the nasal turbinates at 5 dpi, with no detectable infectious virus in the lung, gut or brain at 5 dpi or later timepoints (Fig. 2E and data not shown). Due to limited tissue availability, viral $TCID_{50}$-titers in nasal turbinates were not tested on 14 and 21 dpi.

Infection of cells by SARS-CoV-2 is dependent on the expression of the binding receptor ACE2 (Angiotensin-converting enzyme 2) and the fusion priming protease TMPRSS2 (Transmembrane protease, serine 2) [1, 48, 49]. In order to determine if the reduced replication of SARS-CoV-2 in the LRT of young animals could be explained by lower ACE2 and TMPRSS2 expression, we quantified ACE2 and TMPRSS2 mRNA by RT-qPCR in young and adult placebo animals. ACE2 and TMPRSS2 expression was

however similar between nasal turbinates and lung tissue, indicating that the absence of SARS-CoV-2 replication in the LRT was not due to reduced expression of ACE2 or TMPRSS2 (Fig. 2F). Adult animals did seem to express lower levels of ACE2 and TMPRSS2, but this did not negatively impact viral load (Fig. 2A, B).

Pathology in the URT is higher for i.n. infected animals

Despite active SARS-CoV-2 replication, ferrets did not display any overt clinical signs of COVID-19 disease that are observed for humans. Compared to mock-infected animals, SARS-CoV-2-infected animals did not lose more weight and did not experience fever (Supplemental Fig. 2AB), nor were alterations in respiratory function and physical activity observed. Despite the absence of clinical disease, infection with SARS-CoV-2 did result in pathological aberrations in the respiratory tract as determined by histopathology.

In the nasal turbinates, pathological aberrations were restricted to the respiratory epithelial lining of the naso- and maxilloturbinates (Fig. 3A). The sub- and intraepithelial inflammation resulted in thickened respiratory mucosa and an exudate of polymorphonuclear cells, lymphocytes and some macrophages.

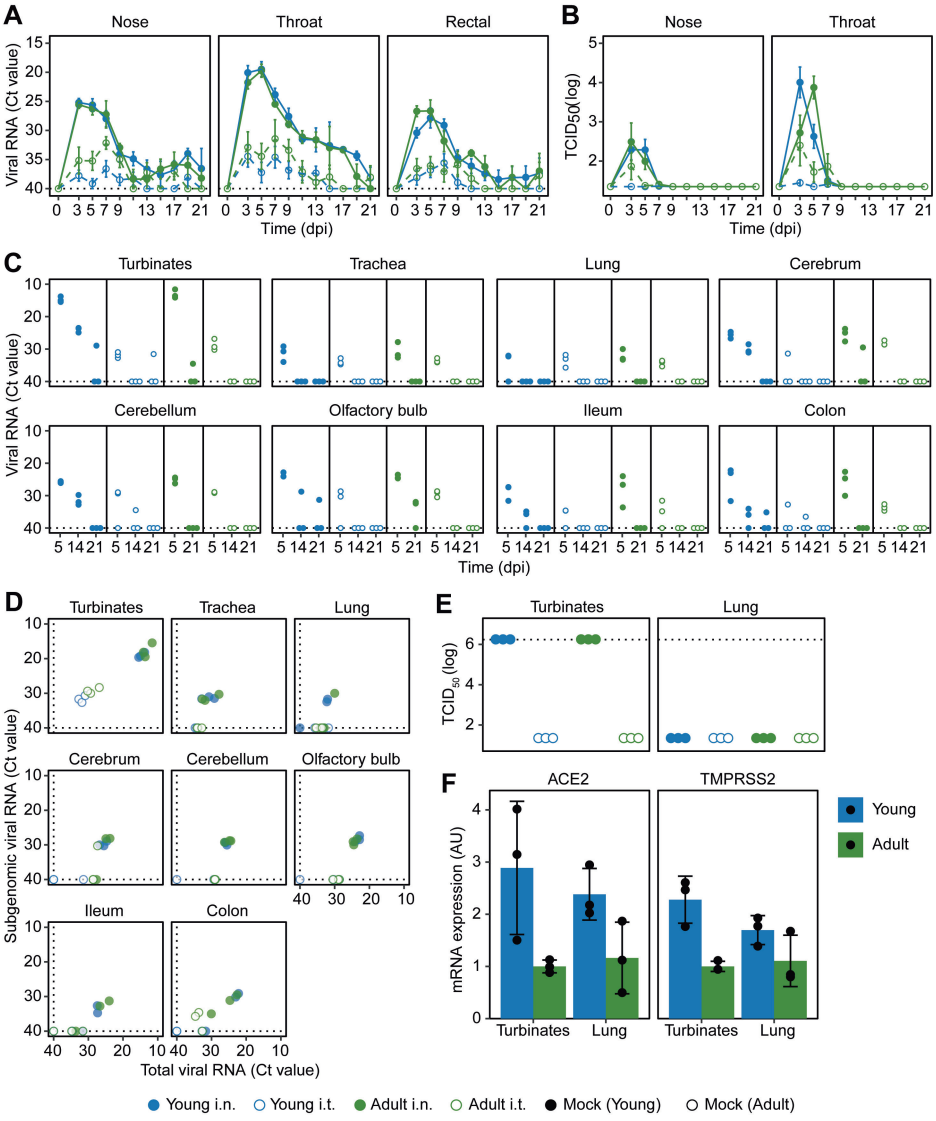

Figure 2: Viral load in swabs and tissues of SARS-CoV-2 infected ferrets. A, B) Viral load measured by RT-qPCR (A) and $TCID_{50}$-assay (B) in swabs collected from SARS-CoV-2 infected ferrets on various days post infection (dpi). **C**) Viral RNA in tissues at 5, 14 and 21 dpi measured by RT-qPCR. **D**) Total viral RNA on 5 dpi as depicted in (C) plotted against subgenomic viral RNA. **E**) Infectious virus detected by $TCID_{50}$-assay in nasal turbinates and lung 5 dpi. **F**) Expression of SARS-CoV-2 receptor ACE2 and TMPRSS2 protease in nasal turbinate and lung tissue of placebo animals, plotted as arbitrary units (AU). In panels A, C and D, RT-qPCR negative specimens were set to a Ct-value of 40 for visualization purposes, which is depicted by dotted lines. In panel E, dotted lines depict the highest dilution tested. For A, B: n = 3-9. For C-F: with exception of 'Adult i.t.' on 14 dpi (n = 2), all groups are n = 3.

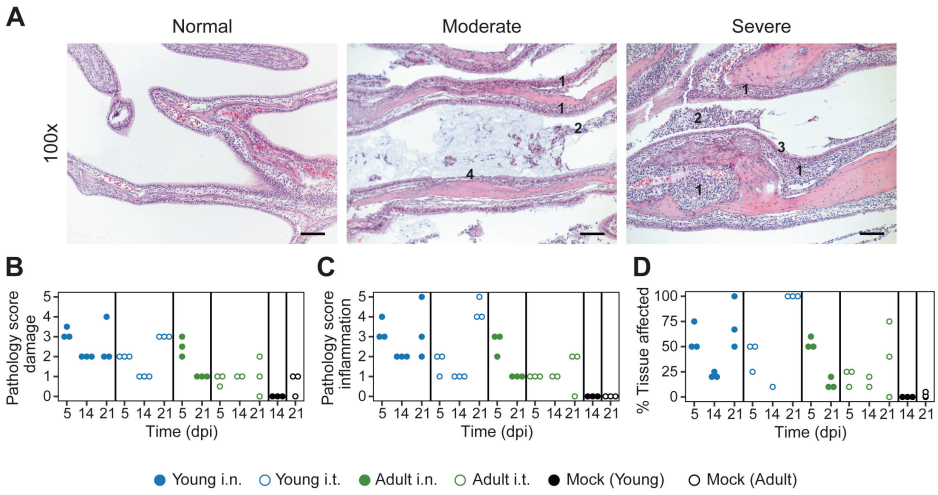

Figure 3: SARS-CoV-2 infection induces more severe URT pathology in young ferrets. A) Representative haematoxylin and eosin stained sections of normal, moderate (score 2) and severe (score 4) affected naso- and maxilloturbinates at 100x magnification. SARS-CoV-2 infection induced infiltration of polymorphonuclear cells into the lamina propria and submucosa of the respiratory epithelium, resulting in thickened respiratory mucosa (indicated with '1'). This was accompanied by exudate containing mucus (moderate) and many polymorphonuclear cells, lymphocytes and some macrophages (2). The infection caused hyperplasia/hypertrophy of the epithelial cells (3) and sometimes the epithelial lining was absent (4). Images are from SARS-CoV-2 infected ferrets at 5 ('moderate and severe) or 21 dpi ('normal'). Bars represent 100µm. **B-D**) Scoring by parameters related to epithelial damage (B), inflammation (C) and percentage of tissue involved in pathologic changes (D). The infection-induced pathology was scored on a scale of 0–5 based on the parameters described in the materials and methods. With exception of 'Adult i.t.' on 14 dpi (n = 2), all groups are n = 3 and each dot represents an animal.

Damage to the epithelial lining was characterized by hypertrophy, hyperplasia, and squamous metaplasia and sporadically the epithelium was absent. Hypertrophy of goblet cells was also present and haemorrhage was sometimes observed. The different pathological facets were categorized into inflammation and damage, for which an end-score was determined as previously described (Fig. 3B, C and Supplemental fig. 3) [50].

In general, the severity of pathology was dependent on age and infection route, although the age-correlation was opposite to our expectations. In the acute phase (5 dpi), i.n. inoculated ferrets displayed more pathological aberrations in the nasal turbinates, which partly resolved by 14 dpi (Fig. 3B, C). Strikingly, inflammation and to a lesser extent epithelial damage increased again by 21 dpi in young animals, but was less pronounced in adult ferrets. Notably, this effect was stronger in i.t. infected young ferrets than in i.n. infected young ferrets and involved 100% of the epithelium

of the naso- en maxilloturbinates (Fig. 3D). Pathology in the nasal turbinates thus increased in young animals even after the infection had been cleared.

Pathology in the LRT is not affected by inoculation route

On a macroscopic level, the lungs of SARS-CoV-2 infected ferrets did not show aberrations in the acute phase (5 dpi), apart from a few darker patches. However, red opalescent coloring along the bronchus and as isolated patches started to appear at 14 and 21 dpi. During the course of this study, there was no increase in lung weight, indicating absence of serious edema (Supplemental Fig. 2C). Microscopically, slight peribronchi(oli)tis – characterized by the presence of infiltrating cells in the submucosa along the bronchi – was observed 5 dpi (Fig. 4A). The bronchus epithelium showed some reaction in the form of mild to minor hyperplasia, sometimes visible as repeated epithelial bumps. Strikingly, hyperplasia of the Bronchus-Associated Lymphoid Tissue (BALT) developed in 1 out of 3 i.n. and in 2 out of 3 i.t. infected young ferrets by 21 dpi, but was absent in adult ferrets. Mild to strong follicular hyperplasia was located at the first branches of the bronchus and in the more severe cases extended to the smaller bronchiole (Fig. 4A). Obstruction of bronchioli occurred regularly due to compression by the hyperplastic follicles. These consisted of activated lymphocytes, which penetrated through the muscle layer of the bronch(iol)us into the lamina propria. In addition, albeit low in number, local patches of mild to moderate desquamative interstitial pneumonia had developed. The pathology score and percentage affected lung parenchyma increased from 5 to 21 dpi, mostly in in the young ferrets (Fig. 4B-C and Supplemental Fig. 4). Of note, young animals that were investigated 21 dpi had tested positive for antibodies against NL-63 and enteric and systemic corona viruses prior to SARS-CoV-2 infection (Supplemental table 1). This combination was absent in adult ferrets, complicating the interpretation of these results.

In concordance with our findings in the lung and nasal turbinates, pathology in the trachea increased by 21 dpi (Fig. 4D, Supplemental Fig. 5). The epithelium of the trachea in all young ferrets and in the i.t. adult group was often hyperplastic and sometimes showed serious damage and pseudo squamous characteristics 21 dpi (Fig. 4E). Inflammatory cells infiltrated the submucosa and epithelium, most prominently in young ferrets. Since SARS-CoV-2 viral RNA was also detected in the gut, histopathological analysis of the ileum and colon was performed, but no deviations were observed. In conclusion, independent of inoculation route, young animals displayed more severe pathology than adult ferrets in both the URT and LRT, but it is uncertain whether the increase until 21 dpi is due to age or prior exposure to other coronaviruses.

Cellular and humoral Immunity

As several ferrets used in this study displayed antibody responses against ferret corona viruses and NL-63 prior to the start of the study (Supplemental table 1), we wondered if cross-reactive responses to SARS-CoV-2 were present in these animals. We measured antibody responses against SARS-CoV-2 spike protein (S) and its receptor binding domain (RBD) by ELISA. Cellular responses were measured by IFNγ-ELISpot in which PBMCs were stimulated with live SARS-CoV-2 or overlapping peptide pools of the S, membrane (M) and nucleoprotein (N) proteins. In three animals the antibody response against SARS-CoV-2 was just above background prior to infection (Supplemental Fig. 6A). Additionally, another animal in the young i.n. infected group clearly responded against an overlapping peptide pool of SARS-CoV-2 spike protein in ELISpot on two separate time-points before infection (Supplemental Fig. 6B). This animal tested positive for antibodies against ferret corona and NL63, but not against SARS-CoV-2 (Supplemental table 1 and Supplemental Fig. 6A), suggesting that there might have been a cross-reactive T cell response. Interestingly, the animal displayed similar viral kinetics as other animals of the same treatment group, but it displayed more severe pathology 21 dpi.

After SARS-CoV-2 infection, i.n. inoculated ferrets displayed high antibody responses against both S and RBD with no evident differences between young and adult animals 14 dpi (Fig. 5A). In contrast, antibody titers in i.t. infected animals were lower with a clear distinction between ages. More adult (4/5) than young (1/6) i.t. inoculated ferrets displayed responses against S-protein after infection. Similar findings were obtained for humoral responses against RBD.

Next, we investigated cellular responses at 14 dpi. PBMCs mainly responded against the larger peptide pools of S (S1 & S2), M and N (Fig. 5B). We additionally measured responses against envelope (E) and accessory proteins (ORF3a-ORF10), but responses against these peptide pools were marginal and did not differ from naïve animals. Consistent with the low viral load, only 1/6 young i.t. infected animals responded to any SARS-CoV-2 stimulus, indicating that almost no cellular immunity was established in this group by 14 dpi. For the other groups, no clear differences between infection routes or age were observed. The responses 21 dpi were similar to those of 14 dpi (Supplemental Fig. 7A). As others have reported the presence of cross-reactive T cell responses in humans [51-54], we also tested if PBMCs from SARS-CoV-2 infected ferrets would respond upon stimulation with spike peptide pools of coronaviruses NL63, OC43, 229E and HKU1. Some animals displayed minor responses, although they were only slightly higher than mock-infected animals (Fig. 5C).

We additionally investigated cellular responses in the lung. To reduce contamination of the lung lymphocytes with circulating lymphocytes, lungs were perfused with saline on 14 and 21 dpi.

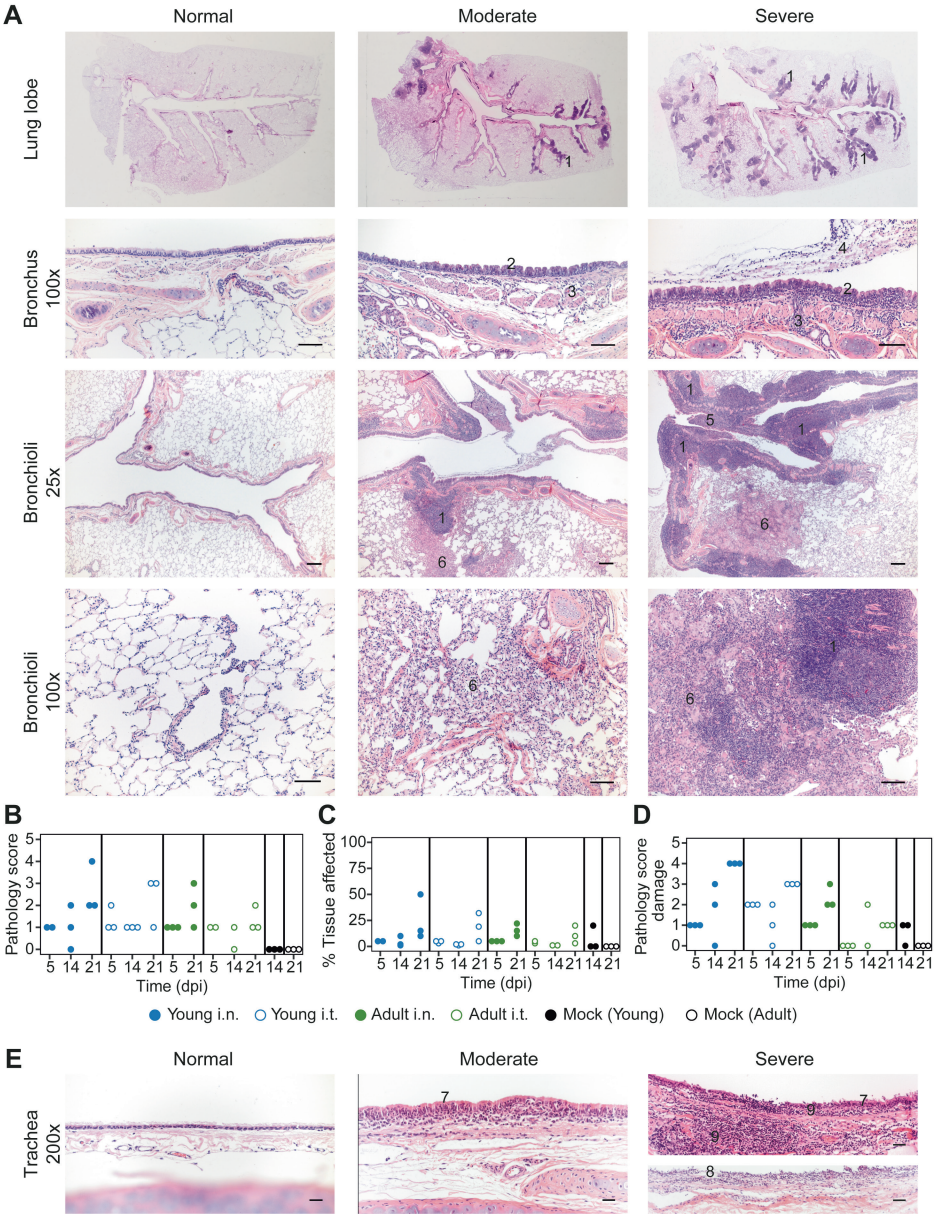

Figure 4: Pathology aspects of lung and trachea. A) Representative haematoxylin and eosin stained sections of normal, moderately and severely affected respiratory tissues at overview, 25x and 100x magnification. Lungs of SARS-CoV-2 infected animals with a clear hyperplasia of the Bronchus-Associated Lymphoid Tissue (BALT), consisting of activated lymphocytes that penetrate through the muscle layer of the bronch(iol)us into the lamina propria and submucosa (indicated in figure with '1'). Hyperplasia of bronchial epithelium visible as repeated bumps (2), cellular infiltrate into the submucosa (3) and exudate in the lumen (4) were also

observed. The presence of hyper-plastic follicles led to obstruction of bronchiole (5). Some animals displayed desquamative interstitial pneumonia, with pulmonary macrophages in the alveoli and to a minor extent, lymphocytes and plasma cells (6). The alveolar epithelium (pneumocytes) exhibited squamous-like characteristics. Images are taken from placebo ferrets ('normal') or SARS-CoV-2 infected ferrets 14 or 21 dpi ('moderate', 'severe'). **B-D**) Pathology was summarized in an overall score ranging from 0-5 based on the parameters described in the materials and methods. Pathology score (B) and % of tissue affected (C) for lung tissue and pathology score for trachea (D). With exception of 'Adult i.t.' on 14 dpi (n = 2), all groups are n = 3. **E**) Representative haematoxylin and eosin stained sections of normal, moderately and severely affected trachea tissue slides at 200x magnification. Pathological aberrations in the trachea consisted of hyperplasia (7), damage and pseudo-squamous characteristics of the epithelium (8) and infiltration of inflammatory cells into the submucosa and epithelium of the trachea (9). Images are taken from SARS-CoV-2 infected ferrets 5 ('normal) or 21 dpi ('moderate', 'severe'). Bars represent 200µm, 100µm and 50µm at respectively 25x, 100x and 200x magnification.

In comparison to PBMCs, responses against the smaller SARS-CoV-2 peptide pools seemed more prominent in lung-derived lymphocytes of young i.n. infected animals. In this group, two out of three ferrets showed responses against ORF3a, ORF6, ORF8, ORF9b and ORF10 peptide pools at 21 dpi (Fig. 5D). Like in PBMC, cellular responses were absent in the lung of i.t. infected young ferrets. Of note, responses in the lungs of i.t. infected old animals differed between day 14 and 21 post infection, with responses being higher overall on 21 dpi (Fig. 5D and Supplemental Fig. 7B). However, the group size (n = 2-3) was too small for reliable statistical testing.

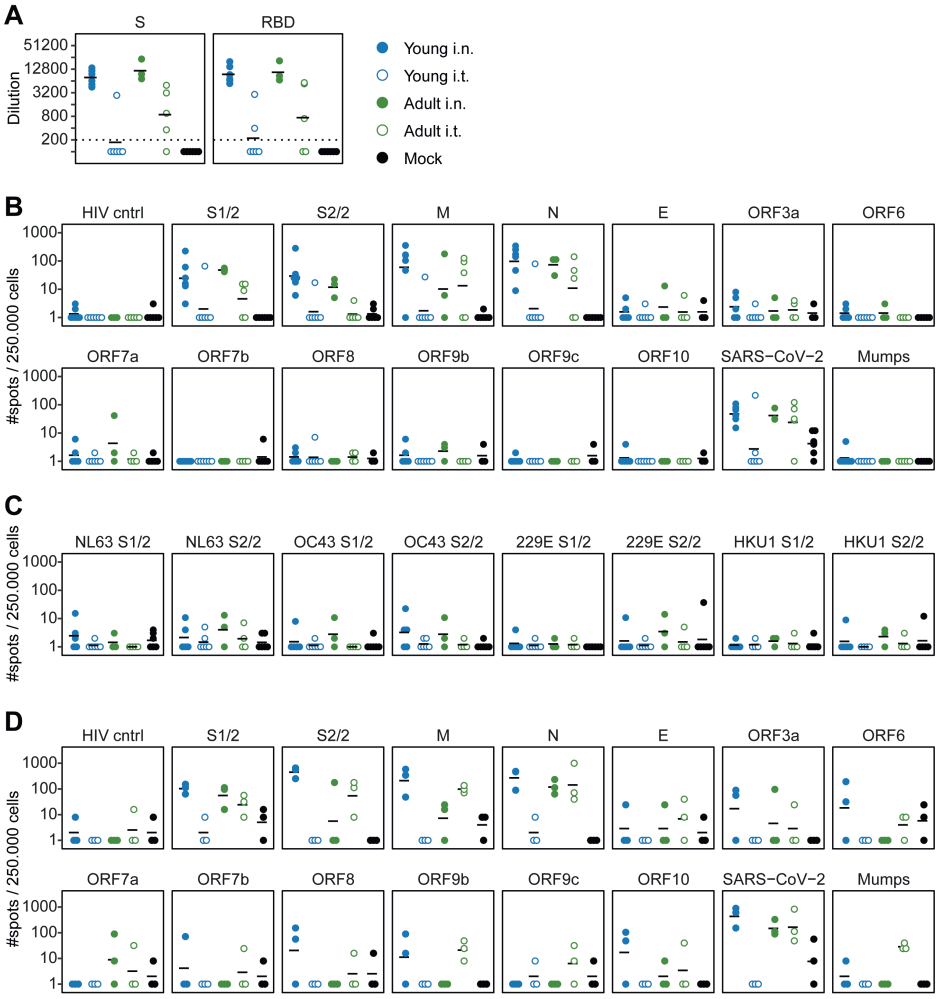

Figure 5: Cellular and humoral responses in SARS-CoV-2 infected ferrets are affected by inoculation route. A) Humoral responses detected by ELISA against whole spike (S) and the receptor binding domain (RBD) region of spike in serum 14 dpi. Responses are depicted as the (modelled) dilution at which the ELISA curve drops below background (mean + 3x SD of SARS-CoV-2 naïve animals at 200x dilution). The dotted line indicates the lowest dilution tested and negative samples were set to half that dilution for visualization purposes. **B-D**) Cellular responses in PBMCs (B, C) and lung-derived lymphocytes (D) as determined by IFNγ-ELISpot. Cells were stimulated with SARS-CoV-2 peptide pools or live virus. HIV cntrl and Mumps are negative controls for peptide pool and virus stimulations respectively. Data shown here were corrected for medium background and were set to a minimum of 1 spot for visualization on a log-scale. **B**) PBMCs isolated 14 or 15 days post infection (dpi). **C**) Frozen PBMCs isolated 14 or 21 dpi were thawed and stimulated with peptide pools of endemic human coronaviruses. **D**) Responses by lung-derived lymphocytes at 21 dpi. For b and c, samples were collected 14 and 15 or 14 and 21 dpi respectively, but visualized as a single group. N = 3-6 for panels A-C and n = 3 for panel D. Black lines indicate (geometric) mean per group.

Discussion

In this study we utilized a male ferret model to assess the influence of age and infection route on SARS-CoV-2 disease and immunity. Intranasal inoculation was more efficient in establishing an infection compared to intratracheal administration. This was especially the case for young ferrets, in which virus hardly replicated after i.t. inoculation. In contrast, disease and pathology were not increased in older animals or upon intratracheal inoculation.

Despite a productive SARS-CoV-2 infection, ferrets did not develop the symptomatic disease that is reported for humans (reviewed in [16]). A slightly more watery defecation was observed in some animals towards the end of the study, but occurrences were too few to confidently attribute this to SARS-CoV-2 infection. We did however detect SARS-CoV-2 genomic RNA and subgenomic mRNA in rectal swabs and gut tissues at multiple time-points. Subgenomic SARS-CoV-2 mRNA is indicative of viral infection, which suggests that SARS-CoV-2 is indeed enterotropic in ferrets, similar to what has been reported for humans [14, 55-58]. In addition, the presence of viral genomic RNA and subgenomic mRNA in the olfactory bulb, cerebrum and cerebellum of ferrets is in line with reports that SARS-CoV-2 can infect the CNS of patients [14, 59, 60]. Infection of the olfactory bulb might explain the anosmia often found in COVID-19 patients. It is however important to note that while the presence of subgenomic mRNA indicates infection of various tissues, there was a lack of infectious virus as measured by $TCID_{50}$-assay. This raises the question whether the production of infectious virus in these tissues is completely absent or only happened within the first few days after inoculation.

The lack of clinical disease in this study is in line with previous SARS-CoV-2 ferret studies. In those studies bodyweight did not decrease after infection, although reduced activity was observed in some instances [25, 29, 32]. Fever was observed in some studies [25, 27], but not in others [29, 32, 33]. Ferrets thus do not model the severe aspects of COVID-19. Despite this knowledge, we initiated this study because existing studies did not investigate intratracheal inoculation in (older) male ferrets. Shi *et al*. did perform an intratracheal infection in female ferrets and found viral RNA in the nasal turbinates and trachea, but not in the lung [30]. In our study, adult male ferrets displayed higher viral titers after i.t. infection compared to young ferrets, indicating that age increases susceptibility to LRT SARS-CoV-2 infection in the ferret model. We postulated that the reduced viral replication in the LRT of especially young ferrets might be due to differential expression of the SARS-CoV-2 receptors ACE2 and TMPRSS2 [1, 49]. However, this does not seem to be the case as ACE2 and TMPRSS2 expression was similar between nasal turbinate and lung tissue and young ferrets actually expressed more ACE2 and TMRPSS2 than adult ferrets. It thus seems that factors other than receptor expression prevent the successful

replication of SARS-CoV-2 in the LRT of young ferrets. Other age-dependent factors that are thought to affect SARS-CoV-2 replication include the immune system, the presence of comorbidities and the status of the vascular endothelium [61]. Further research might clarify to which extent these variables influence the ferret response to SARS-CoV-2 infection.

Notwithstanding the lack of clinical symptoms, we and others [30, 32] did find pathological abnormalities in infected ferrets. While SARS-CoV-2 replicated less efficiently in young i.t. inoculated animals and almost no adaptive immune response was induced, they did display some of the most affected pathology. It is however important to mention that all young ferrets euthanized on 21 dpi tested positive for antibodies against ferret corona and NL63 prior to SARS-CoV-2 infection. We cannot exclude that this might have had an effect and it has been postulated that existing cross-reactive immune responses can worsen COVID-19 disease outcome [62]. Ryan *et al.* also found that pathology was still increasing between 14 and 21 dpi, although they did not report the immune status of their ferrets for other corona viruses. It is tempting to speculate that the increasing pathology post SARS-CoV-2 infection partly resembles aspects of long-COVID that have been described in convalescent patients [22, 63-65]. These patients suffer from sequala up to months after initial infection with SARS-CoV-2. Although the symptoms are diverse, dyspnea is a relatively common occurrence. In theory, the BALT hyperplasia that we observed in ferrets and the resulting constriction of the bronchi(oli) could induce dyspnea, although there is no evidence yet that this is the cause of dyspnea in patients suffering from long-COVID.

After SARS-CoV-2 infection we detected antibodies against SARS-CoV-2 S-protein and RBD. Antibody titers were highest in i.n. infected ferrets, low in adult i.t. infected animals and absent in most young i.t. infected animals. This suggest that sufficient viral replication is required for seroconversion, as ferrets with lower viral loads also displayed lower humoral responses. This was especially clear in the i.t. young group, where the only ferret that developed humoral and cellular immunity also possessed the highest titer of replicative competent virus. Cellular responses were also strongest in i.n. inoculated ferrets. Similar to cellular responses of convalescent patients [54, 66], most responses in ferrets were aimed against S, M and N proteins. In both ferrets and humans [54, 66], almost no response against the E protein was observed. Cellular responses against multiple accessory proteins of SARS-CoV-2 were limited in the blood, but lung-derived lymphocytes did respond against several of these peptide pools. Likely, the relative abundance of SARS-CoV-2 specific T cells is higher in the lung, thereby increasing the sensitivity of the ELISpot assay. As cross-reactive cellular responses for SARS-CoV-2 have been described in humans [51-54], we also measured responses in the blood against peptide pools of S-proteins of other corona viruses. However, responses were low and interpretation of the results will require a larger group size and more sensitive assays.

Due to the global circumstances at the time of this study, there are several caveats present in the experimental set-up. The availability of (male) ferrets was limited and hence we could not investigate all groups at every timepoint. In addition, several ferrets were previously exposed to Aleutian disease and coronaviruses other than SARS-CoV-2 (details in Supplemental data). Although we did not find evidence that this infection history influenced our results, we cannot fully exclude that possibility. Finally, due to the limited availability of animals it will be difficult to model SARS-CoV-2 infections in older ferrets. However, as we did not find strong differences between young and adult ferrets upon intranasal inoculation, the use of young ferrets should suffice for future experiments.

As has been discussed here, ferrets are readily infected with SARS-CoV-2 but do not present clinical symptoms. Infected ferrets might thus represent the asymptomatic COVID-19 that manifests in a significant part of the population [67]. In addition, the derailed immune responses in the respiratory tract in ferrets might model the long-term respiratory effects observed in long-COVID patients, although more in-depth research is required to verify this. Lastly, with the recently developed reagents for humoral and cellular immunology in the ferret model [37, 68-71], vaccine-induced immune responses can be quantified and their effect on viral replication and pathology can be measured. This matured ferret model can help with improving our understanding of SARS-CoV-2, thereby driving the development of new therapies and vaccines.

Supplemental Tables & Figures

Supplemental Table 1 | Immune status before SARS-CoV-2 infection

				HI (dilution)			ELISA (titer)				
Ferret	Age	Inoculation route	Section day post infection	(B/Colorado/06/2017)	(B/Maryland/15/2016)	(A/Michigan/45/15)	Aleution IgG	CDV[1]	FCOV[2]	CCoV[3]	NL-63
1	Young	i.n.	5	neg	neg	neg	<100	280	109	<100	<100
2	Young	i.n.	5	neg	neg	neg	<100	77	<100	<100	<100
3	Young	i.n.	5	neg	neg	neg	<100	360	<100	<100	<100
4	Young	i.n.	14	neg	neg	neg	<100	224	<100	<100	<100
5	Young	i.n.	14	neg	neg	neg	<100	331	126	<100	<100
6	Young	i.n.	14	neg	neg	neg	<100	76	<100	<100	<100
7	Young	i.n.	21	neg	neg	neg	<100	984	<100	450	410
8	Young	i.n.	21	neg	neg	neg	<100	1058	142	163	111
9	Young	i.n.	21	neg	neg	neg	<100	1050	136	506	239
10	Young	i.t.	5	neg	neg	neg	<100	675	<100	<100	<100
11	Young	i.t.	5	neg	neg	neg	<100	570	<100	107	<100
12	Young	i.t.	5	neg	neg	neg	<100	319	<100	<100	<100
13	Young	i.t.	14	neg	neg	neg	<100	267	160	<100	<100
14	Young	i.t.	14	neg	neg	neg	<100	388	106	145	<100
15	Young	i.t.	14	neg	neg	neg	<100	54	150	<100	<100
16	Young	i.t.	21	neg	neg	neg	<100	1053	<100	301	354
17	Young	i.t.	21	neg	neg	neg	<100	1058	123	183	170
18	Young	i.t.	21	neg	neg	neg	<100	1054	121	517	373
19	Adult	i.n.	5	neg	neg	neg	<100	160	134	<100	<100
20	Adult	i.n.	5	neg	neg	neg	<100	102	<100	<100	<100
21	Adult	i.n.	5	neg	neg	neg	<100	213	<100	<100	<100
22	Adult	i.t.	21	neg	neg	neg	<100	505	142	105	<100
23	Adult	i.t.	21	neg	neg	neg	<100	215	113	<100	<100
24	Adult	i.t.	21	neg	neg	neg	<100	675	<100	197	<100

Supplemental Table 1 | Immune status before SARS-CoV-2 infection (continued)

				HI (dilution)			ELISA (titer)				
Ferret	Age	Inoculation route	Section day post infection	(B/Colorado/06/2017)	(B/Maryland/15/2016)	(A/Michigan/45/15)	Aleution IgG	CDV[1]	FCOV[2]	CCoV[3]	NL-63
25	Adult	i.t.	5	neg	neg	neg	<100	347	172	<100	<100
26	Adult	i.t.	5	neg	neg	neg	<100	504	116	<100	<100
27	Adult	i.t.	5	neg	neg	neg	<100	445	174	122	<100
28	Adult	i.t.	14	neg	neg	neg	<100	511	<100	158	<100
29	Adult	i.t.	14	neg	neg	neg	<100	206	<100	<100	<100
31	Adult	i.n.	21	neg	neg	neg	115	125	140	<100	<100
32	Adult	i.n.	21	neg	neg	neg	<100	312	<100	<100	<100
33	Adult	i.n.	21	neg	neg	neg	<100	669	<100	189	<100
34	Young	Mock	14	neg	neg	neg	<100	12	<100	<100	<100
35	Young	Mock	14	neg	neg	neg	149	469	424	116	<100
36	Young	Mock	14	neg	neg	neg	100	276	138	<100	<100
37	Adult	Mock	21	neg	neg	>320	<100	278	<100	<100	<100
38	Adult	Mock	21	neg	neg	160	<100	404	114	107	<100
39	Adult	Mock	21	neg	neg	>320	<100	28	<100	<100	<100

[1]CDV = Canine distemper virus

[2]FCOV = Feline coronavirus, representative of ferret systemic corona virus

[3]CCoV = Canine coronavirus, representative of ferret enteric corona virus

Pre-existing immunity against CCoV and NL-63, but not SARS-CoV-2

Pre-existing cellular responses against SARS-CoV-2

Pre-existing humoral responses against SARS-CoV-2.

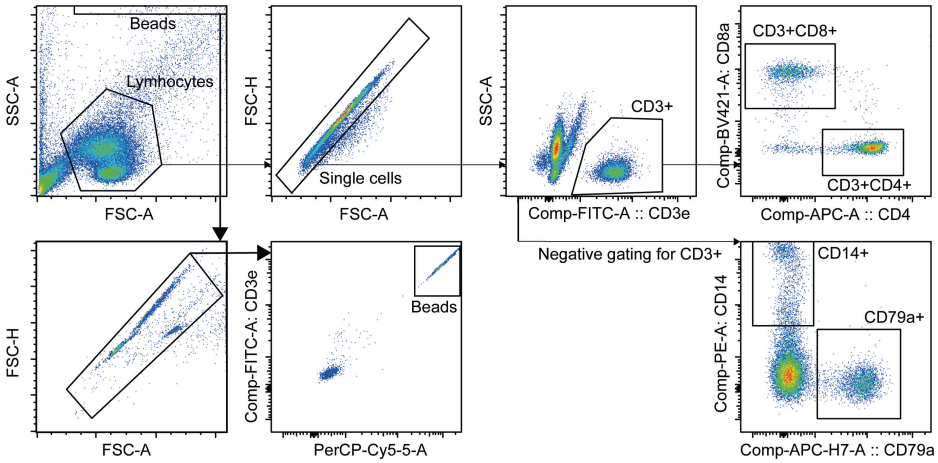

Supplemental figure 1: Gating strategy of whole blood trucount. Plots show the gating strategy for identification of cell subsets in whole blood of young and adult ferrets. CD14 and CD79a subsets were gated in the 'Single cells' population excluding all CD3+ cells. Beads were used to correct cell counts for the volume of measured blood.

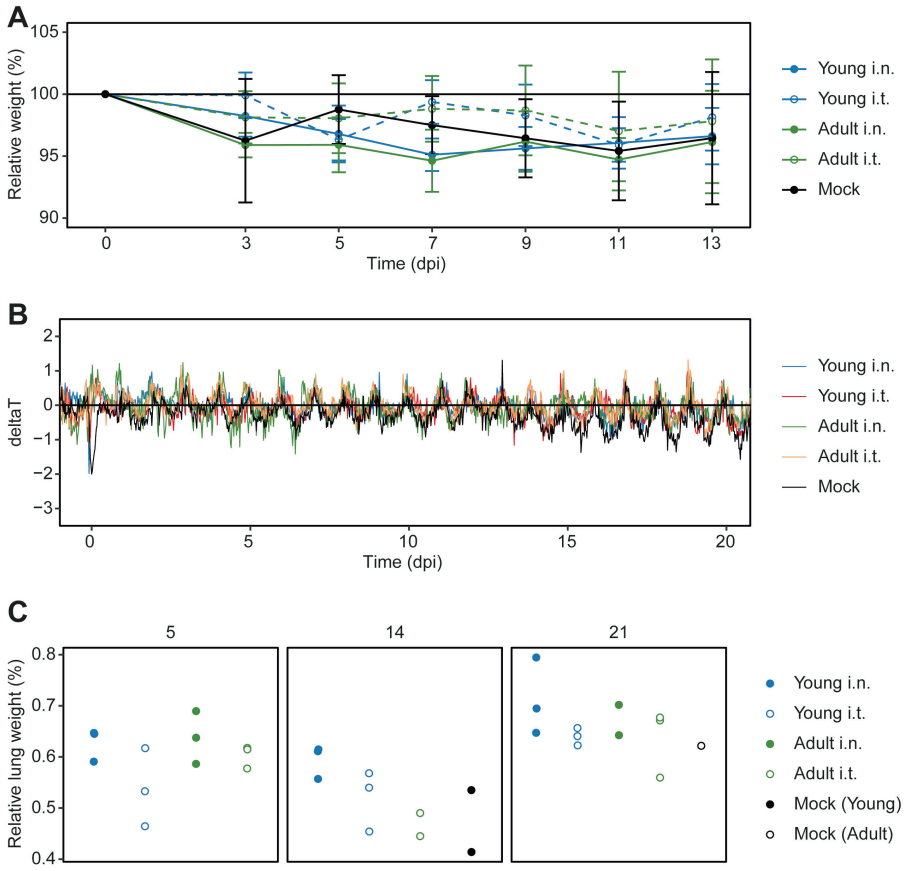

Supplemental figure 2: SARS-CoV-2 infection does not induce clinical disease in male ferrets. A) Body weight was measured on various time points and depicted as % of original bodyweight on the day of infection. **B)** Body temperature was measured continuously in 30-minute intervals by implanted abdominal transponders. The ΔT was calculated by subtracting body temperature during baseline (1-6 days before infection) from the body temperature after SARS-CoV-2 infection. **C)** Relative lung weight depicted as a percentage of total body weight on the day of infection. The different panels depict the relative lung weight on 5, 14 and 21 days post infection (dpi). Lines **(A, B)** depict the group mean while the error bars depict standard error of the mean (**A** only). For **(A, B)**: n = 3-6; for **(C)**: with exception of 'Adult i.t.' on 14 dpi (n = 2), all groups are n = 3.

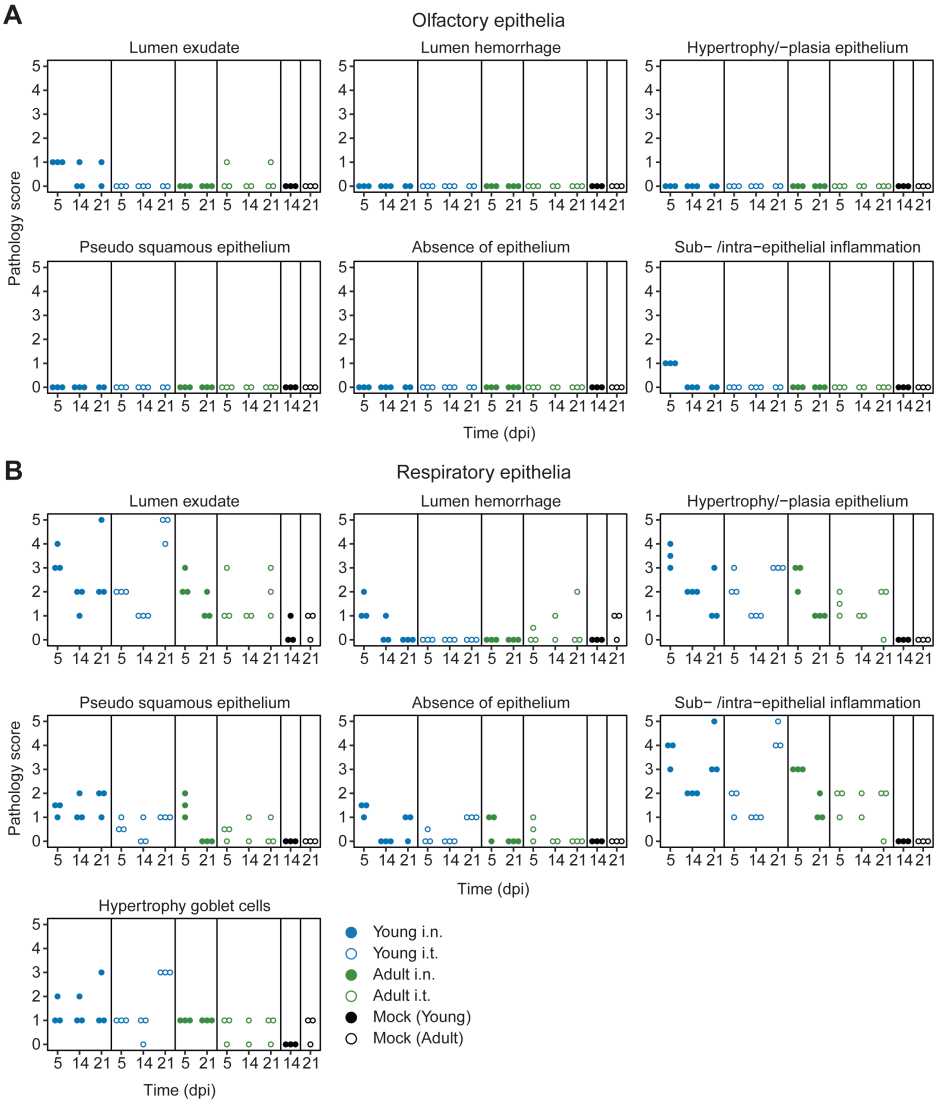

Supplemental figure 3: Extensive pathology scoring nasal turbinates. A, B) Scoring of **(A)** olfactory and **(B)** respiratory turbinates. Panels depict individual parameters related to epithelial damage and inflammation on 5, 14 and 21 days post infection (dpi). The infection-induced pathology was scored on a scale of 0–5 based on the parameters described in the materials and methods. With exception of 'Adult i.t.' on 14 dpi (n = 2), all groups are n = 3.

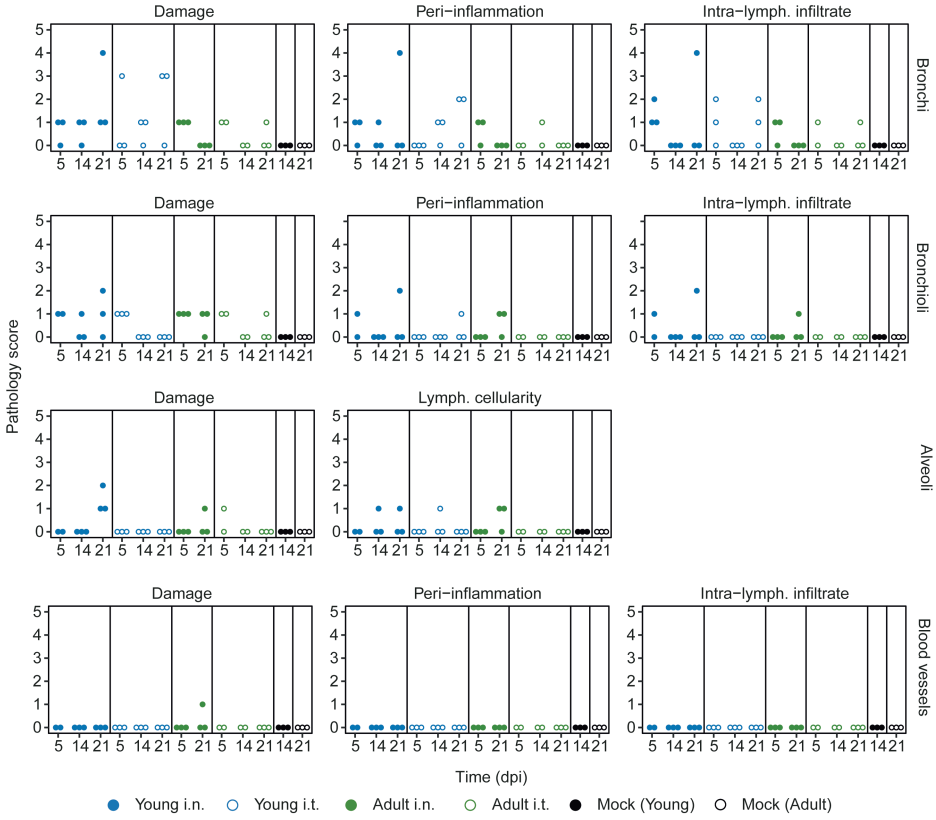

Supplemental figure 4: Extensive pathology scoring lungs. Panels show individual scoring by parameters related to epithelial damage and inflammation. The infection-induced pathology was scored on a scale of 0–5 based on the parameters described in the materials and methods on 5, 14 and 21 days post infection (dpi). With exception of 'Adult i.t.' on 14 dpi (n = 2), all groups are n = 3.

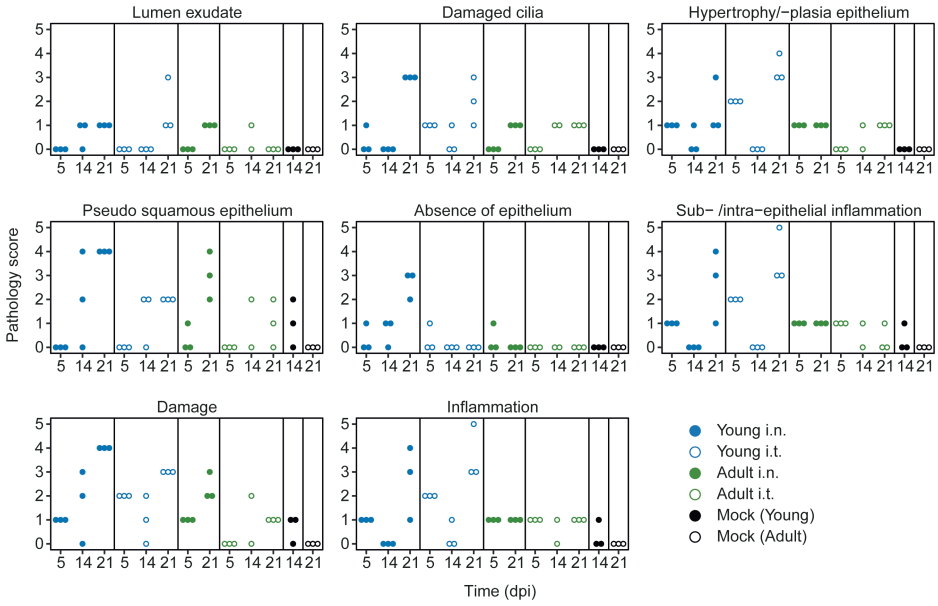

Supplemental figure 5: Extensive pathology scoring trachea. Panels show individual scoring by parameters related to epithelial damage and inflammation. The infection-induced pathology was scored on a scale of 0–5 based on the parameters described in the materials and methods on 5, 14 and 21 days post infection (dpi). With exception of 'Adult i.t.' on 14 dpi (n = 2), all groups are n = 3.

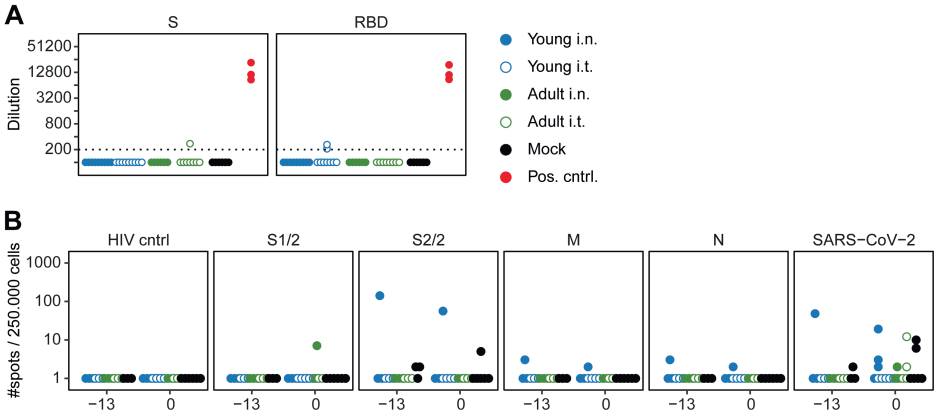

Supplemental figure 6: Pre-existing immune responses against SARS-CoV-2 in ferrets. **A)** Sera from three animals before SARS-CoV-2 infection contained small antibody responses against (the receptor binding domain [RBD] of) spike (S) in ELISA assays, but these were different animals from the one that responded in the ELISpot of panel B. Responses are depicted as the (modelled) dilution at which the ELISA curve drops below background (mean + 3x SD of SARS-CoV-2 naïve animals at 200x dilution). The dotted line indicates the lowest dilution tested and negative samples were set to half that dilution for visualization purposes. Positive control consists of sera of SARS-CoV-2 infected animals collected 21 days post infection (dpi). N= 3 for positive control sera and n = 6-9 for other groups. **B)** IFNγ-ELISpots performed with PBMCs isolated 13 and 0 days before SARS-CoV-2 infection indicate that one animal already possessed (cross-reactive) T cell responses against overlapping peptide pools of the S-protein of SARS-CoV-2. Data shown were corrected for medium background and were set to a minimum of 1 spot for visualization on a log-scale. N = 3 at -13 dpi and n = 5-6 for 0 dpi.

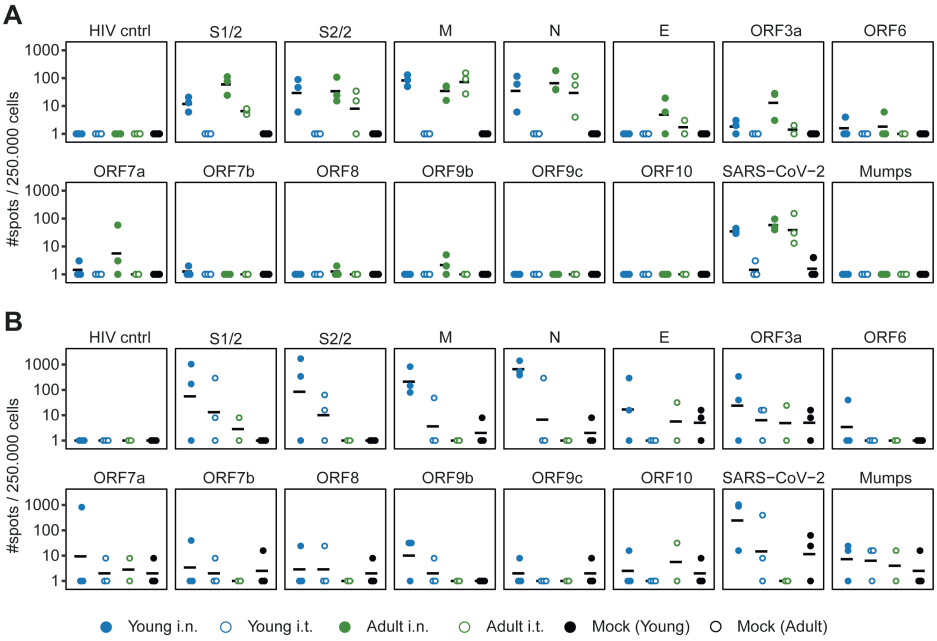

Supplemental figure 7: Cellular responses against SARS-CoV-2 in PBMC and lung. A, B) Cellular responses in PBMCs **(A)** and lung derived lymphocytes **(B)** as determined by IFNγ-ELISpot. Cells were stimulated with various SARS-CoV-2 peptide pools or live virus. Dots show individual ferrets while black lines indicate the group geometric mean. Data were corrected for medium background and were set to a minimum of 1 spot for visualization on a log-scale. **A)** Responses in PBMC isolated 21 days post infection (dpi). **B)** Responses of lung-derived lymphocytes 14 dpi. N = 3 for all panels, with exception of 'Adult i.t.' on 14 dpi (n = 2).

References

1. Zhou, P., et al., *A pneumonia outbreak associated with a new coronavirus of probable bat origin.* Nature, 2020. **579**(7798): p. 270-273.
2. Creech, C.B., S.C. Walker, and R.J. Samuels, *SARS-CoV-2 Vaccines.* JAMA, 2021. **325**(13): p. 1318-1320.
3. Gupta, R.K., *Will SARS-CoV-2 variants of concern affect the promise of vaccines?* Nat Rev Immunol, 2021. **21**(6): p. 340-341.
4. Munoz-Fontela, C., et al., *Animal models for COVID-19.* Nature, 2020. **586**(7830): p. 509-515.
5. Lee, C.Y. and A.C. Lowen, *Animal models for SARS-CoV-2.* Curr Opin Virol, 2021. **48**: p. 73-81.
6. WHO, *Transmission of SARS-CoV-2: implications for infection prevention precautions*. 2020, WHO.
7. Harrison, A.G., T. Lin, and P. Wang, *Mechanisms of SARS-CoV-2 Transmission and Pathogenesis.* Trends Immunol, 2020. **41**(12): p. 1100-1115.
8. Tang, S., et al., *Aerosol transmission of SARS-CoV-2? Evidence, prevention and control.* Environ Int, 2020. **144**: p. 106039.
9. Liu, Y., et al., *Aerodynamic analysis of SARS-CoV-2 in two Wuhan hospitals.* Nature, 2020. **582**(7813): p. 557-560.
10. Chen, Y., et al., *The presence of SARS-CoV-2 RNA in the feces of COVID-19 patients.* J Med Virol, 2020. **92**(7): p. 833-840.
11. Zheng, S., et al., *Viral load dynamics and disease severity in patients infected with SARS-CoV-2 in Zhejiang province, China, January-March 2020: retrospective cohort study.* BMJ, 2020. **369**: p. m1443.
12. Wolfel, R., et al., *Virological assessment of hospitalized patients with COVID-2019.* Nature, 2020. **581**(7809): p. 465-469.
13. Amirian, E.S., *Potential fecal transmission of SARS-CoV-2: Current evidence and implications for public health.* Int J Infect Dis, 2020. **95**: p. 363-370.
14. Schurink, B., et al., *Viral presence and immunopathology in patients with lethal COVID-19: a prospective autopsy cohort study.* Lancet Microbe, 2020. **1**(7): p. e290-e299.
15. Zhou, F., et al., *Clinical course and risk factors for mortality of adult inpatients with COVID-19 in Wuhan, China: a retrospective cohort study.* Lancet, 2020. **395**(10229): p. 1054-1062.
16. Ge, H., et al., *The epidemiology and clinical information about COVID-19.* Eur J Clin Microbiol Infect Dis, 2020. **39**(6): p. 1011-1019.
17. Du, Y., et al., *Clinical Features of 85 Fatal Cases of COVID-19 from Wuhan. A Retrospective Observational Study.* Am J Respir Crit Care Med, 2020. **201**(11): p. 1372-1379.
18. Bradley, B.T., et al., *Histopathology and ultrastructural findings of fatal COVID-19 infections in Washington State: a case series.* Lancet, 2020. **396**(10247): p. 320-332.
19. Cdc Weekly, C., *The Epidemiological Characteristics of an Outbreak of 2019 Novel Coronavirus Diseases (COVID-19) — China, 2020.* China CDC Weekly, 2020. **2**(8): p. 113-122.
20. Karagiannidis, C., et al., *Case characteristics, resource use, and outcomes of 10 021 patients with COVID-19 admitted to 920 German hospitals: an observational study.* The Lancet Respiratory Medicine, 2020. **8**(9): p. 853-862.
21. Verity, R., et al., *Estimates of the severity of coronavirus disease 2019: a model-based analysis.* Lancet Infect Dis, 2020. **20**(6): p. 669-677.
22. Nalbandian, A., et al., *Post-acute COVID-19 syndrome.* Nat Med, 2021. **27**(4): p. 601-615.
23. Belser, J.A., J.M. Katz, and T.M. Tumpey, *The ferret as a model organism to study influenza A virus infection.* Dis Model Mech, 2011. **4**(5): p. 575-9.
24. Bodewes, R., G.F. Rimmelzwaan, and A.D. Osterhaus, *Animal models for the preclinical evaluation of candidate influenza vaccines.* Expert Rev Vaccines, 2010. **9**(1): p. 59-72.

25. Kim, Y.I., et al., *Infection and Rapid Transmission of SARS-CoV-2 in Ferrets.* Cell Host Microbe, 2020. **27**(5): p. 704-709 e2.
26. Liu, H.L., et al., *Gene signatures of SARS-CoV/SARS-CoV-2-infected ferret lungs in short- and long-term models.* Infect Genet Evol, 2020. **85**: p. 104438.
27. Park, S.J., et al., *Antiviral Efficacies of FDA-Approved Drugs against SARS-CoV-2 Infection in Ferrets.* mBio, 2020. **11**(3): p. e01114-20.
28. Richard, M., et al., *SARS-CoV-2 is transmitted via contact and via the air between ferrets.* Nat Commun, 2020. **11**(1): p. 3496.
29. Schlottau, K., et al., *SARS-CoV-2 in fruit bats, ferrets, pigs, and chickens: an experimental transmission study.* Lancet Microbe, 2020. **1**(5): p. e218-e225.
30. Shi, J., et al., *Susceptibility of ferrets, cats, dogs, and other domesticated animals to SARS-coronavirus 2.* Science, 2020. **368**(6494): p. 1016-1020.
31. Wu, S., et al., *A single dose of an adenovirus-vectored vaccine provides protection against SARS-CoV-2 challenge.* Nat Commun, 2020. **11**(1): p. 4081.
32. Ryan, K.A., et al., *Dose-dependent response to infection with SARS-CoV-2 in the ferret model and evidence of protective immunity.* Nat Commun, 2021. **12**(1): p. 81.
33. Everett, H.E., et al., *Intranasal Infection of Ferrets with SARS-CoV-2 as a Model for Asymptomatic Human Infection.* Viruses, 2021. **13**(1): p. 113.
34. Kreijtz, J.H., et al., *Low pathogenic avian influenza A(H7N9) virus causes high mortality in ferrets upon intratracheal challenge: a model to study intervention strategies.* Vaccine, 2013. **31**(43): p. 4995-9.
35. de Jonge, J., et al., *H7N9 Live Attenuated Influenza Vaccine Is Highly Immunogenic, Prevents Virus Replication, and Protects Against Severe Bronchopneumonia in Ferrets.* Mol Ther, 2016. **24**(5): p. 991-1002.
36. Bodewes, R., et al., *Pathogenesis of Influenza A/H5N1 virus infection in ferrets differs between intranasal and intratracheal routes of inoculation.* Am J Pathol, 2011. **179**(1): p. 30-6.
37. van de Ven, K., et al., *Systemic and respiratory T-cells induced by seasonal H1N1 influenza protect against pandemic H2N2 in ferrets.* Commun Biol, 2020. **3**(1): p. 564.
38. Fang, Y., et al., *Molecular characterization of in vivo adjuvant activity in ferrets vaccinated against influenza virus.* J Virol, 2010. **84**(17): p. 8369-88.
39. Corman, V.M., et al., *Detection of 2019 novel coronavirus (2019-nCoV) by real-time RT-PCR.* Euro Surveill, 2020. **25**(3): p. 2000045.
40. Scheltinga, S.A., et al., *Diagnosis of human metapneumovirus and rhinovirus in patients with respiratory tract infections by an internally controlled multiplex real-time RNA PCR.* J Clin Virol, 2005. **33**(4): p. 306-11.
41. Zhang, Y., et al., *In vivo structure and dynamics of the SARS-CoV-2 RNA genome.* Nat Commun, 2021. **12**(1): p. 5695.
42. R Core Team, *R: A Language and Environment for Statistical Computing*. 2021, R Foundation for Statistical Computing.
43. Wickham, H., *ggplot2: Elegant Graphics for Data Analysis*. 2016, Springer-Verlag New York.
44. Wickham, H., et al., *Welcome to the Tidyverse.* Journal of Open Source Software, 2019. **4**(43): p. 1686.
45. Kassambara, A., *ggpubr: 'ggplot2' Based Publication Ready Plots*. 2020, CRAN.
46. Holm, S., *A Simple Sequentially Rejective Multiple Test Procedure.* Scandinavian Journal of Statistics, 1979. **6**(2): p. 65-70.
47. Sansoni, P., et al., *Lymphocyte subsets and natural killer cell activity in healthy old people and centenarians.* Blood, 1993. **82**(9): p. 2767-73.
48. Peacock, T.P., et al., *The furin cleavage site in the SARS-CoV-2 spike protein is required for transmission in ferrets.* Nat Microbiol, 2021. **6**(7): p. 899-909.

49. Hoffmann, M., et al., *SARS-CoV-2 Cell Entry Depends on ACE2 and TMPRSS2 and Is Blocked by a Clinically Proven Protease Inhibitor.* Cell, 2020. **181**(2): p. 271-280 e8.
50. Isakova-Sivak, I., et al., *Development and pre-clinical evaluation of two LAIV strains against potentially pandemic H2N2 influenza virus.* PLoS One, 2014. **9**(7): p. e102339.
51. Braun, J., et al., *SARS-CoV-2-reactive T cells in healthy donors and patients with COVID-19.* Nature, 2020. **587**(7833): p. 270-274.
52. Mateus, J., et al., *Selective and cross-reactive SARS-CoV-2 T cell epitopes in unexposed humans.* Science, 2020. **370**(6512): p. 89-94.
53. Le Bert, N., et al., *SARS-CoV-2-specific T cell immunity in cases of COVID-19 and SARS, and uninfected controls.* Nature, 2020. **584**(7821): p. 457-462.
54. Grifoni, A., et al., *Targets of T Cell Responses to SARS-CoV-2 Coronavirus in Humans with COVID-19 Disease and Unexposed Individuals.* Cell, 2020. **181**(7): p. 1489-1501 e15.
55. Hanley, B., et al., *Histopathological findings and viral tropism in UK patients with severe fatal COVID-19: a post-mortem study.* Lancet Microbe, 2020. **1**(6): p. e245-e253.
56. Lamers, M.M., et al., *SARS-CoV-2 productively infects human gut enterocytes.* Science, 2020. **369**(6499): p. 50-54.
57. Cuicchi, D., T. Lazzarotto, and G. Poggioli, *Fecal-oral transmission of SARS-CoV-2: review of laboratory-confirmed virus in gastrointestinal system.* Int J Colorectal Dis, 2021. **36**(3): p. 437-444.
58. Cheung, K.S., et al., *Gastrointestinal Manifestations of SARS-CoV-2 Infection and Virus Load in Fecal Samples From a Hong Kong Cohort: Systematic Review and Meta-analysis.* Gastroenterology, 2020. **159**(1): p. 81-95.
59. Song, E., et al., *Neuroinvasion of SARS-CoV-2 in human and mouse brain.* J Exp Med, 2021. **218**(3): p. e20202135.
60. Meinhardt, J., et al., *Olfactory transmucosal SARS-CoV-2 invasion as a port of central nervous system entry in individuals with COVID-19.* Nat Neurosci, 2021. **24**(2): p. 168-175.
61. Zimmermann, P. and N. Curtis, *Why is COVID-19 less severe in children? A review of the proposed mechanisms underlying the age-related difference in severity of SARS-CoV-2 infections.* Arch Dis Child, 2020. **106**: p. 429-439.
62. Beretta, A., M. Cranage, and D. Zipeto, *Is Cross-Reactive Immunity Triggering COVID-19 Immunopathogenesis?* Front Immunol, 2020. **11**: p. 567710.
63. Zhao, Y.M., et al., *Follow-up study of the pulmonary function and related physiological characteristics of COVID-19 survivors three months after recovery.* EClinicalMedicine, 2020. **25**: p. 100463.
64. Dennis, A., et al., *Multiorgan impairment in low-risk individuals with post-COVID-19 syndrome: a prospective, community-based study.* BMJ Open, 2021. **11**(3): p. e048391.
65. Ayoubkhani, D., et al., *Post-covid syndrome in individuals admitted to hospital with covid-19: retrospective cohort study.* BMJ, 2021. **372**: p. n693.
66. Peng, Y., et al., *Broad and strong memory CD4(+) and CD8(+) T cells induced by SARS-CoV-2 in UK convalescent individuals following COVID-19.* Nat Immunol, 2020. **21**(11): p. 1336-1345.
67. Gao, Z., et al., *A systematic review of asymptomatic infections with COVID-19.* J Microbiol Immunol Infect, 2021. **54**(1): p. 12-16.
68. DiPiazza, A., et al., *Flow Cytometric and Cytokine ELISpot Approaches To Characterize the Cell-Mediated Immune Response in Ferrets following Influenza Virus Infection.* J Virol, 2016. **90**(17): p. 7991-8004.
69. Music, N., et al., *Influenza vaccination accelerates recovery of ferrets from lymphopenia.* PLoS One, 2014. **9**(6): p. e100926.
70. DiPiazza, A.T., et al., *Analyses of Cellular Immune Responses in Ferrets Following Influenza Virus Infection.* Methods Mol Biol, 2018. **1836**: p. 513-530.
71. Martel, C.J. and B. Aasted, *Characterization of antibodies against ferret immunoglobulins, cytokines and CD markers.* Vet Immunol Immunopathol, 2009. **132**(2-4): p. 109-15.

General discussion

6

Recap of the problem

The most effective and feasible way to reduce the impact of influenza virus infections is by vaccination. The problem, however, is that the current influenza virus vaccines are not effective enough since the immunity they induce is very strain-specific and does not cover drifted or newly emerging influenza viruses. We thus need a new generation of vaccines that offer a broader and longer-lasting protection. T-cell immunity might be key to this since T cells can target conserved influenza virus epitopes, leading to broadly-reactive immunity. However, the development and evaluation of T cell-inducing influenza virus vaccines requires a deeper understanding of what entails a protective T-cell response. Animal models are essential for this, and the ferret model in particular is suited for the evaluation of influenza virus vaccines; ferrets mimic human influenza disease and recent developments have made it possible to measure T-cell immunity.

In this thesis we described how we set up different ferret infection models and demonstrated that T-cell immunity can protect against influenza disease. The key findings of this thesis are summarized below in Box 1. In this chapter, we will first deliberate on the value of the ferret model and how it can be used to mimic human influenza virus and SARS-CoV-2 infections. We will also touch upon the translational value of the adaptive immune response in ferrets, followed by a discussion on the role of T cells in influenza disease and how T-cell immunity can be the backbone of universal influenza virus vaccines.

Translation from ferret to human

The ferret model for influenza virus pathogenesis

Starting with the first experimental influenza virus infection of ferrets in 1933 [1], the ferret model has gradually developed to become one of the standard models for the investigation of influenza virus replication, transmission and disease [2]. The reason why the ferret model is so highly regarded is because ferrets are readily infected with human and avian influenza strains, ferrets mimic human influenza A virus (IAV) subtype-dependent disease and ferrets are a good predictor of transmissibility between humans [3-6]. While the ferret model can accurately mimic human influenza virus infection and disease, there are also minor differences. Below, we discuss the similarities and dissimilarities between the ferret model and the human situation, with the aim to improve the translation from the ferret model to the human situation.

Box 1: Key findings in this thesis

Chapter 2: For an H2N2 influenza virus infection model in ferrets, both intranasal and intratracheal inoculation with H2N2 influenza virus can induce human-like disease. Intratracheal inoculation tends to induce more severe disease than intranasal administration for H2N2 influenza viruses.
Chapter 2: The binding preference of influenza virus for α2,3- and α2,6-sialic acid might affect the location and height of H2N2 influenza virus replication in the respiratory tract. H2N2 influenza viruses with distinct sialic acid binding preferences can lead to different disease severities in the ferret model.
Chapter 3: Ferrets infected with H1N1 influenza virus develop T-cell responses in the circulation and respiratory tract against conserved influenza virus proteins in ferrets. This is associated with reduced disease symptoms of an H2N2 influenza virus infection, illustrating that T-cell immunity can protect against heterosubtypic influenza virus infections.
Chapter 3: Cellular responses against conserved influenza virus proteins are present in both ferrets and healthy human blood donors. Based on our findings in ferrets, boosting of these responses in humans might reduce disease severity upon a heterosubtypic influenza virus infection.
Chapter 4: A new mRNA-LNP vaccine encoding conserved internal influenza virus proteins can induce T-cell responses in naïve ferrets and boost T-cell responses in influenza-experienced ferrets.
Chapter 4: Booster vaccination of influenza-experienced ferrets enhances protection against heterosubtypic avian influenza virus infection, proving that T cell-based vaccines are a valid strategy to establish broadly-protective immune responses against influenza.
Chapter 4: Intramuscular mRNA-LNP vaccination induces and boosts T-cell immunity in the respiratory tract and bone marrow, indicating that mRNA-LNP vaccines can establish T-cell immunity in relevant tissues that are distant from the site of vaccination.
Chapter 5: Ferrets can be readily infected with SARS-CoV-2, show a human-like tropism of infected tissues and develop cellular and humoral immunity against SARS-CoV-2. However, ferrets do not display the clinical signs of COVID-19, which limits the usefulness of the ferret model for human SARS-CoV-2 induced disease.
Chapter 5: Compared to intranasal administration, intratracheal SARS-CoV-2 inoculation leads to lower viral replication and is less potent in inducing cellular and humoral immunity.

How does virus subtype and infection route affect influenza disease?
Influenza disease severity is influenced by both the inoculation route (which determines the site of infection) and the virus subtype (which determines if the virus replicates at the site of inoculation). To start with the latter, the human adapted IAVs H1N1, H2N2 and H3N2 usually replicate in the upper respiratory tract (URT) of humans [7]. In contrast, H5 and H7 avian influenza viruses mostly cause lower respiratory tract (LRT) infections in humans [8, 9]. LRT infections can directly hamper the uptake of oxygen, which is why they tend to induce more severe disease than URT infections. Whether an IAV is able to infect the URT or LRT is influenced in part by the receptor binding affinity and temperature sensitivity. IAV uses either α2,3- or α2,6-linked sialic acid (SA) to infect cells. Both receptors are expressed throughout the respiratory tract of humans and ferrets, but α2,6-SA is thought to be more abundant in the URT and α2,3-SA in the LRT [10-13]. Seasonal influenza viruses typically prefer α2,6-SA and replicate at lower temperatures, leading to a mild URT infection in ferret and human. In contrast, avian influenza viruses tend to preferentially bind α2,3-SA and show optimal replication at higher temperature [14-16], resulting in high viral replication in the LRT.

For both humans and ferrets, an URT infection usually does not extend to a LRT infection and vice versa. This means that the route of infection can have a major impact on disease severity. Ferrets are often inoculated with virus-containing fluid via the intranasal or intratracheal route, which can establish an infection in the URT of LRT respectively [3, 4]. Intranasal inoculation is used more often for human influenza viruses (H1N1 and H3N2) in the ferret model, since it is easier to perform compared to intratracheal administration (reviewed in [5]) and induces a human-like disease (**Chapter 3**, [17-19]). In contrast, avian influenza virus isolates do not produce a typical human disease when administered intranasally. URT infections with H5N1 avian influenza virus in the ferret model – induced by intranasal inoculation – could spread to the central nervous system, which was ultimately lethal [20, 21]. These symptoms are not representative of the human situation since neurological symptoms after H5N1 influenza virus infection seldom occur in H5N1-infected patients [22]. In the case of H7N9, intranasal inoculation can induce mild to robust disease, but not the severe pneumonia that is observed in a significant number of H7N9-infected humans ([23] and unpublished data). For both H5N1 and H7N9 influenza virus isolates, a severe human-like form of disease (pneumonia) can be induced in ferrets by depositing the virus lower in the respiratory tract by intratracheal inoculation (**Chapter 4** and [20, 24-28]). The inoculation route can thus have a major influence on influenza disease severity in the ferret model.

In **Chapter 2** we investigated whether disease severity differed between inoculation routes for multiple H2N2 influenza virus isolates with varying binding preferences for α2,3- and α2,6-SA. In general, intratracheal inoculation resulted in a LRT infection,

which tended to be more severe than the relatively mild URT infection. However, not all virus isolates successfully replicated in the LRT, which could explain why these viruses also seemed to induce less severe disease. The two α2,6-SA preferring viruses replicated in both the URT and LRT, but the two α2,3-SA preferring viruses did not replicate at all or were limited to the URT. It is tempting to speculate that these findings are due to a difference in SA-binding preference, but this would require additional experiments in which the binding preference can be (genetically) altered. Such experiments might tell us whether the differences between H2N2 virus isolates was due to varying SA-binding preferences or due to other factors such as temperature sensitivity.

While ferrets in experimental settings are usually infected intranasally or intratracheally with virus-containing fluid, humans typically contract viral influenza via aerosols or surface-to-surface contact [29]. This difference in infection routes has prompted the development of more natural infection routes for the ferret model. Influenza virus transmission and disease can be investigated using (indirect) contact-to-contact experiments where one infected ferret (donor) can infect other naïve ferrets (recipient) [30]. In these experiments ferrets can either have direct contact or be separated to specifically investigate the role of airborne transmission. The downside of this method is that it requires additional housing and animals (donor and recipient), increases experiment duration and is difficult to reproduce due to the non-standardized infection of recipient animals (reviewed in [5]). As an alternative, ferrets can be directly infected using aerosolized influenza viruses [31, 32]. This does require specialized equipment and has no major impact on disease severity, which might explain why this method is not commonly used. Given the minor impact on disease severity with other inoculation routes, intranasal and intratracheal inoculation thus remain the standard routes of infection in the ferret model.

How does the infection dose affect influenza disease?

Another parameter that might affect viral influenza pathogenesis in the ferret model is the inoculation dose. Ferrets are typically exposed to unnaturally high IAV titers (e.g. 10^6 $TCID_{50}$/EID_{50}/PFU), while humans typically get infected with much lower titers (10^3 $TCID_{50}$; reviewed in [5]). The reasons to use high titers is to ensure that each inoculation results in a successful infection, which might not be guaranteed with lower titers. A higher IAV inoculation dose does not seem to result in more severe disease, but merely expedites the onset of disease symptoms [5, 33]. While it seems that a higher infectious dose does not necessarily impact the translation to humans, others have tried to use a more natural infection dose in the order of 10^3 $TCID_{50}$ [19, 33, 34]. In general, with lower infection doses, the viral replication curve more accurately mimics viral replication in humans. The induction of disease is however less robust, leading to more variation between animals. In conclusion, while the infection route

can determine the site of viral replication and the severity of disease, differences in the infection dose seem to have little impact on IAV disease in ferrets.

How does pre-existing influenza-specific immunity affect findings in the ferret model? One major difference between animal models and the human situation that is not always addressed, is the level of pre-existing immunity. Based on the annual attack rate of influenza viruses, it is expected that every child becomes infected with influenza virus at least once – and probably multiple times – within their first decade of life [35, 36]. Most adults thus have a rich infection history, in which they have encountered multiple IAV and influenza B virus strains. These infections have induced diverse immune responses, which complicates the interpretation of clinical trials as certain therapies or vaccines might have different efficacies related to the level of pre-existing immunity. Animal models do not have the extend of this – often unwanted – heterogeneity in pre-existing immunity and are therefore essential to pre-clinical research. This advantage can, however, also be a disadvantage as studies with naïve animals do not fully resemble the human situation. For example, influenza virus vaccines are often developed for use in (influenza-experienced) adults, but the preclinical development stage primarily uses naïve animals. Such discrepancies might hinder the translation from animal models to humans.

To more accurately mimic adults with pre-existing influenza immunity, we used both naïve and influenza-experienced ferrets when we evaluated a T cell-inducing lipid nanoparticle (LNP)-encapsulated nucleoside-modified mRNA (mRNA-LNP) influenza virus vaccine (**Chapter 5**). The vaccine was more potent in influenza-experienced ferrets – which received a single H1N1 influenza virus infection 6 weeks before vaccination – illustrating that infection history can strongly affect vaccine responses. T-cell responses were of similar magnitude in blood of naïve and influenza-experienced ferrets, but were more diverse and robust in the respiratory tract of influenza-experienced ferrets. This might explain why booster vaccination in influenza-experienced ferrets increased protection against H7N9 influenza disease. In line with our findings, vaccination with an inactivated H3N2-vaccine induced higher HA-titers in mice, hamsters and ferrets if they were previously infected with an H1N1 strain [37]. Although it was not investigated which mechanism was behind this increased vaccination response, CD4 T cells recognizing epitopes shared between H1 and H3 might have supported B cells with their antibody production after H3N2 vaccination. On the other hand, prior vaccination with inactivated influenza virus vaccines (IIV) can also prevent the induction of broadly-reactive T-cell immunity by H3N2 infection in ferrets [38]. These findings show that influenza-specific pre-existing immunity can have a large impact on the outcome of infections and the effectiveness of vaccination. For the evaluation of influenza virus vaccines in animal models, we suggest to always include groups with prior exposure to influenza as a way to more accurately mimic the human situation.

How do other pathogens affect the ferret model?
Pre-existing immunity is not only limited to influenza virus. Humans encounter a variety of pathogens on a daily basis, but lab animals are often housed under specific-pathogen-free (SPF) conditions to minimize variation and to increase reproducibility. However, ferrets are typically sourced from commercial farms that – while adhering to biosafety regulations to prevent infections – are inherently not as 'clean' as lab mice. Combined with the high susceptibility of ferrets for certain (respiratory) infections, it is likely that ferrets have been exposed to viruses or other unwanted pathogens. Hence, it is necessary to screen ferrets for prior infections to exclude potential interference before the start of an experiment. In the case of influenza research, this screening usually includes IAV and influenza B viruses to exclude that any pre-existing immunity might affect the treatment outcome. Additionally, ferrets are screened for Aleutian disease virus (ADV; also named carnivore amdoparvovirus 1) – a chronic infection that might result in clinical symptoms when ferrets are immunosuppressed (reviewed in [39]). There are however other pathogens that might affect how ferrets respond to infections or treatments. Examples include distemper virus, SARS-CoV-2 and several ferret corona viruses ([40-45]). In **Chapters 3 and 4**, we screened ferrets for a range of pathogens. Almost no animals had prior exposure to influenza virus, SARS-CoV-2 or Aleutian disease; likely because animals are often screened for these pathogens. In contrast, virtually all animals showed evidence that they had been infected before with different (ferret) corona viruses. Most ferret studies unfortunately do not investigate or report on prior exposure to these pathogens, which makes it difficult to investigate the spread and impact of these infections on the research presented. To facilitate the comparison and reproducibility of ferret studies, it would be beneficial to agree on a minimal standard for the screening of ferrets involved in respiratory infection studies.

While the relatively open housing conditions at commercial ferret suppliers carries the risk of introducing pathogens, it might also contribute to a developed microbiome of ferrets. This is relevant for influenza research since a healthy microbiome can positively impact the immune response against respiratory infections. For example, in mice the immune system significantly differs between SPF-housed and 'dirty' mice, which could be attributed to differences in the microbiome [46-49]. Furthermore, reconstitution of a 'wild' microbiome by microbiome transplantation in SPF mice resulted in improved protection against a lethal influenza virus infection [50]. This indicates that findings in SPF mice might not always be translatable to the human situation and one study has actually shown that mice with a 'wild' microbiome more accurately predicted the results of clinical trials [51]. We expect that ferrets – unlike lab mice – possess a relatively developed and stable microbiome. Ferrets are outbred and often sourced from commercial farms that – while adhering to a biosafety regiment to prevent certain infections – are inherently not as 'clean' as lab mice. Compared to

mice, ferrets might thus more accurately model human disease and immune response after influenza virus infection.

The ferret model for SARS-CoV-2 pathogenesis

When SARS-CoV-2 swept across the globe in late 2019 and early 2020, there was a high demand for animal models to study the pathogenesis of SARS-CoV-2 and the disease it caused. Like several other research groups, we evaluated if the ferret model would be able to reproduce human COVID-19. The basis for this was that ferrets express ACE2 (angiotensin converting enzyme 2) and TMPRSS2 (transmembrane protease serine 2) in the respiratory tract (**Chapter 5** and [52]); the binding receptor and fusion priming protease respectively that are used by SARS-CoV-2 to infect cells [53-55].

Despite the expression of ACE2 and TMPRSS2, early findings indicated that ferrets do not develop the mild (or severe) COVID-19 that manifests in most human adults [43, 44, 56-62]. However, these studies mostly used young, female ferrets while the severity of COVID-19 in humans increases with age and is more prominent in males and persons that have certain comorbidities [63-67]. For this reason, we infected both young and adult male ferrets, as we postulated that older male ferrets would develop more severe disease (**Chapter 5**). We also compared intranasal and intratracheal inoculation routes since the latter might establish an LRT infection which can lead to more severe disease in the case of influenza virus. We observed a human-like tissue tropism of SARS-CoV-2, with viral RNA detected in the respiratory tract, intestines and brain of infected ferrets. In spite of confirmed viral replication, none of the infected ferrets developed any signs of clinical COVID-19. Likewise, disease did not differ between intranasal and intratracheal inoculation. Young ferrets that were infected intratracheally, however, did differ from the other groups as we detected almost no viral replication in their respiratory tract. Consequently, these ferrets also did not develop cellular or humoral immunity against SARS-CoV-2. While we did not detect any clinical disease symptoms such as body weight loss or fever, histopathological aberrations did develop in the respiratory tract of – mainly – young ferrets. This pathology might have been indicative of the long-COVID that is sometimes observed in humans. Still, this finding has yet to be validated since animal numbers in our study were low (n = 3) and the pathology was not reproduced when ferrets were inoculated with a SARS-CoV-2 beta variant in another study (publication in progress), although in that study the virus hardly replicated in ferrets.

In contrast to our findings, a recent study by Kim et al. did report that SARS-CoV-2 disease was increased in older female ferrets [68]. This study was to a large extent similar to our study, with young (<6 months) and old (>3 years) ferrets that were infected intranasally. However, Kim et al. used female ferrets that were infected with a slightly lower virus dose ($10^{5.8}$ $TCID_{50}$ versus 10^{7} $TCID_{50}$). It is unlikely that the gender

or lower infection dose could explain the discrepancy between their and our study, as symptoms are more likely to increase with dose and there are multiple other studies that did not find SARS-CoV-2 related disease in female ferrets [61, 62, 69]. Importantly, multiple studies that do report clinical symptoms for SARS-CoV-2 infected ferrets, use the same ferret supplier and virus strain [43, 57, 68], that differ from most other ferret studies that do not report symptoms. This could offer an explanation for the discrepancy between SARS-CoV-2 ferret infection studies. In line with this, we found that the SARS-CoV-2 beta variant did not replicate effectively in ferrets, while the earlier SARS-CoV-2 alpha variant did (**Chapter 5** and publication in progress). SARS-CoV-2 viral replication and pathogenesis in the ferret model might thus be variant-dependent and requires a more in-depth investigation.

While it is debatable if the ferret model is suited to study SARS-CoV-2 pathogenesis, it might hold some promise to study adaptive immune responses against SARS-CoV-2. We were able to measure humoral responses against SARS-CoV-2 spike and cellular response against peptide pools covering the most important SARS-CoV-2 proteins (**Chapter 5**). Importantly, immune responses in SARS-CoV-2 infected ferrets seem similar to that of humans, with dominant cellular responses against spike, membrane and nucleoprotein. The ferret model could be used to investigate to which extend a SARS-CoV-2 induced immune response is able to recognize divergent SARS-CoV-2 strains. However, this could also be investigated with other animal models (e.g. humanized mice) or with blood obtained from SARS-CoV-2 infected humans. In conclusion, while the ferret model can be seen as the golden standard for influenza virus research, it is not as suited to mimic the different aspects of SARS-CoV-2 pathogenesis and disease.

Similarities in the immune system of ferret and human

The ferret model accurately mimics human influenza pathogenesis, but (universal) influenza virus vaccines also need to be evaluated based on the immune response they induce. This raises the question if influenza-specific immune responses observed in ferrets are representative of human influenza-specific immunity. It is difficult to answer this question due to a lack of ferret-specific reagents that are needed for the investigation of adaptive immunity [70]. Despite this, in the sections below we will discuss the few known similarities of the ferret and human immune system and what can be done to investigate the ferret immune response in more detail.

Is adaptive immunity conserved between ferret and human?
Like all mammals [71], ferrets are expected to possess all five (primary) classes of immunoglobulins, but it is still unknown if they also possess four IgG subclasses like humans (IgG1, IgG2, IgG3, IgG4) [72]. Nevertheless, the ferret antibody response does hold a certain predictive value for human humoral immunity in the context of whether

an influenza virus vaccine needs to be updated to cope with drifted influenza viruses [73-76]. Every year, ferrets are infected with influenza virus vaccine strains and sera is collected. Haemagglutinin inhibition (HI) titers in serum are measured against both the vaccine and circulating influenza strains. If the HI-titers measured against the circulating strain shows a fourfold reduction compared to the in HI-titer determined against the vaccine strain, the vaccine strain is too antigenically diverse from the circulating strain and a vaccine update is deemed necessary [77]. The fact that ferret antibody responses can be used to assess the impact of antigenic changes on human influenza virus vaccines, indicates that the humoral immunity is relatively similar between ferret and human.

In addition to the humoral immune system, the T-cell compartment also seems similar between humans and ferrets. Both humans and ferrets possess T cells ($CD3^+$) that can be further divided into $CD4^+$ and $CD8^+$ T cells. Like human studies, T-cell immunity in ferrets is typically assessed by the production of IFNγ and sometimes TNF. Proliferation of T cells after antigen stimulation can also be a read-out for T-cell responses [38]. However, we do not know to which extent T-cell responses are similar between humans and ferrets. For example, we compared T-cell responses against H2N2 influenza virus between humans and ferrets on a protein level in **Chapter 3**, but a more in-depth investigation is desirable. The annotation and description of different ferret MHC-alleles is crucial for this, as T-cell responses in an individual are directly related to the composition of MHC alleles. A more thorough understanding of the ferret MHC composition could answer the question why some ferrets develop T-cell responses against certain epitopes and others not.

Another unknown is whether T-cell subsets are similar between humans and ferrets and if the markers used to distinguish them are analogous. An example of this is the tissue-resident memory T (T_{RM}) cell population, which can be identified by expression of CD69 and/or CD103 in humans and mice. Lung T_{RM} cells are important for the protection against influenza disease [78, 79] and the ability to measure their presence and activity can help evaluate vaccines. To this end, we have initiated the development of antibodies against ferret CD69 and CD103. Since it is unknown if the combination of CD69 and CD103 expression can be used to distinguish ferret T_{RM} cells, we first confirmed that lung-derived ferret $CD8^+$ T cells express CD69 and CD103 mRNA (unpublished data). Importantly, CD103 expression was higher in lung-derived T cells compared to blood-derived T cells, suggesting that CD103 can also be used in ferrets to distinguish circulating and tissue-resident memory T cells. We additionally tested whether the mouse-specific anti-CD103 clone M290 stains ferret CD103 as others previously reported this [80], but we could not reproduce their finding (unpublished data). This is probably not due to a lack of CD103 expression on ferret $CD8^+$ T cells, but rather due to a lack of binding affinity of the mouse-specific CD103 antibody for ferret CD103. This example clearly illustrates the difficulty with interpreting the ferret

immune response towards influenza virus infection and vaccination. By developing ferret-specific antibodies and other reagents, the translation of the ferret model to the human situation could be improved.

Can gene-expression analysis support translation from ferret to human?
The lack of ferret-specific reagents can be partly resolved by indirect measurements of immune gene expression. The draft genome of the ferret that has been published in 2014 can facilitate this [81], although its usefulness is hampered by the limited annotation and experimental validation. Still, we (**Chapter 5**) and others have successfully used the ferret genome to identify and measure gene expression to compensate for the lack of ferret-specific reagents [82-86]. Techniques such as quantitative reverse transcriptase polymerase chain reaction (RT-qPCR), RNAseq and oligonucleotide microarrays, have allowed the community to investigate the ferret immune response in more detail. For example, Horman et al. used RT-qPCR to measure the expression of additional cytokines beyond IFNγ and TNF in an attempt to correlate a cytokine expression profile with disease severity [82]. In a different publication, they used gene-expression tools to show that in response to influenza virus infection or IFNα, ferrets upregulate interferon-inducible transmembrane proteins [83]. While they did not directly compare the expression profile of ferrets to humans, this kind of research is invaluable for the translation of the ferret model to the human situation.

Gene-expression analysis is a promising method to investigate the ferret immune response and to translate this to the human situation. In contrast to flow cytometry – which can detect tens of different markers and has been an indispensable technique for the investigation of T-cell immunity – gene-expression analyses such as RNAseq allows for the measurement of thousands of different mRNAs. This facilitates a much broader and in-depth comparison of the immune response. However, gene-expression does not equal protein expression and care should be taken not to translate one into the other. Additionally, gene-expression analysis is currently still limited in resolution as the ferret genome is not fully annotated and most labs do not have the facilities or expertise to perform gene-expression analysis on single cells. To truly realize the potential of gene-expression analysis it is thus necessary to extensively map the ferret genome (DNA) and transcriptome (RNA). Only with this can gene-expression analysis truly become a powerful tool in the translation from the ferret model to human reality.

Recommendations for improvement of the ferret model
The ferret is one of the best models available for investigating the pathogenesis, replication kinetics and transmission of influenza virus. However, further improvements of the ferret model are necessary to utilize its potential as an immunological model for the evaluation of universal influenza virus vaccines. To achieve this, we discussed several recommendations, which are summarized below

in Box 2. With the improvements listed here, we are convinced that the ferret model can be of more value for the development of new universal influenza virus vaccines.

Box 2: recommendations for the improvement of the ferret model

Standardize screening of ferrets for prior infections to improve reproducibility and comparison of ferret infection studies.
Develop ferret-specific reagents to measure systemic and local T-cell immunity in more detail.
Sequence and annotate the genome of ferrets from multiple suppliers to support gene-analysis techniques and to define the diversity in genetic background between individual ferrets and suppliers.
Improved understanding of MHC alleles in the ferret population could facilitate a more detailed understanding of T-cell immunity in the ferret model.

T-cell immunity and universal influenza virus vaccines

Traditional influenza virus vaccines offer limited protection because the immune response they induce is confined to antibodies against strain-specific epitopes in haemagglutinin (HA). In order to improve vaccine effectiveness, vaccines would need to induce broadly-reactive immune responses that target multiple influenza virus subtypes. T cells are indispensable for this since they can recognize conserved epitopes and have been shown to mediate heterosubtypic protection. Therefore, T-cell immunity is considered a key component of future universal influenza virus vaccines. The question is, how can we best induce a long-lived, broadly-protective T-cell response against conserved influenza virus epitopes? Here, we discuss our work in the context of existing literature to define what is needed for a T cell-inducing universal influenza virus vaccine.

T cell-based influenza virus vaccines require a cellular correlate of protection
Vaccine responses are deemed protective when they reach certain criteria, the so-called correlate of protection. For traditional influenza virus vaccines, the antibody-based correlate of protection is defined as an HI-titer of ≥ 40 (reviewed in [87]). This titer is associated with an 50% decrease in risk of contracting viral influenza in adult individuals. Unlike antibodies, T cells cannot prevent infection and this makes it difficult to establish a correlate of protection for T cells. This is further complicated by the fact that most vaccines aim at inducing protective antibody levels. Combined with the difficulty and high cost of cellular assays (compared to antibody assays), T-cell responses in human influenza virus vaccine trials are often not quantified. Even if T-cell responses are quantified, they often cannot be interpreted independently

from the antibody responses. However, the lack of a cellular correlate of protection can hinder the development and market approval of new T cell-based influenza virus vaccines.

What entails a protective T-cell response?
There have been several attempts to define a cellular correlate of protection. One clinical study found that young children with higher IFNy-responses after IIV-vaccination are less likely to develop clinical influenza disease [88]. By stimulating PBMCs with influenza virus in IFNy ELISpot assays, the authors found that ≥ 100 spot forming cells / 10^6 PBMCs was sufficient to protect the majority of children against clinical influenza disease and might be a correlate of protection. Similar findings can be derived from older adults. McElhaney found that T-cell responses are a better correlate of protection than antibody responses in adults > 60 years [89]. Unfortunately, while these studies give clear indications that influenza-specific T cells can protect against disease, they do not designate an undisputable correlate of protection.

While it cannot be regarded as a cellular correlate of protection, there are some rough indications which type of T-cell response is protective. In an early (1983) human infection study, high cytotoxic T-cell responses (>10% lysis of infected cells) prior to infection with H1N1 influenza virus was associated with reduced virus shedding [90]. Later, an observational study during the 2009 H1N1 influenza pandemic reported that pre-existing $CD8^+$ T-cell responses against conserved influenza virus epitopes negatively correlated with influenza disease [91]. Specifically, $IFNy^+IL2^-$ $CD8^+$ T-cell responses were thought to be essential. Some studies also found a role for $CD4^+$ T cells. In one study that focused on zoonotic avian infections, H7N9-specific $CD4^+$ and $CD8^+$ T-cell responses were higher in patients that survived an H7N9 influenza virus infection compared to those that died [92]. Similarly, in a human challenge study, pre-existing $CD4^+$ T-cell responses against nucleoprotein (NP) and matrix protein 1 (M1) and 2 (M2) negatively correlated with viral shedding, disease symptoms and disease duration after H3N2 infection [93].

In addition to the findings in human studies, animal models have clearly demonstrated that migration to, and survival in, the respiratory tract are essential for protective T-cell responses. The problem is that – at least in animal models – lung T_{RM} cells are relatively short-lived [94-98]. This might not necessarily be the case for humans since most adults have repeatedly been infected with influenza virus, which could boost the longevity of the T_{RM} cells population. This is supported by the recovery of donor-derived influenza-specific lung T_{RM} cells in lung-transplant recipients up to a year after transplantation [99]. Given the importance of respiratory T-cell immunity, it is unlikely that a correlate of protection can accurately predict protection against influenza disease if it does not take into account respiratory T cells. Unfortunately,

much is still unknown regarding the size and longevity of the influenza-specific T-cell response in the respiratory tract of humans and it will be practically and ethically challenging to measure T-cell immunity in the respiratory tract of healthy humans.

What can be part of a cellular correlate of protection?
It is not surprising that $CD8^+$ T cells have been found to reduce influenza disease since cytotoxic $CD8^+$ T cells can kill infected cells (**Chapter 1**). In contrast, the exact mechanism by which $CD4^+$ T cells reduce influenza disease is difficult to pinpoint because they have such a wide variety of effector functions [100]. $CD4^+$ T cells have been shown to kill infected cells, but it is unlikely that this plays a major role. Cytotoxic $CD4^+$ T cell activity requires expression of MHC-II on the infected cell, which is only expressed by antigen presenting cells and not on most influenza-infected cells in the respiratory tract [101]. It is more likely that the beneficial role of $CD4^+$ T cells is due to their assistance to B cells and $CD8^+$ T cells, or by recruiting innate immune cells to the site of infection. The idea that $CD4^+$ T cells are primarily protective via other cell types suggests that $CD4^+$ T cells are not suited as an (independent) cellular correlate of protection. In contrast, $CD8^+$ T cells that can directly kill influenza-infected cells, could serve as a relatively straightforward correlate of protection. Alternatively, $CD4^+$ and $CD8^+$ T-cell immunity could both be included, but this might lead to a complicated and impractical correlate of protection. More in-depth investigations are needed to pin-point exactly which aspect of the T-cell response can serve as a correlate of protection. For example, it would be interesting to transfer varying numbers of T cells into naïve animals to determine if – and to which extend – higher T-cell numbers increases protection. Additionally, transferring specific T-cell subsets (e.g. $CD8^+IFN\gamma^+$ cells) might give additional information that could form the basis for a cellular correlate of protection.

Not only the number of T cells, but also their location and effector function can affect the potency of the T-cell response. Given the difficulty to use respiratory T_{RM} cells to study T-cell immunity, a cellular correlate of protection is therefore likely to be based on T-cell responses derived from blood. It might therefore be interesting to investigate if gene expression or DNA methylation profiles of blood-derived T cells can be used to merge the different factors of the T-cell response in a single correlate of protection. For example, it has been shown that gene expression [94, 102] and DNA methylation (reviewed in [103]) in the early phase of an immune response determines to which tissue T cells migrate. If such profiles are (partly) conserved in circulating memory T cells, it might be possible to predict if, and to which tissue, T cells will migrate after booster vaccination. Similarly, T-cell differentiation and effector functions might be predicted by looking at gene expression and DNA methylation. A cellular correlate of protection based on these (or similar) techniques does require further investigation of the assumptions underlying this proposal. Are genetic profiles of blood-derived T-cells predictive of T-cell immunity in the respiratory tract? And how well does the

genetic profile (e.g. DNA) predict the functional profile (e.g. protein expression)? While the answers to these individual questions might be relatively simple, defining an encompassing cellular correlate of protection is difficult and will be a challenging endeavor.

T cell-based influenza virus vaccines should target conserved proteins

The inclusion of conserved epitopes in a universal influenza virus vaccine is essential for the induction of broadly-protective immunity. For this reason, HA and neuraminidase (NA) cannot be the main target of T-cell immunity since they are not conserved between influenza virus subtypes. As we have shown in **Chapter 3** with data from the Immune Epitope Database (IEDB, [104]), very few known human $CD8^+$ T-cell epitopes are conserved between H1 (A/California/07/2009) and H2 (A/Singapore/1/57) proteins. In contrast, over 70 epitopes were conserved in the polymerase basic protein 1 (PB1) of the respective influenza viruses. Similarly, most other internal influenza virus proteins displayed a high degree of epitope conservation. Based on the conservation of T-cell epitopes, internal influenza virus proteins are thus an interesting target for broadly-reactive T-cell immunity.

In addition to the level of conservation, the immunodominance of influenza virus proteins – defined here as their potential to induce T-cell responses – should also be taken into account when selecting a vaccine target. Using the same dataset from the IEDB, we found that most human $CD8^+$ T-cell epitopes of an H1N1 influenza virus are located in PB1, polymerase basic protein 2 (PB2), and polymerase acidic protein (PA), followed by NP and M1. However, in humans most responses are observed against NP and M1, with slightly lower responses against HA and PB1, and subdominant responses against most other influenza virus proteins (Chapter 3 and [105, 106]). This clearly indicates that the number of (predicted) epitopes does not correlate with immunodominance. Our findings are in agreement with a previous study in which the authors found the highest number of $CD4^+$ and $CD8^+$ T-cell epitopes in PB1, but higher responses against the relatively small M1 protein in humans [107]. In addition to being immunodominant, M1 and NP contain epitopes that are conserved between influenza virus strains. In two independent studies, individuals showed T-cell responses against NP and M1 of H5N1 [108] and H7N9 [109] avian influenza, despite never encountering these influenza virus subtypes. Based on their immunodominance and high level of conservation, NP and M1 are thus interesting targets for a universal influenza virus vaccine.

Given the number of conserved epitopes and immunodominant role of NP, M1 and PB1 in humans, we wondered if influenza virus infection also induced strong responses against these proteins in ferrets. In **Chapter 3**, we showed that cellular responses in H1N1-infected ferrets predominantly targeted NP, and to a lesser extend non-structural protein 1 (NS1), PA, PB1, PB2 and M1. Responses could be boosted by an

additional H2N2 infection, after which we detected a broader response, directed against most internal influenza virus proteins. Based on the potent responses against NP, M1 and PB1 in both ferret and human, we decided to evaluate a new influenza virus mRNA-LNP vaccine encoding these proteins (**Chapter 4**). However, while mRNA-LNP vaccination induced potent NP-responses, T-cell responses against M1 and PB1 were relatively low. In contrast, a natural infection with H1N1 influenza virus did induce robust cellular immunity against M1 and PB1 and these responses could be boosted by mRNA-LNP vaccination. For reasons that we could not clarify, the mRNA-LNP vaccination was thus unable to induce T-cell responses against M1 and PB1, but was able to boost existing responses. It is difficult to predict if this vaccine would behave similar in humans, as mRNA-LNP vaccines targeting internal influenza virus proteins have not yet been tested in humans. Still, the high resemblance between ferret and human T-cell immunity after influenza virus infection is promising for the evaluation of T cell-based influenza virus vaccines in the ferret model.

Induction of (local) T-cell immunity is essential for universal influenza virus vaccines

In **Chapters 3** and **4** we showed that T-cell responses against conserved influenza virus proteins are associated with reduced disease after heterosubtypic influenza virus infection in ferrets. It is likely that especially the respiratory T-cell population contributed to protection because murine research has shown that lung T_{RM} cells are essential for the protection against influenza virus [94, 95, 97, 110-112]. Unfortunately, in our experiments we could not clearly distinguish between the contribution of circulating and respiratory T cells since the tools to investigate this in ferrets are still lacking. We did find in **Chapter 4** that mRNA-LNP vaccination was less potent in inducing respiratory T-cell immunity compared to an influenza virus infection. The reduced respiratory T-cell immunity might be the reason why vaccinated ferrets (without prior influenza virus exposure) were less protected against an H7N9 IAV challenge (compared to influenza pre-exposed ferrets). Combined with the existing literature, it is evident that the ability to induce T_{RM} cells in the respiratory tract is an important requirement of T-cell inducing vaccines. Hence, the question is, how can a future T cell-inducing influenza virus vaccine enhance respiratory T cell numbers, even if the vaccine is not administered via the respiratory tract (e.g. intramuscular or intradermal)? We discuss this in the context of two processes that determine the formation of respiratory T_{RM} cells: i) the migration of T cells to the respiratory tract and ii) the survival and persistence of these T_{RM} cells by vaccination.

How can T-cell migration to the respiratory tract be stimulated?

The site of activation and the inflammatory environment has a major impact on the migratory capacity that a T cell is endowed with (reviewed in [113]). This is nicely depicted in a study in which intraperitoneal peptide vaccination was compared with intranasal influenza virus infection [102]. Compared to peptide-primed $CD8^+$ T cells,

IAV-primed $CD8^+$ T cells possessed a gene-expression profile that was associated with higher capacity for migration to the lung parenchyma, including genes encoding CD49a and CCR5. Both CD49a [114] and CCR5 [115] have been shown to be involved in the migration of $CD8^+$ T cells into lung tissue. Although it is not clear whether the difference between IAV-infection and peptide vaccination was due to the different administration routes (i.n. vs i.p.) or antigen (peptide vs IAV), it does illustrate that vaccination can induce a different immune response compared to natural infection. This is important because without the ability to migrate into the respiratory tract, T cells do not protect against influenza virus. One study demonstrated this in mice by inducing NP-specific responses by intravenously injecting NP epitope-expressing DCs, followed by an intravenous booster vaccination with either NP-expressing *Listeria monocytogens* (LM-NP) or vaccinia virus (VV-NP) [110]. Both strategies boosted $CD8^+$ T cells to a similar level, but VV-NP lead to significantly higher influenza-specific $CD8^+$ T-cell numbers in the broncho alveolar lavage. This was due to higher expression of CXCR3 – which facilitates migration into the respiratory tract – and resulted in enhanced protection upon an influenza virus infection. Others have also reported a role for CXCR3 in the migration of $CD4^+$ T cells to the lungs of Sendai virus-infected mice [116].

Ideally, a future T cell-inducing vaccine would endow the newly induced T cells with the capacity to migrate to the respiratory tract. However, depending on the application of the vaccine, this is not always a requirement. Influenza-experienced individuals likely already possess T cells that are primed to migrate to respiratory tissues and it might be sufficient to administer a booster vaccination at a different site than the respiratory tract. In **Chapter 4**, we show that vaccination of influenza-experienced ferrets with a T cell mRNA-LNP vaccine successfully boosted T-cell responses in the lung, bronchoalveolar lavage and nasal turbinates, despite intramuscular administration. This confirmed earlier findings in mice that vaccination after influenza exposure can boost respiratory T cells. Slütter et al. induced tissue resident transgenic P14 T cells by infection with recombinant PR8 influenza expressing the GP33 epitope (recognized by P14 T cells) [94]. A systemic infection with *Listeria monocytogenes* carrying the same GP33 epitope managed to boost P14 T-cell numbers in the lung. The model Slütter et al. propose, is that systemic boosting resulted in higher $CD8^+$ T_{EM} cells, which then seeded into the lung tissue. In time, T_{EM} cells lose the ability to migrate into lung tissue and repeated boosters might be required to keep lung T_{RM} cell numbers stable. A later publication actually showed that repeated boosting of T cells can enhance their capability to populate and survive in the lungs of mice [95]. Repeated exposure to antigens – for example by vaccination – might thus be needed to support replenishment of lung T_{RM} cells.

How can vaccination support respiratory T cells?
After migration to the respiratory tract, primed T cells require additional signals to remain there. In all likelihood, this requires a local signal in the form of antigen presentation and/or inflammation [96, 111, 117-121]. This also explains why intraperitoneal (i.p.) or i.m. administration routes generally do not induce lung T_{RM} cells in naïve animals [97, 112, 120, 122]. However, it is possible to pull circulating T cells into the respiratory tract. Takamura et al. showed that antigen-specific $CD8^+$ T cells induced by intraperitoneal influenza virus infection could be pulled into the lung environment of mice if CpG (Toll-like receptor ligand) was administered intranasally 8 or 30 days post infection [119]. This effect was however temporary, unless cognate antigen was administered together with the CpG, indicating that local antigen recognition is required for long-term maintenance of lung T_{RM} cells. In contrast, a report from Caminschi et al. indicates that the requirement for cognate antigen recognition might also depend on the adjuvant used [123].

While the formation of lung-resident T cells seems to require local antigen recognition or specific adjuvants, this requirement might not apply for other parts of the respiratory tract. Pizzolla et al. have shown that while the formation of lung T_{RM} cells in mice requires local antigen recognition, T_{RM} cells in the nasal turbinates establish themselves without local antigen recognition [111]. T_{RM} cells in the nasal turbinates were long-lived, with no significant decline between 20 and 120 days post infection. Interestingly, antigen-specific T_{RM} cells ($CD103^+CD69^+$) formed in the nasal turbinates in the absence of any infection, inflammation or antigen recognition. This is in agreement with our observation that intramuscular mRNA-vaccination in **Chapter 4** was able to induce cellular responses in the nasal turbinates of naïve ferrets.

T cell-based vaccination strategies should take into account how to induce or boost respiratory immune responses. As we have discussed here, this might require several different approaches depending on the target group and the vaccine format. In influenza-experienced individuals, circulating influenza-specific memory T cells likely already have the ability to migrate to the respiratory tract. Therefore, merely boosting circulating T cells that can then migrate to the respiratory tract might already be sufficient to enhance protection against influenza disease. In contrast, individuals without pre-existing influenza immunity (mainly young children) need vaccines that can induce respiratory T-cell immunity de novo. LAIVs are administered via the airways and can induce respiratory T-cell immunity, but the protection induced by LAIVs has been limited in humans thus far (**Chapter 1**). Other vaccine formats that are administered via different routes (e.g. intramuscular) might induce more robust T-cell immunity, but it is uncertain if this also includes respiratory T cells. We have seen that mRNA-LNP vaccination induced T-cells in the nasal turbinates and lung, but responses were lower than a natural influenza virus infection. In order to enhance the induction of respiratory T-cell immunity in naïve individuals, prime-pull strategies or

the use of certain adjuvants are of interest. For example, children might be primed intramuscularly with a (newly developed) mRNA-LNP vaccine, followed several weeks later by intranasally administered LAIV (or vice versa). In this way, a robust systemic cellular response can be pulled towards the respiratory tract. Of course, this raises a multitude of other questions that require additional investigation. How stable is the immunity induced by a prime-pull strategy? Which combinations of vaccine formats are most efficient and safe? These and other questions require relevant animal models in which we can evaluate the potential of influenza virus vaccines to induce respiratory T-cell responses.

Potential caveats of T cell-based universal influenza virus vaccines

The introduction of universal T cell-based influenza virus vaccines might come with its own set of problems. There are concerns that an increased focus on T-cell immunity could exacerbate the loss of T-cell epitopes. Additionally, too much T-cell immunity carries the risk of inducing immunopathology. In the sections below, we discuss these possible caveats to determine their impact on the success of T cell-based universal T cell-based influenza virus vaccines.

Can increased immunological pressure lead to a loss of T-cell epitopes?

We and others often mention that internal influenza virus proteins are more conserved compared to the external HA and NA proteins. While this is certainly the case, we should place this in the context of immunological pressure. Both HA and NA are dominant targets for the antibody response and immune-escape mutations in HA and NA can be beneficial for viral transmission [124-127]. Hence, the high mutation rate and low conservation of HA and NA is partly due to the high immunological pressure on these proteins. The question then is: are T-cell epitopes in contrast more conserved due to lower immunological pressure? If so, would the introduction of T cell-inducing vaccines increase immunological pressure and lead to a higher mutation rate of T cell-specific influenza virus epitopes?

There is clear evidence that T-cell epitopes are subject to immunological pressure. In time, mutations in NP of H3N2 influenza virus have occurred, which either abolished the presentation of T-cell epitopes by MHC or lead to a mutated peptide that was no longer recognized by a specific T-cell clone [128-130]. This was also demonstrated by Machkovech et al., who measured immunological pressure by comparing the mutation rate of human $CD8^+$ T-cell epitopes in human and swine influenza strains [131]. The idea is that there is no immunological pressure on human $CD8^+$ T-cell epitopes in swine and therefore, these epitopes should be relatively stable in swine influenza viruses. The authors indeed found that in human influenza viruses, $CD8^+$ T-cell epitopes mutated significantly more rapid than in swine influenza viruses, indicating that the human $CD8^+$ T-cell epitopes were subjected to immunological pressure. Similarly, Woolthuis et al. tracked the presence of 142 MHC-I restricted epitopes in H1N1 (pre-2009), pH1N1

(post-2009), H2N2 and H3N2 viruses [132]. They found that on average, circulating influenza viruses lose >1 epitope per 3 years. Influenza viruses both gained and lost epitopes, with the highest turnover in NP. Interestingly, in mice with a transgenic T-cell receptor (TCR) specific for a single NP epitope, the IAV evaded the $CD8^+$ T cell response within 18 days after IAV infection [133]. This was the result of multiple mutations in the NP-epitope. While immune-escape within 18 days post infection does not seem promising for T-cell vaccination, it is unlikely that this finding is representative of the human situation. Humans have a much broader immune response compared to a transgenic-TCR mouse model and the infecting influenza virus would need to accumulate multiple mutations in T-cell epitopes to fully escape the response. Not surprisingly, it is estimated that it takes up to a decade before a given IAV accrues sufficient mutations to escape the host's $CD8^+$ T-cell response [134]. Additionally, mutations can negatively impact the transmission and fitness of influenza viruses, which are not fully captured in an experimental mouse model. T-cell epitopes are thus subject to immunological pressure, but it is questionable if this drives influenza viruses to rapidly escape T-cell immunity in humans.

While there is clear evidence that immunological pressure leads to a loss of T-cell epitopes in influenza viruses, T-cell immunity is not necessarily entirely evaded. The observation that certain T-cell epitopes are conserved between human influenza viruses (**Chapter 3**, [135]) and between human and avian influenza strains [108, 109], indicates that at least some T-cell epitopes do not easily disappear due to immunological pressure. An example of this is the $M1_{58\text{-}66}$ epitope (GILGFVFTL), which is conserved between most IAV strains despite its immunodominance [136]. A reason for this is that functional constraints of (internal) influenza virus proteins can limit viral escape of T-cell epitopes, as some mutations would severely impact viral fitness [137]. This is supported by murine studies in which immune-escaping mutations in IAV are lost when they are transferred to naïve mice, indicating that the evasion of the $CD8^+$ T-cell response comes at the cost of reduced viral fitness [138]. The idea that T-cell epitopes are conserved due to functional constraints is in line with reports that the internal proteins of IAV are more conserved and slower to accumulate mutations compared to HA and NA [139, 140]. Based on the observation that T-cell epitopes are conserved between influenza virus subtypes, the low rate at which T-cell epitopes disappear and the broad T-cell response, it is thus unlikely that influenza viruses can rapidly escape vaccine-induced T-cell immunity.

Can enhanced T-cell immunity lead to immunopathology?
In addition to the concern of immune escape, there is a concern that strong T-cell immunity can negatively impact influenza disease by inducing immunopathology. The rationale behind this is that non-specific effector functions of T cells – such as secretion of inflammatory cytokines – can damage the surrounding tissue and exacerbate pathology. Indeed, multiple studies have shown that removing certain

signals can lead to a derailment of the T-cell response (reviewed in [141]). For example, mice that did not express soluble TNF displayed increased morbidity and lung pathology, which resulted from prolonged $CD8^+$ T-cell activity [142]. In contrast, $CD8^+$ T-cell induced immunopathology could also be reduced by inhibiting TNF activity [143], indicating that too much TNF worsens immunopathology. This nicely illustrates that everything in the immune system requires a certain balance. Very robust T-cell immunity with insufficient inhibitory checkpoints might thus come with the risk of T cell-induced pathology.

While there is evidence that uninhibited T-cell immunity can lead to immunopathology, it is still debatable how big the risk of T cell-induced immunopathology actually is. Most studies that investigated T cell-induced immunopathology either used mice or very artificial models (e.g. expression of influenza antigen in alveolar epithelial cells). Mice do not resemble human influenza disease and constant and wide-spread expression of influenza antigens in epithelial cells hardly mimics a natural influenza virus infection (or vaccination). Additionally, is has been clearly illustrated that influenza-induced T cells are subject to inhibitory signals that prevent excessive immune activation (reviewed in [78, 144]). For example, viral infection in the respiratory tract of mice leads to increased expression of inhibitory receptors (e.g. PD-1) on $CD8^+$ T-cells and inhibitory ligands on airway epithelial cells [145]. These are clear indications that the host can find a balance between immune activation and inhibition. Although T cell-inducing influenza virus vaccines should be developed with the risk of immunopathology in mind, the balance between activation and inhibition might not that easily be broken.

Outdated influenza virus vaccination strategies can hamper heterosubtypic immunity

There are clear benefits of influenza virus vaccination in risk groups and people that are in close contact with those at risk [146]. Vaccination of healthy children and adults with the currently available vaccines might, however, result in negative long-term effects. Whereas unvaccinated, but naturally infected individuals benefit from a broad induction or boosting of their influenza immunity – including T cells – the induction of immunity by vaccination with IIVs is largely limited to the antibody response [147]. For example, in young children a natural infection induced higher NP-specific $CD4^+$ T-cell responses compared to IIV vaccination [148]. The possible negative effects of IIVs are further illustrated by studies using mice and ferrets in which an H3N2 IAV infection resulted in heterosubtypic immunity against H5N1 IAV [38, 149, 150]. However, if mice or ferrets were vaccinated with an H3N2 subunit vaccine prior to H3N2 infection, the induction of heterosubtypic protection was reduced. Similarly, vaccination of mice with H1N1 split vaccine prevented the induction of heterosubtypic immunity by H1N1 infection and did not reduce mortality after H5N1 infection [151]. Thus, vaccination of healthy humans, especially young children that have not yet encountered influenza

virus, might prevent the induction or boosting of heterosubtypic immunity. This increases the risk for severe influenza disease if these individuals become infected with mutated or newly emerging influenza viruses that have escaped the existing antibody response. Paradoxically, long-term influenza virus vaccination might thus create a population of healthy individuals that is at risk of serious influenza disease if (newly emerging) influenza strains escape the vaccine-induced immunity. This problem can be prevented by the introduction of new influenza virus vaccines that induce a broader immune response.

The way forward: universal influenza virus vaccines

The fact that each year influenza virus infections still cause significant morbidity and mortality despite vaccination, demonstrates that there is a need for improved influenza virus vaccines. Universal influenza virus vaccines aim to achieve this by inducing a broader immune response that extends the protection to all influenza virus subtypes that can infect humans, including zoonotic strains [152]. A secondary aim of universal influenza virus vaccines could be to reduce the frequency of vaccinations required to provide protection. Currently, influenza virus vaccine boosters are given yearly to anticipate on changes in circulating strains and to boost antibody responses to protective levels. If a universal influenza virus vaccine induces a sufficiently broad and long-lived immune response, booster vaccination might no longer be required annually.

In this thesis we focused on the role of T-cell immunity as a key-component of universal influenza virus vaccines. T cells can kill virus-infected cells, by which they reduce disease and viral transmission. Not surprisingly, higher T-cell immunity is associated with improved clinical outcome after influenza virus infection. The most important aspect of T cells, however, is that they can recognize conserved influenza virus epitopes. This equips T cells with the ability to respond to a wide range of influenza virus subtypes, which makes T-cell immunity a prime target for universal influenza virus vaccines. Based on our findings and the literature reviewed above, there are several requirements for a T-cell inducing universal influenza virus vaccine. Such a vaccine should be able to:

I. Induce a durable T-cell response against epitopes conserved between influenza virus subtypes
II. Induce, boost and enhance the longevity of respiratory T-cell immunity
III. Find a balance between protective T-cell immunity and possible collateral damage due to excessive immune activation

Since traditional IIVs do not live up to the requirements stated above, a T-cell inducing universal vaccine would require a different vaccine platform. The mRNA-LNP platform is one interesting vaccine concept since we and others have demonstrated

the potential of mRNA-LNP vaccines in reducing the impact of infectious diseases. Other interesting platforms for a universal influenza virus vaccine include (but are not limited to) improved LAIV and vector vaccines. The major benefit of LAIV and vector vaccines is that they can be administered into the respiratory tract, which could tremendously increase the recruitment of respiratory T cells. In the future, other vaccine platforms (including mRNA-LNPs) might also display increased efficacy if they can be inhaled instead of injected.

While we firmly believe that T-cell immunity is essential for an universal influenza virus vaccine, one should not neglect the enormous potential of humoral immunity. New antibody-inducing vaccines targeting conserved epitopes in, for example, M2 and the stalk domain of HA are very promising. In our opinion, a universal influenza virus vaccine should therefore combine the best of two worlds: antibodies and T cells. With further vaccine improvements, the width of the antibody response against HA might be increased by targeting conserved epitopes. Ultimately, this may lead to an antibody response that covers the majority of H1N1, H3N2 and influenza B strains, unlike the strain-specific immunity afforded by current vaccines. A truly protective vaccine might be developed if broadly-reactive antibody responses could be combined with T-cell responses against conserved epitopes, that can serve as a safety measure when influenza viruses evade the antibody response. NP and M1 are logical targets for T-cell immunity as they are immunodominant and highly conserved between human and animal influenza strains, but other proteins might also be interesting if subdominant immune responses can be enhanced by vaccination.

Concluding remarks

In this thesis we have described the potential of T-cell immunity and the value of the ferret model for influenza research. We believe that the work we presented here can benefit the development of new universal influenza virus vaccines. Many obstacles still remain though, and it will take considerable effort to develop and introduce universal influenza virus vaccines. We therefore compiled several recommendations that might aid the development of universal influenza virus vaccines (Box 3). Without improved vaccines, viral influenza will remain a serious problem. With this thesis, we hope to convey that T-cell immunity is part of the solution.

Box 3: Recommendations for future influenza vaccinations

1. Development of universal influenza virus vaccines requires relevant animal models to mimic human influenza disease and immunity. The ferret model is suited to this purpose, but is hampered by the lack of reagents. More focus should be given to the development of ferret-specific reagents to measure T-cell immunity in more detail.
2. The next generation of influenza virus vaccines should include antigens that induce relevant T-cell immunity.
3. T cell-based universal vaccines should focus on the induction and/or boosting of T-cell immunity in the respiratory tract.
4. More attention should be given to vaccine strategies that combine different influenza virus vaccine platforms since the synergistic effect could increase vaccine effectiveness.
5. A cellular correlate of protection is crucial for the evaluation of T cell-based universal influenza virus vaccines. This will likely encompass several parameters of T-cell functioning, which can be impractical. It should be investigated if gene-expression techniques can combine these different parameters and if this can be used to predict vaccine effectiveness.
6. As long as influenza virus vaccines are not improved, influenza virus vaccination should remain limited to risk-groups since there is a risk that vaccination hampers the induction of heterosubtypic immunity in healthy individuals.

References

1. Smith, W., C.H. Andrewes, and P.P. Laidlaw, *A Virus Obtained from Influenza Patients.* The Lancet, 1933. **222**(5732): p. 66-68.
2. Nguyen, T.Q., R. Rollon, and Y.K. Choi, *Animal Models for Influenza Research: Strengths and Weaknesses.* Viruses, 2021. **13**(6).
3. Maher, J.A. and J. DeStefano, *The ferret: an animal model to study influenza virus.* Lab Anim (NY), 2004. **33**(9): p. 50-3.
4. Johnson-Delaney, C.A. and S.E. Orosz, *Ferret respiratory system: clinical anatomy, physiology, and disease.* Vet Clin North Am Exot Anim Pract, 2011. **14**(2): p. 357-67, vii.
5. Oh, D.Y. and A.C. Hurt, *Using the Ferret as an Animal Model for Investigating Influenza Antiviral Effectiveness.* Front Microbiol, 2016. **7**: p. 80.
6. Buhnerkempe, M.G., et al., *Mapping influenza transmission in the ferret model to transmission in humans.* Elife, 2015. **4**.
7. Kuiken, T. and J.K. Taubenberger, *Pathology of human influenza revisited.* Vaccine, 2008. **26 Suppl 4**: p. D59-66.
8. Yuen, K.Y., et al., *Clinical features and rapid viral diagnosis of human disease associated with avian influenza A H5N1 virus.* The Lancet, 1998. **351**(9101): p. 467-471.
9. Ke, C., et al., *Human Infection with Highly Pathogenic Avian Influenza A(H7N9) Virus, China.* Emerg Infect Dis, 2017. **23**(8): p. 1332-1340.
10. Nicholls, J.M., et al., *Sialic acid receptor detection in the human respiratory tract: evidence for widespread distribution of potential binding sites for human and avian influenza viruses.* Respir Res, 2007. **8**: p. 73.
11. Kirkeby, S., C.J. Martel, and B. Aasted, *Infection with human H1N1 influenza virus affects the expression of sialic acids of metaplastic mucous cells in the ferret airways.* Virus Res, 2009. **144**(1-2): p. 225-32.
12. Jayaraman, A., et al., *Decoding the distribution of glycan receptors for human-adapted influenza A viruses in ferret respiratory tract.* PLoS One, 2012. **7**(2): p. e27517.
13. Xu, Q., et al., *Influenza H1N1 A/Solomon Island/3/06 virus receptor binding specificity correlates with virus pathogenicity, antigenicity, and immunogenicity in ferrets.* J Virol, 2010. **84**(10): p. 4936-45.
14. Massin, P., S. van der Werf, and N. Naffakh, *Residue 627 of PB2 is a determinant of cold sensitivity in RNA replication of avian influenza viruses.* J Virol, 2001. **75**(11): p. 5398-404.
15. Massin, P., et al., *Temperature sensitivity on growth and/or replication of H1N1, H1N2 and H3N2 influenza A viruses isolated from pigs and birds in mammalian cells.* Vet Microbiol, 2010. **142**(3-4): p. 232-41.
16. Zeng, H., et al., *Tropism and Infectivity of a Seasonal A(H1N1) and a Highly Pathogenic Avian A(H5N1) Influenza Virus in Primary Differentiated Ferret Nasal Epithelial Cell Cultures.* J Virol, 2019. **93**(10).
17. Bodewes, R., et al., *Infection of the upper respiratory tract with seasonal influenza A(H3N2) virus induces protective immunity in ferrets against infection with A(H1N1)pdm09 virus after intranasal, but not intratracheal, inoculation.* J Virol, 2013. **87**(8): p. 4293-301.
18. Bissel, S.J., et al., *H1N1, but Not H3N2, Influenza A Virus Infection Protects Ferrets from H5N1 Encephalitis.* Journal of Virology, 2014. **88**: p. 3077-3091.
19. Ryan, K.A., et al., *Cellular immune response to human influenza viruses differs between H1N1 and H3N2 subtypes in the ferret lung.* Plos One, 2018. **13**: p. e0202675.
20. Bodewes, R., et al., *Pathogenesis of Influenza A/H5N1 virus infection in ferrets differs between intranasal and intratracheal routes of inoculation.* Am J Pathol, 2011. **179**(1): p. 30-6.

21. Yamada, M., et al., *Multiple routes of invasion of wild-type Clade 1 highly pathogenic avian influenza H5N1 virus into the central nervous system (CNS) after intranasal exposure in ferrets.* Acta Neuropathol, 2012. **124**(4): p. 505-16.
22. Beigel, J.H., et al., *Avian influenza A (H5N1) infection in humans.* N Engl J Med, 2005. **353**(13): p. 1374-85.
23. Xu, L., et al., *The mouse and ferret models for studying the novel avian-origin human influenza A (H7N9) virus.* Virol J, 2013. **10**: p. 253.
24. Zitzow, L.A., et al., *Pathogenesis of avian influenza A (H5N1) viruses in ferrets.* J Virol, 2002. **76**(9): p. 4420-9.
25. Zeng, H., et al., *Tropism and infectivity of influenza virus, including highly pathogenic avian H5N1 virus, in ferret tracheal differentiated primary epithelial cell cultures.* J Virol, 2013. **87**(5): p. 2597-607.
26. Kreijtz, J.H., et al., *Low pathogenic avian influenza A(H7N9) virus causes high mortality in ferrets upon intratracheal challenge: a model to study intervention strategies.* Vaccine, 2013. **31**(43): p. 4995-9.
27. de Jonge, J., et al., *H7N9 Live Attenuated Influenza Vaccine Is Highly Immunogenic, Prevents Virus Replication, and Protects Against Severe Bronchopneumonia in Ferrets.* Mol Ther, 2016. **24**(5): p. 991-1002.
28. Imai, M., et al., *A Highly Pathogenic Avian H7N9 Influenza Virus Isolated from A Human Is Lethal in Some Ferrets Infected via Respiratory Droplets.* Cell Host and Microbe, 2017. **22**: p. 615-626.e8.
29. Killingley, B. and J. Nguyen-Van-Tam, *Routes of influenza transmission.* Influenza Other Respir Viruses, 2013. **7 Suppl 2**: p. 42-51.
30. Belser, J.A., et al., *Complexities in Ferret Influenza Virus Pathogenesis and Transmission Models.* Microbiol Mol Biol Rev, 2016. **80**(3): p. 733-44.
31. Belser, J.A., et al., *Influenza virus infectivity and virulence following ocular-only aerosol inoculation of ferrets.* J Virol, 2014. **88**(17): p. 9647-54.
32. Gustin, K.M., et al., *Influenza virus aerosol exposure and analytical system for ferrets.* Proc Natl Acad Sci U S A, 2011. **108**(20): p. 8432-7.
33. Marriott, A.C., et al., *Low dose influenza virus challenge in the ferret leads to increased virus shedding and greater sensitivity to oseltamivir.* PLoS One, 2014. **9**(4): p. e94090.
34. Gooch, K.E., et al., *Heterosubtypic cross-protection correlates with cross-reactive interferon-gamma-secreting lymphocytes in the ferret model of influenza.* Sci Rep, 2019. **9**(1): p. 2617.
35. Jayasundara, K., et al., *Natural attack rate of influenza in unvaccinated children and adults: a meta-regression analysis.* BMC Infect Dis, 2014. **14**: p. 670.
36. Somes, M.P., et al., *Estimating the annual attack rate of seasonal influenza among unvaccinated individuals: A systematic review and meta-analysis.* Vaccine, 2018. **36**(23): p. 3199-3207.
37. Jennings, R., C.W. Potter, and C. McLaren, *Effect of preinfection and preimmunization on the serum antibody response to subsequent immunization with heterotypic influenza vaccines.* J Immunol, 1974. **113**(6): p. 1834-43.
38. Bodewes, R., et al., *Vaccination against seasonal influenza A/H3N2 virus reduces the induction of heterosubtypic immunity against influenza A/H5N1 virus infection in ferrets.* J Virol, 2011. **85**(6): p. 2695-702.
39. Langlois, I., *Viral diseases of ferrets.* Vet Clin North Am Exot Anim Pract, 2005. **8**(1): p. 139-60.
40. von Messling, V., et al., *A ferret model of canine distemper virus virulence and immunosuppression.* J Virol, 2003. **77**(23): p. 12579-91.
41. Enkirch, T. and V. von Messling, *Ferret models of viral pathogenesis.* Virology, 2015. **479-480**: p. 259-70.

42. *Biology and Diseases of the Ferret*. Third ed, ed. J.G. Fox and R.P. Marini. 2014, Hoboken: John Wiley & Sons, Inc. 65-68.
43. Kim, Y.I., et al., *Infection and Rapid Transmission of SARS-CoV-2 in Ferrets.* Cell Host Microbe, 2020. **27**(5): p. 704-709 e2.
44. Shi, J., et al., *Susceptibility of ferrets, cats, dogs, and other domesticated animals to SARS-coronavirus 2.* Science, 2020. **368**(6494): p. 1016-1020.
45. Wise, A.G., M. Kiupel, and R.K. Maes, *Molecular characterization of a novel coronavirus associated with epizootic catarrhal enteritis (ECE) in ferrets.* Virology, 2006. **349**(1): p. 164-74.
46. Ichinohe, T., et al., *Microbiota regulates immune defense against respiratory tract influenza A virus infection.* Proc Natl Acad Sci U S A, 2011. **108**(13): p. 5354-9.
47. Abt, M.C., et al., *Commensal bacteria calibrate the activation threshold of innate antiviral immunity.* Immunity, 2012. **37**(1): p. 158-70.
48. Steed, A.L., et al., *The microbial metabolite desaminotyrosine protects from influenza through type I interferon.* Science, 2017. **357**(6350): p. 498-502.
49. Bradley, K.C., et al., *Microbiota-Driven Tonic Interferon Signals in Lung Stromal Cells Protect from Influenza Virus Infection.* Cell Rep, 2019. **28**(1): p. 245-256 e4.
50. Rosshart, S.P., et al., *Wild Mouse Gut Microbiota Promotes Host Fitness and Improves Disease Resistance.* Cell, 2017. **171**(5): p. 1015-1028 e13.
51. Rosshart, S.P., et al., *Laboratory mice born to wild mice have natural microbiota and model human immune responses.* Science, 2019. **365**(6452).
52. Zamoto, A., et al. *Identification of ferret ACE2 and its receptor function for SARS-coronavirus*. in *The Nidoviruses*. 2006. Boston, MA: Springer US.
53. Peacock, T.P., et al., *The furin cleavage site in the SARS-CoV-2 spike protein is required for transmission in ferrets.* Nat Microbiol, 2021. **6**(7): p. 899-909.
54. Hoffmann, M., et al., *SARS-CoV-2 Cell Entry Depends on ACE2 and TMPRSS2 and Is Blocked by a Clinically Proven Protease Inhibitor.* Cell, 2020. **181**(2): p. 271-280 e8.
55. Zhou, P., et al., *A pneumonia outbreak associated with a new coronavirus of probable bat origin.* Nature, 2020. **579**(7798): p. 270-273.
56. Liu, H.L., et al., *Gene signatures of SARS-CoV/SARS-CoV-2-infected ferret lungs in short- and long-term models.* Infect Genet Evol, 2020. **85**: p. 104438.
57. Park, S.J., et al., *Antiviral Efficacies of FDA-Approved Drugs against SARS-CoV-2 Infection in Ferrets.* mBio, 2020. **11**(3): p. e01114-20.
58. Richard, M., et al., *SARS-CoV-2 is transmitted via contact and via the air between ferrets.* Nat Commun, 2020. **11**(1): p. 3496.
59. Schlottau, K., et al., *SARS-CoV-2 in fruit bats, ferrets, pigs, and chickens: an experimental transmission study.* Lancet Microbe, 2020. **1**(5): p. e218-e225.
60. Wu, S., et al., *A single dose of an adenovirus-vectored vaccine provides protection against SARS-CoV-2 challenge.* Nat Commun, 2020. **11**(1): p. 4081.
61. Ryan, K.A., et al., *Dose-dependent response to infection with SARS-CoV-2 in the ferret model and evidence of protective immunity.* Nat Commun, 2021. **12**(1): p. 81.
62. Everett, H.E., et al., *Intranasal Infection of Ferrets with SARS-CoV-2 as a Model for Asymptomatic Human Infection.* Viruses, 2021. **13**(1): p. 113.
63. Cdc Weekly, C., *The Epidemiological Characteristics of an Outbreak of 2019 Novel Coronavirus Diseases (COVID-19) — China, 2020.* China CDC Weekly, 2020. **2**(8): p. 113-122.
64. Karagiannidis, C., et al., *Case characteristics, resource use, and outcomes of 10 021 patients with COVID-19 admitted to 920 German hospitals: an observational study.* The Lancet Respiratory Medicine, 2020. **8**(9): p. 853-862.
65. Verity, R., et al., *Estimates of the severity of coronavirus disease 2019: a model-based analysis.* Lancet Infect Dis, 2020. **20**(6): p. 669-677.

66. Du, Y., et al., *Clinical Features of 85 Fatal Cases of COVID-19 from Wuhan. A Retrospective Observational Study.* Am J Respir Crit Care Med, 2020. **201**(11): p. 1372-1379.
67. Zhou, F., et al., *Clinical course and risk factors for mortality of adult inpatients with COVID-19 in Wuhan, China: a retrospective cohort study.* Lancet, 2020. **395**(10229): p. 1054-1062.
68. Kim, Y.I., et al., *Age-dependent pathogenic characteristics of SARS-CoV-2 infection in ferrets.* Nat Commun, 2022. **13**(1): p. 21.
69. Ciurkiewicz, M., et al., *Ferrets are valuable models for SARS-CoV-2 research.* Vet Pathol, 2022: p. 3009858211071012.
70. Wong, J., et al., *Improving immunological insights into the ferret model of human viral infectious disease.* Influenza Other Respir Viruses, 2019. **13**(6): p. 535-546.
71. Vadnais, M.L., M.F. Criscitiello, and V.V. Smider, *Antibodies from Other Species*, in *Protein Therapeutics*, J.O. Tristan Vaughan, Bahija Jallal, Editor. 2017. p. 85-112.
72. Wong, J., et al., *Sequencing B cell receptors from ferrets (Mustela putorius furo).* PLoS One, 2020. **15**(5): p. e0233794.
73. Lipatov, A.S., et al., *Cross-protectiveness and immunogenicity of influenza A/Duck/Singapore/3/97(H5) vaccines against infection with A/Vietnam/1203/04(H5N1) virus in ferrets.* J Infect Dis, 2006. **194**(8): p. 1040-3.
74. Stephenson, I., et al., *Comparison of neutralising antibody assays for detection of antibody to influenza A/H3N2 viruses: an international collaborative study.* Vaccine, 2007. **25**(20): p. 4056-63.
75. Thi Nguyen, D., et al., *Antigenic characterization of highly pathogenic avian influenza A(H5N1) viruses with chicken and ferret antisera reveals clade-dependent variation in hemagglutination inhibition profiles.* Emerg Microbes Infect, 2018. **7**(1): p. 100.
76. Souza, C.K., et al., *Antigenic Distance between North American Swine and Human Seasonal H3N2 Influenza A Viruses as an Indication of Zoonotic Risk to Humans.* J Virol, 2022. **96**(2): p. e0137421.
77. Russell, C.A., et al., *Influenza vaccine strain selection and recent studies on the global migration of seasonal influenza viruses.* Vaccine, 2008. **26 Suppl 4**: p. D31-4.
78. Van Braeckel-Budimir, N. and J.T. Harty, *Influenza-induced lung T rm: Not all memories last forever.* Immunology and Cell Biology, 2017. **95**: p. 651-655.
79. Snyder, M.E. and D.L. Farber, *Human lung tissue resident memory T cells in health and disease.* Curr Opin Immunol, 2019. **59**: p. 101-108.
80. Rutigliano, J.A., et al., *Screening monoclonal antibodies for cross-reactivity in the ferret model of influenza infection.* Journal of immunological methods, 2008. **336**: p. 71-7.
81. Peng, X., et al., *The draft genome sequence of the ferret (Mustela putorius furo) facilitates study of human respiratory disease.* Nature Biotechnology, 2014. **32**: p. 1250-1255.
82. Horman, W.S.J., et al., *The Dynamics of the Ferret Immune Response During H7N9 Influenza Virus Infection.* Front Immunol, 2020. **11**: p. 559113.
83. Horman, W.S.J., et al., *Upregulated expression of ferret Interferon-Inducible Transmembrane genes by IFN-alpha and influenza virus infection.* J Virol, 2021.
84. Bruder, C.E., et al., *Transcriptome sequencing and development of an expression microarray platform for the domestic ferret.* BMC genomics, 2010. **11**: p. 251.
85. Cameron, C.M., et al., *Gene expression analysis of host innate immune responses during Lethal H5N1 infection in ferrets.* Journal of virology, 2008. **82**: p. 11308-11317.
86. Fang, Y., et al., *Molecular characterization of in vivo adjuvant activity in ferrets vaccinated against influenza virus.* J Virol, 2010. **84**(17): p. 8369-88.
87. Cox, R.J., *Correlates of protection to influenza virus, where do we go from here?* Hum Vaccin Immunother, 2013. **9**(2): p. 405-8.

88. Forrest, B.D., et al., *Correlation of cellular immune responses with protection against culture-confirmed influenza virus in young children.* Clin Vaccine Immunol, 2008. **15**(7): p. 1042-53.
89. McElhaney, J.E., et al., *T cell responses are better correlates of vaccine protection in the elderly.* J Immunol, 2006. **176**(10): p. 6333-9.
90. McMichael, A.J., et al., *Cytotoxic T-cell immunity to influenza.* N Engl J Med, 1983. **309**(1): p. 13-7.
91. Sridhar, S., et al., *Cellular immune correlates of protection against symptomatic pandemic influenza.* Nat Med, 2013. **19**(10): p. 1305-12.
92. Wang, Z., et al., *Recovery from severe H7N9 disease is associated with diverse response mechanisms dominated by CD8(+) T cells.* Nat Commun, 2015. **6**: p. 6833.
93. Wilkinson, T.M., et al., *Preexisting influenza-specific CD4+ T cells correlate with disease protection against influenza challenge in humans.* Nat Med, 2012. **18**(2): p. 274-80.
94. Slütter, B., et al., *Dynamics of influenza-induced lung-resident memory T cells underlie waning heterosubtypic immunity.* Sci Immunol, 2017. **2**(7).
95. Van Braeckel-Budimir, N., et al., *Repeated Antigen Exposure Extends the Durability of Influenza-Specific Lung-Resident Memory CD8(+) T Cells and Heterosubtypic Immunity.* Cell Rep, 2018. **24**(13): p. 3374-3382 e3.
96. Uddback, I., et al., *Long-term maintenance of lung resident memory T cells is mediated by persistent antigen.* Mucosal Immunol, 2021. **14**(1): p. 92-99.
97. Wu, T., et al., *Lung-resident memory CD8 T cells (TRM) are indispensable for optimal cross-protection against pulmonary virus infection.* J Leukoc Biol, 2014. **95**(2): p. 215-24.
98. Liang, S., et al., *Heterosubtypic immunity to influenza type A virus in mice. Effector mechanisms and their longevity.* The Journal of Immunology, 1994. **152**(4): p. 1653.
99. Snyder, M.E., et al., *Generation and persistence of human tissue-resident memory T cells in lung transplantation.* Sci Immunol, 2019. **4**(33).
100. Sant, A.J., et al., *CD4 T cells in protection from influenza virus: Viral antigen specificity and functional potential.* Immunol Rev, 2018. **284**(1): p. 91-105.
101. Takeuchi, A. and T. Saito, *CD4 CTL, a Cytotoxic Subset of CD4(+) T Cells, Their Differentiation and Function.* Front Immunol, 2017. **8**: p. 194.
102. Brinza, L., et al., *Immune signatures of protective spleen memory CD8 T cells.* Sci Rep, 2016. **6**: p. 37651.
103. Mueller, S.N., et al., *Memory T Cell Subsets, Migration Patterns, and Tissue Residence.* Annual Review of Immunology, 2013. **31**: p. 137-161.
104. Vita, R., et al., *The Immune Epitope Database (IEDB): 2018 update.* Nucleic Acids Res, 2019. **47**(D1): p. D339-D343.
105. Hayward, A.C., et al., *Natural T cell-mediated protection against seasonal and pandemic influenza: Results of the flu watch cohort study.* American Journal of Respiratory and Critical Care Medicine, 2015. **191**: p. 1422-1431.
106. Chen, L., et al., *Immunodominant CD4+ T-cell responses to influenza A virus in healthy individuals focus on matrix 1 and nucleoprotein.* J Virol, 2014. **88**(20): p. 11760-73.
107. Assarsson, E., et al., *Immunomic analysis of the repertoire of T-cell specificities for influenza A virus in humans.* J Virol, 2008. **82**(24): p. 12241-51.
108. Lee, L.Y., et al., *Memory T cells established by seasonal human influenza A infection cross-react with avian influenza A (H5N1) in healthy individuals.* J Clin Invest, 2008. **118**(10): p. 3478-90.
109. Quinones-Parra, S., et al., *Preexisting CD8+ T-cell immunity to the H7N9 influenza A virus varies across ethnicities.* Proceedings of the National Academy of Sciences, 2014. **111**: p. 1049-1054.

110. Slütter, B., et al., *Lung airway-surveilling CXCR3(hi) memory CD8(+) T cells are critical for protection against influenza A virus.* Immunity, 2013. **39**(5): p. 939-48.
111. Pizzolla, A., et al., *Resident memory CD8(+) T cells in the upper respiratory tract prevent pulmonary influenza virus infection.* Sci Immunol, 2017. **2**(12).
112. Zens, K.D., J.K. Chen, and D.L. Farber, *Vaccine-generated lung tissue–resident memory T cells provide heterosubtypic protection to influenza infection.* JCI Insight, 2016. **1**.
113. Masopust, D. and J.M. Schenkel, *The integration of T cell migration, differentiation and function.* Nat Rev Immunol, 2013. **13**: p. 309-320.
114. Ray, S.J., et al., *The collagen binding alpha1beta1 integrin VLA-1 regulates CD8 T cell-mediated immune protection against heterologous influenza infection.* Immunity, 2004. **20**(2): p. 167-79.
115. Kohlmeier, J.E., et al., *The chemokine receptor CCR5 plays a key role in the early memory CD8+ T cell response to respiratory virus infections.* Immunity, 2008. **29**(1): p. 101-13.
116. Kohlmeier, J.E., et al., *CXCR3 Directs Antigen-Specific Effector CD4+ T Cell Migration to the Lung During Parainfluenza Virus Infection.* Journal of immunology (Baltimore, Md. : 1950), 2009. **183**: p. 4378-84.
117. Wakim, L.M., et al., *Enhanced survival of lung tissue-resident memory CD8$^+$ T cells during infection with influenza virus due to selective expression of IFITM3.* Nature immunology, 2013. **14**: p. 238-45.
118. Lee, Y.T., et al., *Environmental and antigen receptor-derived signals support sustained surveillance of the lungs by pathogen-specific cytotoxic T lymphocytes.* J Virol, 2011. **85**(9): p. 4085-94.
119. Takamura, S., et al., *Specific niches for lung-resident memory CD8+ T cells at the site of tissue regeneration enable CD69-independent maintenance.* The Journal of experimental medicine, 2016. **213**: p. 3057-3073.
120. McMaster, S.R., et al., *Pulmonary antigen encounter regulates the establishment of tissue-resident CD8 memory T cells in the lung airways and parenchyma.* Mucosal Immunol, 2018. **11**(4): p. 1071-1078.
121. Wakim, L.M., et al., *Antibody-targeted vaccination to lung dendritic cells generates tissue-resident memory CD8 T cells that are highly protective against influenza virus infection.* Mucosal Immunology, 2015.
122. Takamura, S., et al., *The route of priming influences the ability of respiratory virus-specific memory CD8+ T cells to be activated by residual antigen.* J Exp Med, 2010. **207**(6): p. 1153-60.
123. Caminschi, I., et al., *Zymosan by-passes the requirement for pulmonary antigen encounter in lung tissue-resident memory CD8(+) T cell development.* Mucosal Immunol, 2019. **12**(2): p. 403-412.
124. Chang, P., et al., *Immune Escape Adaptive Mutations in the H7N9 Avian Influenza Hemagglutinin Protein Increase Virus Replication Fitness and Decrease Pandemic Potential.* J Virol, 2020. **94**(19).
125. Smith, D.J., et al., *Mapping the antigenic and genetic evolution of influenza virus.* Science, 2004. **305**(5682): p. 371-6.
126. Bedford, T., et al., *Integrating influenza antigenic dynamics with molecular evolution.* Elife, 2014. **3**: p. e01914.
127. Lee, J.M., et al., *Mapping person-to-person variation in viral mutations that escape polyclonal serum targeting influenza hemagglutinin.* Elife, 2019. **8**.
128. Voeten, J.T., et al., *Antigenic drift in the influenza A virus (H3N2) nucleoprotein and escape from recognition by cytotoxic T lymphocytes.* J Virol, 2000. **74**(15): p. 6800-7.

129. Boon, A.C., et al., *Sequence variation in a newly identified HLA-B35-restricted epitope in the influenza A virus nucleoprotein associated with escape from cytotoxic T lymphocytes.* J Virol, 2002. **76**(5): p. 2567-72.
130. Rimmelzwaan, G.F., et al., *Sequence variation in the influenza A virus nucleoprotein associated with escape from cytotoxic T lymphocytes.* Virus Res, 2004. **103**(1-2): p. 97-100.
131. Machkovech, H.M., et al., *Positive Selection in CD8+ T-Cell Epitopes of Influenza Virus Nucleoprotein Revealed by a Comparative Analysis of Human and Swine Viral Lineages.* J Virol, 2015. **89**(22): p. 11275-83.
132. Woolthuis, R.G., et al., *Long-term adaptation of the influenza A virus by escaping cytotoxic T-cell recognition.* Scientific Reports, 2016. **6**: p. 1-8.
133. Price, G.E., et al., *Viral escape by selection of cytotoxic T cell-resistant variants in influenza A virus pneumonia.* J Exp Med, 2000. **191**(11): p. 1853-67.
134. Li, Z.T., et al., *Why Are CD8 T Cell Epitopes of Human Influenza A Virus Conserved?* J Virol, 2019. **93**(6).
135. Koutsakos, M., et al., *Human CD8(+) T cell cross-reactivity across influenza A, B and C viruses.* Nat Immunol, 2019. **20**(5): p. 613-625.
136. Rimmelzwaan, G.F., et al., *Influenza virus CTL epitopes, remarkably conserved and remarkably variable.* Vaccine, 2009. **27**(45): p. 6363-6365.
137. Berkhoff, E.G., et al., *Functional constraints of influenza A virus epitopes limit escape from cytotoxic T lymphocytes.* J Virol, 2005. **79**(17): p. 11239-46.
138. Valkenburg, S.A., et al., *Acute emergence and reversion of influenza A virus quasispecies within CD8+ T cell antigenic peptides.* Nat Commun, 2013. **4**: p. 2663.
139. Heiny, A.T., et al., *Evolutionarily conserved protein sequences of influenza a viruses, avian and human, as vaccine targets.* PloS one, 2007. **2**: p. e1190.
140. Bhatt, S., E.C. Holmes, and O.G. Pybus, *The genomic rate of molecular adaptation of the human influenza A virus.* Mol Biol Evol, 2011. **28**(9): p. 2443-51.
141. Duan, S. and P.G. Thomas, *Balancing immune protection and immune pathology by CD8+ T-cell responses to influenza infection.* Frontiers in Immunology, 2016. **7**: p. 1-16.
142. DeBerge, M.P., K.H. Ely, and R.I. Enelow, *Soluble, but not transmembrane, TNF-alpha is required during influenza infection to limit the magnitude of immune responses and the extent of immunopathology.* J Immunol, 2014. **192**(12): p. 5839-51.
143. Srikiatkhachorn, A., et al., *Interference with intraepithelial TNF-alpha signaling inhibits CD8(+) T-cell-mediated lung injury in influenza infection.* Viral Immunol, 2010. **23**(6): p. 639-45.
144. Takamura, S., *Persistence in Temporary Lung Niches: A Survival Strategy of Lung-Resident Memory CD8+ T Cells.* Viral immunology, 2017. **30**: p. 438-450.
145. Erickson, J.J., et al., *Multiple Inhibitory Pathways Contribute to Lung CD8+ T Cell Impairment and Protect against Immunopathology during Acute Viral Respiratory Infection.* J Immunol, 2016. **197**(1): p. 233-43.
146. Dominguez, A., P. Godoy, and N. Torner, *The Effectiveness of Influenza Vaccination in Different Groups.* Expert Rev Vaccines, 2016. **15**(6): p. 751-64.
147. Krammer, F. and P. Palese, *Advances in the development of influenza virus vaccines.* Nat Rev Drug Discov, 2015. **14**(3): p. 167-82.
148. Shannon, I., et al., *Differences in Influenza-Specific CD4 T-Cell Mediated Immunity Following Acute Infection Versus Inactivated Vaccination in Children.* J Infect Dis, 2021. **223**(12): p. 2164-2173.
149. Bodewes, R., et al., *Vaccination against human influenza A/H3N2 virus prevents the induction of heterosubtypic immunity against lethal infection with avian influenza A/H5N1 virus.* PLoS One, 2009. **4**(5): p. e5538.

150. Bodewes, R., et al., *Vaccination with whole inactivated virus vaccine affects the induction of heterosubtypic immunity against influenza virus A/H5N1 and immunodominance of virus-specific CD8+ T-cell responses in mice.* J Gen Virol, 2010. **91**(Pt 7): p. 1743-53.
151. Lee, Y.-N.Y.-T., et al., *A Novel Vaccination Strategy Mediating the Induction of Lung-Resident Memory CD8 T Cells Confers Heterosubtypic Immunity against Future Pandemic Influenza Virus.* Journal of immunology (Baltimore, Md. : 1950), 2016. **196**: p. 2637-45.
152. Erbelding, E.J., et al., *A Universal Influenza Vaccine: The Strategic Plan for the National Institute of Allergy and Infectious Diseases.* J Infect Dis, 2018. **218**(3): p. 347-354.

Appendices

7

Nederlandse samenvatting

De griep

Jaarlijks krijgt ongeveer 5-10% van de volwassen bevolking griep. De ziekte wordt veroorzaakt door het influenzavirus en kenmerkt zich door neusverkoudheid, hoesten, koorts, hoofdpijn, spierpijn en vermoeidheid. Een influenzavirusinfectie loopt in het merendeel van de gevallen goed af. Voor sommige Nederlanders kan een infectie met het influenzavirus echter vrij gevaarlijk zijn. Dit zijn met name mensen die al andere gezondheidsklachten hebben of bij wie het immuunsysteem minder goed functioneert.

Om (kwetsbare) mensen tegen het influenzavirus te beschermen, wordt er jaarlijks een vaccinatiecampagne uitgevoerd waarbij mensen uit risicogroepen het griepvaccin kunnen krijgen. Het vaccin stimuleert het lichaam om antilichamen aan te maken tegen de uitsteeksels van het influenzavirus. Antilichamen zijn eiwitten van het immuunsysteem die bescherming moeten bieden tegen ziekteverwekkers. Zo kunnen antilichamen bijvoorbeeld aan het influenzavirus binden, waardoor het virus niet langer lichaamscellen kan binnen dringen en mensen dus ook niet ziek worden. Helaas is de werking van het influenzavaccin niet optimaal, waardoor gevaccineerde mensen soms alsnog geïnfecteerd kunnen raken met het influenzavirus. Het is daarom belangrijk dat er nieuwe, betere influenzavaccins ontwikkeld worden.

Het influenzavirus

Om te snappen waarom de huidige influenzavaccins niet optimaal werken, is het belangrijk om eerst meer te weten over het influenzavirus. Influenzavirussen kunnen onderverdeeld worden in de groepen A, B, C en D. Het meeste onderzoek richt zich echter op influenza A virus (IAV) en influenza B virus (IBV) omdat deze twee groepen virussen in de menselijke populatie circuleren en daarmee verantwoordelijk zijn voor de jaarlijkse griepgolf. Bovendien heeft IAV in het verleden al meerdere pandemieën veroorzaakt, waaronder de zeer dodelijk ‘Spaanse griep’ in 1918 die naar schatting zo’n 50 miljoen mensen het leven kostte. De Wereldgezondheidsorganisatie (WHO) ziet IAV als een mogelijke veroorzaker van een toekomstige pandemie. Dit gevaar is de reden dat veel onderzoek – inclusief dit proefschrift – zich richt op IAV.

Het influenzavirus is opgebouwd uit genetisch materiaal (RNA) dat ingepakt zit in een vetbolletje (Figuur 1). Aan de buitenkant van dit vetbolletje zitten de hemagglutinine (HA) en neuraminidase (NA) eiwitten. Deze eiwitten zijn belangrijk voor de infectie van een lichaamscel door het virus. Daarnaast worden HA en NA door onderzoekers gebruikt om verschillende subtypes van IAV te onderscheiden. Er zijn namelijk 18 verschillende HA’s (H1-H18) en 11 verschillende NA’s (N1-N11) bekend. Een IAV subtype wordt gevormd door de combinatie van HA en NA. Een influenzavirus met HA type 3 (H3) en NA type 2 (N2) wordt dus H3N2 genoemd.

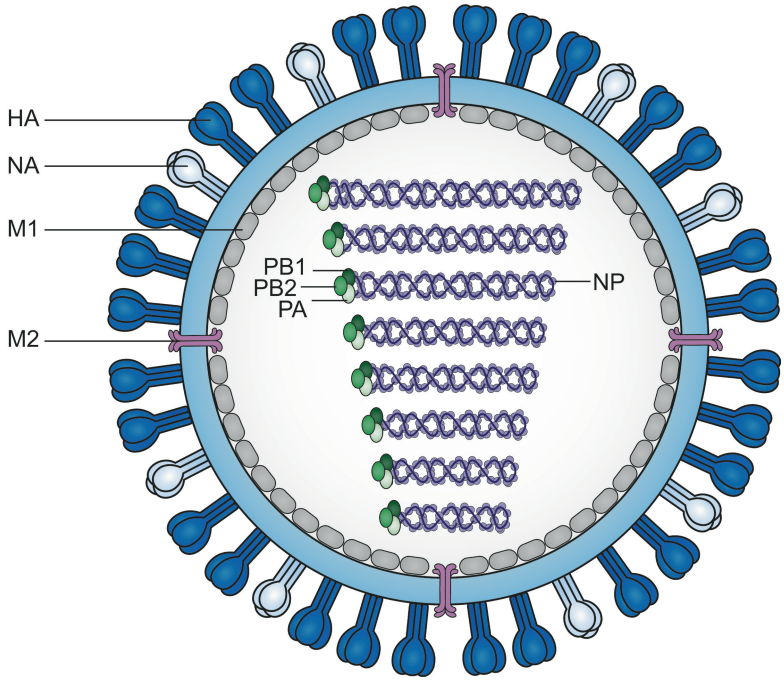

Figuur 1: Een schematische weergave van het influenzavirus. Aan de buitenkant van het virus bevinden zich de hemagglutinine (HA) en neuraminidase (NA) eiwitten. Matrix proteïne 1 (M1) vormt de binnenkant van het virus en matrix proteïne 2 (M2) is een ionkanaal dat een verbinding vormt tussen de binnen- en buitenkant van het virus. Het genetisch materiaal van het virus – RNA – is gewikkeld om nucleoproteïne (NP) en heeft een hoedje van polymerase basic proteïne 1, 2 (PB1, PB2) en polymerase acidic proteïne (PA). Deze drie eiwitten zijn verantwoordelijk voor het kopiëren van het viraal RNA als een virus eenmaal de cel heeft geïnfecteerd.

Veel subtypes komen alleen voor in dieren en slechts een beperkt aantal IAV's kan daadwerkelijk mensen infecteren. H1N1 en H3N2 virussen zijn op dit moment (samen met IBV) verantwoordelijk voor de griepgolf in de winter. H2N2 influenzavirus kan ook mensen infecteren, maar dit virus is omstreeks 1968 verdwenen uit de humane populatie, al zijn soortgelijke virussen nog wel aanwezig in dierlijke populaties. Ten slotte zijn er (sporadische) infecties met influenzavirussen die overspringen van dier op mens, ook wel zoönosen genoemd. Dit gebeurt voornamelijk met H5- en H7-gebaseerde IAV's in gebieden waar mens en dier in nauw contact komen. Deze infecties kunnen zeer dodelijk zijn, maar gelukkig is het virus moeilijk overdraagbaar van mens-op-mens. Echter, dit soort zoönotische infecties vormt een groot risico voor een nieuwe pandemie omdat er slechts enkele mutaties in het virus nodig zijn om makkelijker mensen te infecteren.

Influenzavirus vaccins

Om mensen te beschermen tegen influenzavirus infecties is er in de jaren 40 een vaccin ontwikkeld. Voor dit vaccin werd influenzavirus opgegroeid in (bevruchte) kippeneieren, waarna het virus werd gezuiverd en afgedood. Dit afgedode – en dus ongevaarlijke – virus werd via een injectie in de spieren toegediend bij personen, die vervolgens antilichamen tegen het influenzavirus ontwikkelden. Bijna 80 jaar later berust een groot deel van onze influenzavaccins nog steeds op deze techniek, al is de productiemethode wel aangepast.

Alle influenzavaccins die zijn goedgekeurd voor toediening aan mensen zijn gebaseerd op het opwekken van antilichamen tegen HA. De reden hiervoor is dat HA-bindende antilichamen vaak neutraliserende antilichamen zijn, wat inhoudt dat deze antilichamen kunnen voorkomen dat het virus lichaamscellen infecteert (Figuur 2). HA-specifieke antilichamen kunnen dus erg effectief zijn in het voorkomen van ziekte. Een limitatie van antilichamen is echter dat zij voornamelijk aan die eiwit(delen) kunnen binden die aan de buitenkant van het virus zitten. En in het geval van influenzavirussen veranderen juist de eiwitten aan de buitenkant het snelst waardoor deze ontsnappen aan de antilichaamrespons. Hierdoor zijn er een aantal problemen met de huidige griepvaccins die zich uitsluitend richten op antilichamen tegen HA. Ten eerste is de antilichaamrespons tegen HA erg specifiek, waardoor vaccinatie tegen één influenzastam minder of geen bescherming biedt tegen infecties met andere influenzastammen. Een antilichaam gericht tegen HA type 1 (H1) bindt dus hoogstwaarschijnlijk niet aan HA type 2 (H2). Daarnaast treden er vrij snel veranderingen op in HA, waardoor het virus niet meer herkend kan worden door de antilichamen en zo dus ontsnapt aan de afweer. Ten slotte leidt de focus op antilichamen ertoe dat cellulaire immuniteit – een belangrijk ander deel van ons afweersysteem – niet voldoende benut wordt. Zoals hieronder uitgelegd is juist deze cellulaire afweer een belangrijke factor in de bescherming tegen influenzavirussen.

Cellulaire immuniteit

Het immuunsysteem van de mens (en eigenlijk alle zoogdieren) bestaat uit het aangeboren en het verworven immuunsysteem. De aangeboren immuniteit is niet specifiek, maar kan wel snel reageren op infecties. Het verworven immuunsysteem start wat langzamer op, maar reageert wel erg specifiek op ziekteverwekkers en bouwt daarna ook een geheugen op waardoor het sneller kan reageren bij een volgende infectie. Het doel van vaccinatie is om het geheugen van de verworven immuniteit alvast op te bouwen voordat iemand de echte ziekteverwekker tegenkomt.

De verworven immuniteit kan verder onderverdeeld worden in een humorale en cellulaire component. De humorale immuniteit is hierboven al deels besproken en bestaat uit B-cellen die antilichamen produceren. De cellulaire immuniteit bestaat uit $CD4^+$ en $CD8^+$ T-cellen.

$CD4^+$ T-cellen worden ook wel de 'helper T-cellen' genoemd omdat ze B-cellen en $CD8^+$ T-cellen kunnen helpen bij hun reactie tegen infecties. De $CD8^+$ T-cellen zijn cytotoxische cellen en zijn verantwoordelijk voor het daadwerkelijk opruimen van de infectie. Ze doen dit door geïnfecteerde lichaamscellen te doden en signaalstoffen uit te scheiden die andere cellen van het immuunsysteem kunnen activeren. Het grote verschil tussen het humorale en cellulaire immuunsysteem is dat antilichamen (humorale immuniteit) direct ziekteverwekkers kunnen herkennen, terwijl T-cellen (cellulaire immuniteit) dit niet kunnen. T-cellen zijn afhankelijk van (geïnfecteerde) lichaamscellen die stukjes eiwit – ook wel peptiden genoemd – afkomstig van het virus op het zogenoemde 'major histocompatibility complex' (MHC) presenteren aan T-cellen (Figuur 2). Op deze manier kunnen T-cellen ook viruseiwitten herkennen die aan de binnenkant van het virus zitten. Dit is een groot voordeel in het geval van influenzavirussen omdat de eiwitten aan de binnenkant van het virus minder snel veranderen dan eiwitten aan de buitenkant.

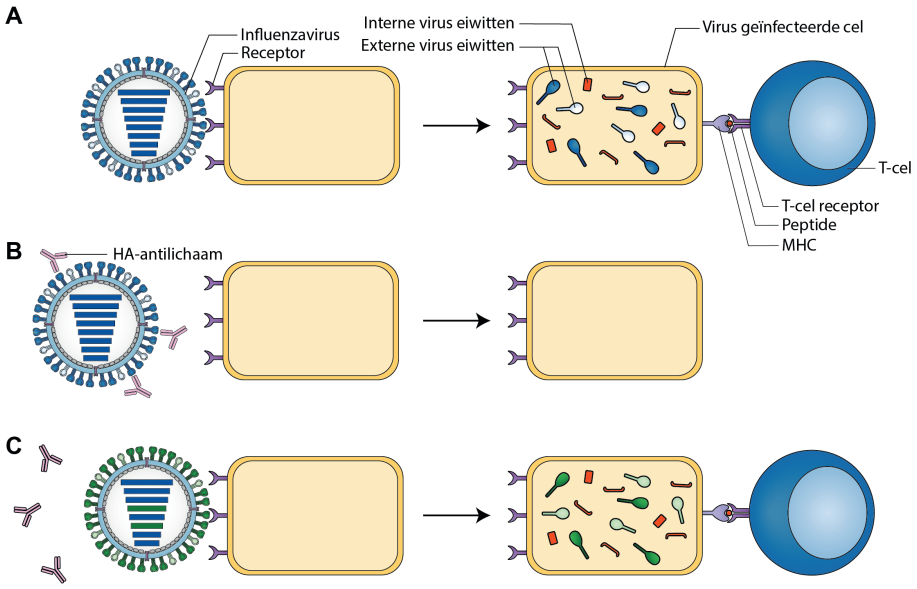

Figuur 2: Antilichaam en T-cel immuniteit tegen influenzavirus. A) In de afwezigheid van antilichamen kan een influenzavirus een cel infecteren door aan receptoren op een cel te binden. Het virus gaat dan de cel binnen en valt uiteen. Stukjes van de viruseiwitten (peptiden) kunnen dan via het MHC gepresenteerd worden aan T-cellen, die vervolgens de geïnfecteerde cel kunnen doden. **B)** Neutraliserende antilichamen tegen hemagglutinine (HA) kunnen voorkomen dat het influenzavirus een cel infecteert. **C)** De HA-antilichamen zijn echter specifiek voor een influenzavirusstam en bieden niet altijd bescherming tegen andere stammen. Hierdoor kunnen gemuteerde virussen wel de cel infecteren. T-cellen herkennen echter de stabiele interne eiwitten van influenza, dus zij kunnen nog steeds geïnfecteerde lichaamscellen doden, ook al is het virus gemuteerd.

Hierdoor kan één T-cel vaak veel verschillende influenzastammen herkennen. Echter, een gastheer moet wel eerst geïnfecteerd zijn voordat T-cellen in actie kunnen komen. Dat betekent dus ook dat T-cellen geen infectie kunnen voorkomen, maar ze kunnen wel de ernst van een ziekte beperken. In dit proefschrift onderzoeken we dan ook of het mogelijk is om doormiddel van vaccinatie een betere T-cel immuniteit op te bouwen die voorkomt dat mensen (ernstig) ziek worden door influenza. Toen in 2019 de wereld overvallen werd door het SARS-CoV-2 virus hebben we deze vraagstelling ook voor dit virus toegepast.

Dit proefschrift

De vraagstelling van dit proefschrift is of cellulaire immuniteit gericht tegen geconserveerde virusonderdelen kan bijdragen aan de bescherming tegen influenza A en SARS-CoV-2 virussen. Voor IAV kan de in dit onderzoek gegenereerde kennis bijdragen aan de ontwikkeling van toekomstige 'universele' influenzavaccins. Hiermee worden vaccins bedoeld die tegen een breed spectrum van influenzavirussen beschermen, waardoor hopelijk de effecten van een influenza pandemie minder ernstig zijn en er minder mensen overlijden aan de jaarlijkse griepgolf. Naast 'T-cel immuniteit' en 'universele vaccins', is ook het gebruikte diermodel een belangrijk onderdeel van dit proefschrift. Het immuunsysteem is erg complex en we kunnen niet zomaar mensen infecteren met influenza om onderzoek te doen. Daarom maken we voor dit onderzoek gebruik van het fretten model. In 1933 werden fretten voor het eerst door onderzoekers geïnfecteerd met influenzavirus, waarna het model door de jaren heen is uitgegroeid tot een van de betere modeldieren voor influenzaonderzoek. De voordelen van het frettenmodel is dat de dieren makkelijk te infecteren zijn met verschillende influenzavirussen en daarbij dezelfde symptomen als mensen (zoals niezen, koorts, etc.) vertonen. Daarnaast zijn volwassen fretten relatief klein (tussen de 500 en 1800 gram), waardoor ze makkelijker te huisvesten zijn dan bijvoorbeeld varkens (een ander model voor influenza). Echter is het frettenmodel niet zo ver ontwikkeld als het in de onderzoekswereld veel gebruikte muizenmodel, waardoor de technische en laboratorium mogelijkheden van het frettenmodel met name voor immunologisch onderzoek nog in de kinderschoenen stond bij aanvang van het proefschrift. We hebben daarom veel moeite gestoken in het verder ontwikkelen van het fretten model.

In **hoofdstuk 2** laten we zien hoe en met welk virus we een fret moeten infecteren om het ziektebeeld van H2N2 influenza in de mens na te kunnen bootsen. H2N2 influenza was de oorzaak van de Aziatische influenza pandemie in 1957, maar komt sinds 1968 niet meer bij mensen voor. Verwante H2 virussen zijn echter nog steeds aanwezig bij vogels, dus het risico bestaat dat er opnieuw een H2N2 virus overspringt op mensen waardoor er een nieuwe pandemie ontstaat. Om hierop voorbereid te zijn, hebben we een frettenmodel opgezet voor infecties met H2N2 influenzavirus zodat er snel vaccins ontwikkeld en getest kunnen worden. Hierbij gebruikten we

vier verschillende H2N2 virusstammen en twee verschillende toedieningsroutes: via de neus of via de luchtpijp. Het idee hierachter is dat toediening via de luchtpijp leidt tot een lagere luchtweginfectie en die zijn over het algemeen ernstiger dan een hogere luchtweginfectie (bereikt door toediening via de neus). We zagen dat H2N2 virus-geïnfecteerde fretten vergelijkbare symptomen vertoonde als influenza-geïnfecteerde mensen en dat een lagere luchtweginfectie een iets erger ziektebeeld leek te geven. Verder vonden we een link tussen de replicatie van het virus (in de hogere en lagere luchtwegen) en de bindingsvoorkeur van het virus voor bepaalde suikerketens op lichaamscellen. Hiermee bevestigen we eerdere waarnemingen en laten we zien dat we bij infecties met het influenzavirus rekening moeten houden met de bindingsvoorkeuren van het virus. Dit kan namelijk invloed hebben op hoe ziekmakend een virus is.

Nadat we het frettenmodel voor H2N2 infecties hadden opgezet, zijn we de cellulaire immuniteit tegen IAV's gaan bestuderen. Voor de ontwikkeling van nieuwe universele T-cel vaccins kan het helpen om eerst te begrijpen wat voor T-cel immuniteit een infectie met het influenzavirus opwekt; dit kan dan dienen als uitgangspunt voor toekomstige vaccins. In **hoofdstuk 3** hebben we daarom een groep fretten eerst geïnfecteerd met het H1N1 influenzavirus. Vervolgens hebben we deze groep – en een groep die niet eerder geïnfecteerd was geweest – geïnfecteerd met het H2N2 influenzavirus.

Het idee hierachter is dat de HA en NA oppervlakte eiwitten van H1N1 en H2N2 virussen zo anders zijn, dat neutraliserende antilichamen geen bescherming bieden. T-cellen daarentegen zouden wél bescherming kunnen bieden omdat T-cellen de interne influenza-eiwitten herkennen die grotendeels overeenkomen tussen H1N1 en H2N2 virussen. Dat was ook wat we zagen, want H1N1 virus-geïnfecteerde fretten werden minder ziek na een H2N2 virusinfectie dan fretten die nog nooit eerder met influenzavirus besmet waren. Verder hebben we laten zien dat infectie met een H1N1 virus cellulaire immuniteit opwekte die ook een H2N2 virus herkende. Deze resultaten impliceren dat 1) infectie met influenzavirus T-cel immuniteit opwekt die een grote variatie aan influenzavirussen kan herkennen en 2) dat deze T-cel immuniteit bescherming kan bieden tegen (ernstige) ziekte.

In **hoofdstuk 4** onderzochten we of beschermende T-cel immuniteit ook opgewekt en versterkt kan worden doormiddel van vaccinatie. Hiervoor gebruikten we een nieuw mRNA prototype vaccin dat T-cel immuniteit tegen een drie interne influenza-eiwitten zou moeten opwekken. We hebben dit vaccin getest in fretten die al eerder een H1N1 influenza-infectie hebben doorgemaakt en in fretten die nog niet eerder geïnfecteerd waren. We kozen voor deze aanpak met het idee dat fretten die eerder geïnfecteerd waren met H1N1 influenza het meest zouden lijken op jongvolwassen personen, want die zijn ook al eerder geïnfecteerd geweest. De groep fretten die geen H1N1

virusinfectie kreeg diende als model voor heel jonge kinderen, die vaak nog niet eerder besmet zijn geweest met influenzavirus. In H1N1-geïnfecteerde fretten versterkte vaccinatie met het mRNA vaccin de T-cel respons. Dit gebeurde zelfs in de hogere en lagere luchtwegen, ondanks dat het vaccin in de achterbenen werd toegediend. Voor veel vaccins is het juist erg lastig om immuniteit in de luchtwegen op te wekken omdat normaal gesproken het vaccin daarvoor ook in de luchtwegen toegediend zou moeten worden. In niet eerder geïnfecteerde fretten induceerde het vaccin sterke responsen tegen één van de drie influenza-eiwitten en wat lagere responsen tegen de overige twee influenza-eiwitten. We zagen dat ook in deze gevaccineerde fretten T-cellen in de luchtwegen opgewekt werden. Vaccinatie met het mRNA vaccin beschermde fretten ook tegen ernstige ziekte met een zoönotische H7N9 influenza-infectie, maar alleen als fretten eerder geïnfecteerd waren geweest met H1N1 influenza. Fretten die wel eerder geïnfecteerd waren, maar geen vaccin toegediend kregen waren niet beschermd. Dit onderzoek geeft aan dat nieuwe influenzavaccins T-cel immuniteit kunnen opwekken en dat deze bescherming tegen ernstige ziekte bieden na een zoönotische infectie met het influenzavirus. Dit is belangrijk in de context van een mogelijke, nieuwe influenzaviruspandemie.

In **hoofdstuk 5** gebruiken we onze opgedane ervaring om onderzoek te doen naar SARS-CoV-2, een coronavirus dat eind 2019 opdook en in 2020 werd uitgeroepen tot pandemie. Voor het begrijpen van de ziekte en ontwikkelen van vaccins was het belangrijk dat er zo snel mogelijk diermodellen beschikbaar zouden komen om onderzoek te doen naar SARS-CoV-2 (het virus) en COVID-19 (de ziekte). Net als influenza is SARS-CoV-2 een virus dat de luchtwegen infecteert. Omdat fretten ook geïnfecteerd kunnen worden met sommige andere coronavirussen, was de vraag of de fret mogelijk een goed model zou zijn voor SARS-CoV-2 infectie en ziekte. Op het moment dat wij het onderzoek begonnen was al bekend dat jonge fretten via de neus geïnfecteerd konden worden met SARS-CoV-2, maar geen ernstige COVID-19 veroorzaakte. Wij bouwden daarop voort door te kijken of toediening via de luchtpijp om een lage luchtweginfectie te veroorzaken een ernstiger ziektebeeld zou geven. Daarnaast waren we benieuwd of de ziekte erger zou zijn in oudere fretten, aangezien de ziekte in mensen vooral ernstig is onder oudere mannen. Fretten die geïnfecteerd waren met SARS-CoV-2 lieten geen symptomen van infectie zien en ontwikkelden geen koorts. De luchtwegen (long, luchtpijp en neusschelpen) vertoonden wel een milde schade aan het weefsel. Deze schade was voor de lagere luchtweg geïnfecteerde groep onverwacht hoger in jonge fretten in vergelijking met oudere fretten, maar leek niet op het ernstige beeld zoals we dat in de mens zien. Verder was de virusreplicatie duidelijk lager in fretten die via de luchtpijp geïnfecteerd waren. Tenslotte konden we duidelijke cellulaire en humorale immuunresponsen meten in fretten 14 of 21 dagen na infectie. Bovendien leek de hoogte van de immuunrespons te correleren met de virusreplicatie, want fretten met een hoge hoeveelheid virus vertoonden ook sterkere immuunresponsen. Uiteindelijk bleek dat ook toediening via de luchtpijp in oudere

fretten niet resulteerde in een goed model om ernstige COVID-19 infectie in mensen na te bootsen, maar het frettenmodel kan wel gebruikt worden om onderzoek te doen naar SARS-CoV-2 virusreplicatie en immuniteit.

Publications in this thesis

K. van de Ven, H. van Dijken, W. Du, F. de Heij, J. Mouthaan, S. Spijkers, S. van den Brink, P. Roholl, C.A.M. de Haan, J. de Jonge (2022). "Varying viral replication and disease profiles of H2N2 influenza in ferrets is associated with virus isolate and inoculation route".
Manuscript accepted at Journal of Virology

K. van de Ven, F. de Heij, H. van Dijken, J.A. Ferreira, J. de Jonge (2020). "Systemic and respiratory T-cells induced by seasonal H1N1 influenza protect against pandemic H2N2 in ferrets".
*Communication Biology; 3(1). doi:*10.1038/s42003-020-01278-5

K. van de Ven, J. Lanfermeijer, H. van Dijken, H. Muramatsu, C. Vilas Boas de Melo, S. Lenz, F. Peters, M.B. Beattie, P.J.C. Lin, J.A. Ferreira, J. van den Brand, D. van Baarle, N. Pardi, J. de Jonge. "A universal influenza mRNA vaccine candidate boosts T-cell responses and reduces zoonotic influenza virus disease in ferrets".
Manuscript submitted

K. van de Ven, H. van Dijken, L. Wijsman, A. Gomersbach, T. Schouten, J. Kool, S. Lenz, P. Roholl, A. Meijer, P. B. van Kasteren, J. de Jonge (2021). "Pathology and Immunity After SARS-CoV-2 Infection in Male Ferrets Is Affected by Age and Inoculation Route".
*Frontiers in Immunology; 12. doi:*10.3389/fimmu.2021.750229

Other publications

K. van de Ven, J. Lanfermeijer, M. Hendriks, H. van Dijken, S. Lenz, M. Vos, J.A.M. Borghans, D. van Baarle, J. de Jonge. "The memory CD8+ T-cell response in mice is not influenced by time since previous infection".
Manuscript submitted

J. Lanfermeijer, **K. van de Ven**, H. van Dijken, M. Hendriks, C.M.P. Talavera Ormeño, F. de Heij, P. Roholl, J.A.M. Borghans, D. van Baarle, J. de Jonge. "Modified influenza M158-66 peptide vaccination induces non-relevant T-cells and may enhance pathology after challenge".
Manuscript submitted

C. Vilas Boas de Melo, F. Peters, H. van Dijken, S. Lenz, **K. van de Ven**, L. Wijsman, A. Gommersbach, T. Schouten, P.B. van Kasteren, J. van den Brand, J. de Jonge. "Influenza infection in ferrets with SARS-CoV-2 infection history".
*Preprint at bioRxiv 2022.03.22.485425; doi:*10.1101/2022.03.22.485425

K. van de Ven and J. Borst (2015). "Targeting the T-cell co-stimulatory CD27/CD70 pathway in cancer immunotherapy: rationale and potential".
Immunotherapy 7:6, 655-667

M. Lezzerini, **K. van de Ven**, M. Veerman, S. Brul, Y.V. Budovskaya (2015). Specific RNA Interference in Caenorhabditis elegans by Ingested dsRNA Expressed in Bacillus subtilis.
*PLOS ONE 10(4): e0124508. doi:*10.1371/journal.pone.0124508

Dankwoord

Toen ik op 16 januari 2017 begon bij het RIVM was dit boekje nog erg ver weg. Met hulp van veel verschillende mensen in allerlei verschillende vormen, is er na ruim vijf jaar dan toch een boekje verschenen. Hier wil ik graag alle mensen bedanken die mij de afgelopen jaren hebben gesteund, kansen hebben geboden en het leven in z'n algemeen leuker hebben gemaakt.

Jørgen, ik ben altijd blij geweest dat ik bij jou als PhD student heb mogen beginnen. Los van het leuke project was je gewoon een enorm goede begeleider. Waar je mij in het begin nog (figuurlijk) bij de hand nam, gaf je me al snel verantwoordelijkheid en vertrouwen op het moment dat ik dat aankon. Met je passie voor wetenschap heb je mij niet zelden aangespoord om toch nog een experiment, groep of conditie toe te voegen aan studies. Soms overbodig, maar ook vaak met hele mooie resultaten. Misschien nog wel het belangrijkste: je gaf me de inspiratie en motivatie om nieuwe dingen op te pakken waardoor ik ook paden buiten de wetenschap heb kunnen bewandelen. Heel veel dank voor deze kans om te leren, de humor en alle steun en feedback die ik van je heb mogen ontvangen de afgelopen jaren.

Debbie, het was even schrikken toen ik bij een dansworkshop opeens met mijn promotor stond te dansen, maar ook erg leuk. Naast de gezellige momenten, zoals de afdelings-BBQ in de achtertuin, heb ik de afgelopen jaren ook veel van je kunnen leren. Je zocht altijd naar de spannendste en strakste insteek van een paper, wat zeker hielp op de momenten dat ik als AIO door de bomen (of negatieve data) het bos niet meer zag. Ik waardeer ook je aansporing om nieuwe dingen te ondernemen, projecten op te zetten en congressen te bezoeken. Heel veel dank voor het benadrukken van de wetenschap binnen een overheidsorganisatie, het eindeloze feedback geven en het meedenken voor projecten en publicaties.

Ik wil ook graag **prof. dr. L. Koenderman, prof. dr. F.J.M. Van Kuppeveld, prof. dr. J.A.M. Borghans, prof. dr. A.L.W. Huckriede** en **dr. S. Herfst** van de leescommissie bedank voor het lezen van mijn proefschrift. Daarnaast ben ik de leden van de AIO-commissie **dr. J. de Wit, dr. W. Luytjes** en **prof. dr. A.L.W. Huckriede** dankbaar voor de jaarlijkse discussie en feedback op mijn promotietraject.

Mijn allerliefste paranimfen, wat ben ik gelukkig dat jullie met mij deze gebeurtenis willen vieren. **Joos,** van het begin tot het eind heb ik mijn promotietraject samen met jou mogen doen. In die tijd hebben we gelachen, gevloekt, geploeterd en gek gedaan. Het was enorm fijn dat ik met jou tegenslagen en twijfels kon bespreken. Ik ben je dankbaar voor ontelbaar veel dingen, dus ik zal er hier maar een select aantal noemen: het managen van m'n interpersoonlijke relaties, het doorsturen van beursaanvragen en congressen, het organiseren van wetenschappelijke bijeenkomsten (T-cel AIO

meeting) en tenslotte het een stukje gezelliger maken van iedere werkdag. Ik wil je nog wel meegeven dat naar mijn inzicht de beste pannenkoek een dikke pannenkoek is. **Fleur**, mijn liefste kleine zusje. Jij kent me al je hele leven, de goede en de slechte kanten. Ik geniet van je humor en de random dingen die we soms doen, zoals tequila shotjes in de Feestfabriek. Maar ik kijk ook met heel veel bewondering naar je. In je ééntje ben je de communicatieafdeling van een heel bedrijf, dus over je competenties bestaat geen twijfel. Dat maakt ook dat ik mij met een gerust hart kan bezighouden met de inhoud van dit boekje in de wetenschap dat jij en Joos de rest regelen. Ik ben blij dat je het aandurfde om op deze dag naast mij te staan.

Ik kijk met veel plezier terug op mijn tijd bij het RIVM, wat voor een groot deel komt door de volgende mensen. Allereerst alle mensen van het influenza-team. **Harry**, wat zou ik (en de afdeling) toch zonder jou moeten? Je staat altijd klaar voor andere mensen en door jouw betrokkenheid voelde ik me direct op de eerste dag welkom. In de afgelopen vijf jaar kon ik altijd op jou rekenen en als ik soms in de stress zat omdat ik vergeten was iets cruciaals te bestellen voor een groot experiment, dan bleek jij dat allang gedaan te hebben. Dit boekje was er zonder jou niet geweest! **Marion**, schatje en paranimf-buddy voor Joos. Naast het feit dat je een ster bent op het lab, ben je ook gewoon een enorm gezellig persoon. Wat heb ik met jou lekker kunnen lachen bij het maken van filmpjes. Bedankt voor het zijn van mijn steun en toeverlaat, het fungeren als interpersoonlijke-relatie problemen-radar en je geweldige droge humor. **Femke**, wat een leuke verassing toen bleek dat jij in hetzelfde team werkte als waar ik ging solliciteren. We hebben samen mooie studies uitgevoerd en ik kon er altijd op vertrouwen dat je experimenten nauwkeurig uitvoerde. Dat gaf mij enorm veel rust, zeker bij hectische sectiedagen. **Stef,** wat ben ik ongelofelijk blij dat jij er was om te helpen bij de laatste grote studies. Naast de extra gezelligheid was het ook enorm prettig dat jij als een (Duitse) machine samples op een recordtempo verwerkte. Anders hadden die sectiedagen nog een aanzienlijk uurtjes langer geduurd. **Floor**, ook jij was een welkome hulp bij de laatste dierproeven. Daarnaast heb ik het antilichaamproject met vol vertrouwen aan jou kunnen overdragen. **Caro**, I will write the rest in Dutch because it is useful to learn the language. Ik vind het erg leuk dat je mijn project hebt overgenomen en meteen met nieuwe ideeën bent gekomen. Ik bewonder je enthousiasme en dank voor alle nieuwe inzichten die je mij hebt gegeven in de korte periode dat we samen proeven hebben gedaan.

Natuurlijk ben ik ook mijn (oud-)kamergenoten erg dankbaar voor alles wat ze betekend hebben de afgelopen vijf jaar. **Marieke**, voor mij zul je altijd de oma van V0.58 blijven. Dank voor de onderbrekingen als ik druk bezig was en bij jou het schrijven niet lukte, het gekloot op de vrijdagmiddagen en het goede voorbeeld. Helaas heb ik wat meer tijd nodig gehad om mijn proefschrift af te ronden. **Iris**, jij was altijd de liefste van de kamer en vormde daarmee een goede balans met Marieke. Ik ben je ook erg dankbaar voor je steun in het niet mega sportief zijn zoals onze

andere roomies. **Eric,** kerel, ik ben blij dat ik na ruim vijf jaar toch eindelijk Debbie heb kunnen ontmoeten. Ik ben je ook erg dankbaar voor de gezelligheid en voor het feit dat je toch een beetje de chauffeur van V0.58 was. Laten we binnenkort eindelijk eens dat biertje in Amsterdam doen. **Joos,** het was een verademing toen Marieke weg ging en jij haar plek kon overnemen zodat je niet enkel je stoel hoefde om te draaien om mij lastig te vallen. Ik heb je wel als paranimf gekozen, dus dat geeft aan dat het (soms) ook wel gewaardeerd werd. **Alp,** you are the coolest science dude I have ever met and a true FlowJo wizard. Although it always made me a bit sad because I could not measure them in ferrets, I really enjoyed your enthusiasm about T-cell subsets and science in general. **Samantha**, you brought the most random, but really tasty snacks. And in contrast to Joos, you were actually willing to share them. I enjoyed your company and stories, especially about the banana dude.

Ik ben ook alle andere (oud-)PhD studenten dankbaar voor de gezelligheid en het voorbeeld dat ze zijn geweest (zowel goed als slecht). **Elise**, dank voor alle gezelligheid die je georganiseerd hebt. Helaas hebben we nooit meer een vervanger voor je gevonden. **Liz,** jouw proefschrift is een grote bron van ideeën en inspiratie geweest voor mijn eigen proefschrift. **Leon,** dank voor het introduceren van R software. Mede daardoor heb ik nu een baan als data scientist. **Daan,** jammer dat je niet mee kon doen met het grote muizenexperiment, maar dank voor alle input en gezelligheid. **Sara,** ik heb heel veel profijt gehad van alle wetenschappelijke en leuke dingen die jij (vaak samen met Joos) bij IIV opgezet of veranderd hebt. **Nora,** we zijn ongeveer tegelijk begonnen, maar jij hebt een dappere keus gemaakt waardoor je toch wat eerder weg was dan ik. Bedankt voor de gezelligheid! **Hella,** je was een eindeloze bron van verhalen over positieve energie en tampons. Dank voor de info en alle gezelligheid. **Milou,** jij bent altijd voor alles in. Dank voor alle gekkigheid zoals de Duracell filmpjes (voor Hella). Hopelijk heb je ooit nog al die vakantiedagen van je PhD kunnen opnemen. **Esther, Michiel** en **Anke,** dank voor het oppakken van ons corona project. Helaas is het op niks uitgelopen, maar ik vond het erg leuk om samen met jullie te sparren. **David,** bedankt voor de verhalen over je date-leven. Aan **alle AIOs**, dank voor alle gezellige dingen die we samen hebben gedaan! De sportdag, brewery run, 'pub'-quizen, VrijMiBo's en kerstborrels zijn toch wel een van de hoogtepuntjes van mijn tijd bij het RIVM geweest.

Natascha, in de corona periode begon jij als masterstudent bij ons op het lab. In die tijd was ik onverwachts ook erg druk met corona experimenten, dus ik waardeer het enorm dat jij met veel motivatie het project zelfstandig tot een mooi einde hebt gebracht.

Er zijn ook een hoop research technicians die direct of indirect hebben bijgedragen aan dit boekje. Iedere promovendus bij het RIVM weet dat hij of zij nergens is zonder de steun van deze mensen. **Jolanda,** ook met jou heb ik enorm kunnen lachen. Ik

ben je ook dankbaar dat je alle uBiome samples hebt voorbereid, anders waren die drukke experimentdagen nog wat extra stressvol geweest. **Hendrik-Jan**, dank dat ik met al mijn vragen over bacteriën en kloneren bij jou terecht kon. **Peter,** zonder jou geen bestellingen, zonder bestelling geen experiment en zonder experiment geen boekje. **Ronald**, fijn dat je altijd insprong bij sectiedagen en dat je onze redder in nood was bij FACS drama's. **Maarten,** ik heb dankbaar gebruik gemaakt van je BOF stock. Jouw aanwezigheid samen met **Martien** maakte V1.24 ook het beste en meeste gezellig lab van het RIVM. **Martien**, ook bedankt voor al je hulp met het opwerken en categoriseren van de MB-donoren. **Martijn**, het was echt enorm relaxed dat jij alle UMAPs hebt uitgewerkt. **Noortje** en **Jeroen**, jullie zijn op cruciale momenten bijgesprongen op het lab. Enorm veel dank ervoor, want dat scheelde mij heel wat stress en late uurtjes.

Ook aan de andere kant van gebouw V zitten een hoop mensen die mij de afgelopen jaren geholpen hebben. **Puck**, je was mijn redder in nood als het aankwam op kloneren of RT-qPCR. Je feedback was ook altijd zeer nuttig en dus ook zeer welkom. Jouw bijdrage heeft het SARS-CoV-2 paper naar een hoger niveau getild. **Susana,** ik kijk uit naar alle fretten-uBiome publicaties die nog gaan komen. Ook dank voor je blik op mannen: liever een met een buikje, want die zijn tenminste gezellig. **Teun,** dank voor je feedback op mijn manuscripten, de wetenschappelijke discussies waar je deur altijd voor openstond en de wekelijkse voetbalsessie in de Galgenwaard. **Gerco,** het was erg fijn dat jij met ons wilde nadenken over het gebruik van in vitro respiratoire celkweken om de vragen uit het frettenmodel te beantwoorden. **Rob Mariman**, dank voor je analyse van het frettengenoom. Jammer dat ik niet meer de tijd had om daar daadwerkelijk wat mee te doen. **Willem,** je bent een echte virus-encyclopedie en ik heb erg veel profijt gehad van jouw input bij mijn jaarlijkse promotietraject voortgangsgesprek. Dat geldt ook voor **Jelle,** sterspeler bij de Galgenwaard en een aanwinst voor mijn AIO-commissie. Ik ben ook **Josine** en **Cécile** dankbaar voor discussies omtrent influenza en T-cellen en alle input die jullie hebben geleverd op de publicaties van dit proefschrift. **Patricia,** het was altijd gezellig om even je kantoor binnen te kunnen lopen voor een praatje (en klaagzang over publiceren). **Elena,** dank voor het wijzen op het belang van innate immunity in een afdeling voor T-cel fanaten.

Tenslotte wil ik ook alle niet-wetenschappelijke medewerkers bedanken. Zonder **Karin, Marjolieke** en **Jessica,** van het secretariaat waren er geen afdelingsuitjes of congressen. Dank dat ik altijd bij jullie mocht binnenlopen voor een lach of een vraag. **Diana**, het was enorm fijn dat jij als centrumhoofd een luisterend oor bood voor de zorgen van promovendi en dat je actief het wetenschappelijke aspect van de afdeling naar een hoger punt probeert te brengen.

Verder wil ik alle collega's van het **ARC** enorm bedanken voor hun inzet gedurende de afgelopen vijf jaar. Jullie zorgen altijd (ook in de weekenden) netjes en met passie

voor de fretten en muizen van onze experimenten. Zonder jullie was dit proefschrift er nooit geweest. In het bijzonder wil ik ook **Tanja** en **Angéla** (of Angéla en Tanja) bedanken. Dames, dit boekje ligt hier voor een groot deel door jullie harde werken en inhoudelijk kennis. Maar waar ik jullie het meest dankbaar voor ben is het warme welkom dat ik altijd ontving in D7. Tussen het werken (en peukje) door lekker grappen en plagen. Dat mis ik toch wel nu ik weg ben bij het RIVM.

I am also grateful to all the co-authors that contributed to the manuscripts presented in this thesis. Most co-authors have already been mentioned above, but I would additionally like to thank **José Ferreira, Paul Roholl, Sharon van den Brink, Lisa Wijsman, Adam Meijer, Justin Mouthaan, Sanne Spijkers, Wenjuan Du, Xander de Haan, Hiromi Muramatsu, Mitchell Beattie, Paulo Lin, Judith van den Brand** and **Norbert Pardi**. De statistische analyse van deze publicaties had er heel anders uit gezien zonder **José Ferreira**. Het was erg prettig dat jij altijd de tijd nam om mij uit te leggen waarom bepaalde analyses wel of niet geoorloofd waren. **Paul Roholl**, pathologie is niet mijn expertise, dus ik ben je erg dankbaar dat jij dit voor veel van onze experimenten hebt uitgezocht. **Lisa Wijsman, Sharon van den Brink** en **Adam Meijer**, enorm veel dank voor de hoeveelheid werk die jullie verzet hebben. De meer dan 1000 samples die jullie voor ons hebben verwerkt waren een essentieel onderdeel van zeker twee publicaties. **Xander de Haan** and **Wenjuan Du**, many thanks for the collaboration. With your help we managed to publish a more exiting H2N2 influenza paper. **Judith,** ook jij bedankt voor de pathologie analyse. De verschillen tussen groepen waren helaas minder klein dan gehoopt, maar het is alsnog een mooie toevoeging aan het paper geworden. **Norbert Pardi**, many thanks for providing the opportunity to test an exciting new influenza vaccine. I really enjoyed our collaboration and learned a lot from your feedback and input.

Dan zijn er ook nog een aantal mensen van buiten het RIVM die ik graag wil bedanken. **José Borghans**, dank voor de leuke discussies en de uitgebreide en goede feedback op de muizenpapers. Ondanks dat ik blij ben met het resultaat, staan die papers bewust niet in dit boekje omdat je anders geen deel kon uitmaken van de (lees) commissie. Ik ben ook **Jolanda van Leeuwen, Irma Rensink en Marieke van Ham** dankbaar voor het aanwakkeren van een passie voor immunologie lang voordat dit PhD-traject bij het RIVM begon. Other people that have played an important part in my scientific education are **Yelena Budovskaya, Martin de Rooij, Marcel Spaargaren, Benedict Chambers** and **Annika Wagner**. I am grateful to you for your supervision and (scientific) passion during my internships. Without you, I might have never started this PhD. Verder ben ik **Jannie Borst** dankbaar voor de kans die zij mij heeft gegeven. Zonder haar was mijn masterthesis nooit gepubliceerd in 'Immunotherapy'. Ten slotte wil ik ook **Bertus Tulleners** en **Joris Buis** bedanken. Met de Tesla minor hebben jullie mij de kans geboden om me verder te ontwikkelen dan enkel als wetenschapper.

Daar heb ik nu nog iedere dag profijt ben, naast het feit dat de Tesla minor zelf ook een enorm leuke periode was.

Het is misschien gek, maar het is tenslotte mijn dankwoord, dus ik wil ook de software benoemen die belangrijk was tijdens mijn PhD. **Flowjo** was zowel de meest essentiële als meest gehate software die draaide op het RIVM. Dank dat je – naast het weer – altijd een onderwerp was waar iedereen over kon klagen. **ImmunoSpot** was een verademing na jaren van ELISpot plaatjes uitponsen en handmatig spots verwijderen. Dank dat je bestond en het werk een stuk aangenamer maakte. **Rstudio** en **R software** zijn ook essentieel (en gratis) geweest voor dit boekje. Vrijwel alle data en figuren zijn met behulp van deze software opgesteld.

Dit vormt ook een mooi brugje naar mij nieuwe collega's (deze is voor jou Ronald), want data analyse met R beviel me zo goed dat ik daar in door wilde gaan. Gelukkig hebben mijn lieve collega's bij **DICA** mij die kans gegeven. In het bijzonder wil ik **Ronald, Steven, Ryanne, Sanne, Mirthe, Mirna, Varisha, Martijn, Berend en Yvon** van de afdeling Informatie bedanken: wat fijn dat ik samen met jullie mag werken en programmeren.

Dan alle vrienden die de soms zware tijd van een PhD toch wat dragelijker maken. Om maar te beginnen bij de **Nerdjes & Claudia**, die als sinds de middelbare school vragen wanneer ik nou eindelijk eens klaar ben met studeren. Ik durf te stellen dat ik met het inleveren van dit boekje – ongeveer 19 jaar na onze eerste kennismaking – eindelijk klaar ben met studeren. **Tjeu,** kerel, vreemd genoeg had je blijkbaar niet verwacht hier genoemd te worden, ondanks dat we elkaar al kennen sinds de basisschool. Maar je hoeft niet aan een proefschrift mee te schrijven om een vermelding in het dankwoord te krijgen. Ik ben je dankbaar voor het lachen, het gamen en vooral het ondernemen van dingen. Je voorstellen zijn soms goed (Rammstein, obstakel run), maar vaak slecht voorbereid (Pack & Track Biesbosch) of ronduit vermoeiend (boerenvoetgolf). Desondanks levert het altijd prachtige verhalen en herinneringen op. **Tom** (de baard van Neusbaard) **& Claudia** (de chillibioloog), dank voor alle lekkere en leuke bieren (ook lof aan JW), het fantastische eten dat bij jullie van de BBQ komt en alle vette feesten die jullie organiseren. **Jordy & Joyce,** helaas zien we elkaar minder nu we verder uit elkaar wonen. Maar als we dan een weekend weg gaan is het toch weer prachtig met mooie herinneringen en een rookworst. Ik hoop snel weer eens in het mooie Breda langs te komen. Allemaal, bedankt voor het slap lullen en alle leuke weekendjes!

Tess, Excel-maatje, ondertussen hebben we al heel wat restaurants in Amsterdam kunnen proberen. Binnenkort kunnen we ons zoekgebied uitbreiden naar Den Haag. Dank voor alle leuke etentjes, de live podcast van 'Tess haar Tinder dates' en het bieden van een luisterend oor. **Dieuwertje**, R-buddy, ondanks dat je het merendeel

van het jaar in Georgië woont lukt het gelukkig nog om elkaar een paar keer per jaar te zien. Deze culturele uitwisseling heeft echter ook zijn voordelen, want anders had ik nooit van het bestaan van 'shemomedjamo' geweten. Hopelijk kunnen we nog regelmatig samen zwemmen, eten en lachen.

Eske, **Isa** en **Emma**, mijn biomedisch maatjes waarmee we veel dronken themafeestjes bedacht en uitgevoerd hebben. Dank voor alle foto's en gekkigheid. **Eske**, je persoonlijke urbandictionary vermelding is nog steeds up-to-date en je bent als wandelende encyclopedie ook handig om bij je te hebben. Maar vooral ben je erg gezellig om mee te zijn. **Isa**, met wie ik mijn eerste (en laatste) vijf sigaretten heb gerookt. Negatief verwoord haal je blijkbaar het slechtste in mij naar boven; positief verwoord laat je mij nieuwe dingen uitproberen. Het is altijd lachen met je en ik ben dankbaar dat je moeite doet om contact te houden. **Emma,** ik denk dat iedere middelbare scholier blij mag zijn met een docent die zo veel passie heeft voor biologie. Dank voor alle etentjes, steun en toeverlaat tijdens onze studie biomedisch.

Ik ben ook **Claire, Sjoerd, Josie, Ruben** en **Kris** van het stabiel presterende pub-quizteam **Boudoir en de Blote Banjo's** zeer dankbaar. Ik hoop dat met het toenemen van het aantal PhD's in het team ook de resultaten gaan stijgen. **Sjoerd**, Mr. Phillips, ik heb er vertrouwen in dat we samen de macht kunnen grijpen in Kings Dilemma. **Josie,** met jouw filmkennis halen we tenminste nog wat puntjes bij de pub-quiz. Je enthousiasme en baldadigheid (provincie spel?) maken iedere avond geslaagd, zolang je Claire maar buiten je snode plannen laat. **Ruben**, uit onderzoek is gebleken dat zonder jou een 2^{e} plek niet haalbaar is. Je bent ook een onuitputtelijke bron van verhalen en nadat we Kings Dilemma hebben uitgespeeld kunnen we misschien verder met Ruben's Dilemma's. **Kris**, jouw tijd gaat nog komen. Ik weet zeker dat ergens in deze wijde wereld een pub-quiz muziekronde met accordeonmuziek bestaat. Dat is het moment dat we onze 2^{e} plek kunnen prolongeren. Boudoir en de Blote Banjo's, dank voor alle (slechte) humor, de excessieve hoeveelheden drank en de nog excessievere drankrekening.

Roos, Lindsey, Marjo, Janneke, Eske en **Josie,** de hindes, samen met Claire zijn jullie de gezelligste vriendinnengroep die ik ken. Dank voor de gezelligheid die jullie brengen; jullie zijn altijd welkom in ons huisje. **Tandarts Roos,** je bent m'n favoriete tandarts, maar daarbuiten ben ik je ook dankbaar dat Claire en ik met een gerust hart op vakantie kunnen gaan omdat ik weet dat jij die twee monsters (Momo & Jiji) verzorgt. **Eske** en **Lindsey**, het maakt mij niet zoveel uit wie de credits krijgt voor het koppelen van mij en Claire. Ik ben jullie er beiden dankbaar voor. **Leo & David,** eten of borrelen, het is altijd gezellig als we samen iets ondernemen. Hopelijk kunnen we Claire ooit nog zo ver krijgen om ook naar Zeist te verhuizen. **Megan & Dion**, dank dat we altijd welkom zijn in jullie prachtige tuintje, of het nu in IJsselstein, Balkbrug of ergens anders is.

Er is ook een hoop familie die mij heeft gesteund voor en tijdens de afronding van dit proefschrift. **Christel**, dank dat Claire en ik altijd je auto mochten lenen. Daardoor konden we even ontsnappen aan de drukte van de stad (en werk). Daarnaast waardeer ik je interesse in de voortgang van m'n boekje en m'n gewicht. **Dave**, fijn dat we altijd welkom zijn in Amerongen en leuk dat we onze passie over (natuur)fotografie kunnen delen. **Britt** en **George**, dank voor alle gezellige etentjes en jullie prachtige cadeau. De kattenmok is een vast onderdeel van m'n bureau geworden.

Bert en **Mai**, de gezelligste peetoom en peettante. Door corona hebben we helaas wat feestjes moeten missen, maar hopelijk kunnen we ooit weer naar Guus Meeuwis. **Ad, Marie-José**, **Rob, Marloes** en **Maartje,** ook jullie verdienen een vermelding in het dankwoord. Uitjes (o.a. varen in de Biesbosch) met onze beide gezinnen waren altijd gezellig en een goed moment om de kindertrauma's weer even naar boven te halen. Chocoladefondue iemand? Ik wil ook graag **Marie-José** nog expliciet bedanken voor de sushi en voor het feit dat ze al 30 jaar mijn favoriete kapper is.

Broertje en zusjes, waarschijnlijk heb ik jullie als grote broer de nodige kindertrauma's bezorgd. Ik hoop dat de chocoladefondue-sessie (en het volwassen worden) dit een beetje heeft goedgemaakt. Het idee is dat de oudere broer het voorbeeld geeft, maar ik heb ook heel veel van jullie kunnen leren. **Evy**, zusje, je was op jonge leeftijd al een fantastisch moederfiguur, ook al had je toen nog geen kinderen. Maar je bent veel meer dan een moeder. Met je duidelijke mening en de daaropvolgende spraakwaterval kom je vooruit en je brengt daarin ook de zorg een stapje verder. Dank voor het altijd alles regelen, je positieve uitstraling en je ontferming over ons als familie. **Mark**, broeder, wat was het leuk om samen bij Rammstein te staan springen en zingen (of schreeuwen). Ik bewonder hoe bekwaam je bent in zo veel verschillende dingen (verbouwen, computers, volle grond teelt) en ik ben je dankbaar voor je karakteristieke ondeugende, maar vriendelijke glimlach. **Fleur**, welpje, als jongste van het stel heb je het misschien wat zwaarder gehad vroeger, maar ik ben enorm trots op wie je bent geworden en waar je staat. Je bent tenslotte niet voor niks mijn paranimf. **Jeroen, Jolien** en **Bart,** dank dat jullie het met deze familie volhouden, dat jullie er bij zijn met leuke en minder leuke dingen. Ik kijk uit naar de toekomst. **Lynn**, misschien gek om iemand te benoemen die nog niet eens kan lezen, maar jij bracht de hele familie een beetje geluk en bracht ons bij elkaar toen dat door corona soms zo lastig was.

Pap & Mam, één paragraaf in één dankwoord van één proefschrift is niet genoeg om alles op te noemen waarvoor ik dankbaar ben. Ik besef me dat dit boekje alleen hier ligt omdat jullie mij al die tijd hebben gesteund en gemotiveerd. Dat begon al op de basisschool met de uitstapjes naar de bibliotheek, waar ik leerde om verder te kijken dan alleen de directe omgeving. Jullie lieten me ook zelf een weg zoeken en steunde mij in de keuzes die ik maakte. Naast deze steun dienden jullie ook als

voorbeeld. Want al zijn er grote verschillen, er zijn ook overeenkomsten tussen de wetenschap en het boerenleven. Als je iets wilt bereiken, dan moet er hard gewerkt worden. Maar soms zit het tegen en is het resultaat ondanks het harde werken toch teleurstellend. Ik heb over de jaren heen gezien hoe jullie hier mee om gaan en dat heeft mij veel geholpen op de momenten dat volle bak gewerkt moest worden tijdens grote experimenten of wanneer het tegenzat. Bedankt voor jullie onvoorwaardelijke steun en vertrouwen.

Toen ik net een paar maanden thuis werkte om dit proefschrift af te ronden is het huishouden uitgebreid met de monsters **Momo** en **Jiji**. Elke dag moet ik weer lachen om de capriolen die jullie uithalen en elke week een beetje huilen als er weer een plant is uitgegraven of er iets anders in het huis overhoop is gehaald. Desondanks ben ik erg blij met jullie, want het schrijven wordt een stuk aangenamer als je af en toe onderbroken wordt door een kat die aandacht wil.

Dan als allerlaatste de persoon die de afgelopen vijf jaar altijd naast me stond en mij steunde door dik en dun. **Claire**, je bent een topwijf. Jij beseft wat het inhoudt om te promoveren, dat je vrijetijd en vakanties soms moet opgeven om nog nét die proef dit jaar gedaan te krijgen. Dat was niet altijd makkelijk, maar we kwamen er altijd samen uit. En als ik dan gesloopt was na een lang experiment met zware sectiedagen, dan was jij er altijd. Om te ontspannen met een biertje of om gewoon even een weekje weg te gaan naar de natuur. Naast dat je er altijd voor mij bent, verrijk je ook mijn leven. Je bedenkt leuke nieuwe dingen om te doen, waarmee je mij toch weer van de bank krijgt. Je daagt me uit om na te denken over maatschappelijke kwesties, die ik anders genegeerd zou hebben. En je hebt na lang aandringen mij toch zo ver gekregen om die twee monsters in huis te halen, waar ik uiteindelijk heel blij mee ben. Dank voor wie je bent en wat je doet. Door jou ben ik een beter mens en een gelukkiger persoon. Hou van je.

Curriculum vitae

Koen van de Ven was born on December 18th, 1990 in Oirschot, The Netherlands. After finishing his secondary education in 2009, he moved to Amsterdam to obtain his bachelor degree in Biomedical Sciences from the University of Amsterdam. He graduated Cum Laude and with honours in 2012, after which he continued his Master's in the same subject. Koen was especially interested in cancer and the immune system. He therefore did an internship at the Amsterdam Medical Centre where he studied multiple myeloma – a B-cell malignancy – in the lab of dr. Marcel Spaargaren. In line with his interests, Koen went on to write a thesis on the application of immunotherapy for the treatment of cancer. This thesis – written under the guidance of prof. dr. Jannie Borst – was later published and was Koen his first scientific publication as first author. For his second internship Koen moved to Stockholm, Sweden, to study the role of PD-1 in the development of natural killer cells in the lab of dr. Benedict Chambers at the Karolinkska Institutet.

In 2016, Koen received his master's degree Cum Laude. He was then welcomed as a PhD student at the Dutch National Institute for Public Health and the Environment (RIVM) under the supervision of dr. Jørgen de Jonge. In the next five years, Koen would study the role of T-cell immunity in the defence against influenza and SARS-CoV-2 pathogens in ferret and mice animal models. This research has accumulated into the thesis presented here.

After finishing his PhD, Koen moved to a different side of the public health domain, where he is currently working as a data scientist at the Dutch Institute for Clinical Auditing (DICA).